

LONDON
SCHOOL of
HYGIENE
& TROPICAL
MEDICINE



**ACCELERATING DEVELOPMENT OF THERAPEUTIC
TUBERCULOSIS VACCINES USING AN *EX VIVO*
IMMUNE ASSAY PLATFORM**

Satria Arief Prabowo

**Thesis submitted in accordance with the requirements for the degree
of Doctor of Philosophy of the University of London**

January 2019

**Department of Immunology and Infection
Faculty of Infectious and Tropical Diseases
LONDON SCHOOL OF HYGIENE AND TROPICAL MEDICINE**

**Research group affiliation(s): Professor Helen Fletcher (Supervisor)
Tuberculosis Centre and Vaccine Centre, LSHTM**

Funded by European Commission (TBVAC2020, grant 643381) and Indonesia
Endowment Fund for Education

Declaration

I, Satria Arief Prabowo, confirm that the work presented in this thesis is my own. Where information has been derived from other sources, I confirm that this has been indicated in the thesis.

Signed:



January 2019

Preface

This PhD thesis is written in a research paper style format in accordance to the applicable and existing regulation at LSHTM. The first chapter is a general introduction to tuberculosis, covering the topic of immunology, vaccines and correlates of protection. It also outlines the gaps in knowledge and sets the rationale of the project presented in the three manuscripts, each as a chapter, that follow. These three manuscripts are currently under review in international peer-reviewed journals. Unpublished pilot investigations and preliminary methodology development data are discussed in a separate chapter following the research paper chapters. The last chapter in the thesis integrates the results of the three discrete but related investigations as well as the unpublished data to give an answer to the problems stated in the introduction chapter. Reference list is provided at the end of each chapter in accordance to the format of LSHTM research paper style PhD thesis.

List of Publications and Presentations

Publications

Submitted articles

- **Prabowo SA**, Zelmer A, Stockdale L, Ohja U, Smith SG, Seifert K, Fletcher HA. *Historical BCG vaccination combined with drug treatment enhances inhibition of mycobacterial growth ex vivo in human peripheral blood cells*. Submitted to *Scientific Reports*, 2018.
- **Prabowo SA**, Painter H, Zelmer A, Smith SG, Seifert K, Amat M, Cardona PJ, Fletcher HA. *RUTI vaccination enhances inhibition of mycobacterial growth ex vivo and induces a shift of monocyte phenotype in mice*. Submitted to *Frontiers in Immunology*, 2018.
- **Prabowo SA**, Smith SG, Seifert K, Fletcher HA. *Impact of individual-level factors on ex vivo mycobacterial growth inhibition: the influence of immune cells phenotype, cytomegalovirus-specific response and sex on immunity following BCG vaccination in human*. Submitted to *Tuberculosis (Edinb)*, 2018.

Published articles/ in preparation

In addition, during my PhD programme at LSHTM, I also contributed to other publications which are not part of my thesis:

- Kewcharoenwong C, **Prabowo SA**, Bancroft GJ, Fletcher HA, Lertmemongkolchai G. *Glibenclamide reduces primary human monocyte functions against mycobacterial infection by enhancing M2 polarization*. *Frontiers in Immunology*. 2018 Sep 19;9:2109. doi: [10.3389/fimmu.2018.02109](https://doi.org/10.3389/fimmu.2018.02109)
- Zelmer A, Stockdale L, **Prabowo SA**, Cia F, Spink N, Gibb M, Eddaoudi A, Fletcher H. *High monocyte to lymphocyte ratio is associated with impaired protection after subcutaneous administration of BCG in a mouse model of tuberculosis*. *F1000Research*. 2018, 7:296. doi: [10.12688/f1000research.14239.2](https://doi.org/10.12688/f1000research.14239.2)
- Rhodes SJ, Zelmer A, Knight GM, **Prabowo SA**, Stockdale L, Evans TG, Lindenstrøm T, White RG, Fletcher H. *TB vaccine H56 dose response curve is n-shaped not saturating: data generation for new mathematical modelling methods to inform vaccine dose decisions*. *Vaccine*. 2016 Dec 7;34(50):6285-6291. doi: [10.1016/j.vaccine.2016.10.060](https://doi.org/10.1016/j.vaccine.2016.10.060)
- Painter H, **Prabowo SA**, Cia F, Stockdale L, Zelmer A, Fletcher HA. *Adaption of the ex vivo mycobacterial growth inhibition assay for use in murine lung cells*. Manuscript in preparation, 2018.
- Additional role in PLoS One as a peer reviewer (2016, 2017).

Presentations

- Keystone Symposia: New Approaches to Vaccines for Human and Veterinary Tropical Diseases, Cape Town, South Africa, 22 – 26 May 2016.
Poster presentation: *The impact of immunotherapeutic tuberculosis vaccination towards drugs control of mycobacterial growth ex-vivo.* (Prabowo SA, Zelmer A, Stockdale L, Amat M, Cardona PJ, Fletcher HA)
- 47th Union World Conference on Lung Health, International Union Against Tuberculosis and Lung Diseases, Liverpool, United Kingdom, 26 – 29 October 2016.
Oral presentation: *The impact of previous BCG vaccination in enhancing the effectiveness of tuberculosis drugs to control mycobacterial growth ex-vivo.* (Prabowo SA, Zelmer A, Stockdale L, Smith SG, Seifert K, Fletcher HA)
- 35th Annual Meeting of European Society for Paediatric Infectious Diseases (ESPID), Madrid, Spain, 23 – 27 May 2017.
Poster discussion session: *The impact of previous BCG vaccination in enhancing the effectiveness of tuberculosis drugs to control mycobacterial growth ex-vivo.* (Prabowo SA, Zelmer A, Stockdale L, Smith SG, Seifert K, Fletcher HA)
- Cell-Weizmann Institute of Science Symposium: Next Generation Immunology, Rehovot, Israel, 11 – 14 February 2018.
Poster presentation: *Historical BCG vaccination combined with drug treatment enhances inhibition of mycobacterial growth ex vivo in human peripheral blood cells.* (Prabowo SA, Zelmer A, Stockdale L, Smith SG, Seifert K, Fletcher HA)
- 5th Global Forum on Tuberculosis Vaccines, New Delhi, India, 20 – 23 February 2018.
Poster presentation: *Historical BCG vaccination combined with drug treatment enhances inhibition of mycobacterial growth ex vivo in human peripheral blood cells.* (Prabowo SA, Zelmer A, Stockdale L, Smith SG, Seifert K, Fletcher HA)
- 62nd Acid Fast Club Summer Meeting, Jenner Institute, University of Oxford, Oxford, United Kingdom, 5 – 6 July 2018.
Oral presentation: *Historical BCG vaccination combined with drug treatment enhances inhibition of mycobacterial growth ex vivo in human peripheral blood cells.* (Prabowo SA, Zelmer A, Stockdale L, Smith SG, Seifert K, Fletcher HA)

Abstract

Drug treatment and vaccination remain the main strategies to control tuberculosis (TB), which is the leading infectious cause of death globally. Lengthy treatment is often cited as a major obstacle towards improved control of TB. It has been proposed that a combination of TB vaccination with pharmacological treatment, termed therapeutic vaccination, may provide a greater therapeutic value. Several therapeutic TB vaccine candidates have been developed and are currently progressing in the pipeline. We hypothesise that an *ex-vivo* mycobacterial growth inhibition assay (MGIA) can be implemented to investigate and accelerate development of therapeutic vaccination strategies for TB, in the context of both human clinical and animal murine studies.

This thesis describes for the first time, the combined effect of immunoprophylaxis by routine vaccination with *Bacillus Calmette–Guérin* (BCG) and chemotherapy using the *ex vivo* immune assay platform. The first research chapter of the thesis elaborates a proof-of-principle study investigating the combined effect between historical BCG vaccination and two major first-line TB drugs (isoniazid and rifampicin), which is considered essential to further expedite the development of therapeutic vaccination strategies for TB. The second part of the thesis describes a study in which immunisation of mice with RUTI, a novel therapeutic TB vaccine candidate, was shown to enhance inhibition of mycobacterial growth *ex vivo* by inducing a shift of monocyte phenotype. We also investigated the effects of RUTI and BCG vaccination towards *ex vivo* drug-mediated killing in mice. The third research part of the thesis discusses the impact of individual-level factors on *ex-vivo* mycobacterial growth inhibition, specifically the influence of immune cell phenotype, cytomegalovirus-specific response and sex on immunity following BCG vaccination in humans.

In the absence of an immune correlate of protection following TB vaccination, implementation of the *ex vivo* MGIA assay could be beneficial to screen TB vaccine candidates at early phases in order to prioritise which candidates should be tested with the available funding and field sites. Collectively, our findings support the implementation of MGIA as an effort to accelerate the development of therapeutic TB vaccines.

Acknowledgement

My heartfelt thanks for volunteers of the study participants who generously donated and allowed us to use their samples for this research.

I would like to express my sincerest gratitude to my supervisor, Prof Helen Fletcher, for allowing me to become her PhD student and learn under her. She has been a huge inspiration and a great example. I am very grateful for her patience, support, enthusiasm, motivation and invaluable advice throughout every stage of my PhD. I would also like to appreciate my advisory committee, Dr Karin Seifert and Dr Steven Smith, for encouragement, support and mentorship throughout. You have all given me the confidence to become an independent researcher.

From the Fletcher group, I would like to convey my gratitude to Dr Andrea Zelmer, Dr Lisa Stockdale and Hannah Painter for helping me with all kinds of laboratory experiments. Coming from a medical background, it took me some time to engage with basic and molecular science. Thank you for allowing me to become a translational researcher. As a doctor, I always believe if we are only performing clinical practice, we can only cure the patients whom we meet. But as a researcher, in addition to a medical practitioner, the innovations we generate could potentially save a lot of patients, not only in the present time but also in the future. This PhD has encouraged me to bring research further from 'bench to bedside'.

I would like to express my special thanks to Carolynne Stanley for arranging blood from LSHTM donors, for all the ordering and for helping me with any technical queries. My appreciation to Ayad Eddaoudi and Stephanie Canning for training, technical assistance and troubleshooting in relation to flow cytometry. Thank you to Rachel Gregory for always being available to discuss anything. I was incredibly lucky to have very supporting colleagues from LSHTM and London. A special thanks to Higinia Fernandes for her relentless help in administrative arrangements and for her kind advice.

My friends and colleagues, in particular from lab 420 and office 480, thank you for the friendship and hospitality, and for making LSHTM my second home. I particularly would like to thank Felipe Cia, Nuha Mansour, Liz McCarthy, Natasha Spink, Sam Willcocks and Henry Surendra for the countless help. I thank the senior staff members of the Immunology Department for the constructive discussion and invaluable feedback during the Tuesday lab meeting: Prof Gregory Bancroft, Dr John Raynes, Dr Helena Helmbly and Dr Theresa Ward. Thank you to Dr Jackie Cliff for providing comments on my research as well as for allowing me to participate in teaching activities at LSHTM. Special thanks also to friends at LSHTM: Masao Iwagami, Mahjannah Hussein, Titus Divala, Mari Kajiwara, Katherine Horton, Ibrahim Maikore, Inke Lubis, Shaheda Anwar, Aishatu Adamu, Anastasia Polycarpou, Nofri Rahmadika, Imran Morhasson-Bello, Sophia Bakon, Abrar Alasmari and Clare Eckold for the discussion and their encouragement. Thank you to several international and domestic scientists who have visited our group at LSHTM and shared their knowledge in various fields: Dr Chidchamai Kewcharoenwong (Wine), Dr Arnone Nithichanon, Ms Pritsana Sawutdeechaikul (Koy), Dr Panjaporn Chaichana (Por) (Thailand), Dr Hyejon Lee, Dr Jake Whang (South Korea), Dr Simon Kimuda (Uganda), Mr Helder Buló (Mozambique), Prof Ben Marais (Australia) and Mr Utkarsh Ohja (Imperial College London).

My best friends, Dr Erni Marlina and Dr Edessa Negera Gobena, thank you for always be on my side and for your constant support. You have allowed me to reach the finish line of this PhD. I will remember the wonderful moments we shared together, supporting each other in our lab work, discussing our confusion as well as the ups and downs in our journey. I would like to thank London School of Hygiene and Tropical Medicine for giving me the opportunity to join the research degree programme in the best Tropical Medicine institution in the world. Thank you for the great chance for me to serve as faculty research degree student representative year 2016/17 with my fellow colleagues: Catherine Hall, Helen Wagstaffe and Ernest-Diez Benavente. Special thanks to the LSHTM Tuberculosis Centre, Vaccine Centre and Faculty of Infectious and Tropical Diseases for the fantastic seminars and events.

I would not have been completed this work without the generous financial support from my sponsor, Indonesia Endowment Fund for Education (LPDP), who provided me with a studentship to accomplish the PhD. The Fletcher group receives support from the European Commission HORIZON TBVAC2020 as well as other funders which has allowed me to perform the PhD research. We are also grateful to Archivel Farma, S.L. (Badalona, Catalonia, Spain) for providing RUTI candidate vaccine vials to be tested in this project. In particular, we are thankful to Merce Amat and Olga Rue for their sincere support in our project. We are also indebted to Prof Pere-Joan Cardona and Dr Cristina Vilaplana from Universitat Autònoma de Barcelona (UAB), Catalonia, Spain for the scientific discussion and insight in relation to the RUTI project. We are very thankful to Prof Tjip van der Werf and Dr Matthias Gröschel from University Medical Centre Groningen (UMCG), The Netherlands for allowing our participation in the clinical trial of RUTI vaccine as well as for introducing me to the field of tuberculosis vaccines prior to this PhD.

My family deserves more than my thanks. I thank my father and my mother for their infinite love, support and blessing. Thank you as well to my late grandmother, my brother and sister for their encouragement and support. I would not have been able to complete this PhD without them. Finally, I thank God the Almighty for giving me the opportunity, courage and strength to undertake and pursue this PhD degree.

I dedicate the work described in this thesis to my home country, Indonesia, in which tuberculosis disease is still a major problem, with a great hope to help alleviating the burden caused by the disease.

Table of Contents

Declaration by Candidate	1
Preface	2
List of Publications and Presentations	3
Abstract	5
Acknowledgement	6
Table of Contents	9
List of Figures	12
List of Tables	16
List of Appendices	18
List of Abbreviation	19
Chapter 1: General Introduction	23
1.1 Tuberculosis (TB)	23
1.1.1 Epidemiology	24
1.1.2 Pathogenesis	26
1.1.3 Diagnostics	28
1.1.4 Treatment and Drug Resistance	31
1.2 Tuberculosis Immunology: Roles of Immune Cells and Cytokines	36
1.2.1 The Innate Immune Response to TB	36
1.2.2 The Adaptive Immune Response to TB	40
1.2.2.1 Cellular Immune Response	41
1.2.2.1.1 Conventional T-cells	41
1.2.2.1.2 Unconventional T-cells	44
1.2.2.2 Humoral Immune Response and B cells	45
1.2.3 Trained Innate Immunity	46
1.3 Tuberculosis Vaccines	48
1.3.1 Bacillus Calmette–Guérin (BCG)	48
1.3.2 Development of Novel Vaccines against TB	52
1.3.3 Therapeutic Vaccination Strategy for TB	55
1.3.3.1 History of Therapeutic Vaccination in TB	55
1.3.3.2 Current Concept and Candidates for Therapeutic Vaccination in TB	56
1.3.4 Preclinical Animal Models and Human Trials for TB Vaccine Testing	59
1.4 Immune Correlates of Protection	62
1.4.1 T-cell–based Signatures as Correlates of Vaccine-induced Immunity	63
1.4.2 Mycobacterial Growth Inhibition Assays (MGIAs)	64
1.4.2.1 Whole blood MGIAs	65
1.4.2.2 PBMC-based MGIAs	67
1.4.2.3 MGIAs in Preclinical Animal Models	68

1.4.2.4 Immune Mechanisms of Growth Inhibition	70
1.4.2.5 The BACTEC Mycobacterial Growth Indicator Tube (MGIT) System	71
1.5 Project Structure	72
1.5.1 Rationale of the Study	72
1.5.2 Hypothesis	73
1.5.3 Study Aims and Objectives	73
1.5.4 Thesis Structure	74
References	77
Chapter 2: Research Paper 1	96
<u>Title:</u> Historical BCG vaccination combined with drug treatment enhances inhibition of mycobacterial growth <i>ex vivo</i> in human peripheral blood cells	
Introduction	100
Materials and Methods	103
Results	108
Discussion	119
References	127
Supplementary Materials	131
Chapter 3: Research Paper 2	135
<u>Title:</u> RUTI vaccination enhances inhibition of mycobacterial growth <i>ex vivo</i> and induces a shift of monocyte phenotype in mice	
Introduction	140
Materials and Methods	143
Results	150
Discussion	157
References	164
Supplementary Materials	167
Chapter 4: Research Paper 3	171
<u>Title:</u> Impact of individual-level factors on <i>ex vivo</i> mycobacterial growth inhibition: the influence of immune cell phenotype, cytomegalovirus-specific response and sex on immunity following BCG vaccination in humans	
Introduction	176
Materials and Methods	180
Results	187
Discussion	197
References	205
Supplementary Materials	210

Chapter 5: Pilot Investigations and Preliminary Methodology Development	221
5.1 Impact of BCG vaccination in mice on MGIA in the presence of TB drugs	221
5.1.1 Introduction	221
5.1.2 Materials and Methods	221
5.1.3 Results	227
5.1.4 Discussion	236
5.2 Impact of RUTI vaccination in mice on MGIA in the presence of isoniazid (INH) and rifampicin (RIF)	240
5.2.1 Introduction	240
5.2.2 Materials and Methods	241
5.2.3 Results	244
5.2.4 Discussion	251
5.3 Optimisation of the murine and human MGIA assays	253
5.1.1 Introduction	253
5.1.2 Materials and Methods	254
5.1.3 Results and Discussion	254
References	261
Chapter 6: General Discussion and Conclusion	263
6.1 Overall Discussion and Key Findings	263
6.2 Strengths and Limitations of the Research Presented	267
6.3 Conclusions	269
6.4 Future Directions	270
References	273
Appendices	275

List of Figures

Chapter 1: General Introduction

Figure 1. Estimated TB incidence rates in 2016	25
Figure 2. Clinical spectrum of TB infection	28
Figure 3. Bacterial subpopulations in TB treatment	34
Figure 4. Cellular adaptive immune response in TB	42
Figure 5. Vaccination strategies against TB targeting different stages of infection	53
Figure 6. Pathway of licensure for a vaccine candidate	61
Figure 7. Classification of various MGIA's which have been developed for human and animal testing	65

Chapter 2: Research Paper 1

Figure 1. Immune response and growth inhibition following historical BCG vaccination	109
Figure 2. Growth inhibition in the absence and presence of INH and RIF	111
Figure 3. Cytokine responses from co-culture with INH and RIF	114
Figure 4. Frequencies of Th1 cytokine-expressing lymphocytes	117
Figure 5. NK cells correlations	119
Figure S1. Standard curve of BCG Pasteur Aeras used to convert TTP to CFU	131
Figure S2. ICS flow cytometry gating strategy	132

Chapter 3: Research Paper 2

Figure 1. Experimental design and vaccination schedule	144
--	-----

Figure 2. ELISpot and MGIA responses	151
Figure 3. The shift of Ly6C ⁺ and Ly6C ⁻ monocytes/macrophages populations following RUTI vaccination in healthy mice	153
Figure 4. mRNA expressions of Ly6C ⁻ -related and Ly6C ⁺ -related genes	156
Figure S1. RUTI vaccination induced mycobacterial growth inhibition in murine splenocytes in comparison with BCG, performed in rotating tubes	167
Figure S2. Naïve control at week 6 following RUTI vaccination	168
Figure S3. The frequency of monocytes/macrophages, ML ratio, T cells and B cells	169
Figure S4. mRNA expressions of β -actin and melting curve analysis	170

Chapter 4: Research Paper 3

Figure 1. Growth inhibition and immune responses following historical BCG vaccination	189
Figure 2. NK cells correlations	192
Figure 3. CMV-specific responses	194
Figure 4. Sex impact on growth inhibition and immune responses following historical BCG vaccination	195
Figure 5. Comparison by sex of immune cells phenotype, T-cell activation and CMV-specific T-cell response	197
Figure S1. Standard curve of BCG Pasteur Aeras used to convert TTP to CFU	210
Figure S2. Cell surface flow cytometry gating strategies	212
Figure S3. ICS flow cytometry gating strategy	213
Figure S4. Frequencies of Th1 cytokine-expressing T-cells	214

Chapter 5: Pilot Investigations and Preliminary Methodology Development

Figure 1. Correlation between TTP and log ₁₀ CFU as MGIT standard curve	224
Figure 2. Production of antigen-specific IFN- γ response measured with ELISpot and <i>ex vivo</i> control of mycobacterial growth between naïve and vaccinated mice	227
Figure 3. Growth inhibition in BCG-vaccinated and saline-injected mice, in the absence and presence of INH	229
Figure 4. Growth inhibition in BCG-vaccinated and saline-injected mice, in the absence and presence of RIF	230
Figure 5. Growth inhibition in BCG-vaccinated and saline-injected mice, in the absence and presence of PZA	231
Figure 6. Growth inhibition in BCG-vaccinated and saline-injected mice, in the absence and presence of EMB	232
Figure 7. Cytokine responses from co-culture with INH	234
Figure 8. Cytokine responses from co-culture with RIF	235
Figure 9. Correlation between cytokine productions and growth inhibition	236
Figure 10. Experiment design of first RUTI experiment	242
Figure 11. Experiment design of second RUTI experiment	243
Figure 12. <i>Ex vivo</i> control of mycobacterial growth between RUTI-vaccinated groups in the absence of drug	245
Figure 13. <i>Ex vivo</i> control of mycobacterial growth following RUTI vaccination in the presence of INH	246
Figure 14. <i>Ex vivo</i> control mycobacterial growth following RUTI vaccination in the presence of RIF	247
Figure 15. <i>Ex vivo</i> control of mycobacterial growth following RUTI vaccination in the presence of INH	249

Figure 16. <i>Ex vivo</i> control mycobacterial growth following RUTI vaccination in the presence of RIF	250
Figure 17. Comparison of different mycobacterial input to identify optimum condition for investigation of vaccine effect in mice	255
Figure 18. Comparison of different cellular input to identify optimum condition for investigation of vaccine effect in mice	255
Figure 19. Comparison of different culture method in rotating tubes or 48-well plate to identify optimum condition for investigation of vaccine effect in mice	256
Figure 20. Comparison of different cellular input and culture media to identify optimum condition for investigation of vaccine effect in human	258
Figure 21. Comparison of different mycobacterial input to identify optimum condition for investigation of vaccine effect in human	259
Figure 22. Comparison of different culture method to identify optimum condition for investigation of vaccine effect in human	260

Chapter 6: General Discussion and Conclusion

Figure 23. Illustration of the contribution of immune cells from various compartments on the <i>ex vivo</i> mycobacterial growth inhibition assay system	266
--	-----

List of Tables

Chapter 1: General Introduction

Table 1. Summary of drugs used to treat TB with various susceptibility	33
Table 2. Profile of several therapeutic vaccine candidates for TB	58

Chapter 2: Research Paper 1

Table 1. Demographics of participants enrolled in the study	108
Table S1. Median cytokine responses in negative and positive control tubes of the ICS assay	133
Table S2. Summary of mean cytokine responses measured with ELISA assays	134

Chapter 3: Research Paper 2

Table 1. Specific sets of primers of real-time PCR	149
--	-----

Chapter 4: Research Paper 3

Table 1. Characteristics of study participants	187
Table 2. Summary of mean cytokine responses measured with ELISA assays	190
Table 3. Correlation of immune cell frequencies in peripheral blood and <i>ex vivo</i> mycobacterial growth inhibition	191
Table 4. Correlation of CMV-specific T-cell responses and T-cell activation	193
Table S1. Correlation of BCG-specific T-cell response and <i>ex vivo</i> mycobacterial growth	215
Table S2. Impact of historical BCG vaccination on immune cell frequencies	215
Table S3. Summary of mean NK cells cytokine responses measured with ELISA	216

Table S4. CMV-specific T-cell responses	216
Table S5. Correlation of activated T-cells and <i>ex vivo</i> mycobacterial growth	217
Table S6. Comparison by sex of mean cytokine responses measured with ELISA assays	218
Table S7. Impact of sex on immune cell frequency, T-cell activation and CMV-specific T-cell response	219

List of Appendices

Appendix 1. Ethical approval 1 for human study	275
Appendix 2. Ethical approval 2 for human study	276
Appendix 3. Information sheet for study participants	277
Appendix 4. Consent form for study participants	278
Appendix 5. Material transfer agreement for RUTI vaccine study	280
Appendix 6. Conference papers	288
Appendix 7. Publications	294
Appendix 8. Additional data	323

List of Abbreviation

Ab	Antibody
AF700	Alexa fluor 700
Ag	Antigen
ALP	Alkaline phosphatase
AMs	Alveolar macrophages
ANOVA	Analysis of variance
APC/Cy7	Allophycocyanin Cy7
APCs	Antigen presenting cells
ATP	Adenosine triphosphate
BCG	Bacillus Calmette-Guérin
BCG- <i>lux</i>	BCG transfected with luciferase
BCIP	5-bromo-4-chloro-3-indolyl phosphate
BD	Becton Dickinson
BSA	Bovine serum albumin
BSF	Biological service facility
BSL	Biosafety level
BV	Brilliant violet
CCL	C-C motif ligand
CD	Cluster of differentiation
cDNA	Complementary deoxyribonucleic acid
CFP-10	Culture filtrate protein 10
CFU	Colony forming unit
CI	Confidence interval
CMV	Cytomegalovirus
CXCL	C-X-C motif chemokine
DCs	Dendritic cells
DC-SIGN	Dendritic cell-specific intracellular adhesion molecule-3-grabbing non-integrin
DFID	Department for international development
DMSO	Dimethyl sulfoxide
DN	Double negative
DNA	Deoxyribonucleic acid
EC	European commission
ELISA	Enzyme-linked immunosorbent assay
ELISpot	Enzyme-linked immunospot assay
EMB	Ethambutol
ESAT-6	Early secretory antigenic target-6
FACS	Fluorescence activated cell sorting
FBS	Fetal bovine serum

FITC	Fluorescein isothiocyanate
FMO	Fluorescence minus one
FSC	Forward scatter
GCP	Good clinical practice
GM-CSF	Granulocyte-macrophage colony-stimulating factor
Hb	Haemoglobin
HIV	Human immunodeficiency virus
HLA-DR	Human Leukocyte Antigen - DR isotype
ICH	International Conference on Harmonisation
ICS	Intracellular cytokine staining
IFN- γ	Interferon gamma
Ig	Immunoglobulin
IGRA	Interferon-gamma release assay
IL	Interleukin
INH	Isoniazid
iNKT cell	Invariant natural killer T-cell
IP10	Inducible protein 10
IQR	Inter-quartile range
LAG3	Lymphocyte-activation gene 3
LPS	Lipopolysaccharides
LSHTM	London School of Hygiene and Tropical Medicine
LTBI	Latent tuberculosis infection
MDP	Monocyte-macrophage DC progenitor
MDR	Multi-drug resistant
M:F ratio	Male to female ratio
MGIA	Mycobacterial growth inhibition assay
MGIT	Mycobacterial growth indicator tube
MHC	Major histocompatibility complex
MIC	Minimum inhibitory concentration
MIP	<i>Mycobacterium indicus pranii</i>
ML ratio	Monocytes to lymphocytes ratio
MOI	Multiplicity of infection
MRC	Medical Research Council
mRNA	Messenger ribonucleic acid
<i>Mtb</i>	<i>Mycobacterium tuberculosis</i>
mTOR	Mammalian target of rapamycin
MVA	Modified vaccinia Ankara
NBT	Nitro blue tetrazolium
ND	Not detected
NF- κ B	Nuclear factor kappa-light-chain-enhancer of activated B-cells
NHPs	Non-human primates

NK cell	Natural killer cell
NKT cell	Natural killer T-cell
NO	Nitric oxide
NOD2	Nucleotide-binding oligomerization domain-containing protein 2
OADC	Oleic acid, Albumin, Dextrose and Catalase
PANTA	Polymyxin B, Amphotericin B, Nalidixic Acid, Trimethoprim, Azlocillin
PAS	Para-aminosalicylic acid
PBMC	Peripheral blood mononuclear cell
PBS	Phosphate-buffered saline
PCR	Polymerase chain reaction
PD1	Programmed cell death protein 1
PE	Phycoerythrin
PerCP	Peridinin-chlorophyll-protein
PHA	Phytohemagglutinin
PhD	Doctor of Philosophy
PMA	Phorbol myristate acetate
PPD	Purified protein derivative
PPL	Procedure project license
PRR	Pattern recognition receptor
PZA	Pyrazinamide
qRT-PCR	Quantitative reverse transcriptase PCR
RBC	Red blood cell
RD1	Region of difference 1
RIF	Rifampicin
RNA	Ribonucleic acid
Rpm	Rotations per minute
RPMI	Roswell Park Memorial Institute
SEB	<i>Staphylococcus</i> enterotoxin B
SD	Standard deviation
SFC	Spot forming cells
SSC	Side scatter
TB	Tuberculosis
TCR	T-cell receptor
TDR	Totally drug-resistant
TGF	Tumour growth factor
Th	T-helper
TLR	Toll-like receptor
TN	Triple negative
TNF	Tumor necrosis factor
Treg	T-regulatory

TST	Tuberculin skin test
TTP	Time to positivity
UK	United Kingdom
US	United States
UV	Ultra-violet
VPM	<i>Vakzine Projekt Management</i>
WHO	World Health Organization
XDR	Extensively drug-resistant

1.1 Tuberculosis

Tuberculosis (TB) continues to be a major cause of morbidity and mortality, mainly in low- and middle-income countries, despite the causative agent being discovered by Robert Koch more than 100 years ago in 1882¹. TB is a treatable airborne infectious disease caused primarily by *Mycobacterium tuberculosis* (*Mtb*) which constitutes the deadliest infection in the past 200 years². The development of antibiotic treatment as well as implementation of the Bacillus Calmette–Guérin (BCG) vaccination in the last 60 years have resulted in a considerable decline of the disease burden³. Nevertheless, the battle against TB is far from over and TB remains as a prominent public health concern in many parts of the world.

TB is a poverty-related disease and often erroneously considered as a disease of the past. This assumption was challenged in 1993, when the World Health Organization (WHO) declared TB as a global emergency, notably following the nosocomial outbreaks of drug-resistant TB in some hospitals in New York city^{4,5}. Since the disease was declared as a global emergency, TB has resulted in 30 million deaths and orphaned at least 10 million children worldwide⁶. Currently, the spread of human immunodeficiency virus (HIV) infection has been fuelling TB epidemics in several parts of the world, particularly in Sub-Saharan Africa⁷. This is due to the fact that the risk of developing the disease is markedly increased in immunocompromised persons⁸. In some other parts of the world including South-East Asia and South America, HIV plays a lesser role and TB is more associated with other immunocompromising conditions, such as diabetes mellitus^{9,10}.

Furthermore, the current situation is aggravated by the emergence of multidrug-resistant (MDR)-TB which has been reported in virtually all countries¹¹.

By 2050, the Stop TB Partnership aims to eliminate TB by reducing the incidence to less than one case per 1 million people¹². In 2015, the WHO also sets some goals with the End TB Strategy which aims to reduce the morbidity and mortality up to 90% and 95% respectively by 2035¹³. To achieve this, an incidence reduction of 4-5% needs to be sustained annually. Such a target is unlikely to be achieved, considering the current global rate of decline is only around 1.5% per year^{12,14}.

1.1.1 Epidemiology

According to the WHO, in 2016, it was estimated that 10.4 million individuals were affected by TB, of which 1.67 million cases resulted in fatality¹¹. TB mostly affects humans in their productive ages, with the risk of developing active disease rising during adolescence, then remaining high at around 25 years of age and throughout adult life¹⁵. As the disease affects socially and economically active adults, the economic burden of the disease is considered to be huge to society¹⁶. TB is a poverty related disease commonly affecting vulnerable populations in less affluent countries (Figure 1). Five countries accounted for 56% of global new cases: India, Indonesia, China, the Philippines and Pakistan in 2016¹¹. The South-East Asia, African and Western Pacific regions contributed to the majority of TB cases in the world, with over 80% cases occurring in 30 high-burden low-income developing countries¹¹. In most high-income countries, improvement in living standards led to significant declines of TB rates over the past few decades. Despite this, TB still shows no signs of disappearing in the near future as the

disease is still affecting high-risk groups such as elderly, immigrant populations, homeless persons, prisoners and people with low socioeconomic status in these countries¹⁷.

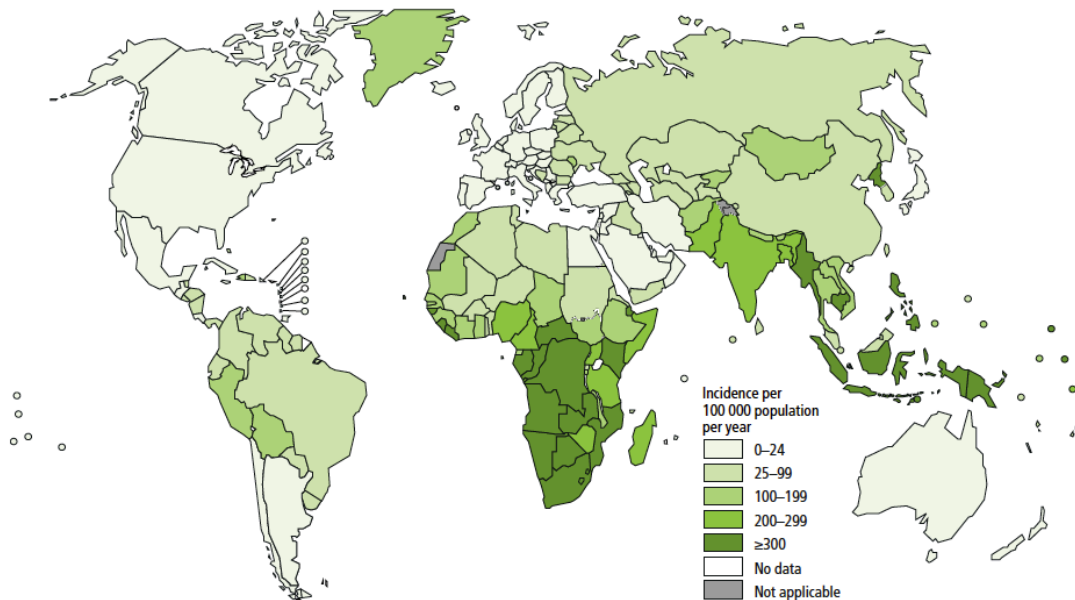


Figure 1. Estimated TB incidence rates in 2016 (taken from WHO¹¹).

The incidence of active TB disease is approximately twofold higher in men than in women¹⁸. Male sex is currently recognised as a risk factor for developing tuberculosis^{19,20}. It is commonly regarded that socioeconomic and cultural factors are responsible for the observed sex bias. This could be due to differences in smoking rates, alcohol or drug use, quality of sputum samples as well as better access to healthcare in males compared to female, thereby leading to higher diagnostic rates of TB in men and under-notification in women^{18,21}. However, it has been suggested that immunology might also play a role, as the male bias also exists in countries without apparent differences between the sexes in access and health-seeking behaviour towards medical care facilities, such as in European and American regions¹⁸. Moreover, the sex bias does not seem to apply to children and

only starts to be observed during adolescence, reflecting the potential contribution of biological factors, such as sex hormones²². Interestingly, such observations are not exclusive to TB and have been described for various other infectious and autoimmune diseases²³. A general consensus exists stating that females exhibit more robust immune responses towards infection and vaccination when compared to males²⁴.

Several risk factors have been identified towards increased susceptibility and progression of active TB disease, such as HIV infection, malnutrition, diabetes mellitus, indoor air pollution, alcohol, use of immunosuppressive drugs and tobacco smoking¹⁹. Among the major known risk factors, HIV infection significantly increases TB risk at least ten times, while type 2 diabetes mellitus as well as excessive alcohol consumption triple the risk, and smoking doubles the risk of developing TB^{19,25}. In developing countries, the high burden of TB is due to a combination of co-morbidities with poor living conditions and lack of health-care resources. In addition, BCG has a low efficacy against adult pulmonary TB disease in countries closer to the equator where the disease is most endemic^{26,27}.

1.1.2 Pathogenesis

Mtb is primarily transmitted by the aerosol route from person to person. Upon inhalation, mycobacteria reach the lower respiratory tract and deposit in alveoli where they predominantly infect alveolar macrophages²⁸. Typically, TB pathogenesis can be divided into two stages, each of them can present as active disease. Some individuals, mainly children, progress rapidly to active disease following primary infection and this is termed as primary or primary-progressive TB. In many others, mostly in immunocompetent

adults, *Mtb* are contained following the primary infection in a structure called granuloma, but the host remains infected in a condition commonly referred to as latent TB infection (LTBI). In the latter scenario, active TB disease can present after many years following exposure, termed reactivation or post-primary TB²⁹. Currently, it is estimated that a quarter or 1.7 billion of the world population is latently-infected with TB³⁰. Among these individuals, there is a 5–10% lifetime risk of developing active TB, with the highest risk being in the first 18 months after the initial infection⁷.

Recognition of mycobacterial components, termed pathogen-associated molecular patterns, by innate immune cells is conducted through pattern recognition receptors (PRRs) on their cell surfaces. Investigations have revealed that PRRs involved in the mycobacterial recognition process include several receptor families such as Toll-Like Receptors (TLRs), nucleotide oligomerization domain-like receptors, C-type lectins, Dendritic Cell-Specific Intercellular Adhesion Molecule-3-Grabbing Non-integrin (DC-SIGN) and dectin-1. These receptors recognise components of *Mtb* such as lipoprotein, CpG-containing DNA, mannose-capped lipoarabinomannan and phosphatidylinositol mannoside^{28,31}. Following this encounter, there could be several possible outcomes: 1) elimination by innate immunity, 2) elimination by acquired immunity, with or without memory, 3) quiescent/ LTBI, 4) subclinical disease with no or minimal symptoms or 5) active TB disease^{29,32} (Figure 2).

In the context of TB, disease development is a function of the host's immune competence, as exemplified by individuals with HIV who are at increased risk of progression to active disease³³. In most cases, TB disease commonly affects the lungs as the primary site of infection (~85% cases)³⁴. However, the infection could also spread outside the lungs and cause extra-pulmonary TB. The most common infection sites outside the lungs are the

lymph nodes, pleura, bone, gastro-intestinal tract and central nervous system⁷. In children, a typical manifestation of extra-pulmonary TB is known as miliary or disseminated TB, in which the infection propagates through the bloodstream and causes a widespread disease, often also manifesting as TB meningitis³⁵.

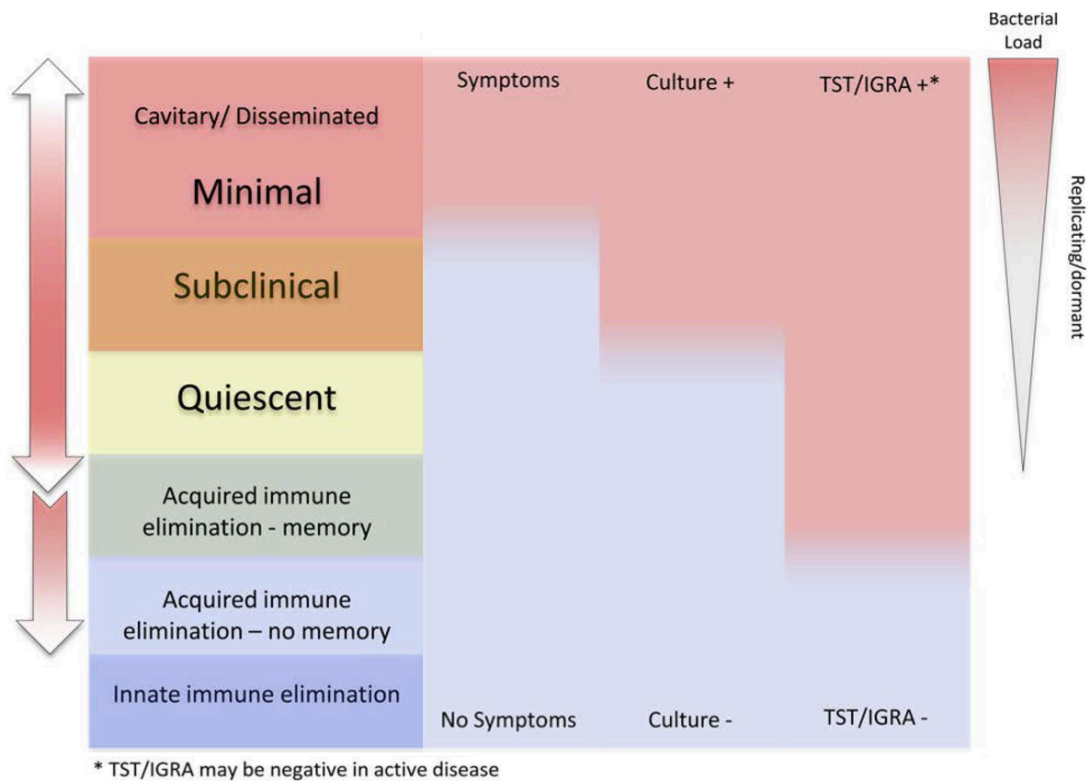


Figure 2. Clinical spectrum of TB infection (modified with permission from Scriba *et al.*³²).

1.1.3 Diagnostics

The cardinal symptoms of active pulmonary TB disease in adults include cough, weight loss, night sweats or chills, fever, anorexia and malaise³⁶. In contrast, LTBI does not show any clinical symptoms and the host is considered to be healthy, despite harbouring latent *Mtb* bacilli. Even in high-burden community settings, the symptoms of active pulmonary TB could mimic some other diseases, such as chronic obstructive pulmonary disease, lung

cancer, bronchiectasis, asthma or fungal infections³⁷. Therefore, diagnostic tests have been developed in order to help distinguish active TB from other conditions, as well as to diagnose LTBI to help identifying persons who are at increased risk of developing active disease (i.e. individuals who are undergoing immunosuppressive therapy).

Latent infection can be diagnosed with either a tuberculin skin test (TST) or an interferon-gamma release assay (IGRA). TST was introduced over 100 years ago and involves injection of mycobacterial antigen (purified protein derivative/ PPD) to assess cellular immune reactivity based on the size of induration in the skin. The conventional threshold for TST positivity is 10 mm, although this threshold is reduced to 5 mm in high risk groups such as immunocompromised patients or household contacts of active TB patients^{7,34}. Generally, 75% to 90% of active TB patients also react to TST³⁸, although the test cannot be used to diagnose active TB by itself and requires clinical investigation as well as other diagnostic measures (Figure 2). Moreover, prior vaccination with BCG and exposure to environmental mycobacteria also affect the results of TST, rendering the results false positive³⁸. Despite this, the test is inexpensive and therefore preferred in low-income regions³⁹.

Immune response to TB infection is recognised to be associated with a strong type 1 immunity, in which the hallmark is the release of interferon-gamma (IFN- γ) cytokine by CD4 T-cells^{40,41}. Hence, two techniques of IGRAs have been developed to measure IFN- γ in blood cells in response to *Mtb*-specific antigens. QuantiFERON TB Gold In Tube (Qiagen, The Netherlands; QFTGIT) or the newer QFT-GIT Plus measures the amount of IFN- γ released in response to *in vitro* stimulation of whole blood using enzyme-linked immunosorbent assay (ELISA). T-SPOT.TB (Oxford Immunotec, Marlborough, MA, USA) uses separated mononuclear cells from peripheral blood in an enzyme-linked

immunospot (ELISpot) assay to count the number of IFN- γ producing cells⁴². Both techniques have the advantage of measuring responses to antigens specific to *Mtb*, namely early secreted antigenic target 6 (ESAT-6) and culture filtrate protein 10 (CFP-10), which are encoded from the RD1 region of the *Mtb* genome that is absent in BCG and most environmental mycobacteria⁴³. Therefore, the specificity of IGRA is highly increased in comparison to the TST. Still, the inability of IGRA to differentiate latent tuberculosis infection from active disease⁴⁴ led WHO not to endorse their use in countries with a high burden of TB and replacement of TST by IGRA is not recommended in middle-to-high incidence settings^{34,42}.

Laboratory diagnosis of active TB currently relies on sputum microscopy and culture with subsequent drug-susceptibility testing to identify resistance. Sputum microscopy identifies *Mtb* acid-fast bacilli from sputum samples of a suspected pulmonary TB case. It remains the most commonly used test for TB, as it is a low-cost test which can be done in basic laboratories attached to primary health-care clinics. Sensitivity of the test ranges from 65% to 80% with multiple specimens⁴⁵. In many settings, the limited sensitivity of sputum microscopy is augmented by conventional diagnostic methods, such as clinical evaluation and chest radiography²⁵. Culture remains the gold standard for diagnosis of TB, with sensitivity greater than 80% and specificity reported to be as high as 98%⁴⁶. The use of solid culture medium is more cost-effective in resource-poor countries⁷, although the major limitation is the delay in obtaining results (> 3-4 weeks). The use of newer liquid-based culture systems (BACTEC-460 or BACTEC MGIT-960, Becton Dickinson, Maryland, USA) allows an automated and more rapid identification of *Mtb* within 10-14 days⁴⁷. A molecular diagnostic test called Xpert MTB/RIF assay could detect *Mtb* within 2 hours and allow identification of rifampicin resistance⁴⁸. The latter assay is currently

endorsed by WHO and could potentially replace microscopy as a first line diagnostic, despite being considered to be more sophisticated and expensive, and technical implementation of the assay in resource-limited settings also remains challenging⁴².

1.1.4 Treatment and Drug Resistance

The current treatment regimen for TB, in most parts of the world, is based on a WHO guideline which was published in 2010⁴⁹. The regimen consists of several first-line drugs, specifically isoniazid – H, rifampicin – R, pyrazinamide – Z, ethambutol – E and streptomycin – S in the case of drug-sensitive TB. For individuals with no history of previous TB treatment or who have received anti-TB drugs for less than 1 month, the regimen consists of 2 months of intensive phase treatment with isoniazid (INH), rifampicin (RIF), pyrazinamide (PZA) and ethambutol (EMB), followed by a 4-month continuation phase with INH and RIF [2HRZE/4HR]. The retreatment regimen for relapsed, treatment failed or treatment interrupted patients lasts for eight months and includes insertion of streptomycin injections in the first two months and administration of ethambutol throughout the treatment duration [2HRZES/1HRZE/5HRE]. LTBI can also be treated as a preventative measure in high risk groups, in which a regimen of INH for 6-9 months is recommended⁴⁹.

Resistance towards the two major first-line anti-TB drugs, INH and RIF, is referred to as multi-drug resistant TB, while further resistance against at least one of the fluoroquinolones and a second-line injectable anti-TB drugs is defined as extensively drug-resistant (XDR)-TB⁵⁰. The emergence of a type of TB resistant to virtually all available first- and second-line drugs termed totally drug-resistant (TDR)-TB has also been

reported in the past several years⁵¹⁻⁵³. Drug-resistant TB poses a further threat towards global efforts to control the disease. Approximately 490,000 cases of MDR-TB occurred worldwide in 2016 and XDR-TB has been reported in 123 countries¹¹. Treatment success rates of MDR-TB vary with only 50-60% success in most settings^{54,55}, while in the case of XDR-TB the success is only around 30%³. Various risk factors leading to the development of drug-resistant TB have been identified⁵⁶. Notably, the length of the standard, drug-sensitive regimen is often cited as responsible for low compliance of patients leading to unsuccessful treatment, eventually increasing the risk of the development of drug-resistance⁵⁷. In addition, it has also been proposed that inter-individual pharmacokinetic variability of a single drug in the regimen, leading to a sub-therapeutic level in the plasma, is a contributing factor in the development of drug-resistant TB⁵⁸.

In the context of MDR-TB, treatment is based on either a standard MDR regimen that is specific for each country or individually tailored regimen based on drug susceptibility testing⁴⁹. The treatment duration could last up to 24 months with administration of drugs with less certain efficacy, and includes poorly tolerated second-line injectable drugs in the first six months⁴⁹. In 2016, WHO recommended a shorter, standardised 9-12 month regimen for people with pulmonary MDR- or RIF-resistant TB susceptible to aminoglycosides and fluoroquinolones³. The 4–6-month intensive phase includes moxifloxacin, an injectable aminoglycoside, ethionamide or prothionamide, clofazimine, high-dose INH, EMB and PZA, and the 5-month continuation phase includes moxifloxacin, clofazimine, EMB and PZA. This regimen applies to non-pregnant patients, pulmonary TB cases and patients who have not undergone previous treatment with second-line drugs. The newer regimen was shown to have a comparable efficacy in

eligible patients compared to the individualised 20-24 months treatment³. More recently in August 2018, WHO introduced some further improvement to the MDR-TB regimen by creating a new priority ranking of the available drugs (Table 1) and introducing a fully oral regimen by the replacement of injectable agents, such as with bedaquiline⁵⁹.

Table 1. Summary of drugs used to treat TB with various susceptibility (adapted from Zumla *et al.*⁷ and WHO Guidance August 2018⁵⁹).

Drugs	Drug regimen
Standard regimen for drug-sensitive TB	6 months rifampicin and isoniazid supplemented by ethambutol and pyrazinamide in the first two months
Latent infection	6-9 months isoniazid
Multi-drug resistant TB	<p>Group A (Medicines to be prioritised): levofloxacin/moxifloxacin, bedaquiline and linezolid</p> <p>Group B (Medicines to be added next): clofazimine, cycloserine/terizidone</p> <p>Group C (Medicines to be included to complete the regimens and when agents from Groups A and B cannot be used): ethambutol, delamanid, pyrazinamide, imipenem-cilastatin, meropenem, amikacin (streptomycin), ethionamide/prothionamide, p-aminosalicylic acid</p>
Extensively-drug resistant TB	Use drugs that remains sensitive from the MDR regimen, including drugs with less certain efficacy in group C, as well as new drugs (i.e. delamanid)

Each of the anti-TB drugs possesses different mechanism of action⁶⁰. INH acts primarily by inhibiting cell wall mycolic acid synthesis. RIF interferes with RNA synthesis by binding to the bacterial DNA-dependent RNA polymerase β -subunit encoded by *rpoB* gene. PZA acts by depleting membrane energy potential and is active against tubercle bacilli at acid pH. EMB works by interfering the biosynthesis of arabinogalactan as a major polysaccharide of mycobacterial cell wall. EMB is the only first-line drug that

exerts bacteriostatic effect. Combined treatment of several drugs with different mechanism of actions is necessary due to the fact that populations of *Mtb* are not uniform in their susceptibility to antimycobacterial agent (Figure 3). Hence, it is crucial to treat with more than one drug to which the organisms are susceptible⁷.

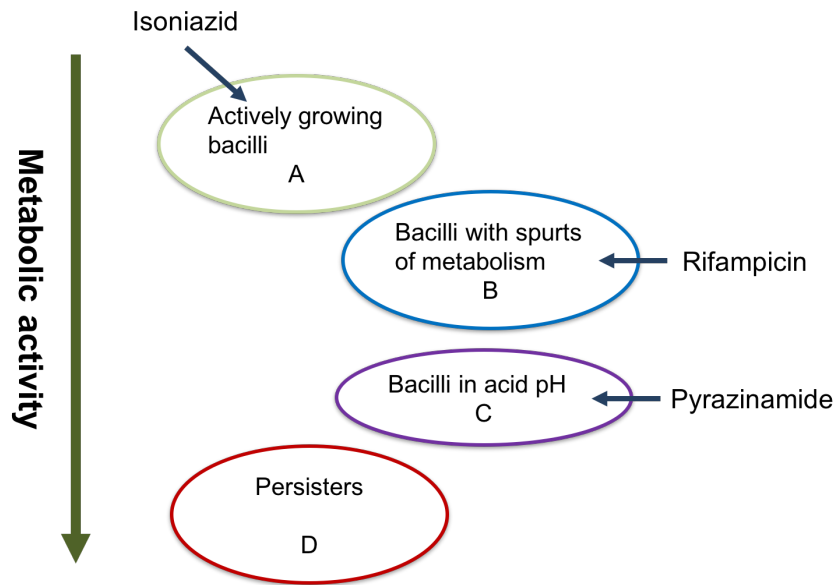


Figure 3. Bacterial subpopulations in TB treatment (taken with modification from Zhang⁶⁰).

Mutations in *katG* and *inhA* genes are the main cause of INH resistance. *katG* encodes multifunctional enzymes that exhibit both catalase-peroxidase and peroxy-nitritase activities, each of these considered important for activating INH prodrug and having a role in pathways involving reactive nitrogen as well as oxygen intermediates, respectively. The second main cause of resistance to INH is due to mutations in the promoter region of *inhA* and is typically more associated with low level INH resistance. *RpoB* is a target of RIF which catalyses the transcription of DNA into mRNA by using four ribonucleoside triphosphates as substrates. Conformational changes caused by mutations in *rpoB* can lead to RIF-resistance. Resistance to PZA is associated with *pncA*,

rpsA and *panD* genes. PZA resistance is most commonly due to mutations of *pncA* gene which encoded pyrazinamidase that converts the pro-drug PZA into active-form pyrazinoic acid. Mutations in *embB* and *embC* genes cause resistance against EMB, through restricting the action of drug to cease the biosynthesis of mycobacterial cell wall⁶¹.

The current standard 6-month therapy for TB has been used for more than 3 decades. Although the regimen provides 95% cure rates for drug sensitive TB⁶², it is still considered lengthy and has failed to accelerate current efforts to eliminate TB as a global health concern. Figure 3 further exemplifies the need for lengthy treatment in TB. Current TB chemotherapy is highly effective in reducing bacterial load and rendering the patients non-infectious after only a few weeks after the initiation of therapy⁶³. However, the therapy needs to be continued for a considerable amount of time due to the presence of persists bacteria⁶⁴. Although these dormant *Mtb* are regarded as genetically identical to actively replicating bacteria, they are not sensitive to anti-TB drugs thus not effectively targeted with the current regimen⁶⁴. It has been proposed that in their metabolically inactive state, there is less uptake and subsequent processing of drugs⁶⁵.

Improvement to currently available chemotherapy is needed. Two approaches have been tentatively identified for this purpose, either by developing a novel more effective drug or by enhancing the host immune response to augment treatment^{66,67}. Development of new TB drugs is appealing as some candidates are already in the pipeline⁶⁸. However, results from several recent phase 3 trials aimed at shortening treatment suggested that although introduction of novel drugs was associated with better sputum conversion rates at 2 months, long-term risks of relapse are not non-inferior compared to current regimens⁶⁹⁻⁷¹. Several modalities in enhancing the host immune response during TB

treatment have been proposed⁶⁶. Current knowledge in TB immunology needs to be translated into intervention in order to maximise the benefit for patients in clinical settings.

1.2 Tuberculosis Immunology: Roles of Immune Cells and Cytokines

Understanding TB immunology is essential for augmenting management and treatment strategies for patients. This importance is exemplified by the fact that the immune system is able to control *Mtb* growth in 90% of infected individuals⁷². Both the innate and adaptive arms of the immune system play crucial roles in controlling mycobacterial growth. The interaction of innate and adaptive components eventually determines the outcome of natural infections with pathogenic mycobacteria, which can range from early asymptomatic clearance to latent infection and clinical disease.

1.2.1 The Innate Immune Response to TB

The cells of the innate system recognise and respond to pathogens in a nonspecific way and provide immediate defence against pathogens. The major innate cell types involved in immune responses towards *Mtb* infection are macrophages, neutrophils, dendritic cells (DCs) and natural killer cells.

Macrophages

Following its transmission and upon reaching lung parenchyma, *Mtb* can be phagocytosed either by alveolar macrophages (AMs), dendritic cells, epithelial cells or neutrophils⁷³.

AMs are phagocytes that primarily take up *Mtb* and serve as a habitat for *Mtb* which have developed evasion mechanisms for phagocytic destruction⁷⁴. AM is a type of tissue-resident macrophage which is derived from blood monocytes. Inside AMs, *Mtb* may resist bactericidal actions by inhibiting phagolysosome function. Typically, macrophages acidify their phagosomes to pH 5.2 in order to kill the bacteria^{75,76}. Production of antimicrobial peptides such as cathelicidin, which is involving the vitamin-D-dependent pathway, as well as the release of nitric oxide (NO) are also considered essential mechanisms^{77,78}. By reducing recruitment of vacuolar H-ATPases, *Mtb* hampers the acidification process and thus enables *Mtb* to persist inside the phagosomal vacuole⁷⁶. Using this mechanism, mycobacteria prevent the phagosome from maturing, while also subsequently inhibiting trafficking to the lysosome, thus preventing phagolysosome fusion⁷⁹. Therefore, while AMs function as the first line defence against infection, they also provide the main reservoir for bacterial survival and replication. Additionally, AMs also act as antigen presenting cells (APCs) which provide recognition for initiation of an adaptive immune response²⁸.

Macrophages can be activated by two different pathways, each serving distinct functions. Classically-activated macrophages, commonly referred to as M1, are induced by immune signals such as from TLRs and by the cytokine IFN- γ . Conversely, alternatively-activated (nonclassical) macrophages, termed M2, are promoted in the absence of strong TLR signals, and induced by cytokines such as interleukin (IL)-4 and IL-13⁸⁰. In humans, CD14 and CD16 markers are used to distinguish the two distinct subsets of monocytes and macrophages. Classical CD14^{bright}CD16⁻ monocytes will subsequently develop into M1 macrophages, while nonclassical CD14^{dim}CD16⁺ monocytes are regarded to be the precursor of M2 macrophages^{81,82}. In mouse, a Ly6C marker is used to distinguish M1

and M2, represented by classical Ly6C⁺ and nonclassical Ly6C⁻ monocytes/macrophages, respectively^{81,83}. Traditionally, M1 macrophages are considered part of the host response against intracellular bacteria and involved in killing of *Mtb*, while M2 macrophages are associated with tissue repair and bacterial persistence³². However, a recent finding by Joosten *et al.* suggested that nonclassical monocytes can also produce CXCL10 or inducible protein-10 (IP-10), which was associated with reduced mycobacterial growth using an *ex vivo* assay system, and the observation was linked to the trained innate immunity mechanism⁸⁴.

Dendritic cells and neutrophils

The most effective role of antigen presentation to T-cells is played by dendritic cells²⁸. DCs and AMs express PRRs that bind molecules from *Mtb* leading to activation of the innate immune system⁷⁹. Once infected, dendritic cells migrate to regional lymph nodes, where they prime naïve T-cells and produce IL-12 leading to T-cell expansion and secretion of cytokines²⁹. Hence, the role of DCs is critical in bridging the innate and adaptive immune response. It has also been proposed that *Mtb* is capable of subverting DC function, leading to impaired T-cell responses, thus evading adaptive immunity⁸⁵.

On the other hand, neutrophils are less well studied than other immune components of the host response to *Mtb*, perhaps due to the difficulties in working with these cells⁸⁶. Optimum killing by neutrophils and other immune cells could halt the infection at an early stage, while inefficient killing allows the disease to progress⁸⁷. In a study of pulmonary TB contacts, it was identified that the risk of TB infection could be reduced with a higher number of neutrophils in the blood⁸⁸. Neutrophils influence the development of acquired immunity through the production of IL-12, monocyte chemoattractant protein and other

cytokines, which can attract T-cells and help their maturation⁸⁹. Conversely, the accumulation of neutrophils is seen in active TB patients where protective immunity is ineffective, and it has been proposed that such accumulation could limit the interaction between infected phagocytes and antigen-specific T-cells^{90,91}. The role of neutrophils is still complex and under investigation by researchers, but their contribution is perhaps essential in the early response against *Mtb*, while their build-up could be associated with loss of *Mtb* containment.

Natural Killer cells

CD3⁻CD56⁺ natural killer (NK) cells are granular innate lymphocytes possessing potent cytolytic capacity. As a component of the innate immune system, NK cells are capable of destroying cells that harbour persistent *Mtb* without prior sensitisation⁹². Direct mechanisms of control by NK cells are largely through secretory products namely perforin, granulysin and granzymes, as well as multiple membrane-bound death receptors that facilitate target directed lysis, such as NKp44 which recognises various *Mtb* cell wall components, including mycolic acids⁹³. Human NK cells exhibit the capacity to lyse *Mtb*-infected macrophages *in vitro*, and there is increasing evidence that highlights the importance of NK cell function during TB disease, especially when T-cell responses are suboptimal⁹⁴⁻⁹⁶. In newly-diagnosed pulmonary TB patients, decreased frequencies of NK cell subsets were observed, which had been associated with lowered expression of NKp30, NKp46 and IFN- γ . This suggests that their presence is required for effective containment of *Mtb*. Meanwhile, following anti-TB treatment, partial restoration of cytolytic capabilities of NK cells was achieved upon the reduction of mycobacterial load in the lung^{97,98}. In a recent study enrolling three independent longitudinal cohorts, the NK

cell frequency was also decreased in active TB patients and this was restored upon treatment in all cohorts⁹⁹.

While the majority of NK cells are cytotoxic, a considerable proportion of NK cells also produce cytokines, which is a typical feature of other lymphocytes of the adaptive immune system⁹². NK cells can produce IFN- γ and IL-22, which inhibit intracellular growth of *Mtb in vitro* by enhancing phagolysosomal fusion, and can also promote the production of IFN- γ from CD8 T-cells by stimulating IL-15 and IL-18 production from *Mtb*-infected monocytes^{100,101}. In humans, NK cells are distinguished by varying expression levels of CD16 and CD56, which can be used to discriminate two different subpopulations of NK cells. CD56^{dim}CD16⁺ cells are considered cytotoxic NK cells which have high cytotoxic activity, while CD56^{bright}CD16^{+/-} cells are regarded as cytokine-producing NK cells that have less lytic activity, but could produce cytokine upon stimulation⁹⁶. As NK cells do not express CD4 or CD8, they are also sometimes known as triple negative (TN) cells (CD3⁻ CD4⁻ CD8⁻)¹⁰². Although for many years the role of NK cells has been attributed to their cytotoxic properties, cytokine production is also an essential function which could place these cells as key orchestrators and regulators of innate and adaptive immunities. Along with IFN- γ and tumour necrosis factor (TNF)- α which are the signature of Th1-type cytokines, NK cells can produce IL-2 to promote T-cell proliferation after clustering in multicellular groups^{96,103}.

1.2.2 The Adaptive Immune Response to TB

The adaptive immune response against TB consists of both humoral and cell-mediated arms. Most of the cellular functions are carried out by the T and B lymphocytes, which

have extremely diverse and clonally specific repertoires, generated by gene rearrangement during their development.

1.2.2.1 Cellular Immune Response

1.2.2.1.1 Conventional T-cells

Mtb is an intracellular pathogen thus the cell-mediated immune response is often regarded to play a dominant role²⁹. T lymphocytes that express an $\alpha\beta$ T-cell receptor (TCR), as well as a co-receptor CD4 or CD8, are considered conventional T-cells¹⁰⁴. CD4⁺ T lymphocytes or T-helper (Th) cells which are major histocompatibility complex (MHC) class II restricted, are able to polarise into several subsets of cells upon activation and stimulation. CD4 T-cells have been shown to be important for the control of *Mtb*, as HIV patients are highly susceptible to TB, with a correlation between decreasing CD4 count and increased susceptibility as well as HIV disease progression¹⁰⁵. Secretion of chemokines, such as C-C motif ligand (CCL) 2, CCL3, CCL5 and TNF- α by infected macrophages, attracts T-cells to the site of infection¹⁰⁶. Each subset of CD4 T-cells produces distinct cytokines with different roles and functions, with the 4 main notable subsets being Th1, Th2, Th17 and Treg.

Th1 cells produce IFN- γ upon IL-12 stimulation by activated DCs and macrophages, and are considered central in control of *Mtb* (Figure 4). Mutations in the IFN- γ and IL-12 receptors have been shown to highly increase the susceptibility to mycobacterial infection in humans¹⁰⁷. Mice, in which the gene for IFN- γ has been knocked out, also become very susceptible to TB^{108,109}. IFN- γ promotes macrophage activation by inducing NO-dependent apoptosis, reviving phagosomal maturation and modulating autophagy¹¹⁰. In

addition, activated macrophages also become more bactericidal through increased production of reactive oxygen and nitrogen intermediates¹¹¹. Th1 cells also produce TNF- α that plays a role in the formation and maintenance of granulomas¹¹². Administration of anti-TNF antibodies causes activation of latent TB infection in rheumatoid arthritis patients¹¹³. In addition, Th1 cells produce IL-2 which is essential for T-cell proliferation¹¹⁴. T-cells which are capable of making IFN- γ , TNF- α and IL-2 are termed multifunctional or polyfunctional T-cells.

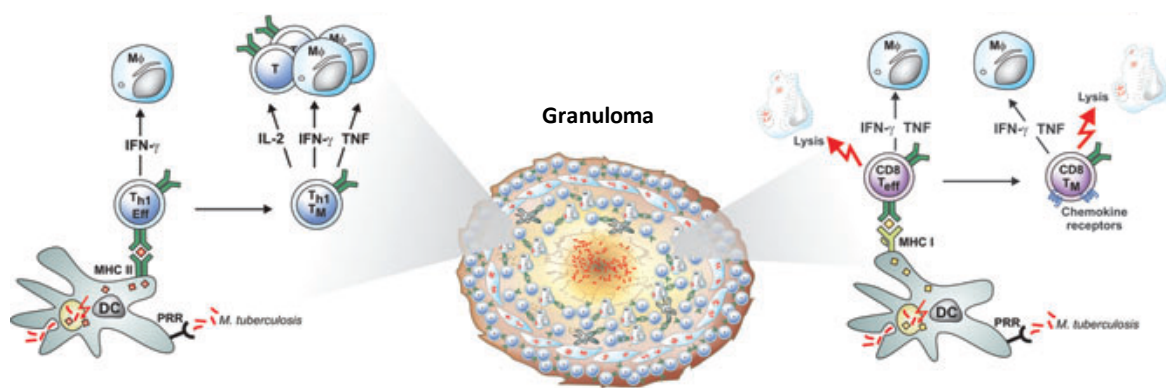


Figure 4. Cellular adaptive immune response in TB (modified from Kaufmann⁷⁴). Essential cytokines produced by important subsets of T-cells are denoted. In addition, several lymphocytes, including CD8 T-cells, are also capable of lysing *Mtb* infected cells (shaded illustration).

Th2 cells produce IL-4, IL-5, IL-10 and IL-13 which promote a humoral immune response but counter-regulate the Th1 response⁷³. In humans, active TB is associated with reduced Th1 and increased Th2 activity with upregulation of IL-4¹¹⁵. The effect of IL-4 is counterbalanced by its antagonist, IL-4 δ 2, and healthy individuals who successfully controlled LTBI were shown to express high levels of Th1 cytokines and IL-4 δ 2¹¹⁶. Helminth infection has been associated with reduced immunity towards *Mtb* due to an increased Th2 response²⁸, and reduced protection by BCG vaccination was linked to

elevated IL-4 and IL-5 in mice infected with *Schistosoma mansoni*¹¹⁷. Th17 cells produce IL-17, IL-21 and IL-22 that are involved in early host defence by recruitment of macrophages and neutrophils to the site of infection¹¹⁰. While IL-17 deficient mice were shown to succumb from infection by a hypervirulent strain of *Mtb*, they could still survive infection with less pathogenic strains¹¹⁸. On the other hand, excessive IL-17 production can lead to tissue damage due to extensive neutrophil recruitment¹¹⁹.

CD4⁺CD25⁺Foxp3⁺ Treg cells are characterized by TGF- β and IL-10 production and can inhibit other subsets of CD4 T-cells²⁸. Although the role of Treg cells could be beneficial in limiting excessive inflammation, an increased number of Treg cells are observed in active TB patients with high bacterial burden²⁹. IL-10 is an immunoregulatory cytokine which is a potent suppressor of macrophage activation and may also inhibit the recruitment of T-cells to the lung by suppressing the expression of recruiting chemokines¹²⁰. Certain mouse strains that produce more IL-10 are known to be naturally more susceptible to *Mtb* infection¹²¹. MHC class I-restricted CD8 T-cells also play a major role in immune response against TB, by secreting perforin and granulysin and lysing *Mtb* infected cells. CD8 T-cells also produce Th1 type cytokines⁷². Through a cross-presentation mechanism by APCs, mycobacterial antigens could access the class I MHC pathway and initiate responses by CD8 T-cells²⁹. Following primary infection, most effector T-cells will die upon pathogen clearance and the remaining 10% that survive are known as memory T-cells. These long-lived cells have high sensitivity to specific antigens and will provide a more rapid and robust response following a secondary encounter with the same antigen³².

In the context of *Mtb* infection, many of the above mentioned innate and adaptive immune cells will contribute to the formation of an organised structure known as the granuloma

(Figure 4). Granulomas are formed primarily by recruited macrophages which surround *Mtb*-infected macrophages, interspersed with recruited neutrophils and are encircled by a lymphocyte cuff, consisting of T-cells and B-cells³². The function of the granuloma is to wall off the pathogen and limit the spread of *Mtb*. While at the same time, a granuloma also provides a ‘secured’ environment for *Mtb*, allowing them to persist in a dormant state for many years¹¹².

1.2.2.1.2 Unconventional T-cells

Unconventional T-cells comprise those lymphocytes that express $\gamma\delta$ TCR and typically reside in an epithelial environment, including the respiratory tract. Another subset is the natural killer T (NKT) cell, which has phenotypic and functional capacities of conventional T-cells, as well as features of NK cells (cytolytic activity). NKT cells recognise glycolipids when presented in the context of CD1d. Unconventional T-cells have a more limited TCR repertoire in the form of cells expressing either an alternative $\gamma\delta$ TCR, or a non-diverse $\alpha\beta$ TCR in the context of NKT cells^{122,123}. The roles of $\gamma\delta$ T-cells in protection against TB include phagocytosis, cytotoxicity and induction of maturation of DCs¹²⁴. The $\gamma\delta$ T-cells are also the main source of IL-17¹²⁵, and human $\gamma\delta$ T-cells activated *in vitro* by phosphoantigens are capable of inducing maturation of DCs. They also possess phagocytosis capability similar to innate immune cells such as neutrophils, monocytes and DCs¹²⁶. In addition, a smaller subset of $\alpha\beta$ T-cells which do not express either CD4 or CD8, termed double negative (DN) T-cells (CD3⁺CD4⁻CD8⁻), also produce IFN- γ together with CD4 T-cells, NK cells and $\gamma\delta$ T-cells following BCG vaccination in infants¹²⁷.

CD1-restricted NKT cells, which can recognize lipid of mycobacteria, are also thought to be involved in protection against *Mtb*²⁹. Among NKT cells, type I or invariant NKT (iNKT) cells are the most well studied, and these cells are known to carry preformed IFN- γ mRNA in their cytoplasm, allowing rapid secretion of the cytokine upon stimulation¹²³. Furthermore, iNKT cells are also thought to play roles in inducing maturation of DCs as well as facilitating cross-presentation of soluble antigens, leading to increased priming of CD8 T-cells¹²². In active TB patients, the frequency of iNKT cells is lower compared to healthy uninfected controls¹²⁸. The importance of these unconventional T-cells remains to be further explored in TB. Nevertheless, they could potentially be targeted for vaccination or treatment of the disease.

1.2.2.2 Humoral Immune Response and B-cells

Antibodies as the central component of adaptive humoral immune response are produced by B-cells. Upon recognition of antigens by naïve B-cells, they will differentiate into antibody-secreting plasma cells. Earlier studies have supported a protective role for antibodies against *Mtb*, despite mycobacteria being intracellular pathogens. A higher titre of immunoglobulin (Ig)G specific to mycobacterial antigen has been associated with improvement upon treatment in adults with pulmonary TB and prevention of disseminated TB in children^{129,130}. Maturation of antibody-producing cells is governed by a Th2 response which also favours production of neutralising antibodies, while Th1 cells mediate class-switching towards opsonising antibodies⁷⁴. Opsonising antibodies are particularly important in enhancing phagocytosis of extracellular *Mtb*, thus they may provide protection by preventing dissemination of *Mtb* and any further progression of the disease¹³¹. In addition, B-cells can assist the cellular immune response by serving as

antigen presenting cells which influence T-cell activation, polarisation and effector functions and the establishment of T-cell memory¹³². In lung granuloma, B-cells contribute as a cellular component which can process and present antigen to T-cells, secrete antibodies and modulate inflammation through the production of IL-10^{32,120}.

Mice lacking B-cells exhibit suboptimal anti-tuberculous immunity associated with exacerbated pulmonary pathology in acute *Mtb* infection¹³³. On the other hand, human plasmablasts and memory B-cells are elevated in *Mtb*-infected compared to uninfected individuals¹³⁴. Revisiting the role of B-cells and antibody may lead to better understanding of the mechanisms underlying the host response to *Mtb* infection in order to generate better intervention strategies against TB.

1.2.3 Trained innate immunity

During the last half century, it has been widely believed that innate immunity does not possess immunological memory, which was considered specific for the adaptive immune response. However, in the past few years, increasing evidence has indicated that some innate immune cells can build immunologic memory by adapting to previous exposure to vaccination, pathogen or microbial components¹³⁵. This phenomenon is termed “trained innate immunity”. To date, it has been mainly characterised in monocytes and NK cells, which can produce increased amounts of pro-inflammatory cytokines and display higher levels of surface activation markers in response to restimulation with different unrelated microorganisms or toll-like receptor ligands¹³⁶⁻¹³⁹. β -Glucan, a major cell wall component of *Candida albicans*, as well as the BCG vaccine are known to be able to induce trained immunity. β -Glucan and BCG induce trained immunity in monocytes via PRRs dectin-1

and NOD2 respectively, leading to enhanced signalling of the Akt (protein kinase B)-mTOR (mammalian target of rapamycin)-hypoxia-inducible factor-1 α pathway^{136,140}. Moreover, induction of trained immunity is achieved by epigenetic modifications and metabolic changes.

Histone modification with chromatin reconfiguration in monocytes has been shown to be a central mechanism of trained immunity and can influence long-term transcriptional regulation¹³⁶. Such changes are linked with a metabolic shift from oxidative phosphorylation toward aerobic glycolysis, thereby increasing the capacity of innate immune cells to respond to stimulation¹³⁹. In NK cells, BCG is also able to induce trained immunity through specific DNA methylation patterns as well as modulated cytokine responses in cytomegalovirus (CMV)-infected individuals^{138,141}. These changes lead to enhanced secondary response following re-exposure to both the same or unrelated stimuli. In addition, NK cells also possess antigen-specific mechanisms of immune memory, distinct to the trained immunity phenomenon, leading to an increased IFN- γ production upon re-exposure of the cells with same stimulus⁹⁶. This antigen-specific NK cell memory develops after exposure to cytokine combinations, such as IL-12, IL-15 and IL-18, which induce long-lived NK cells and recall responses independent of B-cells and T-cells¹⁴². The activated NK cells could then provide protection against reinfection by rapidly degranulating and producing cytokines^{96,141}.

1.3 Tuberculosis Vaccines

1.3.1 Bacillus Calmette–Guérin (BCG)

BCG remains the only licensed TB vaccine and has been in use since 1921¹⁴³. It was developed through over 230 successive *in vitro* subcultures of a strain of *Mycobacterium bovis* every 3 weeks for 13 years, until a non-pathological strain was obtained¹⁴⁴. WHO estimates that the vaccine is given to over 120 million children every year¹⁴⁵. It has been an important part of the Expanded Program on Immunization since the 1970s and has since been given more than 4 billion times¹⁴⁶.

BCG vaccination induces Th1 responses which are considered essential in protective immunity against TB, as was shown in multiple human and animal studies. Following BCG immunisation in infants and children, CD4 T-cell responses associated with IFN- γ expression, as well as cytotoxic activity were observed^{147,148}. BCG also induces DCs maturation and production of IL-12 that leads to Th1 differentiation¹⁴⁹. Activation of CD8 T-cells producing IFN- γ , TNF- α and perforin upon BCG vaccination has also been reported^{148,150}. In a study by Fletcher *et al.*¹⁵¹, the BCG-specific IFN- γ response measured with the ELISpot assay was associated with reduced TB disease risk over the following 1 to 3 years of life in South African infants. This immune response following BCG vaccination was predominantly polyfunctional CD4 T-cells response, with less contribution from antigen-specific CD8 T-cells. In mice, BCG vaccination was shown to increase Th1-type cytokine production in the lung from CD4 and CD8 T-cells following aerosol challenge with *Mtb* compared to unvaccinated mice^{146,152}. In a recent clinical trial by the Scriba group (2016)¹⁵³, protection after BCG vaccination in adults were not associated with CD4 or CD8 T-cells, but rather with IFN- γ -producing NK cells. In this

study enrolling 72 participants with LTBI, BCG vaccination was given after isoniazid preventive therapy.

Most published studies have reported good protection of BCG vaccination in infants and children against miliary and meningitis TB, two severe forms of the disease commonly affecting young children. In a systematic review by Mangtani *et al.* (2014)²⁷, BCG is associated with 85% reduction in the risk of meningeal and/or miliary tuberculosis in children. Pulmonary TB disease in children is rare and difficult to diagnose, although BCG may also protect children against childhood pulmonary disease^{27,154}. Despite this, among many trials and observational studies which have been conducted, the estimated BCG protection against pulmonary tuberculosis in adults ranges from 0 to 80%^{26,27}. In the UK, BCG was shown to provide a strong protective effect up to 80% in a trial conducted by the British MRC¹⁵⁵, while in some other countries such as India and Malawi, the vaccine provides no evidence of efficacy^{156,157}. There are several hypotheses for this variable protection demonstrated in clinical trials: geographical differences and prevalence of environmental mycobacteria between trial sites, genetic differences between trial populations, variable virulence of the *Mtb* strains encountered by the trial populations and differences between strains of the BCG vaccine¹⁵².

The systematic review by Mangtani *et al.* found the average BCG efficacy against pulmonary TB to be 73% at latitudes of $\geq 40^\circ$, while this figures were only 33% at latitudes of 20-40° and 13% at latitudes of 0-20°²⁷. This is consistent with greater exposure to the environmental mycobacteria in the warm and wet climates nearer the equator, which may cause masking or blocking to the effects of BCG vaccination¹⁵⁸. There are also some evidences showing that UK infants make stronger Th1-type responses, including IFN- γ , whereas Malawian infants make stronger Th2- and regulatory-type responses¹⁵⁹. Thus far,

the impact of different BCG vaccine strains has been inconclusive and the recent systematic review did not find evidence of such effect^{27,148}.

In places where BCG is protective, the duration of protection conferred by vaccination generally lasts up to 15 years, although studies conducted in Brazil and US (American Indians and Alaska Natives population) found that protection could last until 20 years and 50 years, respectively^{160,161}. The protection from BCG may wane overtime¹⁶², albeit analysis from participants of clinical trials of a TB vaccine candidate in the UK did not show waning of IFN- γ responses between 10 years and 30 years after BCG vaccination¹⁶³. In the UK, school-aged BCG vaccination was recently found to offer protection against TB for at least 20 years, which is longer than previously thought¹⁶⁴.

Furthermore, BCG is known to provide protection not only against TB, but also towards other pathogens and diseases not related to TB, known as the non-specific effect. It is perhaps not surprising that BCG could provide protection against leprosy and severe forms of Buruli ulcer, caused by *Mycobacterium leprae* and *Mycobacterium ulcerans*, respectively^{165,166}. However, BCG is also demonstrated to have a beneficial effect on reducing all-cause mortality in infants. A meta-analysis of three clinical trials conducted in West Africa on low birth-weight infants showed BCG administration reduced mortality by 38% within the neonatal period, due to a lower sepsis as well as respiratory infections not related to TB¹⁶⁷. Interestingly, these studies as well as some previous studies reported that the non-specific effect after BCG vaccination is more pronounced in females rather than males¹⁶⁸⁻¹⁷⁰. This may suggest that females respond better to BCG vaccination, as has also been observed with measles, influenza and vaccinia vaccines^{171,172}, although this sex-specific effect is yet to be demonstrated towards the prevention of adult pulmonary disease.

Trained innate immunity is considered to be the main mechanism behind the non-specific protective effect of BCG. Investigations by Kleinnijenhuis *et al.* in the past few years have revealed the mechanisms by which BCG could induce trained immunity. In a proof-of-principle trial in which BCG vaccine was given in healthy adult volunteers in The Netherlands, the vaccination led to enhanced release of monocyte-derived cytokines, including TNF- α and IL-1 β , in response to unrelated bacterial and fungal pathogens, such as *Candida albicans* (yeasts and hyphae), *Staphylococcus aureus* and *Eschericia coli* (LPS). In addition, immunodeficient mice lacking B- and T-cell function and vaccinated with BCG, also had better survival following challenge with candida infection compared to naïve mice (survival rate 100% and 30%, respectively)¹³⁶. The nonspecific protective effect of BCG has also been linked to NK cells. NK cells from BCG-vaccinated individuals have enhanced proinflammatory cytokine production (IL-6, TNF- α and IL-1 β) in response to mycobacteria and other unrelated pathogens, and studies in mice have shown that BCG confers nonspecific protection against candidiasis partially through NK cells¹³⁸. Isolated peripheral blood mononuclear cells (PBMCs) from BCG-vaccinated healthy adults also displayed long-lasting heterologous Th1 and Th17 responses upon restimulation with unrelated pathogens and TLR-ligands¹⁷³. More recently, Smith *et al.* demonstrated whole blood signatures of BCG-induced trained innate immunity in UK infants, which includes secretion of IL-6, epidermal growth factor, platelet-derived growth factor -AB/BB and NK cell activation¹⁷⁴.

Despite the extensive work which has been conducted to decipher the BCG mechanism of action, new TB vaccines are still needed as BCG only provides partial protection worldwide^{27,145}. Improving understanding of the mechanisms of protection induced by

BCG could aid the development of new vaccines. Introduction of new vaccines is indispensable by 2025 if we would like to achieve the WHO End TB target by 2035¹³.

1.3.2 Development of Novel Vaccines against TB

In the past 2 decades, considerable progress has been observed in the development of novel vaccines against TB. From a vaccine pipeline that was practically empty of candidates prior to 2000, there are currently 13 TB vaccine candidates in the clinical trial pipeline and dozens more in preclinical development¹⁷⁵. These candidates can be classified into several categories based on the proposed strategy and targeted population (Figure 5). Most TB vaccines in the pipeline are preventive vaccines, which aim to prevent the occurrence of TB infection and/or disease in healthy naïve individuals (pre-exposure) or in already infected individuals (post-exposure). The preventive vaccines can be in a form that aims to substitute BCG (BCG replacement) or to boost the immune response after priming with BCG (prime-boost strategy)^{176,177}.






Target populations	Infection/Disease	Vaccine type 	Advanced Candidates
Infant 	Uninfected	Preexposure/Preventive BCG replacement	rBCG: VPM1002 r-Mtb: MTBVAC
Infant 	Uninfected BCG	Preexposure/Preventive Prime-boost	Viral vectored: MVA85A/Aeras-485 Protein/adjuvant: H4:IC-31
Adolescent/ Adult 	LTBI/BCG (TST ⁺)	Postexposure/Preventive Prime-boost	Viral vectored: MVA85A/Aeras-485 Protein/adjuvant: M72:AS01 _E H56:IC-31 ID93:GLA-SE
Adolescent/ Adult 	Active TB	Therapeutic	Killed mycobacteria: <i>M. indicus pranii</i> <i>M. vaccae</i> RUTI

Figure 5. Vaccination strategies against TB targeting different stages of infection (taken from Weiner & Kaufmann¹⁷⁶).

VPM 1002 is a recombinant BCG vaccine candidate which has been developed based on the notion of improving access to the intracellular compartment by the insertion of a listeriolysin gene and the deletion of a urease gene, which would allow presentation to MHC class I molecules and enables better cross-priming for CD8 T-cells¹⁷⁸. MTBVAC is a recombinant *Mtb* manufactured by gene deletion of virulence factors which should ensure safety, while the presence of antigens found in human *Mtb* isolates in MTBVAC is expected to provide enhanced protection¹⁷⁹. These two vaccines are initially aimed to replace BCG by potentially providing superior protection. On the other hand, prime-boost vaccine candidates are expected to induce stronger immune responses after priming with BCG. Such vaccines could employ a viral vector system to express one or more *Mtb* antigens, or be formulated in a protein–adjuvant combination to present *Mtb* antigens as fusion proteins^{180,181}. MVA85A uses the viral vector system to deliver antigen 85A, a

highly conserved *Mtb* antigen, as well as several other candidate vaccines such as Ad5Ag85A, ChAdOx185A and TB/FLU-04L¹⁸². The use of viral vector systems is considered to induce high levels of antigen-specific CD4 and CD8 T-cells in individuals who have been primed by BCG vaccination or been exposed to environmental mycobacteria¹⁸³. Another type of prime-boost vaccine candidate uses adjuvanted subunit protein to deliver various *Mtb* antigens. H1, H56 and H4 candidate vaccines use the IC-31 adjuvant to deliver antigen 85B, with the addition of TB10.4 antigen for H4 vaccine and ESAT-6 as well as Rv2660c for H56^{184,185}. Two other vaccine candidates, namely M72 and ID93, use different adjuvants developed by their manufacturers, AS01E and GLA-SE respectively^{186,187}, to deliver *Mtb* antigens (hence their names, Figure 5). Adjuvants stimulate the immune system to make stronger responses to antigens, but do not directly induce immune responses themselves¹⁸⁸.

MVA85A is the pioneer sub-unit TB vaccine candidate to enter human trials and the first in infants since BCG was last tested. The results of MVA85A efficacy trial in infants were published in 2013. Even though the vaccine appeared to provide promising immunogenicity when tested in various pre-clinical animal models as well as in early phase human trials¹⁸⁹⁻¹⁹³, no significant efficacy was observed with MVA85A towards the prevention of TB disease in a trial enrolling 2,797 infants in South Africa¹⁹⁴. Nevertheless, the work from the MVA85A efficacy trial has resulted in several findings which provide important insights on immunology and correlates of protection following TB vaccination^{102,151,195}. H4:IC-31 vaccine was tested in a large phase 2 trial using a prevention of infection trial design. Although the preventive vaccine candidate showed some efficacy signals when given in adolescents previously primed with BCG at birth, the protection offered by H4:IC-31 was not superior compared to BCG given in

adolescents¹⁹⁶. More recently, M72:AS01E vaccine was shown to provide 54% efficacy against active pulmonary TB disease when given in latently-infected adults¹⁹⁷.

Therapeutic vaccination is a unique strategy compared to preventive vaccination which aims to combine vaccination with drug treatment (Figure 5). Such an approach is expected to enhance the effectiveness and shorten the duration of TB drug treatment, as well as to prevent or reduce the risk of TB relapse¹⁹⁸. This concept has gained much interest recently, due to the threat posed by drug-resistant TB, where drug treatment is less or no longer effective.

1.3.3 Therapeutic Vaccination for Tuberculosis

1.3.3.1 History of Therapeutic Vaccination in TB

An initial attempt of therapeutic vaccination for tuberculosis was conducted in 1884 by Robert Koch following his discovery of *Mtb*, when he inoculated active TB patients with tuberculin, a suspension of powdered *Mtb*¹⁹⁹. An exacerbated immune response termed a Koch phenomenon occurred following tuberculin administration. With present knowledge, it is possible that administration of *Mtb* antigens to already infected individuals resulted in a cytokine storm, such as by TNF- α , which would likely have been tissue-damaging and caused the harmful response attributable to the many deaths following tuberculin therapy^{200,201}. Such a phenomenon has been the main discouraging factor in the development of therapeutic vaccination for TB for many years, as the activated immune state during TB disease is considered perilous for the introduction of additional *Mtb* antigens by a vaccine. At that time, however, due to the unavailability of drug treatment, Koch administered tuberculin alone when mycobacterial load would have

been high. A recent study provided evidence that the occurrence of the Koch response is associated with bacterial load²⁰². Administering chemotherapy in advance could significantly reduce bacterial load and prevent the exacerbated immune response from therapeutic vaccination²⁰¹. More recent attempts to administer a pre-exposure vaccine in a therapeutic manner without initial chemotherapy also resulted in strong tissue toxicity resembling the Koch phenomenon^{203,204}.

Favourable results with tuberculin had been observed during the 1950s, in which tuberculin was administered in adjunct to chemotherapy²⁰⁵⁻²⁰⁷. In a study conducted in 1957, administration of tuberculin with para-aminosalicylic acid (PAS) and streptomycin as the only available TB chemotherapy at that time was associated with a better sputum conversion rate²⁰⁷. Similar studies were also conducted in TB meningitis patients, in which tuberculin administration was associated with improvement of clinical parameters^{205,206}. These results suggested that therapeutic vaccination could be safely implemented when administered with chemotherapy during TB treatment. Nevertheless, due to the discovery of a ‘highly effective’ chemotherapy in 1960 led by Sir John Crofton, attention was withdrawn from the initial successes of tuberculin²⁰⁸. With the current emergence of *Mtb* strains that are no longer susceptible to currently available TB drugs^{66,209}, the effectiveness of the chemotherapy has been challenged and an alternative modality apart from drug treatment is needed.

1.3.3.2 Current Concept and Candidates for Therapeutic Vaccination in TB

A concept of therapeutic TB vaccination has been reviewed by Prabowo *et al.* (2013)²⁰¹, in which a revisited approach is considered essential to allow implementation of therapeutic vaccination into current practice. Persister bacteria are responsible for the

lengthy treatment of TB and transcriptome analysis has shown that these bacilli may express different antigens termed latency antigens²¹⁰. Introduction of a latency antigen to overcome persisters *Mtb* could create further synergy between drugs and vaccines²⁰¹. For drug-sensitive TB, a therapeutic vaccine containing latency antigens could shorten the current regimen and prevent the occurrence of relapse, while it could potentially increase the low treatment success rate in the context of drug-resistant TB^{66,209}.

Several TB vaccine candidates are currently available in the pipeline and this has recently been systematically reviewed by Gröschel & Prabowo *et al.* (2014)²¹¹. Table 2 summarises the profile of these candidates. Among the candidates, the RUTI vaccine is considered a leading candidate based on the quality of the published clinical reports. The RUTI vaccine is composed of purified fragments of *Mtb* in liposomes grown under stress conditions which induces the expression of latency antigens²¹². The vaccine is purified to decrease the risk of the exacerbated immune response and fragmented to facilitate processing and presentation of cell wall antigens. The cell wall antigen preparation has an average size of 0.1 µm and exerts adjuvant properties^{212,213}. RUTI was specifically developed as an adjunct for treatment for TB, both in the context of active TB treatment and isoniazid preventive therapy for LTBI. The vaccine has completed a phase 2a trial and was shown to be safe and immunogenic when given after subsequent chemotherapy in latent TB patients with and without HIV co-infection²¹⁴. Previous pre-clinical studies in mice, guinea pig, goat and mini-pig have shown that RUTI was able to reduce bacterial load after chemotherapy and improve lung pathology compared to control²¹⁵⁻²¹⁸. A RUTI clinical trial in MDR-TB patients receiving chemotherapy is currently ongoing (NCT02711735).

Table 2. Profile of several therapeutic vaccine candidates for TB (taken from Gröschel & Prabowo *et al.*²¹¹)

Vaccine Candidate Name	Manufacturer	Route of Administration	Immune Response	Safety	Remark
<i>M. vaccae</i>	Immodulon, London	Intradermal, Oral	Promotes Th1 response	Only mild local reactions were observed	Multiple doses required
	Anhui Longcom, China	Intramuscular, Oral	Suppresses Th2 response		
RUTI	Archivel, Barcelona	Subcutaneous	Mixed Th1/Th2/Th3 response toward latency antigen	No hypersensitivity observed	Further study to ensure safety is required
<i>M. smegmatis</i>	Wuhan Institute of Biological Product, China	Subcutaneous	Two-way immune modulation function	Only mild local reactions were observed	Further larger studies required
<i>M. indicus-pranii</i>	Immuvac, Cadila Pharmaceuticals, India	Subcutaneous, Aerosol	Promotes Th1 response	No human infection has ever been reported	Aerosol administration may increase compliance
V5	Immunitor, Canada	Oral	Improved clinical parameters, attenuates TB-associated inflammation	No exacerbated immune response reported	The exact content remains to be further investigated

Mycobacterium vaccae is an older therapeutic vaccine candidate which has been tested in a large efficacy trial²¹⁹. A recent meta-analysis showed that *M. vaccae* provided some benefit in improving sputum conversion rate and radiographic healing, although a single dose of *M. vaccae* failed to provide protection when tested in a phase 3 trial²²⁰. Further genomic characterisation has shown that the *M. vaccae* strain used in the trial was actually *Mycobacterium obuense*²²¹. The use of multiple doses of *M. vaccae/ obuense* is probably needed when added to chemotherapy in TB. Another candidate is *Mycobacterium indicus pranii* (MIP) which was initially developed as a vaccine for leprosy, but has been retrospectively shown to be beneficial in TB co-infected patients²¹¹. In a large study

randomising 1,400 adults with pericarditis TB, MIP did not have a significant effect on morbidity and mortality of the disease when administered therapeutically²²². MIP is currently in preparation for a large efficacy trial in India as a preventive vaccine, in a head-to-head comparison with VPM1002¹⁷⁸. The next candidate is *M. smegmatis*, which in mice could promote Th1 and inhibit Th2 responses, thus resembling *M. vaccae*²¹¹. V5 is an oral therapeutic vaccine initially developed and approved for management of chronic hepatitis, with some evidence to suggest it may also protect against TB²²³. In addition to the above mentioned candidates, H56 as a fusion protein vaccine could also be considered a therapeutic vaccine. The presence of Rv2660c, a latency antigen, enables its application as a multistage vaccine and it has been shown in mouse and non-human primate models to effectively control reactivation of latent TB^{185,224}.

1.3.4 Preclinical Animal Models and Human Trials for TB Vaccine Testing

Animal models have been used extensively in the development of new TB vaccines, with the clear aim to demonstrate better protection compared to BCG prior to progressing to human clinical trials¹¹¹. Typically, the main indicator for testing the potency of new vaccine candidates in animal models is the reduction of the bacillary load in the lungs at the acute phase of the infection. While in human, protection is defined as prevention of TB disease and/or infection using clinical and diagnostic endpoints, and any individuals becoming infected are considered not protected²²⁵. Despite the difference, animal models are still regarded valuable as a ‘bridge’ between vaccine discovery and human testing. Murine models are currently the most widely used and characterised, perhaps due to the inexpensive and in-bred nature of the model, therefore allowing straightforward standardised adaptation between centres^{111,225}. Three murine models currently exist for

TB vaccines testing: 1) low dose aerosol, 2) murine latent TB and 3) intratracheal models²²⁶. The first model is also generally known as the ‘*in vivo Mtb* challenge model’, where a preventive vaccine candidate is expected to reduce bacterial load in the lung few weeks following a low dose *Mtb* challenge (~ 50 colony forming units [CFUs])²²⁷. The second model is developed to test therapeutic vaccine candidates, in which infection from a low dose aerosol is allowed to progress for 6 weeks or more, at which time antibiotic treatment is started for several weeks followed by vaccination, as an attempt to assess the impact of therapeutic vaccine on top of TB treatment. This model was notably used to test RUTI and H56 candidate vaccines^{185,215}. The intratracheal model involves inoculation of a high dose of *Mtb* and is less commonly used as it is considered not to reflect the natural history of TB infection²²⁸.

Several differences exist between murine models and humans in terms of *Mtb* infection. The largely used C57Bl/6 and Balb/c mouse strains do not develop similar granuloma when compared to human, and they also have a different distribution of TLRs^{111,225}. To overcome these issues, larger mammals can be used, such as guinea pigs and non-human primates (NHPs), with the latter being the closest species to humans²²⁶. However, the use of such mammals, especially NHPs, is very costly and requires advanced technical expertise, leading to only a few groups globally who are capable of conducting these experiments. In terms of cost, performing the murine latent TB model to test therapeutic TB vaccines is also considered expensive, as the experiment could last for over 20 weeks. Furthermore, there is an ethical consideration for performing animal experiments, as they endure suffering classified as moderate in severity during the study, while at the same time large numbers of animals may be required in order to reach statistical power²²⁹. Development of an *ex vivo* testing system, which could reduce the numbers of animals

used, or refine the experiment by negating the need of an *in vivo* challenge experiment, would be greatly appreciated.

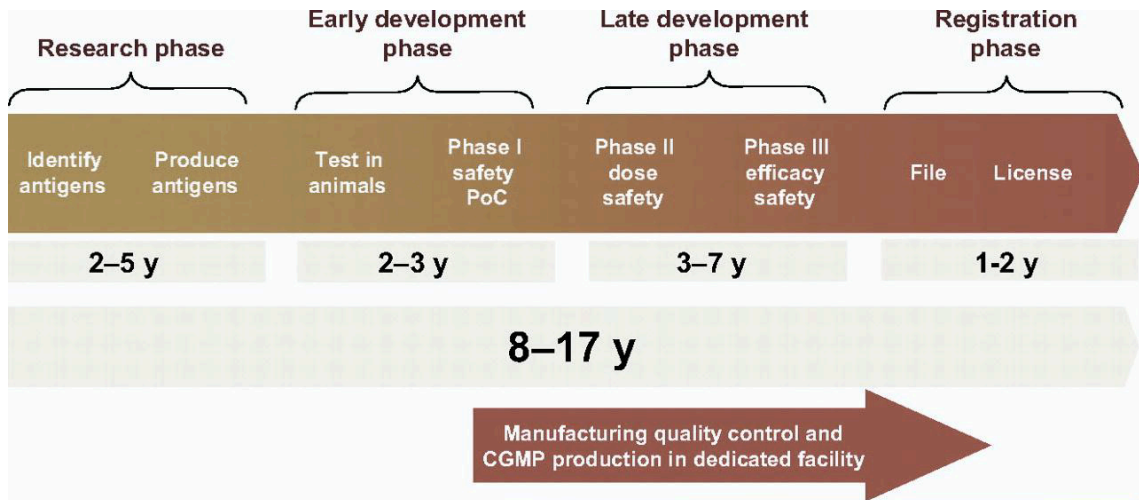


Figure 6. Pathway of licensure for a vaccine candidate (taken from Kanesa-Thanan *et al.*²³⁰).

In order for a TB vaccine candidate to be licensed, several stages of testing in humans known as clinical trials need to be conducted. A phase 1 clinical trial in TB vaccine development aims to assess safety in healthy volunteers and also to gain the first insight of vaccine immunogenicity. Further, in a phase 2 clinical trial, a vaccine candidate is tested in the target population. In a phase 2a study, typically optimum dose and route, immunogenicity and safety of a vaccine are assessed. In a phase 2b trial, efficacy as an outcome is assessed in addition to safety and immunogenicity. Lastly, a phase 3 study aims to demonstrate efficacy in a larger number of participants in target population, often in multiple trial sites with different settings. Following licensure, a post marketing surveillance known as phase 4 should also be performed^{175,230}. Figure 6 exemplifies the pathway of licensure for a vaccine candidate which could take up to a couple of decades from discovery. Currently, not less than US \$100 million per year of global investment

is dedicated for TB vaccine development at various stages²³¹. In the case of MVA85A, the efficacy trial itself costed US \$30 million and took 5 years to complete, yet showed no protection^{194,231}. The lengthy and costly clinical trials have emphasised the need for an immune correlate of protection following TB vaccination which could identify promising candidates in early pre-clinical or clinical development.

1.4 Immune Correlates of Protection

A biomarker is defined as “an objective characteristic that indicates a normal or pathogenic biological process, or a pharmacological response to a therapeutic intervention or vaccination”²³². Immune biomarkers or correlates of vaccine efficacy will substantially accelerate TB vaccine development by potentially reducing the need of lengthy and costly efficacy trials²³³. Biomarkers will be expected to be implemented to screen dozens of vaccine candidates currently available in the pipeline, by predicting the likely efficacy of these candidates and subsequently selecting the most promising candidates to progress to efficacy trials²³⁴. As exemplified by the case of MVA85A trial, it could take a decade or more to determine the efficacy for just one vaccine candidate²³⁵. Vaccine candidates should also be screened in the preclinical stage to determine which candidates should advance to human trials. Such screening efforts would be beneficial as well to find optimum doses for pre-clinical and clinical studies, especially in the case of therapeutic vaccination in which optimum combinations of vaccine and drug dose may need to be identified.

1.4.1 T-cell–based Signatures as Correlates of Vaccine-induced Immunity

IFN- γ has been extensively used as a marker of immunogenicity in TB vaccine experiments and human trials¹²⁶. IFN- γ is a robust cytokine, which is mainly produced by T-cells in large quantities and not easily degraded in culture or with storage, and its production can be measured by counting IFN- γ –secreting spot forming cells in an ELISpot assay, by ELISA or multiplex assay, or by using flow cytometry with intracellular cytokine staining (ICS)²³⁶. Despite this, there are discrepancies between studies towards the value of IFN- γ as a correlate of protection. In mice, although BCG vaccination induced protective T-cells *in vivo*, production of IFN- γ by these cells does not predict vaccine protection^{237,238}. In humans, a study by Kagina *et al.* (2010)²³⁹ found that measurement of polyfunctional T-cells, making IFN- γ , TNF- α and IL-2, in BCG-stimulated whole blood cultures from BCG-vaccinated infants at 10 weeks of age did not distinguish between infants who subsequently progressed to TB disease and those who remained healthy. However, in a more recent study by Fletcher *et al.* (2016)¹⁵¹, the frequencies of cells producing BCG-specific IFN- γ measured with ELISpot was associated with a reduced risk of developing disease, using the infants cohort of the MVA85A efficacy trial. Although both the Kagina and Fletcher studies were conducted in the same South African infant populations, the number of case infants in the latter study was almost double, with a higher number of controls per TB case infants (3 controls per case) and IFN- γ measurement was performed later in infants of the Fletcher study (4-6 months old). On the other hand, MVA85A also induced a modestly higher polyfunctional T-cells than BCG alone, and this did not translate into protection¹⁹⁴. Therefore, it is likely that IFN- γ production by conventional T-cells is necessary but insufficient to be used solely as a correlate of protection.

These findings have led researchers to look at other immune cell populations which could be associated with protection, such as $\gamma\delta$ T-cells, Th17, CD4⁻ CD8⁻ DN T-cells as well as NK cells^{126,240}. NK cells, in particular, are quickly recruited and secrete large quantities of IFN- γ and cytotoxic molecules following infection or vaccination^{241,242}. In this context, it is plausible to consider that immune protection from TB is a result of coordinated activities from multiple cells types and immune mechanisms, rather than exclusively from IFN- γ or CD4 T-cells. Gene expression analysis may help to identify which pathways contribute to protection, and transcriptomics has previously highlighted the role of neutrophils and type I interferons which were once overlooked⁹⁰. Yet, data analysis is complex and such technology is perhaps not readily applicable to resource-limited clinical trial sites. Consequently, an assay which could measure the summative effect of host immune responses following TB vaccination i.e. the ability of cells from vaccinated subjects to control the growth of mycobacteria *ex vivo*, would be of value and could allow a screening effort of vaccine candidates in early pre-clinical and clinical studies.

1.4.2 Mycobacterial Growth Inhibition Assays (MGIAs)

The mycobacterial growth inhibition assay (MGIA) is a functional assay which assess the ability of immune cells to kill or inhibit the growth of mycobacteria in an *ex vivo* system. Using intracellular inhibition of mycobacterial growth as a measure of vaccine potency, the MGIA is developed and expected to be able to predict clinical efficacy of TB vaccines, therefore allowing screening efforts in early phase of vaccine testing²⁴³. The MGIA involves co-culture of whole blood, human PBMCs or mouse splenocytes with mycobacteria, and subsequent measurement of mycobacterial growth inhibition, and thereby could also be regarded as an ‘*ex vivo* challenge model’.

In the past several years, many efforts have been focused on strengthening reproducibility as well as to standardise assays between laboratories, therefore allowing comparison of results between centres. Several groups have demonstrated the use of *ex vivo* MGIA in various different systems in human and animals in the past few decades (Figure 7), and this was recently reviewed by and Tanner *et al.* and Brennan *et al.*^{243,244}. Further application of the MGIA to screen TB vaccine candidates is justified and their use in TB vaccine clinical trials and pre-clinical animal testing should be considered by vaccine developers.

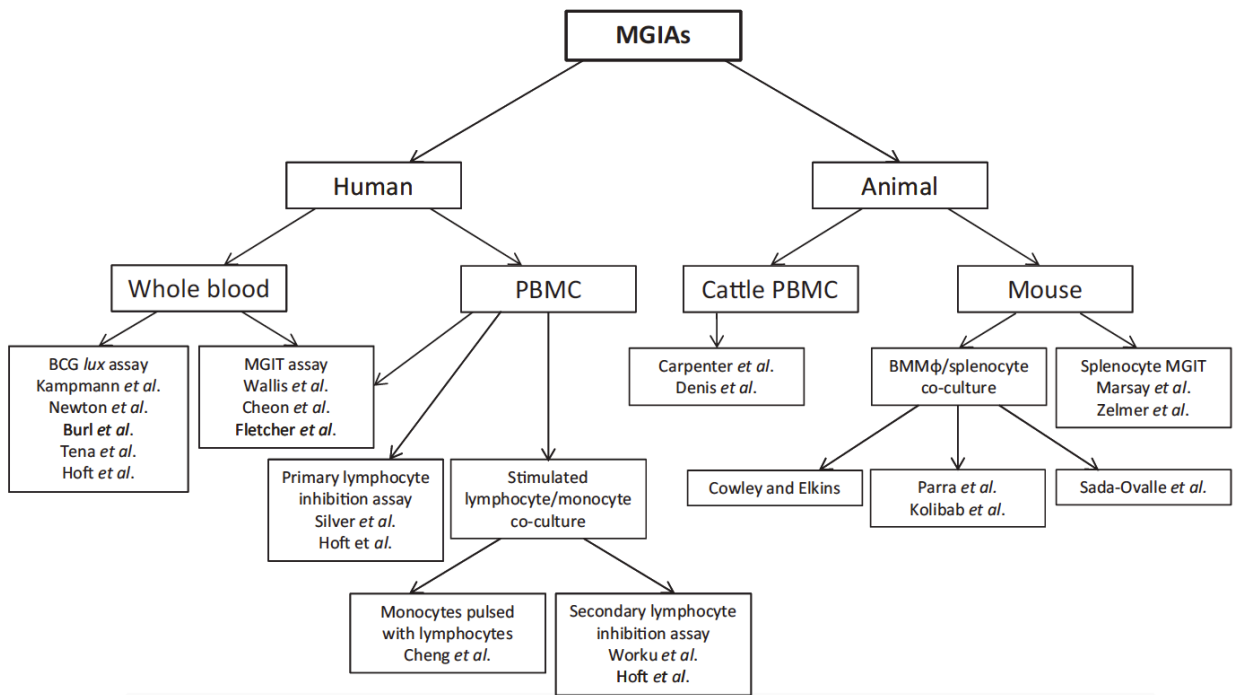


Figure 7. Classification of various MGIA's which have been developed for human and animal testing (taken with permission from Tanner *et al.*²⁴⁴).

1.4.2.1 Whole blood MGIA's

MGIA's can be performed using whole blood or PBMC samples from humans. In 2001, Wallis *et al.* established a whole blood MGIA to measure the bactericidal activity of anti-

TB drugs using the BACTEC mycobacterial growth indicator tube (MGIT) system²⁴⁵. The assay was then used to monitor drug treatment of active TB patients²⁴⁶. Around the same time, Kampmann *et al.* also developed a whole blood assay using BCG transfected with luciferase (BCG-*lux*) as a reporter²⁴⁷. In this context, both the MGIT and BCG-*lux* systems are used for quantification of mycobacteria. Cheon *et al.* applied the MGIT assay and found that both primary vaccination and revaccination with BCG in US adults enhanced *ex vivo* mycobacterial growth inhibition²⁴⁸. Using the BCG-*lux* system, enhanced growth inhibition was also observed following BCG vaccination in South African infants, and this capacity was impaired with HIV infection^{249,250}.

In 2013, Fletcher *et al.* implemented the MGIT-based whole blood MGIA alongside a PBMC-based adaptation. In the UK where primary BCG vaccination is known to have a high efficacy, primary BCG vaccination was associated with enhanced inhibition of growth, but not following revaccination²⁵¹. In this study, it was observed that a higher magnitude of mycobacterial growth inhibition was achieved with PBMC, rather than whole blood. Recently, it was discovered that the level of haemoglobin (Hb) and iron correlate with the *ex vivo* growth of mycobacteria²⁵², thereby denoting a confounding factor for the use of whole blood, as Hb levels may vary between study participants. Mycobacteria are known to be able to utilise haemoglobin as an iron source for metabolism²⁵³, hence a vaccine effect could be masked due to high growth in the presence of abundant iron. A study by the Scriba group (2017) also did not find differences in growth inhibition in children aged 4 to 12 years old, which epidemiologically is immune from developing TB disease (known as the ‘golden age’), as well as in LTBI subjects compared to uninfected individuals in South Africa using the whole blood MGIA²⁵⁴. While this could be due to universally high levels of mycobacterial sensitisation in this

high TB burden setting (through environmental mycobacteria and/or universal BCG vaccination) that could affect inhibition of mycobacterial growth, the impact of varying levels of Hb in their study participants also could not be excluded.

1.4.2.2 PBMC-based MGIAs

Silver *et al.* developed a system utilising low-level infection of isolated monocytes with *Mtb* H37Rv for 1 hour, followed by a 7 day culture either alone or with unstimulated autologous lymphocytes. This assay is termed the ‘primary lymphocyte inhibition assay’²⁵⁵. In addition, Worku *et al.* also established another assay, in which antigen-specific T-cells were expanded by stimulation prior to co-culture with infected monocytes, referred to as the ‘secondary lymphocyte inhibition assay’²⁵⁶. In 2002, Hoft *et al.* compared these two different PBMC-based assays head-to-head with the whole blood assay²⁵⁷, and found that BCG revaccination in midwestern US adults enhanced mycobacterial growth inhibition using the three assays, similar to the finding of Cheon *et al.*²⁴⁸. However, it was soon realised that both of the lymphocyte inhibition assays, which require separation of lymphocytes and monocytes as well as pre-culture, might not be suitable for field use and especially considering the small volumes of infant blood²³⁶.

The PBMC-based ‘direct’ MGIA as described by Fletcher *et al.*²⁵¹ is considered to provide technical simplicity for field implementation, and the use of PBMC would allow cryopreserving of samples from different time points in a vaccine study. The samples can then be analysed altogether upon completion of the study thus minimising the potential impact of batch variability. In addition, using PBMC allows for any natural variation in monocyte phenotype or frequency to be incorporated into the readout of the assay. In terms of distinguishing protection following BCG vaccination, the PBMC assay did not

detect enhanced inhibition of growth after BCG revaccination in a UK adult population, in contrast to the IFN- γ response measured with ELISpot which saw an increase following revaccination. While both assays detected increased response following primary vaccination, the PBMC-based MGIA is regarded to better reflect epidemiological data, in which BCG revaccination is considered not providing an additional benefit where primary BCG vaccination is known to be highly efficacious, such as in the UK^{27,258}. Later, Smith *et al.* found that BCG vaccination in UK infants enhanced *ex vivo* mycobacterial growth control using the PBMC-based assay and such control was correlated with a higher frequency of polyfunctional CD4 T-cells²⁵⁹. Most recently, Joosten and colleagues (2018) discovered that recent exposure with *Mtb* and BCG vaccination also enhanced the capacity of PBMC to control *ex vivo* mycobacterial growth by the role of nonclassical monocytes⁸⁴. This observation was associated with the trained innate immune mechanism, and has further supported the notion that an assay which can detect a comprehensive summative effect of both innate and adaptive host-immune responses, such as the PBMC MGIA, is needed.

1.4.2.3 MGIA in Preclinical Animal Models

MGIA assays have also been adapted for animal models to allow pre-clinical screening of TB vaccine candidates prior to further investigation in human studies. This would be particularly useful where there is a need to test vaccine candidates for antigen dose, adjuvant dose or antigen-adjuvant combinations, in which MGIA could save time, animals and funds. Thus far, the assays have been described using cells from mice²⁶⁰⁻²⁶³, cattle^{264,265} and non-human primates²⁵². Using the animal models, the MGIA outcomes

could be correlated with protection from *in vivo* challenges with *Mtb*, hence providing biological validation.

In mice, initially the MGIA was performed using infected macrophages cultured separately from mouse splenocytes, and then combined together. Using this MGIA, splenocytes from mice vaccinated with five different TB vaccines inhibited mycobacterial growth *ex vivo*, compared to naive controls²⁶⁰. Work by Marsay *et al.* in 2013 applied a murine splenocyte MGIA using the BACTEC MGIT system to develop a ‘direct’ splenocyte MGIA in order to simplify the assay and include the innate cell compartment. Splenocytes from BCG-vaccinated mice were better able to inhibit growth of mycobacteria compared to the naïve animals, and this *ex vivo* inhibition correlated with protection from *in vivo* challenge with *Mtb*²⁶¹. Further optimisation work by Zelmer *et al.*²⁶² found that detection of vaccine-induced inhibition could be improved by decreasing the multiplicity of infection (MOI) in the direct splenocyte MGIA. It was also demonstrated that the capacity to detect mycobacterial growth inhibition in BCG-vaccinated mice was time sensitive, with the peak of growth inhibition being detected at 6 weeks after vaccination in C57Bl/6 mice²⁶².

In general, the MGIA assay both in human and animals, employs a low MOI in the *ex vivo* system (~ 1 CFU/10,000 PBMCs or splenocytes) in order to prevent overwhelming of the vaccine effect. Performing a time course experiment in mice might also be necessary to identify the time point of the peak immune response when screening different TB vaccine candidates. Among different studies, it has been concluded that splenocytes are the most practical tissue to use, due to the small volume of blood in mice which impedes the use of whole blood or PBMCs. An adaptation of the direct *ex vivo* MGIA using murine lung cells is currently underway (Hannah Painter, personal communication).

It was also identified that splenocyte viability might pose as a problem in the direct splenocyte MGIA, and this was later improved in the work of Jensen and colleagues (2017) by enrichment of culture media and incubation without rotation²⁶³.

1.4.2.4 Immune Mechanisms of Growth Inhibition

Earlier works in humans using the lymphocyte inhibition assays have shown the contribution of CD4 and CD8 T-cells in mycobacterial growth inhibition, by the addition or depletion of these cell populations in the *ex vivo* culture system^{248,255,266}. Moreover, following BCG vaccination, IFN- γ was increased when cytokine production was measured in MGIA culture supernatant^{250,251,257}. However, in many of these studies, IFN- γ did not correlate with mycobacterial growth inhibition, supporting the notion that it is essential but could not be used a sole marker of protection. Interestingly, in one MGIA study, BCG vaccination was found to enhance *ex vivo* responsiveness of $\gamma\delta$ T-cells to mycobacteria, and this was achieved through granzyme A production from a subset of $\gamma\delta$ T-cells, namely $\gamma_9\delta_2$ T-cells, in a TNF- α -dependent manner^{266,267}. Moreover, NK cells isolated from the primary lymphocyte inhibition assay were also shown to enhance inhibition of intracellular *Mtb* growth in an apoptosis-dependent manner²⁶⁸.

IgG antibody responses to arabinomannan increased significantly following BCG vaccination in humans, with phagocytosis and intracellular growth inhibition being enhanced when mycobacteria were opsonised with post vaccination sera, and these enhancements were correlated with the IgG titres²⁶⁹. A higher proportion of monocytes to lymphocytes (ML ratio) is associated with increased mycobacterial growth and altering the ML ratio *in vitro* also affects the control of mycobacterial growth²⁷⁰. In addition, trained innate immunity has also recently been discovered to play a role in mycobacterial

growth inhibition, with non-classical CD14^{dim} monocytes being associated with enhanced growth control following recent *Mtb* exposure and BCG vaccination⁸⁴. In the latter study employing direct PBMC MGIA, several cytokines previously identified as associated with trained immunity, such as TNF- α , IL-1 β and IL-6, were elevated in the culture supernatants of individuals with superior mycobacterial growth control. Moreover, Joosten *et al.* also identified CXCL10, CXCL9 and CXCL11 as additional cytokines associated with trained immunity based on their study⁸⁴.

In mice, IFN- γ appears to play a more dominant role as demonstrated by Marsay *et al.* with the direct splenocyte MGIA, in which IFN- γ mRNA expression was significantly correlated with mycobacterial growth inhibition²⁶¹. This may be due to the in-bred nature of mice, in contrast to humans. The positive impact of CD4 and CD8 T-cells when added to murine splenocyte co-culture has also been demonstrated²⁷¹. Interestingly, in a recent murine study by Jensen *et al.*, IFN- γ production measured in the MGIA supernatant was also correlated with growth inhibition following immunisation with a vaccine candidate (H56), but the cellular source could not be identified from the measured vaccine-specific T-cells. This suggests that other cells, such as NK cells, may produce IFN- γ which could enhance growth inhibition. In summary, these studies of various immune pathways have shown that the MGIA could more broadly represent complex host-pathogen interactions and may be a more accurate surrogate of protective immunity, when compared to measurement of a single cytokine.

1.4.2.5 The BACTEC Mycobacterial Growth Indicator Tube (MGIT) System

Quantification of bacterial count for the MGIA can be performed using several methods such as quantification of BCG-*lux*^{247,250}, CFU counting of infected monocytes²⁵⁵⁻²⁵⁷ or the

BACTEC MGIT system^{245,246,248,251,272}. Use of the MGIT system allows an automated quantification of mycobacteria with a greater dynamic range compared to culture on solid media and with less variability²⁷³. The BACTEC MGIT system was initially developed to detect mycobacteria in human clinical samples. The system uses tubes that contain modified Middlebrook 7H9 liquid broth medium. The MGIT tube contains an oxygen-quenched fluorochrome at the bottom that acts as a sensor towards depletion of the free oxygen level upon growth of mycobacteria. A decrease in oxygen level leads to disinhibition of the fluorochrome leading to a fluorescent colour under UV light. This change is recorded in the MGIT instrument by computer algorithm as time to positivity (TTP) measured in hours²⁷⁴. A positive MGIT tube typically contains $10^5 - 10^6$ CFU per ml of medium²⁷⁴. The TTP value has been shown to correlate well with the actual CFU count in culture samples²⁷⁵. In the instrument, MGIT tubes are incubated at a temperature of 37° C and monitored for increasing fluorescence every 60 minutes²⁷⁴.

1.5 Project Structure

1.5.1 Rationale of the Study

Several therapeutic TB vaccine candidates have been developed and are currently progressing through the TB vaccine pipeline. It is hypothesised that the ability of a therapeutic vaccine to enhance capacity to control mycobacterial growth can be measured *ex vivo* and that a vaccine effect will still be observed even in the presence of TB drugs. This study will implement the MGIA to investigate the impact of vaccination with BCG in humans and mice, as well as immunisation with the RUTI vaccine in the mouse model, in the absence and presence of TB drugs *ex vivo*. To our knowledge, no other studies have

used the *ex vivo* MGIA system to assess therapeutic TB vaccine candidates and none have assessed vaccine-induced growth inhibition in the presence of drugs. The results of this study will provide information for TB vaccine researchers regarding the value of MGIA as a screening tool for therapeutic TB vaccine candidates.

1.5.2 Hypothesis

Immunisation with therapeutic tuberculosis vaccines enhances the ability of immune cells to control the growth of mycobacteria, in the absence and in the presence of TB drugs and this effect can be measured *ex vivo* in a growth inhibition assay. Further, the growth inhibition assay can be used to gain insight into the immune pathways important for the control of mycobacterial growth.

1.5.3 Study Aims and Objectives

The aims of the study are:

1. To a) establish a human cohort of healthy, previously BCG immunised and BCG naïve individuals to be able to assess the impact of historical BCG vaccination on mycobacterial growth inhibition. To b) use frozen PBMC from this cohort to investigate if *ex vivo* mycobacterial growth inhibition can still be observed when cells are co-cultured with TB drugs.
2. To use the mouse model to determine the impact of recent vaccination with BCG and with the RUTI vaccine towards *ex vivo* control of mycobacterial growth, in the absence and presence of TB drugs.

3. To assess the impact of individual-level factors and immune cell phenotype on immunity following historical BCG vaccination in a human cohort of healthy, previously BCG immunised and BCG naïve individuals.
4. To elucidate the immune mechanisms underlying vaccine-induced mycobacterial growth control both in humans and the mouse model.

The objectives of the study are:

1. To establish a human cohort with sufficient statistical power to be able to assess the impact of historical BCG vaccination on mycobacterial growth inhibition.
2. To optimise and implement *ex vivo* growth inhibition assays using human PBMCs and mouse splenocytes for testing therapeutic TB vaccine candidates.
3. To identify optimum drug concentrations for assessing the therapeutic effect of first line TB drugs (INH and RIF) using the growth inhibition assay.
4. To explore essential immune mechanisms for protective immunity using ELISpot and ELISA to identify cytokine production, as well as using flow cytometry with surface staining and/or intracellular cytokine staining to characterise immune cell phenotype.
5. To assess the impact of sex, CMV-specific response and immune cell phenotype on *ex vivo* growth inhibition in humans following historical BCG vaccination.

1.5.4 Thesis Structure

The overarching theme of this thesis is the use of mycobacterial growth inhibition assay as a potential platform to test therapeutic TB vaccines *ex vivo*. This thesis is divided into

6 chapters, of which 4 chapters will describe the results and discuss the main findings from the PhD project, mainly in manuscript style in accordance with the research paper style thesis format. As has been elaborated, **Chapter 1** presents a literature review of the topic of this thesis as well as outlining the project structure.

In **Chapter 2**, the combined effect of historical BCG vaccination and TB drugs is demonstrated for the first time using the *ex vivo* MGIA system in a cohort of adult, healthy volunteers. This study provides proof-of-principle that immune mediated mycobacterial growth inhibition can be observed and measured in the presence of two major first-line TB drugs, which is considered an essential first-step to further expedite the development of MGIA as a screening tool for therapeutic TB vaccines. Data discussed in this chapter indicates that the efficacy of INH can be augmented following historical BCG vaccination, which supports findings from previous observational and animal studies. The observation also suggests a role for NK cells in the combined effect between BCG vaccination and INH.

The impact of RUTI vaccination in the mouse model is discussed in **Chapter 3**, in which for the first time the vaccine was shown to inhibit the growth of mycobacteria *ex vivo* in a time course experiment. The nature of the *ex vivo* assay does not require the immune mechanism that underlies growth control of a vaccine candidate to be known *a priori*, while in turn could help to determine underlying mechanisms by investigating immune factors in samples with efficient growth inhibition. The data in this chapter show that RUTI vaccination induces a shift towards nonclassical monocytes phenotypes which is associated with enhanced growth inhibition. This finding suggests that RUTI has an important impact on the myeloid compartment which has not previously been identified. This demonstrates the value of assays such as the MGIA which assess changes in the

innate myeloid compartment as well as changes in adaptive immunity following vaccination.

Chapter 4 will discuss the impact of individual-level factors on *ex vivo* mycobacterial growth inhibition in a cohort of healthy, adult volunteers. Specifically, it was found that immune cells phenotype, cytomegalovirus-specific response and sex have impacts on immunity following BCG vaccination, reflecting epidemiological data and previous human studies. Although this chapter does not directly address the therapeutic vaccination strategy, it provides important insights into the factors that influence mycobacterial growth inhibition which may need to be considered if using this assay in the context of clinical trials. This is important as vaccine developers will need to understand the factors which may confound their ability to observe a vaccine effect when they move from pre-clinical to clinical studies.

In **Chapter 5**, several unpublished pilot investigations and preliminary methodology development data sets will be described and discussed, such as the impact of BCG vaccination and RUTI towards *ex vivo* drug-mediated killing in the mouse model, as well as our early optimisation work with the MGIA in human and mouse. Finally, **Chapter 6** will integrate the discussion of the three discrete yet related investigations as well as the unpublished data to give answers to the problems posed in the present chapter.

References

1. Keshavjee S, Farmer PE. Tuberculosis, drug resistance, and the history of modern medicine. *N Engl J Med* 2012; **367**(10): 931-6.
2. Paulson T. Epidemiology: A mortal foe. *Nature* 2013; **502**(7470): S2-3.
3. Tiberi S, du Plessis N, Walzl G, et al. Tuberculosis: progress and advances in development of new drugs, treatment regimens, and host-directed therapies. *Lancet Infect Dis* 2018; **S1473-3099**(18): 30110-5.
4. Frieden TR, Sterling T, Pablos-Mendez A, Kilburn JO, Cauthen GM, Dooley SW. The emergence of drug-resistant tuberculosis in New York City. *N Engl J Med* 1993; **328**(8): 521-6.
5. World Health Organization. Tuberculosis: A Global Emergency. *WHO, Geneva*, 1994.
6. Herbert N, George A, Masham of Ilton B, et al. World TB Day 2014: finding the missing 3 million. *Lancet* 2014; **383**(9922): 1016-8.
7. Zumla A, Raviglione M, Hafner R, von Reyn CF. Tuberculosis. *N Engl J Med* 2013; **368**(8): 745-55.
8. Harries AD, Zachariah R, Corbett EL, et al. The HIV-associated tuberculosis epidemic—when will we act? *Lancet* 2010; **375**(9729): 1906-19.
9. van Crevel R, Dockrell HM. TANDEM: understanding diabetes and tuberculosis. *Lancet Diabetes Endocrinol* 2014; **2**(4): 270-2.
10. McMurry HS, Mendenhall E, Aravind LR, Nambiar L, Satyanarayana S, Shivashankar R. Co-prevalence of type 2 diabetes mellitus and tuberculosis in low- and middle-income countries: A systematic review. *Diabetes Metab Res Rev* 2018: e3066.
11. World Health Organization. Global Tuberculosis Report. *WHO, Geneva*, 2017.
12. Lonnroth K, Castro KG, Chakaya JM, et al. Tuberculosis control and elimination 2010-50: cure, care, and social development. *Lancet* 2010; **375**(9728): 1814-29.
13. Uplekar M, Weil D, Lonnroth K, et al. WHO's new End TB Strategy. *Lancet* 2015; **S0140-6736**(15): 60570-3.
14. Dye C, Maher D, Weil D, Espinal M, Raviglione M. Targets for global tuberculosis control. *Int J Tuberc Lung Dis* 2006; **10**(4): 460-2.
15. Marais BJ, Gie RP, Schaaf HS, Beyers N, Donald PR, Starke JR. Childhood pulmonary tuberculosis: old wisdom and new challenges. *Am J Respir Crit Care Med* 2006; **173**(10): 1078-90.
16. Floyd K, Glaziou P, Zumla A, Raviglione M. The global tuberculosis epidemic and progress in care, prevention, and research: an overview in year 3 of the End TB era. *Lancet Respir Med* 2018; **6**(4): 299-314.

17. Abubakar I, Stagg HR, Cohen T, et al. Controversies and unresolved issues in tuberculosis prevention and control: a low-burden-country perspective. *J Infect Dis* 2012; **205**(Suppl 2): S293-300.
18. Neyrolles O, Quintana-Murci L. Sexual inequality in tuberculosis. *PLoS Med* 2009; **6**(12): e1000199.
19. Narasimhan P, Wood J, Macintyre CR, Mathai D. Risk factors for tuberculosis. *Pulm Med* 2013; **2013**: 828939.
20. Horton KC, MacPherson P, Houben RM, White RG, Corbett EL. Sex differences in tuberculosis burden and notifications in low- and middle-income countries: A systematic review and meta-analysis. *PLoS Med* 2016; **13**(9): e1002119.
21. Rhines AS. The role of sex differences in the prevalence and transmission of tuberculosis. *Tuberculosis (Edinb)* 2013; **93**(1): 104-7.
22. Nhamoyebonde S, Leslie A. Biological differences between the sexes and susceptibility to tuberculosis. *J Infect Dis* 2014; **209**(Suppl 3): S100-6.
23. van Lunzen J, Altfeld M. Sex differences in infectious diseases-common but neglected. *J Infect Dis* 2014; **209**(Suppl 3): S79-80.
24. Fish EN. The X-files in immunity: sex-based differences predispose immune responses. *Nat Rev Immunol* 2008; **8**(9): 737-44.
25. Pai M, Behr MA, Dowdy D, et al. Tuberculosis. *Nat Rev Dis Primers* 2016; **2**: 16076.
26. Fine PE. Variation in protection by BCG: implications of and for heterologous immunity. *Lancet* 1995; **346**(8986): 1339-45.
27. Mangtani P, Abubakar I, Ariti C, et al. Protection by BCG vaccine against tuberculosis: a systematic review of randomized controlled trials. *Clin Infect Dis* 2014; **58**(4): 470-80.
28. Dheda K, Schwander SK, Zhu B, van Zyl-Smit RN, Zhang Y. The immunology of tuberculosis: from bench to bedside. *Respirology* 2010; **15**(3): 433-50.
29. O'Garra A, Redford PS, McNab FW, Bloom CI, Wilkinson RJ, Berry MP. The immune response in tuberculosis. *Annu Rev Immunol* 2013; **31**: 475-527.
30. Houben RMGJ, Dodd PJ. The global burden of latent tuberculosis infection: A re-estimation using mathematical modelling. *PLoS Med* 2016; **13**(10): e1002152.
31. Kleinnijenhuis J, Oosting M, Joosten LA, Netea MG, van Crevel R. Innate immune recognition of *Mycobacterium tuberculosis*. *Clin Dev Immunol* 2011; **2011**: 405310.
32. Scriba TJ, Coussens AK, Fletcher HA. Human immunology of tuberculosis. *Microbiol Spectr* 2016; **4**(5): TBTB2-0016.
33. Wejse C, Patsche CB, Kuhle A, et al. Impact of HIV-1, HIV-2 and HIV-1+2 dual infection on the outcome of tuberculosis. *Int J Infect Dis* 2014; **32**(2015): 128-34.

34. Dheda K, Barry CE, Maartens G. Tuberculosis. *Lancet* 2016; **387**(10024): 1211-26.
35. Perez-Velez CM, Marais BJ. Tuberculosis in children. *N Engl J Med* 2012; **367**(4): 348-61.
36. Zumla A. The white plague returns to London--with a vengeance. *Lancet* 2011; **377**(9759): 10-1.
37. Lawn SD, Zumla AI. Tuberculosis. *Lancet* 2011; **378**(9785): 57-72.
38. Huebner RE, Schein MF, Bass JB, Jr. The tuberculin skin test. *Clin Infect Dis* 1993; **17**(6): 968-75.
39. Cobelens F, van den Hof S, Pai M, et al. Which new diagnostics for tuberculosis, and when? *J Infect Dis* 2012; **205**(Suppl 2): S191-8.
40. Walzl G, Ronacher K, Hanekom W, Scriba TJ, Zumla A. Immunological biomarkers of tuberculosis. *Nat Rev Immunol* 2011; **11**(5): 343-54.
41. Ernst JD. The immunological life cycle of tuberculosis. *Nat Rev Immunol* 2012; **12**(8): 581-91.
42. Walzl G, McNerney R, du Plessis N, et al. Tuberculosis: advances and challenges in development of new diagnostics and biomarkers. *Lancet Infect Dis* 2018; **S1473-3099**(18): 30111-7.
43. Cole ST, Brosch R, Parkhill J, et al. Deciphering the biology of *Mycobacterium tuberculosis* from the complete genome sequence. *Nature* 1998; **393**(6685): 537-44.
44. Rangaka MX, Wilkinson KA, Glynn JR, et al. Predictive value of interferon- γ release assays for incident active tuberculosis: a systematic review and meta-analysis. *Lancet Infect Dis* 2012; **12**(1): 45-55.
45. McNerney R, Cunningham J, Hepple P, Zumla A. New tuberculosis diagnostics and rollout. *Int J Infect Dis* 2015; **32**(2015): 81-6.
46. Escalante P. In the clinic. Tuberculosis. *Ann Intern Med* 2009; **150**(11): ITC61-614; quiz ITV6.
47. Pardini M, Varaine F, Bonnet M, et al. Usefulness of the BACTEC MGIT 960 system for isolation of *Mycobacterium tuberculosis* from sputa subjected to long-term storage. *J Clin Microbiol* 2007; **45**(2): 575-6.
48. Boehme CC, Nabeta P, Hillemann D, et al. Rapid molecular detection of tuberculosis and rifampin resistance. *N Engl J Med* 2010; **363**(11): 1005-15.
49. World Health Organization. Treatment of Tuberculosis Guideline: Fourth Edition. Geneva, 2010.
50. Zumla A, Abubakar I, Raviglione M, et al. Drug-resistant tuberculosis--current dilemmas, unanswered questions, challenges, and priority needs. *J Infect Dis* 2012; **205**(Suppl 2): S228-40.

51. Migliori GB, De Iaco G, Besozzi G, Centis R, Cirillo DM. First tuberculosis cases in Italy resistant to all tested drugs. *Euro Surveill* 2007; **12**(5): E070517 1.
52. Velayati AA, Masjedi MR, Farnia P, et al. Emergence of new forms of totally drug-resistant tuberculosis bacilli: super extensively drug-resistant tuberculosis or totally drug-resistant strains in iran. *Chest* 2009; **136**(2): 420-5.
53. Udhwadia ZF. Totally drug-resistant tuberculosis in India: who let the djinn out? *Respirology* 2012; **17**(5): 741-2.
54. Zumla A, Kim P, Maeurer M, Schito M. Zero deaths from tuberculosis: progress, reality, and hope. *Lancet Infect Dis* 2013; **13**(4): 285-7.
55. World Health Organization. Global Tuberculosis Report. Geneva, 2014.
56. Faustini A, Hall AJ, Perucci CA. Risk factors for multidrug resistant tuberculosis in Europe: a systematic review. *Thorax* 2006; **61**(2): 158-63.
57. Dheda K, Gumbo T, Gandhi NR, et al. Global control of tuberculosis: from extensively drug-resistant to untreatable tuberculosis. *Lancet Respir Med* 2014; **2**(4): 321-38.
58. Pasipanodya JG, Srivastava S, Gumbo T. Meta-analysis of clinical studies supports the pharmacokinetic variability hypothesis for acquired drug resistance and failure of antituberculosis therapy. *Clin Infect Dis* 2012; **55**(2): 169-77.
59. World Health Organization. Rapid Communication: Key changes to treatment of multidrug- and rifampicin-resistant tuberculosis (MDR/RR-TB) *WHO, Geneva* 2018.
60. Zhang Y. The magic bullets and tuberculosis drug targets. *Annu Rev Pharmacol Toxicol* 2005; **45**: 529-64.
61. Hameed HMA, Islam MM, Chhotaray C, et al. Molecular Targets Related Drug Resistance Mechanisms in MDR-, XDR-, and TDR-Myco**acterium** tuberculosis Strains. *Front Cell Infect Microbiol* 2018; **8**.
62. Stop TB Partnership. The Global Plan to Stop TB. Geneva, 2011-2015.
63. Joshi JM. Tuberculosis chemotherapy in the 21 century: Back to the basics. *Lung India* 2011; **28**(3): 193-200.
64. Zhang Y, Yew WW, Barer MR. Targeting persisters for tuberculosis control. *Antimicrob Agents Chemother* 2012; **56**(5): 2223-30.
65. Gengenbacher M, Kaufmann SH. Mycobacterium tuberculosis: success through dormancy. *FEMS Microbiol Rev* 2012; **36**(3): 514-32.
66. Schon T, Lerm M, Stendahl O. Shortening the 'short-course' therapy- insights into host immunity may contribute to new treatment strategies for tuberculosis. *J Intern Med* 2013; **273**(4): 368-82.
67. Warner DF, Mizrahi V. Shortening treatment for tuberculosis--to basics. *N Engl J Med* 2014; **371**(17): 1642-3.

68. Mitchison D, Davies G. The chemotherapy of tuberculosis: past, present and future. *Int J Tuberc Lung Dis* 2012; **16**(6): 724-32.
69. Gillespie SH, Crook AM, McHugh TD, et al. Four-month moxifloxacin-based regimens for drug-sensitive tuberculosis. *N Engl J Med* 2014; **371**(17): 1577-87.
70. Jindani A, Harrison TS, Nunn AJ, et al. High-dose rifapentine with moxifloxacin for pulmonary tuberculosis. *N Engl J Med* 2014; **371**(17): 1599-608.
71. Merle CS, Fielding K, Sow OB, et al. A four-month gatifloxacin-containing regimen for treating tuberculosis. *N Engl J Med* 2014; **371**(17): 1588-98.
72. Kaufmann SH, Hussey G, Lambert PH. New vaccines for tuberculosis. *Lancet* 2010; **375**(9731): 2110-9.
73. Axelsson-Robertson R, Magalhaes I, Parida SK, Zumla A, Maeurer M. The immunological footprint of Mycobacterium tuberculosis T-cell epitope recognition. *J Infect Dis* 2012; **205**(Suppl 2): S301-15.
74. Kaufmann SH. Novel tuberculosis vaccination strategies based on understanding the immune response. *J Intern Med* 2010; **267**(4): 337-53.
75. Rohde KH, Abramovitch RB, Russell DG. Mycobacterium tuberculosis invasion of macrophages: linking bacterial gene expression to environmental cues. *Cell Host Microbe* 2007; **2**(5): 352-64.
76. Welin A, Lerm M. Inside or outside the phagosome? The controversy of the intracellular localization of Mycobacterium tuberculosis. *Tuberculosis (Edinb)* 2012; **92**(2): 113-20.
77. Liu PT, Modlin RL. Human macrophage host defense against Mycobacterium tuberculosis. *Curr Opin Immunol* 2008; **20**(4): 371-6.
78. Fabri M, Stenger S, Shin DM, et al. Vitamin D is required for IFN-gamma-mediated antimicrobial activity of human macrophages. *Sci Transl Med* 2011; **3**(104): 104ra2.
79. Gupta A, Kaul A, Tsolaki AG, Kishore U, Bhakta S. Mycobacterium tuberculosis: immune evasion, latency and reactivation. *Immunobiology* 2012; **217**(3): 363-74.
80. Marino S, Cilfone NA, Mattila JT, Linderman JJ, Flynn JL, Kirschner DE. Macrophage Polarization Drives Granuloma Outcome during Mycobacterium tuberculosis Infection. *Infect Immun* 2015; **83**(1): 324-38.
81. Yang J, Zhang L, Yu C, Yang XF, Wang H. Monocyte and macrophage differentiation: circulation inflammatory monocyte as biomarker for inflammatory diseases. *Biomark Res* 2014; **2**(1): 1.
82. Sampath P, Moideen K, Ranganathan UD, Bethunaickan R. Monocyte Subsets: Phenotypes and Function in Tuberculosis Infection. *Front Immunol* 2018; **9**: 1726.
83. Mildner A, Marinkovic G, Jung S. Murine Monocytes: Origins, Subsets, Fates, and Functions. *Microbiol Spectr* 2016; **4**(5).

84. Joosten SA, van Meijgaarden KE, Arend SM, et al. Mycobacterial growth inhibition is associated with trained innate immunity. *J Clin Invest* 2018; **128**(5): 1837-51.
85. Hanekom WA, Mendillo M, Manca C, et al. Mycobacterium tuberculosis inhibits maturation of human monocyte-derived dendritic cells in vitro. *J Infect Dis* 2003; **188**(2): 257-66.
86. Eum SY, Kong JH, Hong MS, et al. Neutrophils are the predominant infected phagocytic cells in the airways of patients with active pulmonary TB. *Chest* 2010; **137**(1): 122-8.
87. Eruslanov EB, Lyadova IV, Kondratieva TK, et al. Neutrophil responses to Mycobacterium tuberculosis infection in genetically susceptible and resistant mice. *Infect Immun* 2005; **73**(3): 1744-53.
88. Martineau AR, Newton SM, Wilkinson KA, et al. Neutrophil-mediated innate immune resistance to mycobacteria. *J Clin Invest* 2007; **117**(7): 1988-94.
89. Hartmann P, Becker R, Franzen C, et al. Phagocytosis and killing of Mycobacterium avium complex by human neutrophils. *J Leukoc Biol* 2001; **69**(3): 397-404.
90. Berry MP, Graham CM, McNab FW, et al. An interferon-inducible neutrophil-driven blood transcriptional signature in human tuberculosis. *Nature* 2010; **466**(7309): 973-7.
91. Orme IM, Robinson RT, Cooper AM. The balance between protective and pathogenic immune responses in the TB-infected lung. *Nat Immunol* 2015; **16**(1): 57-63.
92. Vankayalapati R, Barnes PF. Innate and adaptive immune responses to human Mycobacterium tuberculosis infection. *Tuberculosis (Edinb)* 2009; **89 Suppl 1**: S77-80.
93. Barcelos W, Sathler-Avelar R, Martins-Filho OA, et al. Natural killer cell subpopulations in putative resistant individuals and patients with active Mycobacterium tuberculosis infection. *Scand J Immunol* 2008; **68**(1): 92-102.
94. Vankayalapati R, Garg A, Porgador A, et al. Role of NK cell-activating receptors and their ligands in the lysis of mononuclear phagocytes infected with an intracellular bacterium. *J Immunol* 2005; **175**(7): 4611-7.
95. Sia JK, Georgieva M, Rengarajan J. Innate Immune Defenses in Human Tuberculosis: An Overview of the Interactions between Mycobacterium tuberculosis and Innate Immune Cells. *J Immunol Res* 2015; **2015**: 747543.
96. Choreno Parra JA, Martinez Zuniga N, Jimenez Zamudio LA, Jimenez Alvarez LA, Salinas Lara C, Zuniga J. Memory of Natural Killer Cells: A New Chance against Mycobacterium tuberculosis? *Front Immunol* 2017; **8**: 967.
97. Nirmala R, Narayanan PR, Mathew R, Maran M, Deivanayagam CN. Reduced NK activity in pulmonary tuberculosis patients with/without HIV infection: identifying the defective stage and studying the effect of interleukins on NK activity. *Tuberculosis (Edinb)* 2001; **81**(5-6): 343-52.

98. Bozzano F, Costa P, Passalacqua G, et al. Functionally relevant decreases in activatory receptor expression on NK cells are associated with pulmonary tuberculosis in vivo and persist after successful treatment. *Int Immunol* 2009; **21**(7): 779-91.
99. Roy Chowdhury R, Vallania F, Yang Q, et al. A multi-cohort study of the immune factors associated with M. tuberculosis infection outcomes. *Nature* 2018; **s41586**: 018-0439-x.
100. Vankayalapati R, Klucar P, Wizel B, et al. NK cells regulate CD8+ T cell effector function in response to an intracellular pathogen. *J Immunol* 2004; **172**(1): 130-7.
101. Dhiman R, Indramohan M, Barnes PF, et al. IL-22 produced by human NK cells inhibits growth of Mycobacterium tuberculosis by enhancing phagolysosomal fusion. *J Immunol* 2009; **183**(10): 6639-45.
102. Muller J, Matsumiya M, Snowden MA, et al. Cytomegalovirus infection is a risk factor for TB disease in Infants. *bioRxiv* 2017: 222646.
103. Kim M, Kim TJ, Kim HM, Doh J, Lee KM. Multi-cellular natural killer (NK) cell clusters enhance NK cell activation through localizing IL-2 within the cluster. *Sci Rep* 2017; **7**: 40623.
104. Pennington DJ, Vermijlen D, Wise EL, Clarke SL, Tigelaar RE, Hayday AC. The integration of conventional and unconventional T cells that characterizes cell-mediated responses. *Adv Immunol* 2005; **87**: 27-59.
105. Geldmacher C, Schuetz A, Ngwenyama N, et al. Early depletion of Mycobacterium tuberculosis-specific T helper 1 cell responses after HIV-1 infection. *J Infect Dis* 2008; **198**(11): 1590-8.
106. Mendez-Samperio P. Expression and regulation of chemokines in mycobacterial infection. *J Infect* 2008; **57**(5): 374-84.
107. Casanova JL, Abel L. Genetic dissection of immunity to mycobacteria: the human model. *Annu Rev Immunol* 2002; **20**: 581-620.
108. Cooper AM, Dalton DK, Stewart TA, Griffin JP, Russell DG, Orme IM. Disseminated tuberculosis in interferon gamma gene-disrupted mice. *J Exp Med* 1993; **178**(6): 2243-7.
109. Flynn JL, Chan J, Triebold KJ, Dalton DK, Stewart TA, Bloom BR. An essential role for interferon gamma in resistance to Mycobacterium tuberculosis infection. *J Exp Med* 1993; **178**(6): 2249-54.
110. van Altena R, Duggirala S, Groschel MI, van der Werf TS. Immunology in tuberculosis: challenges in monitoring of disease activity and identifying correlates of protection. *Curr Pharm Des* 2011; **17**(27): 2853-62.
111. Kaufmann SH. Immune response to tuberculosis: experimental animal models. *Tuberculosis (Edinb)* 2003; **83**(1-3): 107-11.
112. Ramakrishnan L. Revisiting the role of the granuloma in tuberculosis. *Nat Rev Immunol* 2012; **12**(5): 352-66.

113. Keane J, Gershon S, Wise RP, et al. Tuberculosis associated with infliximab, a tumor necrosis factor alpha-neutralizing agent. *N Engl J Med* 2001; **345**(15): 1098-104.
114. Nelson BH. IL-2, regulatory T cells, and tolerance. *J Immunol* 2004; **172**(7): 3983-8.
115. Lienhardt C, Azzurri A, Amedei A, et al. Active tuberculosis in Africa is associated with reduced Th1 and increased Th2 activity in vivo. *Eur J Immunol* 2002; **32**(6): 1605-13.
116. Demissie A, Abebe M, Aseffa A, et al. Healthy individuals that control a latent infection with Mycobacterium tuberculosis express high levels of Th1 cytokines and the IL-4 antagonist IL-4delta2. *J Immunol* 2004; **172**(11): 6938-43.
117. Elias D, Akuffo H, Pawlowski A, Haile M, Schon T, Britton S. Schistosoma mansoni infection reduces the protective efficacy of BCG vaccination against virulent Mycobacterium tuberculosis. *Vaccine* 2005; **23**(11): 1326-34.
118. Gopal R, Monin L, Slight S, et al. Unexpected role for IL-17 in protective immunity against hypervirulent Mycobacterium tuberculosis HN878 infection. *PLoS Pathog* 2014; **10**(5): e1004099.
119. Torrado E, Cooper AM. IL-17 and Th17 cells in tuberculosis. *Cytokine Growth Factor Rev* 2010; **21**(6): 455-62.
120. Redford PS, Murray PJ, O'Garra A. The role of IL-10 in immune regulation during M. tuberculosis infection. *Mucosal Immunol* 2011; **4**(3): 261-70.
121. Beamer GL, Flaherty DK, Assogba BD, et al. Interleukin-10 promotes Mycobacterium tuberculosis disease progression in CBA/J mice. *J Immunol* 2008; **181**(8): 5545-50.
122. Arora P, Foster EL, Porcelli SA. CD1d and natural killer T cells in immunity to Mycobacterium tuberculosis. *Adv Exp Med Biol* 2013; **783**: 199-223.
123. Huang S. Targeting Innate-Like T Cells in Tuberculosis. *Front Immunol* 2016; **7**: 594.
124. Meraviglia S, El Daker S, Dieli F, Martini F, Martino A. gammadelta T cells cross-link innate and adaptive immunity in Mycobacterium tuberculosis infection. *Clin Dev Immunol* 2011; **2011**: 587315.
125. Lockhart E, Green AM, Flynn JL. IL-17 production is dominated by gammadelta T cells rather than CD4 T cells during Mycobacterium tuberculosis infection. *J Immunol* 2006; **177**(7): 4662-9.
126. Abebe F. Is interferon-gamma the right marker for bacille Calmette-Guerin-induced immune protection? The missing link in our understanding of tuberculosis immunology. *Clin Exp Immunol* 2012; **169**(3): 213-9.
127. Zufferey C, Germano S, Dutta B, Ritz N, Curtis N. The contribution of non-conventional T cells and NK cells in the mycobacterial-specific IFNgamma response in Bacille Calmette-Guerin (BCG)-immunized infants. *PLoS One* 2013; **8**(10): e77334.

128. Snyder-Cappione JE, Nixon DF, Loo CP, et al. Individuals with pulmonary tuberculosis have lower levels of circulating CD1d-restricted NKT cells. *J Infect Dis* 2007; **195**(9): 1361-4.
129. Daniel TM, Oxtoby MJ, Pinto E, Moreno E. The immune spectrum in patients with pulmonary tuberculosis. *Am Rev Respir Dis* 1981; **123**(5): 556-9.
130. Costello AM, Kumar A, Narayan V, et al. Does antibody to mycobacterial antigens, including lipoarabinomannan, limit dissemination in childhood tuberculosis? *Trans R Soc Trop Med Hyg* 1992; **86**(6): 686-92.
131. Kaufmann SH. The contribution of immunology to the rational design of novel antibacterial vaccines. *Nat Rev Microbiol* 2007; **5**(7): 491-504.
132. Kozakiewicz L, Phuah J, Flynn J, Chan J. The Role of B Cells and Humoral Immunity in Mycobacterium tuberculosis Infection. In: Divangahi M, ed. *The New Paradigm of Immunity to Tuberculosis*. New York, NY: Springer New York; 2013: 225-50.
133. Maglione PJ, Xu J, Chan J. B cells moderate inflammatory progression and enhance bacterial containment upon pulmonary challenge with Mycobacterium tuberculosis. *J Immunol* 2007; **178**(11): 7222-34.
134. Sebina I, Biraro IA, Dockrell HM, Elliott AM, Cose S. Circulating B-lymphocytes as potential biomarkers of tuberculosis infection activity. *PLoS One* 2014; **9**(9): e106796.
135. Netea MG, Joosten LA, Latz E, et al. Trained immunity: A program of innate immune memory in health and disease. *Science* 2016; **352**(6284): aaf1098.
136. Kleinnijenhuis J, Quintin J, Preijers F, et al. Bacille Calmette-Guerin induces NOD2-dependent nonspecific protection from reinfection via epigenetic reprogramming of monocytes. *Proc Natl Acad Sci U S A* 2012; **109**(43): 17537-42.
137. Cheng SC, Quintin J, Cramer RA, et al. mTOR- and HIF-1 α -mediated aerobic glycolysis as metabolic basis for trained immunity. *Science* 2014; **345**(6204): 1250684.
138. Kleinnijenhuis J, Quintin J, Preijers F, et al. BCG-induced trained immunity in NK cells: Role for non-specific protection to infection. *Clin Immunol* 2014; **155**(2): 213-9.
139. Arts RJW, Carvalho A, La Rocca C, et al. Immunometabolic Pathways in BCG-Induced Trained Immunity. *Cell Rep* 2016; **17**(10): 2562-71.
140. Quintin J, Saeed S, Martens JHA, et al. Candida albicans infection affords protection against reinfection via functional reprogramming of monocytes. *Cell Host Microbe* 2012; **12**(2): 223-32.
141. Sun JC, Madera S, Bezman NA, Beilke JN, Kaplan MH, Lanier LL. Proinflammatory cytokine signaling required for the generation of natural killer cell memory. *J Exp Med* 2012; **209**(5): 947-54.
142. Sun JC, Beilke JN, Lanier LL. Adaptive immune features of natural killer cells. *Nature* 2009; **457**(7229): 557-61.
143. Luca S, Mihaescu T. History of BCG Vaccine. *Maedica (Buchar)* 2013; **8**(1): 53-8.

144. Fine PE. Bacille Calmette-Guerin vaccines: a rough guide. *Clin Infect Dis* 1995; **20**(1): 11-4.
145. Dockrell HM, Smith SG. What Have We Learnt about BCG Vaccination in the Last 20 Years? *Front Immunol* 2017; **8**: 1134.
146. McShane H. Tuberculosis vaccines: beyond bacille Calmette-Guerin. *Philos Trans R Soc Lond B Biol Sci* 2011; **366**(1579): 2782-9.
147. Hussey GD, Watkins ML, Goddard EA, et al. Neonatal mycobacterial specific cytotoxic T-lymphocyte and cytokine profiles in response to distinct BCG vaccination strategies. *Immunology* 2002; **105**(3): 314-24.
148. Ritz N, Dutta B, Donath S, et al. The influence of bacille Calmette-Guerin vaccine strain on the immune response against tuberculosis: a randomized trial. *Am J Respir Crit Care Med* 2012; **185**(2): 213-22.
149. Kim KD, Lee HG, Kim JK, et al. Enhanced antigen-presenting activity and tumour necrosis factor-alpha-independent activation of dendritic cells following treatment with Mycobacterium bovis bacillus Calmette-Guerin. *Immunology* 1999; **97**(4): 626-33.
150. Smith SM, Malin AS, Pauline T, et al. Characterization of human Mycobacterium bovis bacille Calmette-Guerin-reactive CD8+ T cells. *Infect Immun* 1999; **67**(10): 5223-30.
151. Fletcher HA, Snowden MA, Landry B, et al. T-cell activation is an immune correlate of risk in BCG vaccinated infants. *Nat Commun* 2016; **7**: 11290.
152. Pitt JM, Blankley S, McShane H, O'Garra A. Vaccination against tuberculosis: how can we better BCG? *Microb Pathog* 2013; **58**: 2-16.
153. Suliman S, Geldenhuys H, Johnson JL, et al. Bacillus Calmette-Guerin (BCG) Revaccination of Adults with Latent Mycobacterium tuberculosis Infection Induces Long-Lived BCG-Reactive NK Cell Responses. *J Immunol* 2016; **197**(4): 1100-10.
154. Marais BJ, Graham SM, Maeurer M, Zumla A. Progress and challenges in childhood tuberculosis. *Lancet Infect Dis* 2013; **13**(4): 287-9.
155. B.C.G. AND vole bacillus vaccines in the prevention of tuberculosis in adolescents; first (progress) report to the Medical Research Council by their Tuberculosis Vaccines Clinical Trials Committee. *Br Med J* 1956; **1**(4964): 413-27.
156. Baily GV. Tuberculosis prevention Trial, Madras. *Indian J Med Res* 1980; **72 Suppl**: 1-74.
157. Black GF, Weir RE, Floyd S, et al. BCG-induced increase in interferon-gamma response to mycobacterial antigens and efficacy of BCG vaccination in Malawi and the UK: two randomised controlled studies. *Lancet* 2002; **359**(9315): 1393-401.
158. Dockrell HM, Smith SG, Lalor MK. Variability between countries in cytokine responses to BCG vaccination: what impact might this have on protection? *Expert Rev Vaccines* 2012; **11**(2): 121-4.

159. Lalor MK, Floyd S, Gorak-Stolinska P, et al. BCG vaccination induces different cytokine profiles following infant BCG vaccination in the UK and Malawi. *J Infect Dis* 2011; **204**(7): 1075-85.
160. Aronson NE, Santosham M, Comstock GW, et al. Long-term efficacy of BCG vaccine in American Indians and Alaska Natives: A 60-year follow-up study. *JAMA* 2004; **291**(17): 2086-91.
161. Barreto ML, Cunha SS, Pereira SM, et al. Neonatal BCG protection against tuberculosis lasts for 20 years in Brazil. *Int J Tuberc Lung Dis* 2005; **9**(10): 1171-3.
162. Abubakar I, Pimpin L, Ariti C, et al. Systematic review and meta-analysis of the current evidence on the duration of protection by bacillus Calmette-Guerin vaccination against tuberculosis. *Health Technol Assess* 2013; **17**(37): 1-372, v-vi.
163. Rhodes SJ, Knight GM, Fielding K, et al. Individual-level factors associated with variation in mycobacterial-specific immune response: Gender and previous BCG vaccination status. *Tuberculosis (Edinb)* 2016; **96**: 37-43.
164. Mangtani P, Nguipdop-Djomo P, Keogh RH, et al. The duration of protection of school-aged BCG vaccination in England: a population -based case-control study. *Int J Epidemiol* 2017: 1-9.
165. Portaels F, Aguiar J, Debacker M, et al. Mycobacterium bovis BCG vaccination as prophylaxis against Mycobacterium ulcerans osteomyelitis in Buruli ulcer disease. *Infect Immun* 2004; **72**(1): 62-5.
166. Setia MS, Steinmaus C, Ho CS, Rutherford GW. The role of BCG in prevention of leprosy: a meta-analysis. *Lancet Infect Dis* 2006; **6**(3): 162-70.
167. Biering-Sorensen S, Aaby P, Lund N, et al. Early BCG-Denmark and Neonatal Mortality Among Infants Weighing <2500 g: A Randomized Controlled Trial. *Clin Infect Dis* 2017; **65**(7): 1183-90.
168. Stensballe LG, Nante E, Jensen IP, et al. Acute lower respiratory tract infections and respiratory syncytial virus in infants in Guinea-Bissau: a beneficial effect of BCG vaccination for girls community based case-control study. *Vaccine* 2005; **23**(10): 1251-7.
169. Roth A, Sodemann M, Jensen H, et al. Tuberculin reaction, BCG scar, and lower female mortality. *Epidemiology* 2006; **17**(5): 562-8.
170. Stensballe LG, Sorup S, Aaby P, et al. BCG vaccination at birth and early childhood hospitalisation: a randomised clinical multicentre trial. *Arch Dis Child* 2017; **102**(3): 224-31.
171. Haralambieva IH, Ovsyannikova IG, Kennedy RB, Larrabee BR, Shane Pankratz V, Poland GA. Race and sex-based differences in cytokine immune responses to smallpox vaccine in healthy individuals. *Hum Immunol* 2013; **74**(10): 1263-6.
172. de Bree LCJ, Koeken V, Joosten LAB, et al. Non-specific effects of vaccines: Current evidence and potential implications. *Semin Immunol* 2018; **06**(002): 1044-5323.

173. Kleinnijenhuis J, Quintin J, Preijers F, et al. Long-lasting effects of BCG vaccination on both heterologous Th1/Th17 responses and innate trained immunity. *J Innate Immun* 2014; **6**(2): 152-8.
174. Smith SG, Kleinnijenhuis J, Netea MG, Dockrell HM. Whole Blood Profiling of Bacillus Calmette-Guerin-Induced Trained Innate Immunity in Infants Identifies Epidermal Growth Factor, IL-6, Platelet-Derived Growth Factor-AB/BB, and Natural Killer Cell Activation. *Front Immunol* 2017; **8**: 644.
175. Kaufmann SHE, Dockrell HM, Drager N, et al. TBVAC2020: Advancing Tuberculosis Vaccines from Discovery to Clinical Development. *Front Immunol* 2017; **8**: 1203.
176. Weiner J, 3rd, Kaufmann SH. Recent advances towards tuberculosis control: vaccines and biomarkers. *J Intern Med* 2014; **275**(5): 467-80.
177. Kaufmann SH, Weiner J, von Reyn CF. Novel approaches to tuberculosis vaccine development. *Int J Infect Dis* 2017; **56**: 263-7.
178. Nieuwenhuizen NE, Kulkarni PS, Shaligram U, et al. The Recombinant Bacille Calmette-Guerin Vaccine VPM1002: Ready for Clinical Efficacy Testing. *Front Immunol* 2017; **8**: 1147.
179. Marinova D, Gonzalo-Asensio J, Aguilo N, Martin C. MTBVAC from discovery to clinical trials in tuberculosis-endemic countries. *Expert Rev Vaccines* 2017; **16**(6): 565-76.
180. Andersen P, Woodworth JS. Tuberculosis vaccines--rethinking the current paradigm. *Trends Immunol* 2014; **35**(8): 387-95.
181. Ottenhoff TH, Kaufmann SH. Vaccines against tuberculosis: where are we and where do we need to go? *PLoS Pathog* 2012; **8**(5): e1002607.
182. Kaufmann SHE, Lange C, Rao M, et al. Progress in tuberculosis vaccine development and host-directed therapies—a state of the art review. *Lancet Respir Med* 2014; **2**(4): 301-20.
183. McShane H, Pathan AA, Sander CR, et al. Recombinant modified vaccinia virus Ankara expressing antigen 85A boosts BCG-primed and naturally acquired antimycobacterial immunity in humans. *Nat Med* 2004; **10**(11): 1240-4.
184. Weinrich Olsen A, van Pinxteren LA, Meng Okkels L, Birk Rasmussen P, Andersen P. Protection of mice with a tuberculosis subunit vaccine based on a fusion protein of antigen 85b and esat-6. *Infect Immun* 2001; **69**(5): 2773-8.
185. Aagaard C, Hoang T, Dietrich J, et al. A multistage tuberculosis vaccine that confers efficient protection before and after exposure. *Nat Med* 2011; **17**(2): 189-94.
186. Day CL, Tameris M, Mansoor N, et al. Induction and regulation of T-cell immunity by the novel tuberculosis vaccine M72/AS01 in South African adults. *Am J Respir Crit Care Med* 2013; **188**(4): 492-502.

187. Baldwin SL, Reese VA, Huang PW, et al. Protection and Long-Lived Immunity Induced by the ID93/GLA-SE Vaccine Candidate against a Clinical Mycobacterium tuberculosis Isolate. *Clin Vaccine Immunol* 2015; **23**(2): 137-47.
188. Montagnani C, Chiappini E, Galli L, de Martino M. Vaccine against tuberculosis: what's new? *BMC Infect Dis* 2014; **14**(Suppl 1): S2.
189. Minassian AM, Rowland R, Beveridge NE, et al. A Phase I study evaluating the safety and immunogenicity of MVA85A, a candidate TB vaccine, in HIV-infected adults. *BMJ Open* 2011; **1**(2): e000223.
190. Scriba TJ, Tameris M, Smit E, et al. A phase IIa trial of the new tuberculosis vaccine, MVA85A, in HIV- and/or Mycobacterium tuberculosis-infected adults. *Am J Respir Crit Care Med* 2012; **185**(7): 769-78.
191. Kashangura R, Sena ES, Young T, Garner P. Effects of MVA85A vaccine on tuberculosis challenge in animals: systematic review. *Int J Epidemiol* 2015: 1–12.
192. McShane H, Hatherill M, Hanekom W, Evans T. Effects of MVA85A vaccine on tuberculosis challenge in animals: systematic review. *Int J Epidemiol* 2016; **45**(2): 580.
193. Williams A, Sharpe S, Verreck F, Vordermeier M, Hewinson G. Response to: Systematic review: animal studies of TB vaccines. *Int J Epidemiol* 2016; **45**(2): 583-4.
194. Tameris MD, Hatherill M, Landry BS, et al. Safety and efficacy of MVA85A, a new tuberculosis vaccine, in infants previously vaccinated with BCG: a randomised, placebo-controlled phase 2b trial. *Lancet* 2013; **381**(9871): 1021-8.
195. Tanner R, Kakalacheva K, Miller E, et al. Serum indoleamine 2,3-dioxygenase activity is associated with reduced immunogenicity following vaccination with MVA85A. *BMC Infect Dis* 2014; **14**: 660.
196. Nemes E, Geldenhuys H, Rozot V, et al. Prevention of M. tuberculosis Infection with H4:IC31 Vaccine or BCG Revaccination. *N Engl J Med* 2018; **379**(2): 138-49.
197. Van Der Meeren O, Hatherill M, Nduba V, et al. Phase 2b Controlled Trial of M72/AS01E Vaccine to Prevent Tuberculosis. *N Engl J Med* 2018.
198. Hawn TR, Matheson AI, Maley SN, Vandal O. Host-directed therapeutics for tuberculosis: can we harness the host? *Microbiol Mol Biol Rev* 2013; **77**(4): 608-27.
199. Koch R. A Further Communication on a Remedy for Tuberculosis. *Br Med J* 1891; **1**(1568): 125-7.
200. Gradmann C. Robert Koch and the pressures of scientific research: tuberculosis and tuberculin. *Med Hist* 2001; **45**(1): 1-32.
201. Prabowo SA, Groschel MI, Schmidt ED, et al. Targeting multidrug-resistant tuberculosis (MDR-TB) by therapeutic vaccines. *Med Microbiol Immunol* 2013; **202**(2): 95-104.

202. Gil O, Guirado E, Gordillo S, et al. Intragranulomatous necrosis in lungs of mice infected by aerosol with *Mycobacterium tuberculosis* is related to bacterial load rather than to any one cytokine or T cell type. *Microbes Infect* 2006; **8**(3): 628-36.
203. Moreira AL, Tsenova L, Aman MH, et al. Mycobacterial antigens exacerbate disease manifestations in Mycobacterium tuberculosis-infected mice. *Infect Immun* 2002; **70**(4): 2100-7.
204. Turner J, Rhoades ER, Keen M, Belisle JT, Frank AA, Orme IM. Effective preexposure tuberculosis vaccines fail to protect when they are given in an immunotherapeutic mode. *Infect Immun* 2000; **68**(3): 1706-9.
205. Smith HV, Vollum RL. Effects of intrathecal tuberculin and streptomycin in tuberculous meningitis; an interim report. *Lancet* 1950; **2**(6625): 275-86.
206. Smith HV. Tuberculin in the treatment of tuberculous meningitis and other conditions. *Proc R Soc Med* 1953; **46**(7): 588-90.
207. Howells CH, Swithinbank J. A trial of tuberculin with chemotherapy in the treatment of pulmonary tuberculosis. *Tubercle* 1957; **38**(1): 1-15.
208. Crofton J. Chemotherapy of pulmonary tuberculosis. *Br Med J* 1959; **1**(5138): 1610-4.
209. McMurray DN. Therapeutic vaccination: hope for untreatable tuberculosis? *J Infect Dis* 2013; **207**(8): 1193-4.
210. Keren I, Minami S, Rubin E, Lewis K. Characterization and transcriptome analysis of *Mycobacterium tuberculosis* persisters. *MBio* 2011; **2**(3): e00100-11.
211. Gröschel MI, Prabowo SA, Cardona P-J, Stanford JL, Werf TSvd. Therapeutic vaccines for tuberculosis—A systematic review. *Vaccine* 2014; **32**(26): 3162-8.
212. Cardona PJ. RUTI: a new chance to shorten the treatment of latent tuberculosis infection. *Tuberculosis (Edinb)* 2006; **86**(3-4): 273-89.
213. Cardona PJ. The progress of therapeutic vaccination with regard to tuberculosis. *Front Microbiol* 2016; **7**: 1536.
214. Nell AS, D'Lom E, Bouic P, et al. Safety, tolerability, and immunogenicity of the novel antituberculous vaccine RUTI: randomized, placebo-controlled phase II clinical trial in patients with latent tuberculosis infection. *PLoS One* 2014; **9**(2): e89612.
215. Cardona PJ, Amat I, Gordillo S, et al. Immunotherapy with fragmented *Mycobacterium tuberculosis* cells increases the effectiveness of chemotherapy against a chronic infection in a murine model of tuberculosis. *Vaccine* 2005; **23**(11): 1393-8.
216. Guirado E, Gil O, Caceres N, Singh M, Vilaplana C, Cardona PJ. Induction of a specific strong polyantigenic cellular immune response after short-term chemotherapy controls bacillary reactivation in murine and guinea pig experimental models of tuberculosis. *Clin Vaccine Immunol* 2008; **15**(8): 1229-37.
217. Domingo M, Gil O, Serrano E, et al. Effectiveness and safety of a treatment regimen based on isoniazid plus vaccination with *Mycobacterium tuberculosis* cells' fragments:

- field-study with naturally *Mycobacterium caprae*-infected goats. *Scand J Immunol* 2009; **69**(6): 500-7.
218. Gil O, Diaz I, Vilaplana C, et al. Granuloma encapsulation is a key factor for containing tuberculosis infection in minipigs. *PLoS One* 2010; **5**(4): e10030.
 219. Immunotherapy with *Mycobacterium vaccae* in patients with newly diagnosed pulmonary tuberculosis: a randomised controlled trial. Durban Immunotherapy Trial Group. *Lancet* 1999; **354**(9173): 116-9.
 220. Yang XY, Chen QF, Li YP, Wu SM. *Mycobacterium vaccae* as adjuvant therapy to anti-tuberculosis chemotherapy in never-treated tuberculosis patients: a meta-analysis. *PLoS One* 2011; **6**(9): e23826.
 221. Lalvani A, Sridhar S, von Reyn CF. Tuberculosis vaccines: time to reset the paradigm? *Thorax* 2013; **68**(12): 1092-4.
 222. Mayosi BM, Ntsekhe M, Bosch J, et al. Prednisolone and *Mycobacterium indicus pranii* in tuberculous pericarditis. *N Engl J Med* 2014; **371**(12): 1121-30.
 223. V. Arjanova O, D. Prihoda N, V. Yurchenko L, Sokolenko NI, M. Frolov V. Phase 2 Trial of V-5 Immunitor (V5) in Patients with Chronic Hepatitis C Co-infected with HIV and *Mycobacterium tuberculosis*. *J Vaccines Vaccin* 2010; **01**(01).
 224. Lin PL, Dietrich J, Tan E, et al. The multistage vaccine H56 boosts the effects of BCG to protect cynomolgus macaques against active tuberculosis and reactivation of latent *Mycobacterium tuberculosis* infection. *J Clin Invest* 2012; **122**(1): 303-14.
 225. Young D. Animal models of tuberculosis. *Eur J Immunol* 2009; **39**(8): 2011-4.
 226. Cardona PJ, Williams A. Experimental animal modelling for TB vaccine development. *Int J Infect Dis* 2017; **56**: 268-73.
 227. Orme IM. Prospects for new vaccines against tuberculosis. *Trends Microbiol* 1995; **3**(10): 401-4.
 228. Hernandez-Pando R, Aguilar D, Orozco H, Cortez Y, Brunet LR, Rook GA. Orally administered *Mycobacterium vaccae* modulates expression of immunoregulatory molecules in BALB/c mice with pulmonary tuberculosis. *Clin Vaccine Immunol* 2008; **15**(11): 1730-6.
 229. Reduce, refine, replace. *Nat Immunol* 2010; **11**(11): 971.
 230. Kanesa-Thanan N, Shaw A, Stoddard JJ, Vernon TM. Ensuring the optimal safety of licensed vaccines: a perspective of the vaccine research, development, and manufacturing companies. *Pediatrics* 2011; **127**(Suppl 1): S16-22.
 231. Kaufmann SH, Evans TG, Hanekom WA. Tuberculosis vaccines: Time for a global strategy. *Sci Transl Med* 2015; **7**(276): 276fs8.
 232. Biomarkers Definitions Working G. Biomarkers and surrogate endpoints: preferred definitions and conceptual framework. *Clin Pharmacol Ther* 2001; **69**(3): 89-95.

233. Ottenhoff THM, Ellner JJ, Kaufmann SHE. Ten challenges for TB biomarkers. *Tuberculosis (Edinb)* 2012; **92**: S17-S20.
234. Fletcher HA, Dockrell HM. Human biomarkers: can they help us to develop a new tuberculosis vaccine? *Future Microbiol* 2016; **11**: 781-7.
235. Zumla AI, Schito M, Maeurer M. Advancing the portfolio of tuberculosis diagnostics, drugs, biomarkers, and vaccines. *Lancet Infect Dis* 2014; **14**(4): 267-9.
236. Dockrell HM. Towards new TB vaccines: what are the challenges? *Pathog Dis* 2016; **74**(2016): ftw016.
237. Elias D, Akuffo H, Britton S. PPD induced in vitro interferon gamma production is not a reliable correlate of protection against *Mycobacterium tuberculosis*. *Trans R Soc Trop Med Hyg* 2005; **99**(5): 363-8.
238. Mittrucker HW, Steinhoff U, Kohler A, et al. Poor correlation between BCG vaccination-induced T cell responses and protection against tuberculosis. *Proc Natl Acad Sci U S A* 2007; **104**(30): 12434-9.
239. Kagina BM, Abel B, Scriba TJ, et al. Specific T cell frequency and cytokine expression profile do not correlate with protection against tuberculosis after bacillus Calmette-Guerin vaccination of newborns. *Am J Respir Crit Care Med* 2010; **182**(8): 1073-9.
240. Bhatt K, Verma S, Ellner JJ, Salgame P. Quest for correlates of protection against tuberculosis. *Clin Vaccine Immunol* 2015; **22**(3): 258-66.
241. White MJ, Nielsen CM, McGregor RH, Riley EH, Goodier MR. Differential activation of CD57-defined natural killer cell subsets during recall responses to vaccine antigens. *Immunology* 2014; **142**(1): 140-50.
242. Fletcher HA, Schragger L. TB vaccine development and the End TB Strategy: importance and current status. *Trans R Soc Trop Med Hyg* 2016; **110**(4): 212-8.
243. Brennan MJ, Tanner R, Morris S, et al. The Cross-Species Mycobacterial Growth Inhibition Assay (MGIA) Project, 2010-2014. *Clin Vaccine Immunol* 2017; **24**(9).
244. Tanner R, O'Shea MK, Fletcher HA, McShane H. *In vitro* mycobacterial growth inhibition assays: A tool for the assessment of protective immunity and evaluation of tuberculosis vaccine efficacy. *Vaccine* 2016: 0264-410X.
245. Wallis RS, Palaci M, Vinhas S, et al. A whole blood bactericidal assay for tuberculosis. *J Infect Dis* 2001; **183**(8): 1300-3.
246. Wallis RS, Vinhas SA, Johnson JL, et al. Whole blood bactericidal activity during treatment of pulmonary tuberculosis. *J Infect Dis* 2003; **187**(2): 270-8.
247. Kampmann B, Gaora PO, Snewin VA, Gares MP, Young DB, Levin M. Evaluation of human antimycobacterial immunity using recombinant reporter mycobacteria. *J Infect Dis* 2000; **182**(3): 895-901.

248. Cheon SH, Kampmann B, Hise AG, et al. Bactericidal activity in whole blood as a potential surrogate marker of immunity after vaccination against tuberculosis. *Clin Diagn Lab Immunol* 2002; **9**(4): 901-7.
249. Tena GN, Young DB, Eley B, et al. Failure to control growth of mycobacteria in blood from children infected with human immunodeficiency virus and its relationship to T cell function. *J Infect Dis* 2003; **187**(10): 1544-51.
250. Kampmann B, Tena GN, Mzazi S, Eley B, Young DB, Levin M. Novel human in vitro system for evaluating antimycobacterial vaccines. *Infect Immun* 2004; **72**(11): 6401-7.
251. Fletcher HA, Tanner R, Wallis RS, et al. Inhibition of mycobacterial growth in vitro following primary but not secondary vaccination with *Mycobacterium bovis* BCG. *Clin Vaccine Immunol* 2013; **20**(11): 1683-9.
252. Tanner R, O'Shea MK, White AD, et al. The influence of haemoglobin and iron on in vitro mycobacterial growth inhibition assays. *Sci Rep* 2017; **7**: 43478.
253. Tullius MV, Harmston CA, Owens CP, et al. Discovery and characterization of a unique mycobacterial heme acquisition system. *Proc Natl Acad Sci U S A* 2011; **108**(12): 5051-6.
254. Baguma R, Penn-Nicholson A, Smit E, et al. Application of a whole blood mycobacterial growth inhibition assay to study immunity against *Mycobacterium tuberculosis* in a high tuberculosis burden population. *PLoS One* 2017; **12**(9): e0184563.
255. Silver RF, Li Q, Boom WH, Ellner JJ. Lymphocyte-dependent inhibition of growth of virulent *Mycobacterium tuberculosis* H37Rv within human monocytes: requirement for CD4+ T cells in purified protein derivative-positive, but not in purified protein derivative-negative subjects. *J Immunol* 1998; **160**(5): 2408-17.
256. Worku S, Hoft DF. In vitro measurement of protective mycobacterial immunity: antigen-specific expansion of T cells capable of inhibiting intracellular growth of bacille Calmette-Guerin. *Clin Infect Dis* 2000; **30 Suppl 3**: S257-61.
257. Hoft DF, Worku S, Kampmann B, et al. Investigation of the relationships between immune-mediated inhibition of mycobacterial growth and other potential surrogate markers of protective *Mycobacterium tuberculosis* immunity. *J Infect Dis* 2002; **186**(10): 1448-57.
258. Mangtani P, Nguipdop-Djomo P, Keogh RH, et al. Observational study to estimate the changes in the effectiveness of bacillus Calmette-Guerin (BCG) vaccination with time since vaccination for preventing tuberculosis in the UK. *Health Technol Assess* 2017; **21**(39): 1-54.
259. Smith SG, Zelmer A, Blitz R, Fletcher HA, Dockrell HM. Polyfunctional CD4 T-cells correlate with in vitro mycobacterial growth inhibition following *Mycobacterium bovis* BCG-vaccination of infants. *Vaccine* 2016; **34**(44): 5298-305.
260. Parra M, Yang AL, Lim J, et al. Development of a murine mycobacterial growth inhibition assay for evaluating vaccines against *Mycobacterium tuberculosis*. *Clin Vaccine Immunol* 2009; **16**(7): 1025-32.

261. Marsay L, Matsumiya M, Tanner R, et al. Mycobacterial growth inhibition in murine splenocytes as a surrogate for protection against *Mycobacterium tuberculosis* (M. tb). *Tuberculosis (Edinb)* 2013; **93**(5): 551-7.
262. Zelmer A, Tanner R, Stylianou E, et al. A new tool for tuberculosis vaccine screening: Ex vivo Mycobacterial Growth Inhibition Assay indicates BCG-mediated protection in a murine model of tuberculosis. *BMC Infect Dis* 2016; **16**: 412.
263. Jensen C, Lindebo Holm L, Svensson E, Aagaard C, Ruhwald M. Optimisation of a murine splenocyte mycobacterial growth inhibition assay using virulent *Mycobacterium tuberculosis*. *Sci Rep* 2017; **7**(1): 2830.
264. Carpenter E, Fray L, Gormley E. Cellular responses and *Mycobacterium bovis* BCG growth inhibition by bovine lymphocytes. *Immunol Cell Biol* 1997; **75**(6): 554-60.
265. Denis M, Wedlock DN, Buddle BM. Ability of T cell subsets and their soluble mediators to modulate the replication of *Mycobacterium bovis* in bovine macrophages. *Cell Immunol* 2004; **232**(1-2): 1-8.
266. Worku S, Hoft DF. Differential effects of control and antigen-specific T cells on intracellular mycobacterial growth. *Infect Immun* 2003; **71**(4): 1763-73.
267. Spencer CT, Abate G, Sakala IG, et al. Granzyme A produced by gamma(9)delta(2) T cells induces human macrophages to inhibit growth of an intracellular pathogen. *PLoS Pathog* 2013; **9**(1): e1003119.
268. Brill KJ, Li Q, Larkin R, et al. Human natural killer cells mediate killing of intracellular *Mycobacterium tuberculosis* H37Rv via granule-independent mechanisms. *Infect Immun* 2001; **69**(3): 1755-65.
269. Chen T, Blanc C, Eder AZ, et al. Association of Human Antibodies to Arabinomannan With Enhanced Mycobacterial Opsonophagocytosis and Intracellular Growth Reduction. *J Infect Dis* 2016; **214**(2): 300-10.
270. Naranbhai V, Fletcher HA, Tanner R, et al. Distinct Transcriptional and Anti-Mycobacterial Profiles of Peripheral Blood Monocytes Dependent on the Ratio of Monocytes: Lymphocytes. *EBioMedicine* 2015; **2**(11): 1619-26.
271. Cowley SC, Elkins KL. CD4+ T cells mediate IFN-gamma-independent control of *Mycobacterium tuberculosis* infection both in vitro and in vivo. *J Immunol* 2003; **171**(9): 4689-99.
272. Kolibab K, Parra M, Yang AL, Perera LP, Derrick SC, Morris SL. A practical in vitro growth inhibition assay for the evaluation of TB vaccines. *Vaccine* 2009; **28**(2): 317-22.
273. Diacon AH, Maritz JS, Venter A, van Helden PD, Dawson R, Donald PR. Time to liquid culture positivity can substitute for colony counting on agar plates in early bactericidal activity studies of antituberculosis agents. *Clin Microbiol Infect* 2012; **18**(7): 711-7.
274. Siddiqi SH, Rüsç-Gerdes S. Procedure Manual For BACTEC MGIT 960 TB System 2006. http://www.finddiagnostics.org/export/sites/default/resource-centre/find_reports/pdfs/mgit_manual_nov_2007.pdf (accessed 20 February 2018).

275. Bowness R, Boeree MJ, Aarnoutse R, et al. The relationship between *Mycobacterium tuberculosis* MGIT time to positivity and cfu in sputum samples demonstrates changing bacterial phenotypes potentially reflecting the impact of chemotherapy on critical sub-populations. *J Antimicrob Chemother* 2015; **70**(2): 448-55.

Title: Historical BCG vaccination combined with drug treatment enhances inhibition of mycobacterial growth *ex vivo* in human peripheral blood cells

Author list:

Satria Arief Prabowo (1)(2), Andrea Zelmer (1)(2), Lisa Stockdale (1)(2), Utkarsh Ojha (3), Steven G. Smith (1)(2), Karin Seifert (1), Helen A. Fletcher (1)(2)

Affiliations:

- (1) Department of Immunology and Infection, Faculty of Infectious and Tropical Diseases, London School of Hygiene and Tropical Medicine, UK
- (2) Tuberculosis Centre, London School of Hygiene and Tropical Medicine, UK
- (3) Faculty of Medicine, Imperial College School of Medicine, Imperial College London, London, UK

Correspondence to: Satria Arief Prabowo, Department of Immunology and Infection, Faculty of Infectious and Tropical Diseases, London School of Hygiene and Tropical Medicine, London, WC1E 7HT, UK. satria.prabowo@lshtm.ac.uk

Registry

T: +44(0)20 7299 4646

F: +44(0)20 7299 4656

E: registry@lshtm.ac.uk

RESEARCH PAPER COVER SHEET

PLEASE NOTE THAT A COVER SHEET MUST BE COMPLETED FOR EACH RESEARCH PAPER INCLUDED IN A THESIS.

SECTION A – Student Details

Student	Satria Arief Prabowo
Principal Supervisor	Prof Helen A. Fletcher
Thesis Title	Accelerating Development of Therapeutic Tuberculosis Vaccines using an <i>Ex Vivo</i> Immune Assay Platform

If the Research Paper has previously been published please complete Section B, if not please move to Section C

SECTION B – Paper already published

Where was the work published?	-		
When was the work published?	-		
If the work was published prior to registration for your research degree, give a brief rationale for its inclusion	-		
Have you retained the copyright for the work?*	Choose an item.	Was the work subject to academic peer review?	Choose an item.

**If yes, please attach evidence of retention. If no, or if the work is being included in its published format, please attach evidence of permission from the copyright holder (publisher or other author) to include this work.*

SECTION C – Prepared for publication, but not yet published

Where is the work intended to be published?	Scientific Reports
Please list the paper's authors in the intended authorship order:	Satria Arief Prabowo, Andrea Zelmer, Lisa Stockdale, Utkarsh Ojha, Steven G. Smith, Karin Seifert, Helen A. Fletcher
Stage of publication	Submitted, undergoing review

SECTION D – Multi-authored work

<p>For multi-authored work, give full details of your role in the research included in the paper and in the preparation of the paper. (Attach a further sheet if necessary)</p>	<p>I conceived the research idea, designed the experiments, performed laboratory works and analysed the results with advice from my supervisor and co-authors. I lead the preparation and wrote the draft of the manuscript, and implemented revisions following discussion and comments from my supervisor and co-authors.</p>
---	---

Student Signature:  _____

Date: 17/09/2018

Supervisor Signature:  _____

Date: 18/09/2018

Abstract

Tuberculosis (TB) is a leading infectious cause of death globally. Drug treatment and vaccination with Bacillus Calmette-Guérin (BCG) remain the main strategies to control TB. With the emergence of drug resistance, it has been proposed that a combination of TB vaccination with pharmacological treatment may provide a greater therapeutic value. We implemented an *ex vivo* mycobacterial growth inhibition assay (MGIA) to discriminate vaccine responses in historically BCG-vaccinated human volunteers and to assess the contribution of vaccine-mediated immune response towards the killing effect of mycobacteria in the presence of the antibiotics: isoniazid (INH) and rifampicin (RIF), in an attempt to develop the assay as a screening tool for therapeutic TB vaccines. BCG vaccination significantly enhanced the ability of INH to control mycobacterial growth *ex vivo*. The BCG-vaccinated group displayed a higher production of IFN- γ and IP-10 when peripheral blood mononuclear cells (PBMC) were co-cultured with INH, with a similar trend with RIF. A significantly higher frequency of IFN- γ^+ and TNF- α^+ CD3 $^-$ CD4 $^-$ CD8 $^-$ cells was observed, suggesting the role of Natural Killer (NK) cells in the combined effect between BCG vaccination and INH. Taken together, our data indicate the efficacy of INH can be augmented following historical BCG vaccination, which support findings from previous observational and animal studies.

Introduction

Tuberculosis (TB) is a leading infectious cause of death worldwide. Over the past 200 years, the disease has killed one billion people, surpassing any other infectious disease¹. In 2016, it is estimated that TB affected 10.4 million people and killed 1.7 million individuals². The WHO “End TB” strategy aims to end the global TB epidemic in 2035 by reducing TB incidence by up to 90% and deaths by 95%³. Optimising the use of current, and developing new tools are essential to achieve the desired goals.

Drug treatment and vaccination remain the main strategies currently being used to control the TB epidemic caused by *Mycobacterium tuberculosis* (*Mtb*). The current treatment regimen for drug-sensitive TB lasts for 6 months and consists of several first-line drugs. Although the regimen provides 95% cure rates for drug-sensitive TB⁴, it is still considered lengthy and has led to poor adherence for patients in many settings⁵. Moreover, the emergence of multi-drug resistant (MDR)-TB, which is defined as resistance towards isoniazid (INH) and rifampicin (RIF) – the two major first-line TB drugs – has challenged the effectiveness of chemotherapy in the future⁶.

Bacillus Calmette-Guérin (BCG), a live attenuated strain of *Mycobacterium bovis*, is the only vaccine licensed for TB. BCG is widely used to prevent TB in children since the 1970s as an important part of the Expanded Program on Immunization and has since been given more than 4 billion times⁷. BCG is known to be 80% protective in the UK, although the vaccine is considered to have a variable efficacy in countries closer to the equator towards the prevention of pulmonary TB in adults^{8,9}. Combining TB vaccination with

drug treatment has been proposed to shorten treatment duration and prevent relapse, an approach known as therapeutic vaccination^{10,11}. An early animal study by Dhillon and Mitchison (1989) demonstrated the beneficial effect of drug therapy combined with previous BCG vaccination in the guinea pig¹². In a more recent study by Shang *et al* (2012), prior BCG vaccination as an adjunct to chemotherapy significantly improved survival of guinea pigs challenged with a virulent strain of *Mtb*¹³.

A therapeutic vaccination strategy for TB is expected to provide benefits in the context of treatment for both active and latent TB. Evidence from leprosy, a disease caused by the same genus of mycobacteria, demonstrates the synergistic effect between historical BCG vaccination and rifampicin prophylaxis treatment for the disease, increasing treatment efficacy up to 80%^{14,15}. Despite this, there are few studies which attempt to administer TB vaccines therapeutically after infection for enhancement of TB drug efficacy. This is partly due to the historical experience with tuberculin, a crude extract of *Mtb*, which resulted in an exacerbated immune response when administered therapeutically in active TB patients (known as the “Koch phenomenon”). However, at that time tuberculin was administered alone due to the lack of treatment options. Recently, it was shown that the occurrence of such exacerbated response is associated with bacterial load¹⁶. Therefore, it is suggested that a therapeutic TB vaccine needs to be administered following chemotherapy after the bacterial load has been sufficiently reduced, hence ensuring safety and allowing a beneficial synergistic effect⁷.

In order for a novel TB vaccination strategy to be implemented, its efficacy needs to be demonstrated in large and expensive trials¹⁷. Recently, funders have become more

reluctant to provide the required investment due to the risk of failure¹⁸. As there are currently at least a dozen TB vaccine candidates in the clinical trial pipeline and more candidates under pre-clinical development¹⁹, an effort to screen these candidates at early phases is needed to prioritise which candidates should be tested with the available funding and field sites. In the context of therapeutic vaccination, a screening effort will be essential to narrow down the optimum vaccine and drug regimen before progressing to larger clinical trials.

In this study, an *ex vivo* mycobacterial growth inhibition assay (MGIA) was implemented to measure vaccine-induced bacterial growth inhibition in combination with drug treatment following historical BCG vaccination in healthy human volunteers. In the absence of an immune correlate of protection following TB vaccination, the use of MGIA as a functional assay has gained much interest recently for its ability to assess the cumulative effect of multiple immune components on the control of mycobacterial growth²⁰⁻²². Various cell types are known to play roles in protection against TB, such as lymphocytes, macrophages, dendritic cells and natural killer (NK) cells²³. Here, the findings of our study, which evaluates the ability of the MGIA to discriminate the impact of historical BCG vaccination towards the *ex vivo* killing effect of mycobacteria in the presence of the antibiotics INH and RIF, were presented. This study, which provides proof-of-principle of the potential of the MGIA to measure a synergistic effect between vaccination and chemotherapy, is important as the MGIA can be used to further expedite the development of therapeutic vaccination strategies for TB. Our study shows the ability of the MGIA to capture vaccine mediated growth inhibition, even in the presence of

effective drugs that substantially reduce mycobacterial growth, and supports the implementation of the MGIA as a screening tool for therapeutic TB vaccine candidates.

Materials and Methods

Ethics statement. Participants were recruited under a protocol approved by the LSHTM Observational Research Ethics Committee (ref 8762). Written informed consent was obtained from all individuals prior to enrolment in the study. All procedures were performed in accordance with the Declaration of Helsinki, as agreed by the World Medical Association General Assembly (Washington, 2002) and ICH Good Clinical Practice (GCP).

Study participants and blood sampling. This was an observational study in healthy adults with (i) no history of BCG vaccination or (ii) a history of BCG vaccination more than 6 months before study enrolment. Participants were aged 18 to 70 years with no evidence of exposure or infection with TB. Participants were excluded if they were suffering from any persistent medical condition or infection. Sample size was calculated based on the assumption of effect size 0.75, with power 0.8 and significance level 0.05 (participants per group = 29). Peripheral blood was collected at the amount of 50 ml and processed within 6 hours. Blood samples were collected in tubes containing sodium heparin (Sigma-Aldrich, Dorset, UK).

PBMCs isolation and IFN- γ ELISpot. Peripheral blood mononuclear cells (PBMCs) were isolated from heparinised whole blood by centrifugation over 15 ml LymphoPrep (Stemcell, Cambridge, UK) in a LeucoSep tube (Greiner Bio-One, Stonehouse, UK) according to the manufacturer's instruction. PBMCs were cryopreserved in FBS (Labtech International Ltd, Uckfield, UK) containing 10% DMSO (Sigma-Aldrich) and stored in -80 °C freezer using CoolCell containers (VWR International, Lutterworth, UK). PBMCs were thawed and an *ex vivo* interferon (IFN)- γ enzyme-linked immunospot (ELISpot) assay was performed to assess antigen-specific response as previously described²². In brief, PBMCs were incubated overnight for 18 hours with 20 μ g/ml purified protein derivative (PPD) (Oxford Biosystem, Oxfordshire, UK). Positive control Phytohemagglutinin (PHA) (10 μ g/ml, Sigma-Aldrich) and negative control (medium-only) wells were included for each participant samples.

***Ex vivo* Mycobacterial Growth Inhibition Assay (MGIA).** Cryopreserved PBMCs were thawed and rested for 2 hours at 37 °C in antibiotic-free medium [RPMI-1640 (Sigma-Aldrich) + 10% pooled human AB serum (Sigma-Aldrich) + 2 mM L-Glutamine (Fisher Scientific, Loughborough, UK)] containing 10 U/ml benzonase (Insight Biotechnology, Wembley, UK). After the rest, the cells were counted, washed and re-suspended in the above-mentioned medium without benzonase. The percent viability of recovered cells was around 70 to 90% per vial. A 2-ml screw-cap tube containing 3×10^6 PBMCs in 600 μ l of medium was co-cultured with ~100 Colony Forming Units (CFU) of BCG for 4 days on a 360° rotator (VWR International, UK) at 37°C. BCG Pasteur Aeras strain was obtained from Aeras (Rockville, MD, USA) and used as the immune target in the MGIA. In order to assess the potential enhancing effect of historical BCG

vaccination towards *ex vivo* drug-mediated killing of mycobacteria, 6 μ l of drug at different concentrations was added in the MGIA system to the samples from each participant. The drug final concentrations on the co-culture system were 1; 0.1 and 0.01 μ g/ml for INH and 0.5; 0.1 and 0.01 μ g/ml for RIF. A control tube without drug was also set-up for each participant. INH and RIF were obtained from Sigma-Aldrich, UK and stock solutions were prepared in sterile tissue culture grade water and DMSO, respectively, as per manufacturer's instruction.

After 4 days, the 2-ml tubes were centrifuged at 12,000 rpm for 10 minutes. The MGIA supernatants (500 μ l) were transferred to other 2 ml tubes and frozen at -80 °C for further analysis. The remaining cells were then lysed by addition of 400 μ l of sterile tissue culture grade water and vortexed 3 times with 5-minutes intervals. Lysate containing mycobacteria was transferred to a Bactec MGIT tube supplemented with PANTA antibiotics and oleic acid-albumin-dextrose-catalase (OADC) enrichment broth (all from Becton Dickinson, Oxford, UK). The tube was placed in a Bactec MGIT 960 and incubated until registered positive (measured as time to positivity [TTP]). Use of a standard curve enables conversion of the TTP into bacterial numbers (log CFU) (Supplementary Fig. S1). All work with cells pre-BCG infection and involving BCG infected samples was done in a Biosafety Level (BSL) 2 laboratory.

ELISA. MGIA supernatants were analysed to assess cytokine concentrations by enzyme-linked immunosorbent assay (ELISA). The levels of following cytokines were measured: IFN- γ , tumor necrosis factor alpha (TNF- α), interleukin (IL)-12p40, IL-10, IL-17, IL-6, granulocyte-macrophage colony-stimulating factor (GM-CSF) and interferon-gamma-

induced protein 10 (IP-10). The concentrations of IFN- γ , IL-12p40 and IL-6 were measured using BD OptiEIA kits (Becton Dickinson, UK), while TNF- α , GM-CSF and IP-10 DuoSet ELISA kits were obtained from R&D Systems (Abingdon, UK) and IL-10 ELISA MAX Standard and IL-17 ELISA MAX Deluxe kits were supplied from BioLegend (London, UK). Assays were performed as described by the manufacturers.

Intracellular cytokine staining (ICS) assay and flow cytometry. PBMCs were thawed and rested for 2 hours in a 37°C incubator with 5% CO₂ after addition of 10 U/ml of benzonase. PBMCs were then incubated alone (medium only as negative control), with 5 μ g/ml *Staphylococcus* enterotoxin B (SEB; Sigma, UK) as a positive control and with ~100 CFU BCG (as per the MGIA protocol), with and without 1 μ g/ml of INH for the latter. Incubation with BCG was performed for 4 days and the addition of SEB was performed on Day 3. Two hours after the addition of SEB to the positive control tubes, brefeldin A (Sigma, UK) was added to all tubes which were then incubated for 18 hours at 37°C until Day 4.

Following incubation, cells were washed with ICS FACS buffer (PBS + 0.1% BSA + 0.01% sodium azide) and stained with Vivid live/dead reagent (Invitrogen) for 10 minutes at 4°C in the dark. Cells were then surface stained with anti-CD4-APC (BD Biosciences), anti-CD19-eFluor450 and anti-CD14-eFluor450 (eBiosciences) for 30 minutes at 4°C in the dark. After washing with FACS buffer, cells were permeabilised with Cytofix/Cytoperm reagent (BD Biosciences) at 4°C for 20 min, washed in Perm Wash buffer (BD Biosciences) and stained with anti-CD3-Horizon-BV510, anti-IL-2-FITC, anti-TNF α -PE-Cy7 (BD Biosciences), anti-CD8-PE (eBiosciences) and anti-IFN γ -

PerCPCy5.5 (Biolegend) for 30 min at room temperature in the dark. Cells were finally resuspended in 250 μ L 1% paraformaldehyde (Sigma, UK) and filtered prior to acquisition.

Data was acquired using an LSRII flow cytometer (BD Biosciences) and FACSDiva acquisition software (BD Biosciences). Compensation was performed using tubes of OneComp eBeads (ThermoFisher, UK) individually stained with each fluorophor and compensation matrices were calculated with FACSDiva. ICS flow cytometry data was analysed using FlowJo software version 10.4 (TreeStar Inc., Ashland, OR, USA). Samples were gated sequentially on singlet, live, CD14⁻CD19⁻, CD3⁺ (lymphoid), CD4⁺, CD8⁺, CD3⁺ CD4⁻ CD8⁻ (double negative = DN), CD3⁻ CD4⁻ CD8⁻ (triple negative = TN) cells and negative control stimulation tubes were used to set cytokine gates (see Supplementary Fig. S2).

Median cytokine responses in negative control tubes, as a percentage of the gated CD4⁺ T-cell population, were as follows: IFN- γ – 0.07%; IL-2 – 0.09%; TNF- α – 0.40%. Median cytokine responses in positive control tubes (SEB-stimulated) were as follows: IFN- γ – 3.16%; IL-2 – 4.24%; TNF- α – 24.35%. See Supplementary Table S1 for median cytokine responses of the gated CD8⁺ and DN T-cells as well as TN cells. Cytokine responses reported for all stimuli were after subtraction of background values measured in un-stimulated tubes. The median number of cellular events acquired for all tubes was 168,591 (IQR: 103871 – 225963).

Statistical analysis. Statistical analyses were performed in GraphPad Prism 7 (GraphPad, La Jolla, CA, USA). To identify statistical significance of *ex vivo* growth inhibition (log

CFU values) and ELISA responses, one-way analysis of variance (ANOVA) and students *t*-test were used. Mann-Whitney *U* Test was performed to identify significant differences of the ELISpot and ICS responses between groups. Spearman’s correlation coefficient was used to test for correlations between growth inhibition and immune responses.

Results

Study participants. Fifty participants were enrolled in the study; 21 vaccine-naïve volunteers with no history of BCG vaccination and 29 volunteers previously vaccinated with BCG (average time since vaccination 25.4 years prior to enrolment). Table 1 summarises the demographic characteristics of the study participants. Almost 70% of the BCG-vaccinated participants were from the UK.

Table 1. Demographics of participants enrolled in the study.

Characteristic	Total Participants : 50	
	BCG-naïve (n = 21)	BCG-vaccinated (n = 29)
Female [no. (%)]	17 (81.0 %)	15 (51.7 %)
Median age [yr (range)]	30 (22 – 69)	33 (22 – 63)
Average time since BCG vaccination [yr (range)]	-	25.4 (9 – 52)
Country of Origin UK [no. (%)]	5 (23.8 %)	20 (69 %)

IFN- γ ELISpot response to PPD and assessment of *ex vivo* growth inhibition. The IFN- γ ELISpot assay was performed to measure the magnitude of mycobacteria-specific response from historically BCG-vaccinated and BCG-naïve participants. The secretion of IFN- γ in response to PPD was elevated in the samples from vaccinated individuals in comparison to unvaccinated individuals (median SFC 106.5 and 24, $P < 0.0001$, Fig. 1A). The growth inhibition assay was performed to assess impact of BCG vaccination on *ex vivo* mycobacterial growth. The assay was termed ‘growth inhibition’ as the immune responses in the vaccinated group are expected to inhibit the growth of mycobacteria compared to the naïve group during the 4-days co-culture. Using cryopreserved PBMCs, the assay showed enhanced mycobacterial growth inhibition in PBMCs from BCG-vaccinated compared to BCG-naïve individuals (median log CFU 2.027 and 2.334, $P < 0.05$, Fig. 1B). There was no statistically significant correlation between IFN- γ ELISpot response and mycobacterial growth ($P = 0.121$, Spearman $r = -0.22$, data shown in Appendix 8A of this thesis).

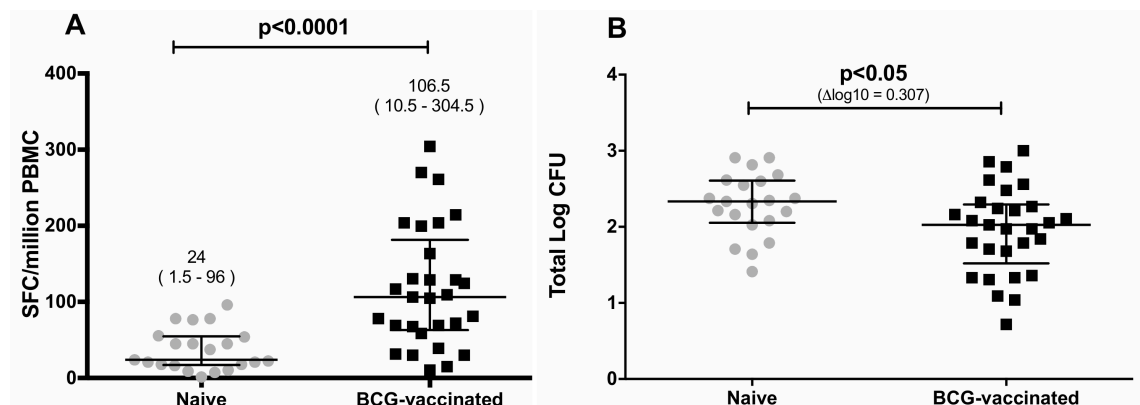


Figure 1. Immune response (A) and growth inhibition (B) following historical BCG vaccination. Assessment was performed from 21 BCG-naïve and 29 BCG-vaccinated participants. (A) IFN- γ production following stimulation with PPD was compared (Mann-Whitney test). Numbers above each group represent median (range). SFC, spot forming cells. (B) Growth inhibition was compared using BCG input ~ 100 CFU as immune target

(unpaired t-test). Data are presented as total number of log CFUs per sample, which was determined by use of a standard curve. Dots and squares represent individual data points, and the central lines indicate the median response with inter-quartile range (IQR).

Drug titration curves and impact of historical BCG vaccination on drug-mediated *ex vivo* growth inhibition. Drug concentrations were selected to achieve a concentration range where we could observe a decrease in bacterial growth, but sufficient bacterial load to identify any synergistic effect of vaccination in addition to the drug. Previous studies have identified the minimum inhibitory concentration (MIC) of INH and RIF towards BCG Pasteur to be 0.1 and 0.063-0.125 µg/ml, respectively²⁴. The drug concentration of 0.1 µg/ml was chosen as it closely depicts the MIC value of INH and RIF. Concentrations were then selected above and below that to assess potential synergistic effects. As expected, there were significant reductions of bacterial growth when BCG was co-cultured with PBMC and 0.1 and 1 µg/ml of INH ($P = 0.0001$, Fig. 2A and 2B), as well as 0.1 and 0.5 µg/ml of RIF ($P = 0.0053$ and $P = 0.0001$, Fig. 2D and 2E) in both BCG-naïve and vaccinated groups. Findings in this study were consistent with previously published results regarding the MIC and drug susceptibility of BCG Pasteur²⁴.

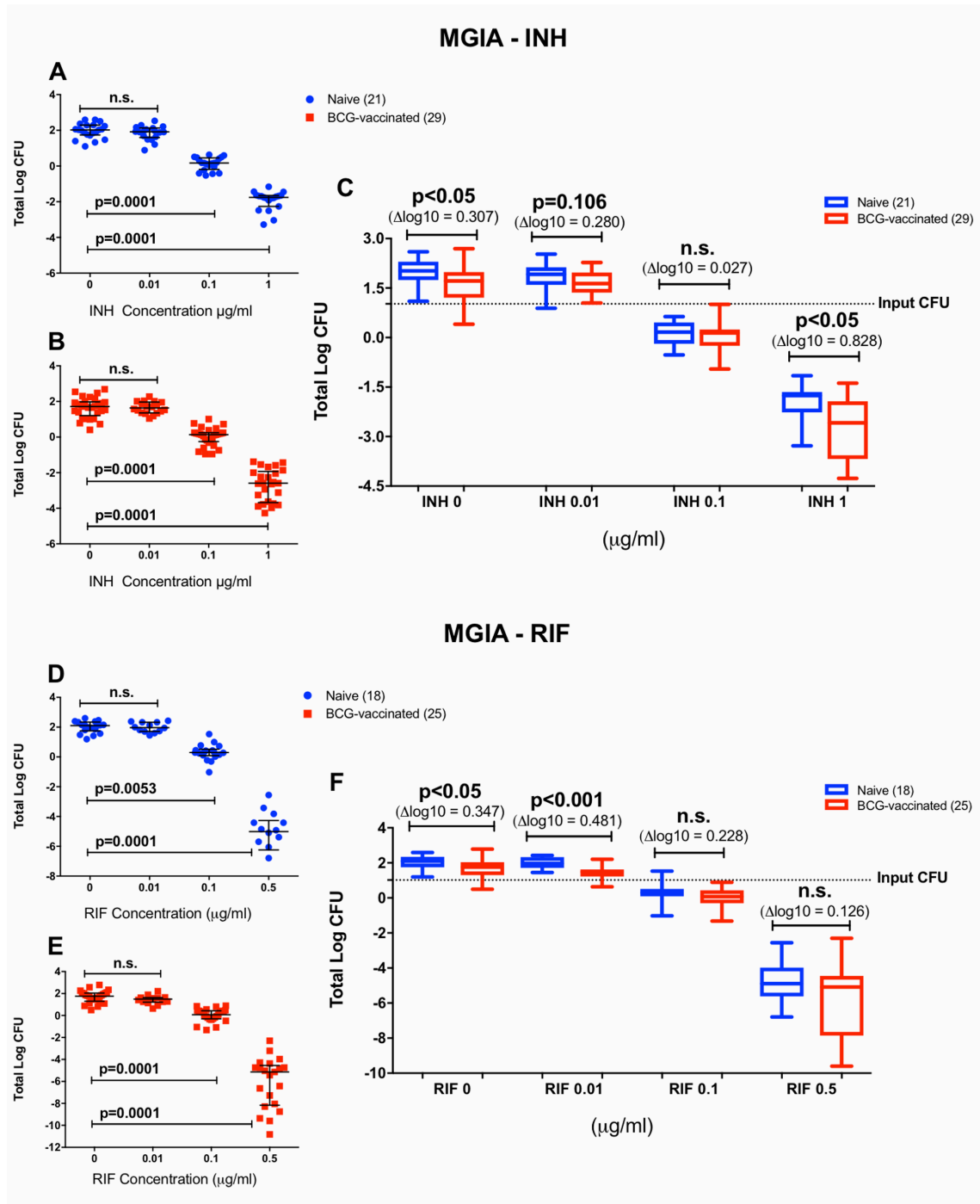


Figure 2. Growth inhibition in the absence and presence of INH (A-C) and RIF (D-E). Mycobacterial growth was assessed in titration curves. INH inhibited mycobacterial growth in a dose-dependent manner in the naïve and vaccinated groups (A and B), as well as RIF (D and E). Data from both groups was compiled in dose-response box plots to identify the BCG effect in addition to the INH- and RIF-mediated killing (C and F). Dots and squares in the titration curves (A – B and D – E) represent individual data points from the participants and the central lines indicate the median response with IQR. Each group is represented in a single box plot with range in the dose-response analysis (C and F).

Samples size is indicated in the figure (for INH: n=29 BCG-vaccinated and n=21 BCG-naïve participants; for RIF: n=25 BCG-vaccinated and n=18 BCG-naïve participants). Statistical significances were tested using one-way ANOVA (A– B and D – E) and unpaired t-test (C and F).

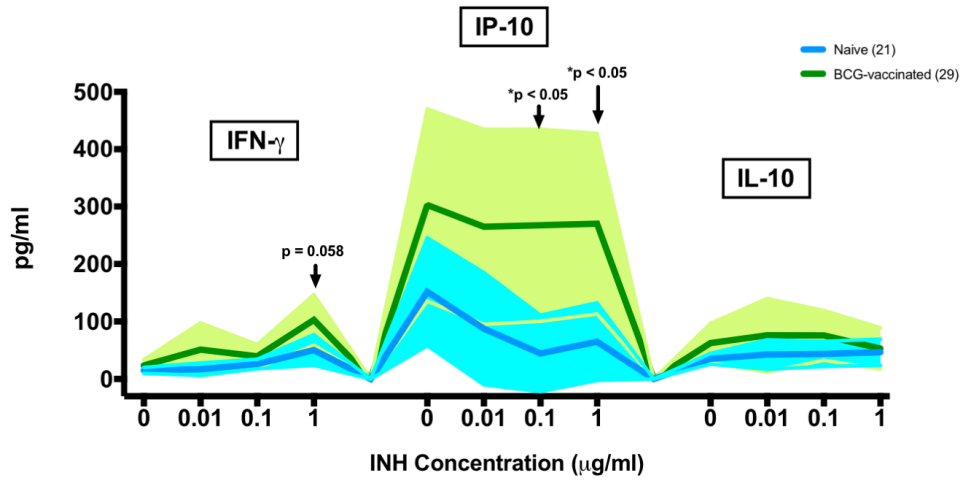
To determine if historical BCG vaccination enhanced the drug effect, data from each BCG-naïve and vaccinated group were plotted in dose response box plots to observe the vaccine impact at various drug concentrations (Fig. 2C and 2F). BCG vaccination significantly enhanced the ability of INH to control mycobacterial growth at the concentration of 1 µg/ml ($P < 0.05$), with a similar trend at 0.01 µg/ml but not at 0.1 µg/ml (Fig. 2C). The effect size of growth inhibition at INH concentration of 1 µg/ml was greater (0.8 log) compared to at the absence of drug (0.3 log). Meanwhile, BCG vaccination did not enhance the control of mycobacterial growth at RIF concentrations of 0.1 and 0.5 µg/ml and the difference was only statistically significant at 0.01 µg/ml (Fig. 2F). The slope of the titration curve was steeper with RIF compared to INH even though a lower maximum concentration of RIF was used (0.5 µg/ml). The log CFU values were obtained by converting the recorded time to positivity (TTP) of the Bactec MGIT 960 used for quantification using a standard curve (see Supplementary Fig. S1). Negative log CFU values indicate low growth of mycobacteria which were still detected using the MGIT machine and extrapolated using the standard curve.

Cytokine release associated with *ex vivo* growth inhibition. ELISA assays were performed using the MGIA supernatant to investigate cytokine productions (IFN- γ , IP-10, IL-10, TNF- α , IL-12p40, GM-CSF, IL-6 and IL-17) which may be associated with *ex vivo* growth inhibition at all drug concentrations. A higher production of IP-10 was

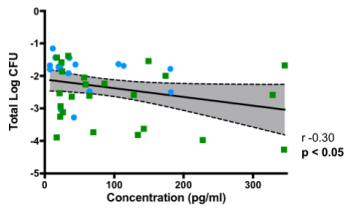
observed in the BCG-vaccinated group compared to the BCG-naïve group when PBMC were co-cultured with 1 µg/ml of INH ($P < 0.05$, Fig. 3A), with a similar non-significant increase of IFN- γ ($P = 0.058$). At this drug concentration, there was a statistically significant inverse correlation between IFN- γ production and *ex vivo* growth inhibition (Spearman $r = -0.30$, $P < 0.05$, Fig. 3B). Notably, this was where we observed a significant difference in the MGIA assay. A significant increase of IP-10 was also observed in the BCG-vaccinated group at INH concentration of 0.1 µg/ml (Fig. 3A). Moreover, there was a significant positive correlation between IL-10 production and higher growth of mycobacteria at 1 µg/ml INH (Spearman $r = 0.33$, $P < 0.05$, Fig. 3D), although we did not see significant differences of IL-10 production between vaccination groups at various INH concentrations (Fig. 3A). Other cytokines measured using co-culture supernatants with INH are summarised in Supplementary Table S2. In general, there appears to be higher cytokine productions in the historically BCG-vaccinated participants when compared to the BCG-naïve, in the presence and absence of drugs.

Similarly to INH, a higher production of IP-10 in the vaccinated group was also observed during the co-culture with RIF at the concentration of 0.1 and 0.5 µg/ml ($P < 0.05$, Fig. 3E), compared to the BCG-naïve group. There was a significant positive correlation between IL-10 production and higher growth of mycobacteria at a RIF concentration of 0.1 µg/ml (Spearman $r = 0.37$, $P < 0.05$, Supplementary Table S2), with a similar trend at the concentration of 0.01 µg/ml (Spearman $r = 0.34$, $P = 0.087$, Fig. 3H). Other cytokines measured using co-culture supernatants with RIF are summarised in Supplementary Table S2.

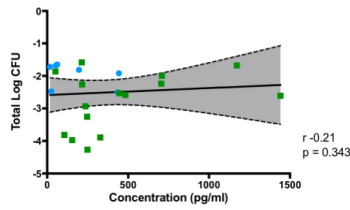
A INH Cytokine Production



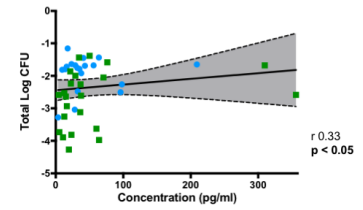
B IFN- γ - Mycobacterial growth (INH 1 $\mu\text{g/ml}$)



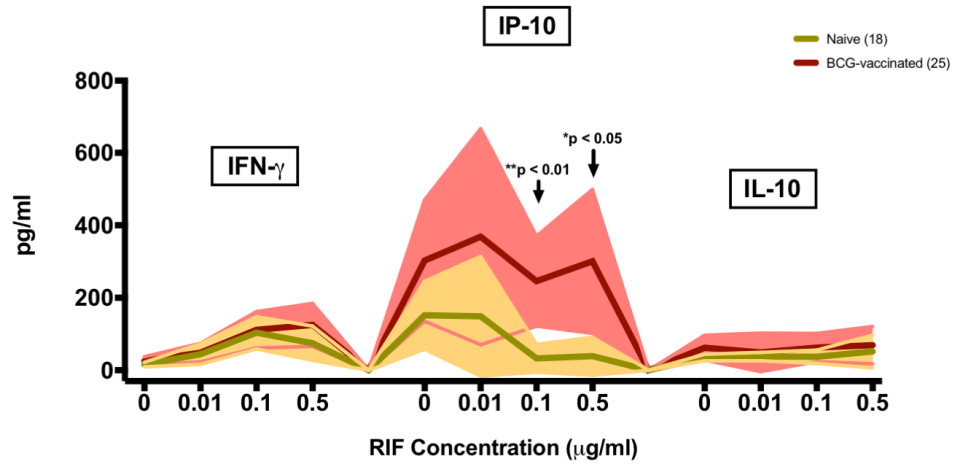
C IP-10 - Mycobacterial growth (INH 1 $\mu\text{g/ml}$)



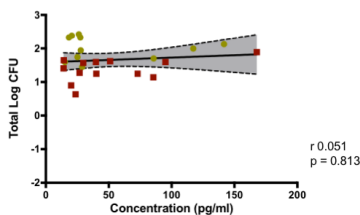
D IL-10 - Mycobacterial growth (INH 1 $\mu\text{g/ml}$)



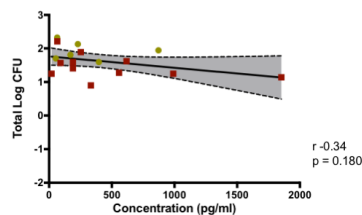
E RIF Cytokine Production



F IFN- γ - Mycobacterial growth (RIF 0.01 $\mu\text{g/ml}$)



G IP-10 - Mycobacterial growth (RIF 0.01 $\mu\text{g/ml}$)



H IL-10 - Mycobacterial growth (RIF 0.01 $\mu\text{g/ml}$)

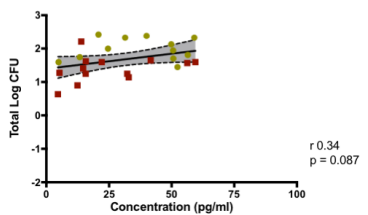


Figure 3. Cytokine responses from co-culture with INH (A-D) and RIF (E-H). MGIA supernatants were analysed for the released cytokines IFN- γ , IP-10 and IL-10. For INH, dark blue and dark green lines and symbols indicate BCG-naïve and BCG-vaccinated groups, respectively. For RIF, these were represented by dark brown (BCG-naïve) and dark red (BCG-vaccinated). Lines indicate mean response and shadings indicate range (A and E). Comparison of responses between BCG-vaccinated and BCG-naïve groups at different drug concentrations were performed using unpaired *t*-test. Correlation between mycobacterial growth at INH concentration of 1 $\mu\text{g/ml}$ and the production of IFN- γ (B), IP-10 (C) and IL-10 (D) were assessed using Spearman's correlation. Correlation between mycobacterial growth at RIF concentration of 0.01 $\mu\text{g/ml}$ (based on the significant difference in the MGIA assay) and the production of IFN- γ (F), IP-10 (G) and IL-10 (H) were also assessed (Spearman's). Note: for the correlations, non-responders were excluded, defined as responses below the following cut-off of the ELISA assays: 7.5 pg/ml (IFN- γ), 5 pg/ml (IP-10) and 3.5 pg/ml (IL-10). Refer to Supplementary Table S2 for comparison and correlation of other cytokines responses.

Intracellular Staining Flow Cytometry. Intracellular cytokine staining of BCG-stimulated PBMCs followed by flow cytometry analysis was performed to detect the ability of historical BCG vaccination to induce cytokine-secreting lymphocytes during the co-culture with drug and BCG. ICS flow cytometry enabled the simultaneous detection of CD4⁺ and CD8⁺ T-cells as well as CD3⁺ CD4⁻ CD8⁻ DN T-cells and CD3⁻ CD4⁻ CD8⁻ TN cells, and secretion of cytokines such as IFN- γ , TNF- α and IL-2 in BCG-stimulated PBMCs (see Supplementary Fig. S2 for gating strategy). The selected drug concentration was 1 $\mu\text{g/ml}$ of INH as the vaccine effect was most notable at this concentration and a significant correlation with cytokine response, in particular with IFN- γ and IP-10, was observed.

In this experiment, a low dose input of BCG (~100 CFU) was used for the stimulation over 4 days to mimic the condition of the *ex vivo* MGIA experiment. Historical BCG vaccination was shown to result in an antigen-specific Th-1 response which was detectable in the ICS assay upon stimulation with BCG bacteria (Fig. 4). There was a

significantly higher frequency of BCG-specific CD4⁺ T-cells expressing IL-2 in the historically BCG-vaccinated group compared to the naïve in the absence of drug (mean frequency 0.160% and 0.011%, respectively, $P < 0.01$, Fig. 4B). Although statistical significance was not arrived at, there was also slightly higher expressions of IFN- γ (mean frequency 0.01% and 0.0075%) and TNF- α (mean frequency 0.0875% and 0.015%) in the BCG-vaccinated group compared to the naïve (Fig. 4A and 4C, respectively). Cytokine expression of BCG-specific CD8⁺ T-cells appeared to follow the same pattern, despite the responses were lower compared to the CD4⁺ T-cells and did not reach significance (Fig. 4 D-E). The ICS panel used in this experiment allowed us to further look at two other lymphocyte populations: double-negative CD3⁺ CD4⁻ CD8⁻ T-cells, which consist primarily of $\gamma\delta$ T-cells and CD4⁻ CD8⁻ TCR- $\alpha\beta$ ⁺ T-cells, and triple-negative CD3⁻ CD4⁻ CD8⁻ cells which are primarily natural-killer cells²³. In the absence of drug, the frequencies of TN cells expressing IFN- γ and TNF- α appeared to be higher in the BCG-vaccinated group compared to the naïve, although it did not reach significance (Fig. 4 J-L), and no observed difference of the cytokine expression from DN T-cells (Fig. 4 G-I).

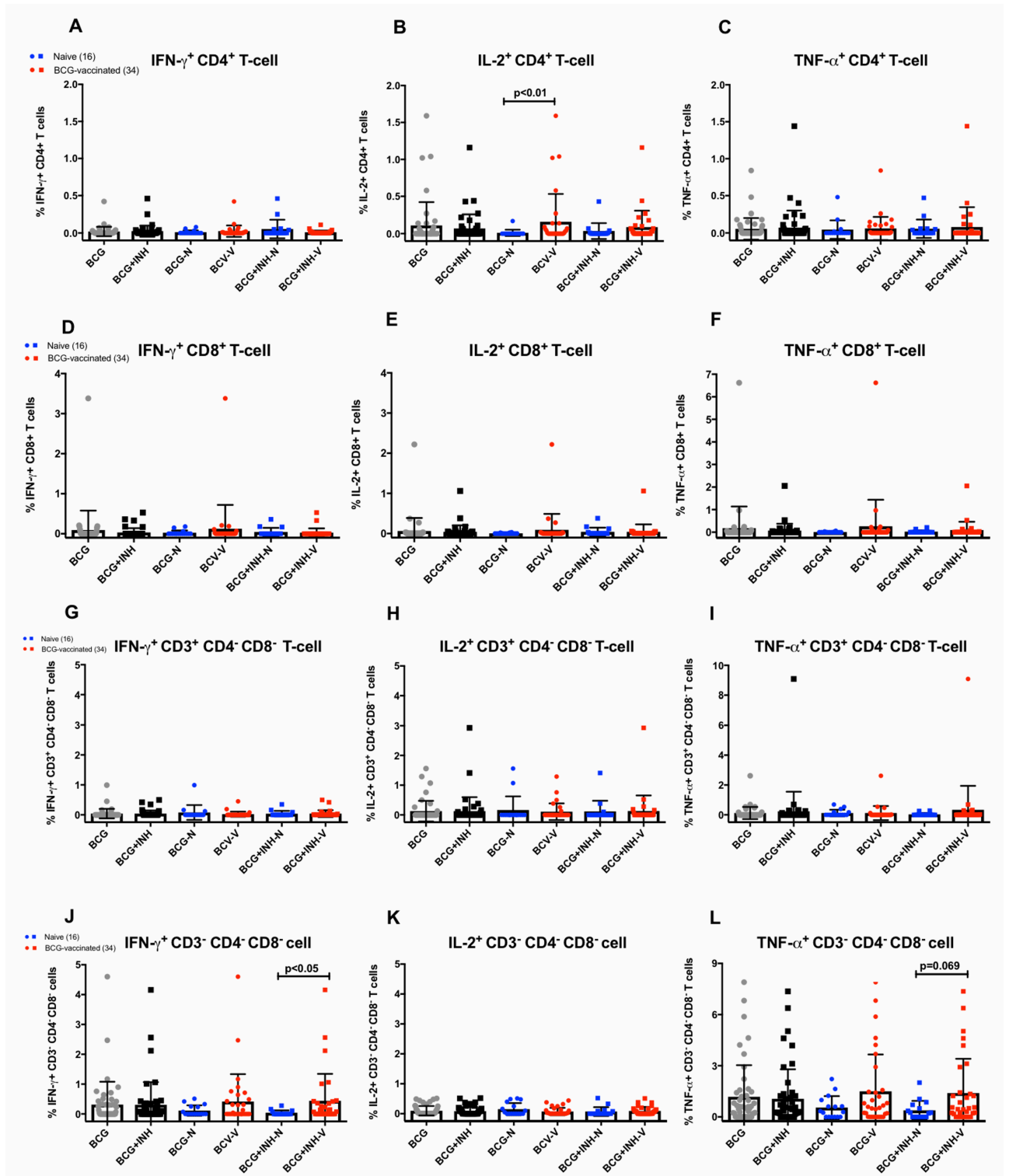


Figure 4. Frequencies of Th1 cytokine-expressing lymphocytes. Expressions were measured from PBMCs after stimulation with BCG, with and without 1 μ g/ml of INH, for 4 days. The grey dot symbols represent stimulation with BCG only, while the black squares represent BCG+INH. Comparisons were made between the naïve (blue) and historically BCG-vaccinated (red) groups. Data is displayed as bar graphs and error bars

represent mean \pm standard deviation (SD). For this experiment, PBMCs from a different cohort of participants were used, consisted of 16 naïve and 34 historically BCG-vaccinated participants, with a similar demographics profile and immune responses as the previously described. The Mann-Whitney U test was used to determine significance. The P value < 0.05 is considered statistically significant.

When the co-culture stimulation was performed in the presence of INH to investigate the source of increased IFN- γ production observed in the ELISA assay, a significantly higher frequency of IFN- γ ⁺ triple-negative cells was observed in the BCG-vaccinated group compared to the naïve (mean frequency 0.439% and 0.04%, respectively, $P < 0.05$, Fig. 4J), suggesting NK cells as a potential source of IFN- γ which could be enhanced in the presence of drugs. A trend of a higher frequency of TNF- α ⁺ TN cells was also observed (mean frequency 1.4% and 0.388%, $P = 0.069$, Fig. 4L). There was no differential cytokine expression from CD4⁺, CD8⁺ and double-negative T-cells during the co-culture with 1 $\mu\text{g/ml}$ of INH, proposing the role of a T-cell independent mechanism on the potential synergistic effect of historical BCG vaccination and drug-mediated growth inhibition which has been observed in our *ex vivo* MGIA assay.

As the triple-negative CD3⁻ CD4⁻ CD8⁻ cells identified in this study were thought to be mostly NK cells, surface-staining flow cytometry was performed on unstimulated PBMCs from the above cohort using markers for NK cells (CD3⁻ CD56⁺). There was a significant correlation between the frequency of CD3⁻ CD4⁻ CD8⁻ cells and the frequency of NK cells ($P = 0.0001$, Fig. 5A). Moreover, a trend of inverse correlation was observed between the frequency of NK cells and *ex vivo* mycobacterial growth in the absence of drug ($P = 0.059$, Spearman $r = -0.27$, Fig. 5B), suggesting a role for NK cells in the control of mycobacterial growth. As the frequency of the triple-negative CD3⁻ CD4⁻ CD8⁻ cells

was also increased in the BCG-vaccinated group during co-culture with 1 µg/ml of INH, evidence suggests that the triple-negative cells represent NK cells and they contribute to the increased IFN- γ production associated with the combined effect between historical BCG-vaccination and *ex vivo* drug-mediated killing of INH.

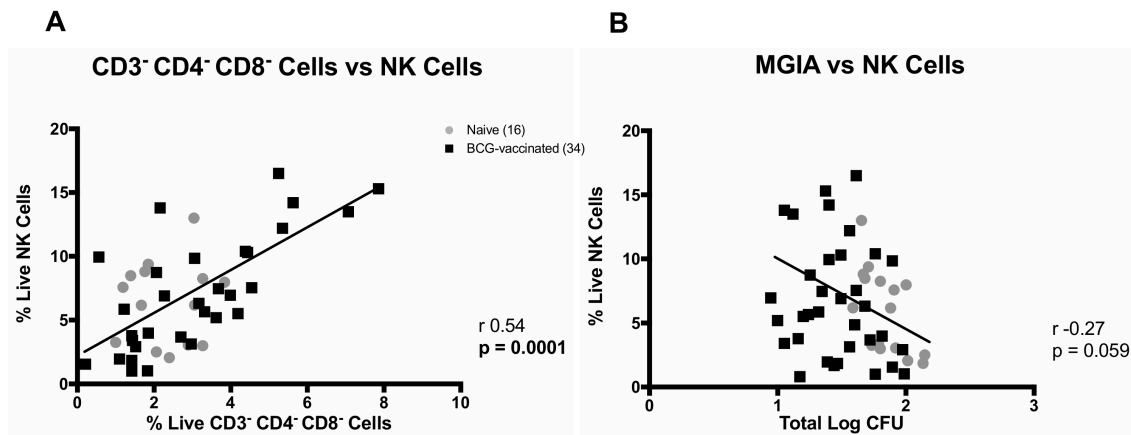


Figure 5. NK cells correlations. The frequency of CD3⁺ CD4⁺ CD8⁺ cells was correlated with NK cells (CD3⁺ CD56⁺) (A) and the *ex vivo* mycobacterial growth was associated with the NK cells frequency (Spearman's correlation) (B). Surface-staining flow cytometry was performed to characterise NK cells. PBMCs from 16 naïve and 34 historically BCG-vaccinated participants were used.

Discussion

Participants with historical BCG vaccination in our study were shown to elicit stronger IFN- γ response towards PPD antigen as well as better control of mycobacterial growth *ex vivo*. The average time since BCG vaccination was 25.4 years. Here, most of the BCG-vaccinated participants were from the UK, where BCG vaccination is known to be 80% protective⁸. Recent studies by Mangtani *et al.* provided evidence that protection from BCG in the UK population could last at least up to 20 years^{25,26}, which is consistent with

the finding of our study. Several studies in other settings also reported detectable protection following BCG vaccination for over than 20 years²⁷⁻²⁹.

There was no significant correlation between IFN- γ production and *ex vivo* control of mycobacterial growth in our study cohort. This supports the notion that an IFN- γ response is only in part essential for control of mycobacterial growth. Recently, higher IFN- γ has been shown to correlate with lower risk of developing TB disease following BCG vaccination³⁰, although some studies suggested otherwise^{23,31}. In the Fletcher *et al.* study, CD4 T-cell activation was shown to correlate with increased TB risk, suggesting an interplay of immune pathways of risk and protection in the same individual³⁰. The IFN- γ based assay has been recommended by a WHO panel to be used in TB vaccine trials³² and our findings support the notion that a functional assay, which measures the summative effect of immune response following vaccination, might be useful in addition to the IFN- γ -based assay.

In this study using human PBMC, INH and RIF as two front-line anti-TB drugs were tested. Both drugs are used for drug-sensitive TB treatment and have been regarded as key for success in current short-course chemotherapy. However, their effectiveness has been challenged by the emergence of MDR-TB and the effort to improve current treatment is indispensable. As BCG is a live, replicating mycobacteria, administration of BCG at the time of treatment may lead to clearance of BCG, thereby preventing the establishment of a vaccine-specific immune response. In this study, however, the impact of historical BCG vaccination was investigated towards mycobacterial growth inhibition in the presence of effective anti-mycobacterial drugs. This study serves as a proof-of-

principle for testing and screening therapeutic TB vaccine candidates in combination with drugs using the *ex vivo* MGIA system prior or in adjunct to *in vivo* animal or human testing.

Historical BCG vaccination was shown to enhance the ability of PBMC to inhibit mycobacterial growth in the absence of drug and to further enhance the efficacy of INH at the concentration of 1 µg/ml. Interestingly, this concentration is close to the therapeutic level of INH in the plasma during treatment in human, which ranges from 2 – 5 µg/ml^{33,34}. As the effect size of the growth inhibition was greater during the co-culture with 1 µg/ml INH compared to the absence of drug, this is considered to reflect a specific combined effect of historical BCG vaccination with INH. We did not observe any impact of historical BCG vaccination at the higher concentration of RIF. Rifampicin has been known to be very potent *in vitro*³⁵, as demonstrated in our *ex vivo* system at the tested RIF concentration (0.1 and 0.5 µg/ml) and reflected in the steeper dose-response curve compared to INH. Therefore, as RIF was highly effective we could not observe any impact of historical BCG vaccination on RIF efficacy, despite the increased cytokine production observed in the ELISA assay.

The enhancement of the *ex vivo* INH killing effect with BCG vaccination is consistent with a survival study in guinea-pigs conducted by Shang *et al* (2012) in which the vaccination was shown to improve the effectiveness of combined therapy and prolong survival¹³. In that study, prior administration of BCG in adjunct to therapy was superior compared to therapy alone. An earlier study by Dhillon and Mitchison (1989) also assessed the impact of previous BCG vaccination in animal models towards INH and

RIF¹². The study used an intravenous infection model of TB and chemotherapy was started soon after challenge. In the guinea-pig, BCG vaccination reduced the bacterial count in the spleen after 20 days when administered in adjunct to INH. A similar trend was also observed with RIF notably during the first 14 days of the experiment, although the difference did not reach significance, comparable to our findings using the *ex vivo* MGIA system.

With regard to INH, the drug is currently used as a prophylaxis treatment for individuals with latent TB, given for 9 months with an efficacy ranging from 60 – 90% for prevention of active TB³⁶. A large observational prospective cohort study in Lima, Peru demonstrated the synergistic effect between historical BCG vaccination and INH prophylaxis, which was greater than each of the interventions alone in preventing active TB in household contacts of TB patients³⁷. In the context of leprosy, historical BCG vaccination is known to boost the efficacy of RIF prophylaxis therapy. While RIF prophylaxis and historical BCG vaccination alone were shown to provide 58% and 57% protection against leprosy, the combination of both provided 80% protection in the study enrolling a large number of participants¹⁴. Findings in these studies suggest that there might be a beneficial effect of historical BCG vaccination on drug treatment which could have been underappreciated. This is the first time the additive effect of immunoprophylaxis by routine BCG vaccination and chemoprophylaxis with INH was demonstrated using an *ex vivo* system and our results warrant further investigation in future epidemiological studies.

The mechanism of BCG-induced protection is thought to be via a CD4⁺ Th1 type response, with evidence showing that BCG-specific IFN- γ response measured with ELISpot was associated with reduced TB disease risk over the early years of life³⁰. Nevertheless, there is emerging evidence that other T-cell subsets (such as CD8⁺ and $\gamma\delta$ T-cells) and NK cells may play a role in BCG-induced immune protection²³. The guinea-pig study by Shang *et al* suggested a possible mechanism for BCG enhancement of TB drug efficacy. In the animal study, combining BCG with drug therapy induced an increase in activated CD4 T cells co-expressing CD45^{hi} and CT4⁺ as measured in blood, which was not observed in guinea-pigs receiving BCG alone¹³. In our study, although the *ex vivo* IFN- γ ELISPOT was not associated with growth inhibition, we observed increased IFN- γ and IP-10 in the vaccinated group compared to the naïve, measured by ELISA, in the MGIA culture supernatant when PBMCs were co-cultured with INH. Moreover, IL-10 was shown to enhance the growth of mycobacteria *ex vivo* in the presence of drugs, although the impact appears to be independent from the vaccine effect. IFN- γ promotes macrophage activation by enhancing phagosomal maturation, inducing NO-dependent apoptosis and modulating autophagy thus enhancing mycobacterial clearance³⁸. While CD4 T-cells are known to be a major source of IFN- γ ; CD8 T-cells, NK cells, $\gamma\delta$ T-cells and CD1-restricted T-cells also produce IFN- γ during infection with mycobacteria³⁹.

Flow-cytometry was used to identify the cellular source of IFN- γ in MGIA supernatants and the assay provided evidence in supporting NK cells as the likely source of the cytokine. Recently, it was demonstrated that the production of IFN- γ and TNF- α by NK cells is functionally linked to their cytotoxic activities⁴⁰. In this study, increased frequencies of IFN- γ ⁺ and TNF- α ⁺ triple-negative CD3⁻ CD4⁻ CD8⁻ cells were associated

with the combined effect of BCG vaccination and INH. On the basis of our results, it is alluded that historical BCG vaccination enhances an NK cell response which contributes to *ex vivo* killing effect through the release of pro-inflammatory cytokines and cytotoxic granules.

Findings of this study are consistent with, and provide an explanation to, a recently published study by Jensen and colleagues (2017)⁴¹, in which a similar *ex vivo* MGIA system was used to assess protection from a TB vaccine candidate using a mouse model. While their study demonstrated a correlation between IFN- γ release and growth inhibition, the cellular source was not found among the investigated vaccine-specific T-cells, suggesting other cell populations such as the NK cells as a potential source. In a human study conducted in South Africa by the Scriba group, administration of BCG following isoniazid preventive therapy in latently-infected TB adults was associated with long-lived NK cells responses⁴². Evidence from immunological studies following immunisation with malaria and rabies vaccines have revealed the important role of NK cells in protection from vaccine-preventable diseases through their activation by antigen-specific CD4 T cell-derived IL-2^{43,44}. Moreover, a distinct subset of human NK cells expressing HLA-DR are known to expand in response to IL-2 and might aid immune responses to BCG⁴⁵. In this study, an increased frequency of IL-2⁺ CD4 T-cells was observed in the historically-vaccinated participants upon stimulation with BCG, suggesting that this cytokine could drive a BCG-specific enhancement of the NK cells responsible for improved *ex vivo* killing effect in the presence of INH.

In conclusion, this study has demonstrated the combined effect between historical BCG vaccination and INH using an *ex vivo* system which support findings from previous observational and animal studies. Therapeutic vaccination aims to administer vaccine during TB treatment with the hope to improve treatment success and shorten duration of treatment⁷, and although several therapeutic TB vaccine candidates are available in the pipeline (reviewed in⁴⁶), more are needed. Therefore, the MGIA platform offers an *ex vivo* assay that could help to identify and accelerate the development of candidate therapeutic TB vaccines using human PBMC samples. The present human study has highlighted the role of NK cells in the combined effect between vaccination and drug treatment, suggesting that NK cells could be further explored as a target for a novel therapeutic vaccine against TB.

Acknowledgements

We would like to thank Carolynne Stanley for participant recruitment and blood sample collection, and Ayad Eddaoudi for assistance with flow cytometry. We thank Dr Gregory Bancroft for useful discussion. We also thank Erni Marlina for technical advices. H.A.F. has received support for this project from EC HORIZON2020 TBVAC2020 (grant no. 643381). S.A.P. received a PhD scholarship from the Indonesian Endowment Fund for Education (LPDP). K.S. was supported by the UK Medical Research Council (MRC) and the UK Department for International Development (DFID) under the MRC/DFID Concordat agreement (grant reference MR/J008702/1).

Author Contributions

S.A.P. and H.A.F. designed the experiments. S.A.P. performed laboratory work and analysed the results supervised by H.A.F., K.S. and S.G.S. A.Z., L.S. and U.O. participated in the MGIA and ELISpot experiments. S.A.P. wrote the draft of the manuscript. All authors reviewed and approved the final version of the manuscript.

Competing interest: All authors declare no competing interests.

References

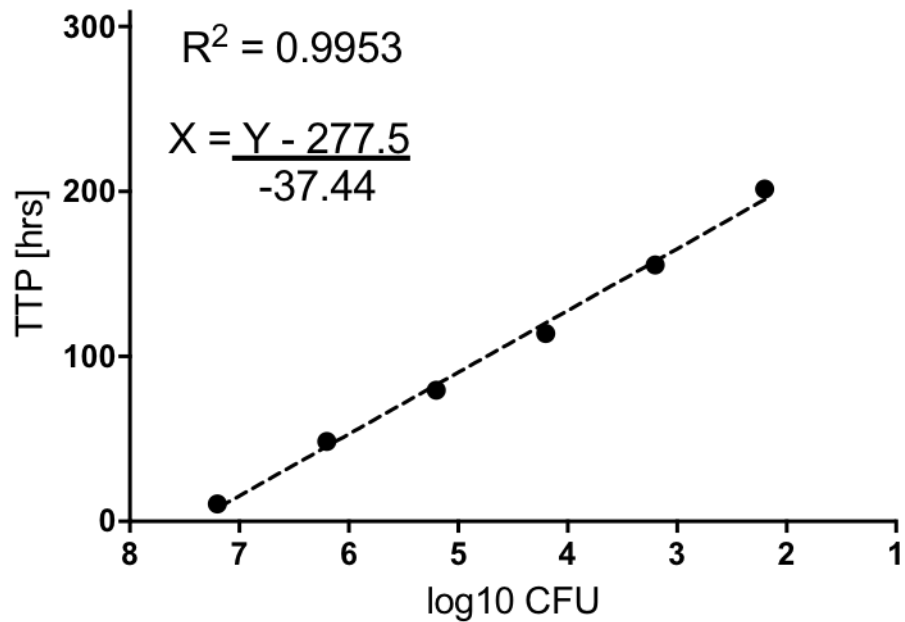
1. Paulson T. Epidemiology: A mortal foe. *Nature* 2013; **502**(7470): S2-3.
2. World Health Organization. Global Tuberculosis Report. *WHO, Geneva*, 2017.
3. Uplekar M, Weil D, Lonnroth K, et al. WHO's new End TB Strategy. *Lancet* 2015; **S0140-6736**(15): 60570-3.
4. World Health Organization. Treatment of Tuberculosis Guideline: Fourth Edition. Geneva, 2010.
5. Dheda K, Barry CE, Maartens G. Tuberculosis. *Lancet* 2016; **387**(10024): 1211-26.
6. Dheda K, Gumbo T, Maartens G, et al. The epidemiology, pathogenesis, transmission, diagnosis, and management of multidrug-resistant, extensively drug-resistant, and incurable tuberculosis. *Lancet Respir Med* 2017; **5**(4): 291-360.
7. Prabowo SA, Groschel MI, Schmidt ED, et al. Targeting multidrug-resistant tuberculosis (MDR-TB) by therapeutic vaccines. *Med Microbiol Immunol* 2013; **202**(2): 95-104.
8. Mangtani P, Abubakar I, Ariti C, et al. Protection by BCG vaccine against tuberculosis: a systematic review of randomized controlled trials. *Clin Infect Dis* 2014; **58**(4): 470-80.
9. Kaufmann SH, Weiner J, von Reyn CF. Novel approaches to tuberculosis vaccine development. *Int J Infect Dis* 2017; **56**: 263-7.
10. Schon T, Lerm M, Stendahl O. Shortening the 'short-course' therapy- insights into host immunity may contribute to new treatment strategies for tuberculosis. *J Intern Med* 2013; **273**(4): 368-82.
11. Zumla A, Chakaya J, Hoelscher M, et al. Towards host-directed therapies for tuberculosis. *Nat Rev Drug Discov* 2015; **14**(8): 511-2.
12. Dhillon J, Mitchison DA. Influence of BCG-induced immunity on the bactericidal activity of isoniazid and rifampicin in experimental tuberculosis of the mouse and guinea-pig. *Br J Exp Pathol* 1989; **70**(1): 103-10.
13. Shang S, Shanley CA, Caraway ML, et al. Drug treatment combined with BCG vaccination reduces disease reactivation in guinea pigs infected with *Mycobacterium tuberculosis*. *Vaccine* 2012; **30**(9): 1572-82.
14. Schuring RP, Richardus JH, Pahan D, Oskam L. Protective effect of the combination BCG vaccination and rifampicin prophylaxis in leprosy prevention. *Vaccine* 2009; **27**(50): 7125-8.
15. Richardus JH, Oskam L. Protecting people against leprosy: chemoprophylaxis and immunoprophylaxis. *Clin Dermatol* 2015; **33**(1): 19-25.

16. Gil O, Guirado E, Gordillo S, et al. Intragranulomatous necrosis in lungs of mice infected by aerosol with *Mycobacterium tuberculosis* is related to bacterial load rather than to any one cytokine or T cell type. *Microbes Infect* 2006; **8**(3): 628-36.
17. Tameris MD, Hatherill M, Landry BS, et al. Safety and efficacy of MVA85A, a new tuberculosis vaccine, in infants previously vaccinated with BCG: a randomised, placebo-controlled phase 2b trial. *Lancet* 2013; **381**(9871): 1021-8.
18. Fletcher HA, Dockrell HM. Human biomarkers: can they help us to develop a new tuberculosis vaccine? *Future Microbiol* 2016; **11**: 781-7.
19. Fletcher HA, Schrager L. TB vaccine development and the End TB Strategy: importance and current status. *Trans R Soc Trop Med Hyg* 2016; **110**(4): 212-8.
20. Cheon SH, Kampmann B, Hise AG, et al. Bactericidal activity in whole blood as a potential surrogate marker of immunity after vaccination against tuberculosis. *Clin Diagn Lab Immunol* 2002; **9**(4): 901-7.
21. Hoft DF, Worku S, Kampmann B, et al. Investigation of the relationships between immune-mediated inhibition of mycobacterial growth and other potential surrogate markers of protective *Mycobacterium tuberculosis* immunity. *J Infect Dis* 2002; **186**(10): 1448-57.
22. Fletcher HA, Tanner R, Wallis RS, et al. Inhibition of mycobacterial growth in vitro following primary but not secondary vaccination with *Mycobacterium bovis* BCG. *Clin Vaccine Immunol* 2013; **20**(11): 1683-9.
23. Abebe F. Is interferon-gamma the right marker for bacille Calmette-Guerin-induced immune protection? The missing link in our understanding of tuberculosis immunology. *Clin Exp Immunol* 2012; **169**(3): 213-9.
24. Ritz N, Tebruegge M, Connell TG, Sievers A, Robins-Browne R, Curtis N. Susceptibility of *Mycobacterium bovis* BCG vaccine strains to antituberculous antibiotics. *Antimicrob Agents Chemother* 2009; **53**(1): 316-8.
25. Mangtani P, Nguipdop-Djomo P, Keogh RH, et al. The duration of protection of school-aged BCG vaccination in England: a population -based case-control study. *Int J Epidemiol* 2017: 1-9.
26. Mangtani P, Nguipdop-Djomo P, Keogh RH, et al. Observational study to estimate the changes in the effectiveness of bacillus Calmette-Guerin (BCG) vaccination with time since vaccination for preventing tuberculosis in the UK. *Health Technol Assess* 2017; **21**(39): 1-54.
27. Aronson NE, Santosham M, Comstock GW, et al. Long-term efficacy of BCG vaccine in American Indians and Alaska Natives: A 60-year follow-up study. *JAMA* 2004; **291**(17): 2086-91.
28. Barreto ML, Cunha SS, Pereira SM, et al. Neonatal BCG protection against tuberculosis lasts for 20 years in Brazil. *Int J Tuberc Lung Dis* 2005; **9**(10): 1171-3.
29. Nguipdop-Djomo P, Heldal E, Rodrigues LC, Abubakar I, Mangtani P. Duration of BCG protection against tuberculosis and change in effectiveness with time since

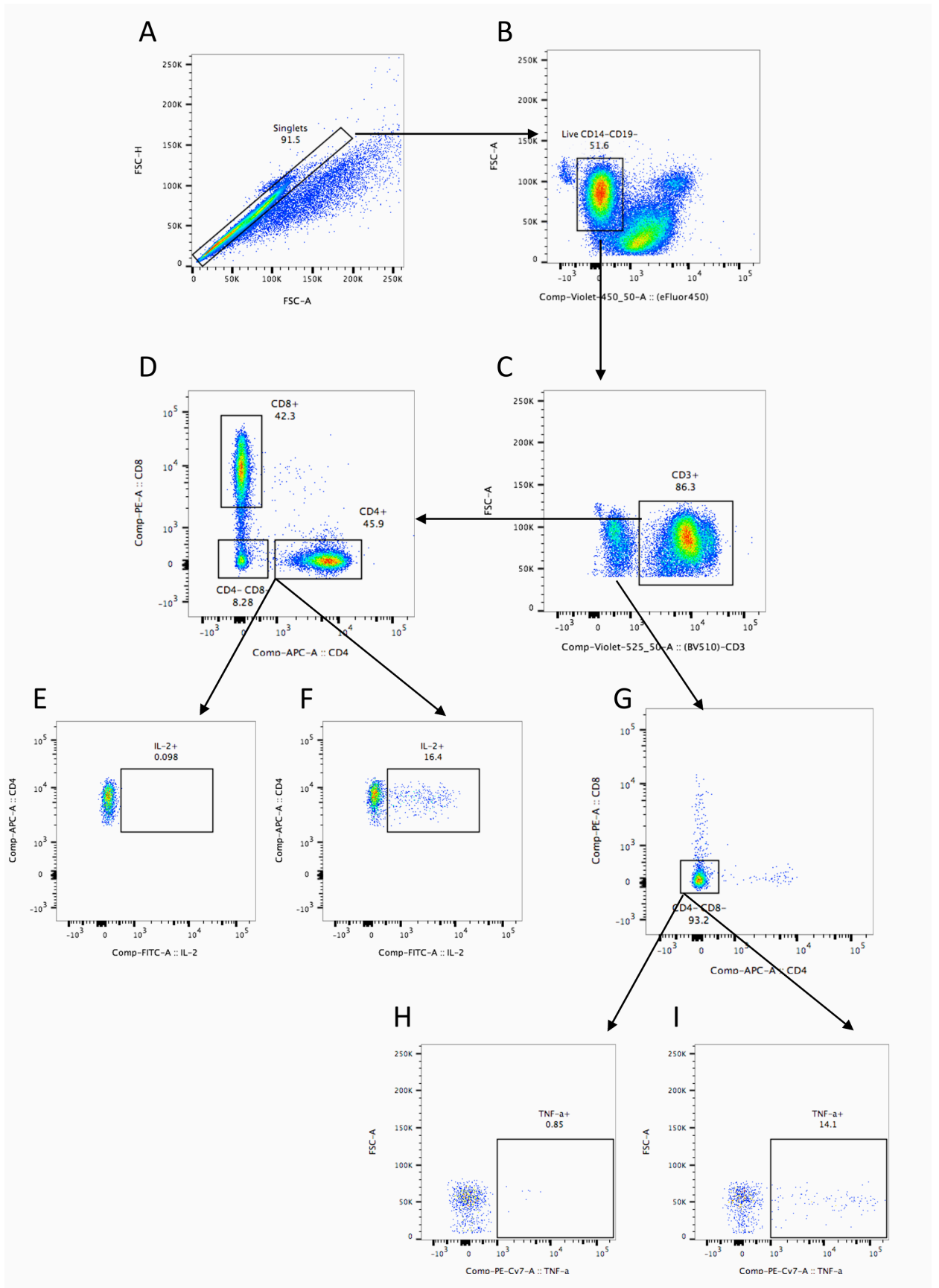
- vaccination in Norway: a retrospective population-based cohort study. *Lancet Infect Dis* 2016; **16**(2): 219-26.
30. Fletcher HA, Snowden MA, Landry B, et al. T-cell activation is an immune correlate of risk in BCG vaccinated infants. *Nat Commun* 2016; **7**: 11290.
 31. Kagina BM, Abel B, Scriba TJ, et al. Specific T cell frequency and cytokine expression profile do not correlate with protection against tuberculosis after bacillus Calmette-Guerin vaccination of newborns. *Am J Respir Crit Care Med* 2010; **182**(8): 1073-9.
 32. Hanekom WA, Dockrell HM, Ottenhoff TH, et al. Immunological outcomes of new tuberculosis vaccine trials: WHO panel recommendations. *PLoS Med* 2008; **5**(7): e145.
 33. Babalik A, Babalik A, Mannix S, Francis D, Menzies D. Therapeutic drug monitoring in the treatment of active tuberculosis. *Can Respir J* 2011; **18**(4): 225-9.
 34. Park JS, Lee JY, Lee YJ, et al. Serum Levels of Antituberculosis Drugs and Their Effect on Tuberculosis Treatment Outcome. *Antimicrob Agents Chemother* 2015; **60**(1): 92-8.
 35. Wallis RS, Palaci M, Vinhas S, et al. A whole blood bactericidal assay for tuberculosis. *J Infect Dis* 2001; **183**(8): 1300-3.
 36. Jasmer RM, Nahid P, Hopewell PC. Clinical practice. Latent tuberculosis infection. *N Engl J Med* 2002; **347**(23): 1860-6.
 37. Zelner JL, Murray MB, Becerra MC, et al. Bacillus Calmette-Guerin and isoniazid preventive therapy protect contacts of patients with tuberculosis. *Am J Respir Crit Care Med* 2014; **189**(7): 853-9.
 38. Herbst S, Schaible UE, Schneider BE. Interferon gamma activated macrophages kill mycobacteria by nitric oxide induced apoptosis. *PLoS One* 2011; **6**(5): e19105.
 39. O'Garra A, Redford PS, McNab FW, Bloom CI, Wilkinson RJ, Berry MP. The immune response in tuberculosis. *Annu Rev Immunol* 2013; **31**: 475-527.
 40. Wang R, Jaw JJ, Stutzman NC, Zou Z, Sun PD. Natural killer cell-produced IFN-gamma and TNF-alpha induce target cell cytolysis through up-regulation of ICAM-1. *J Leukoc Biol* 2012; **91**(2): 299-309.
 41. Jensen C, Lindebo Holm L, Svensson E, Aagaard C, Ruhwald M. Optimisation of a murine splenocyte mycobacterial growth inhibition assay using virulent *Mycobacterium tuberculosis*. *Sci Rep* 2017; **7**(1): 2830.
 42. Suliman S, Geldenhuys H, Johnson JL, et al. Bacillus Calmette-Guerin (BCG) Revaccination of Adults with Latent Mycobacterium tuberculosis Infection Induces Long-Lived BCG-Reactive NK Cell Responses. *J Immunol* 2016; **197**(4): 1100-10.
 43. Horowitz A, Behrens RH, Okell L, Fooks AR, Riley EM. NK cells as effectors of acquired immune responses: effector CD4+ T cell-dependent activation of NK cells following vaccination. *J Immunol* 2010; **185**(5): 2808-18.

44. Horowitz A, Hafalla JC, King E, et al. Antigen-specific IL-2 secretion correlates with NK cell responses after immunization of Tanzanian children with the RTS,S/AS01 malaria vaccine. *J Immunol* 2012; **188**(10): 5054-62.
45. Evans JH, Horowitz A, Mehrabi M, et al. A distinct subset of human NK cells expressing HLA-DR expand in response to IL-2 and can aid immune responses to BCG. *Eur J Immunol* 2011; **41**(7): 1924-33.
46. Gröschel MI, Prabowo SA, Cardona P-J, Stanford JL, Werf TSvd. Therapeutic vaccines for tuberculosis—A systematic review. *Vaccine* 2014; **32**(26): 3162-8.

Supplementary Figures



Supplementary Figure S1. Standard curve of BCG Pasteur Aeras used to convert TTP to CFU. A titration experiment was conducted to establish the relationship between log₁₀ CFU and MGIT time to positivity (TTP). Linear regression analysis was carried out in GraphPad Prism. The resulting equation was used to calculate log₁₀ CFU.



Supplementary Figure S2. ICS flow cytometry gating strategy. Gating of singlet (A), dump negative (live, CD14⁻, CD19⁻) (B), CD3⁺ lymphocytes (C) and CD4⁺, CD8⁺ as well as CD4⁻ CD8⁻ T-cells (D) was performed in sequence for each sample. Furthermore, CD3⁻ CD4⁻ CD8⁻ lymphocytes (NK cells) was also gated (G). Cytokine gates were then set on unstimulated tubes (E and H) and copied to stimulated tubes (F and I). Gating for the following cytokines were set: IFN- γ , TNF- α and IL-2, with E & F and H & I represent examples for IL-2 and TNF- α , respectively.

Supplementary Tables

Supplementary Table S1. Median cytokine responses in negative and positive control tubes of the ICS assay.

Gated cell population	Negative Control			Positive Control (SEB-stimulated)		
	IFN- γ	IL-2	TNF- α	IFN- γ	IL-2	TNF- α
CD4 ⁺ T-cell	0.07%	0.09%	0.40%	3.16%	4.24%	24.35%
CD8 ⁺ T-cell	0.19%	0.05%	0.27%	11.55%	1.88%	23.65%
CD3 ⁺ CD4 ⁻ CD8 ⁻ (DN) T-cell	0.63%	1.47%	0.80%	0.20%	0.09%	1.05%
CD3 ⁻ CD4 ⁻ CD8 ⁻ (TN) cell	0.12%	0.10%	0.85%	2.10%	1.80%	4.68%

Supplementary Table S2. Summary of mean cytokine responses measured with ELISA assays, assessed from MGIA supernatant samples from the co-culture with INH and RIF. Responses between BCG-naïve and BCG-vaccinated groups were compared using unpaired *t*-test. Correlations were investigated using Spearman's correlation at certain drug concentrations (INH 1 μ g/ml; RIF 0.01 and 0.1 μ g/ml) based on the MGIA data. For the correlations, non-responders were excluded, defined as responses below the following cut-off of the ELISA assays: 7.5 pg/ml (IFN- γ), 5 pg/ml (IP-10), 3.5 pg/ml (IL-10), 20 pg/ml (TNF- α), 8 pg/ml (IL-12p40), 1 pg/ml (GM-CSF), 10 pg/ml (IL-6) and 0 pg/ml (IL-17). ND, not detected.

Cytokines	Mean Cytokine Response (pg/ml)															
	INH								RIF							
	Without drug		0.01 µg/ml		0.1 µg/ml		1 µg/ml		Without drug		0.01 µg/ml		0.1 µg/ml		0.5 µg/ml	
	Naïve	BCG	Naïve	BCG	Naïve	BCG	Naïve	BCG	Naïve	BCG	Naïve	BCG	Naïve	BCG	Naïve	BCG
IFN-γ	15.07	23.53	17.12	51.18	26.1	39.46	50.38	102.7	15.84	25.8	44.49	48.63	103.5	111.7	74.69	125.4
	p=0.177		p=0.141		p=0.289		p=0.058		p=0.163		p=0.815		p=0.809		p=0.191	
Correlation with MGIA							r -0.30 *p=0.049				r 0.051 p=0.813		r -0.021 p=0.896			
IP-10	151.7	302.7	87.51	264.7	44.45	267.5	64.9	270.2	151.7	302.7	149	368.6	33.01	245.8	38.86	300.5
	p=0.151		p=0.064		*p=0.034		*p=0.031		p=0.151		p=0.195		*p=0.0055		*p=0.035	
Correlation with MGIA							r -0.21 p=0.343				r -0.34 p=0.180		r -0.26 p=0.258			
IL-10	35.31	62.44	42.54	76.05	43.62	75.86	46.65	53.1	35.31	62.44	37.83	49.3	37.18	62.66	51.75	69.38
	p=0.184		p=0.310		p=0.236		p=0.772		p=0.184		p=0.676		p=0.284		p=0.615	
Correlation with MGIA							r 0.33 *p=0.033				r 0.34 p=0.087		r 0.37 *p=0.019			
TNF-α	10.97	82.04	25.6	113.9	17.91	132.2	23.87	43.82	10.97	82.04	22.82	49.68	17.61	81.85	65.19	129.2
	p=0.156		p=0.199		p=0.102		p=0.499		p=0.156		p=0.610		p=0.274		p=0.510	
Correlation with MGIA							r -0.22 p=0.529				r 0.60 p=0.350		r 0.53 p=0.098			
IL-12p40	5.588	47.71	33.56	111.4	76.3	120.9	30.42	32.98	5.588	47.71	22.35	33.07	81.68	92.55	42.45	139.5
	p=0.179		p=0.169		p=0.602		p=0.923		p=0.179		p=0.722		p=0.824		p=0.324	
Correlation with MGIA							r -0.30 p=0.407				r 0.64 p=0.139		r 0.44 p=0.075			
GM-CSF	0.024	45.11	0	44.08	15.75	89.94	7.536	9.88	0.024	45.11	0.9781	8.111	5.658	35.87	4.117	57.44
	p=0.126		p=0.139		p=0.241		p=0.803		p=0.126		p=0.427		p=0.311		p=0.331	
Correlation with MGIA							r 0.080 p=0.333				r - p= -		r -0.058 p=0.933			
IL-6	250.4	335.3	289	227.4	203.3	299.7	233.6	238.4	250.4	335.3	375.8	189.9	277.5	264.1	272.1	267.1
	p=0.324		p=0.558		p=0.274		p=0.954		p=0.324		p=0.139		p=0.886		p=0.965	
Correlation with MGIA							r 0.021 p=0.911				r 0.22 p=0.424		r 0.059 p=0.759			
IL-17	ND	ND	ND	ND	ND	ND	ND	ND	ND	ND	ND	ND	ND	ND	ND	ND
	p= -		p= -		p= -		p= -		p= -		p= -		p= -		p= -	
Correlation with MGIA							r - p= -				r - p= -		r - p= -			

Title: RUTI vaccination enhances inhibition of mycobacterial growth *ex vivo* and induces a shift of monocyte phenotype in mice

Author list:

Satria Arief Prabowo (1)(2), Hannah Painter (1)(2), Andrea Zelmer (1)(2), Steven G. Smith (1)(2), Karin Seifert (1)(3), Merce Amat (4), Pere-Joan Cardona (5)(6), Helen A. Fletcher (1)(2)

Affiliations:

- (1) Department of Immunology and Infection, Faculty of Infectious and Tropical Diseases, London School of Hygiene and Tropical Medicine, London, UK
- (2) Tuberculosis Centre, London School of Hygiene and Tropical Medicine, London, UK
- (3) Department of Pharmacovigilance, Federal Institute for Drugs and Medical Devices, Bonn, Germany
- (4) Archivel Farma S.L., Badalona, Catalonia, Spain
- (5) Experimental Tuberculosis Unit (UTE), Fundació Institut Germans Trias i Pujol (IGTP), Universitat Autònoma de Barcelona (UAB), Badalona, Catalonia, Spain
- (6) Centro de Investigación Biomédica en Red de Enfermedades Respiratorias (CIBERES), Madrid, Spain

Correspondence to: Satria Arief Prabowo, Department of Immunology and Infection, Faculty of Infectious and Tropical Diseases, London School of Hygiene and Tropical Medicine, London, WC1E 7HT, UK. satria.prabowo@lshtm.ac.uk

Registry

T: +44(0)20 7299 4646

F: +44(0)20 7299 4656

E: registry@lshtm.ac.uk

RESEARCH PAPER COVER SHEET

PLEASE NOTE THAT A COVER SHEET MUST BE COMPLETED FOR EACH RESEARCH PAPER INCLUDED IN A THESIS.

SECTION A – Student Details

Student	Satria Arief Prabowo
Principal Supervisor	Prof Helen A. Fletcher
Thesis Title	Accelerating Development of Therapeutic Tuberculosis Vaccines using an <i>Ex Vivo</i> Immune Assay Platform

If the Research Paper has previously been published please complete Section B, if not please move to Section C

SECTION B – Paper already published

Where was the work published?	-		
When was the work published?	-		
If the work was published prior to registration for your research degree, give a brief rationale for its inclusion	-		
Have you retained the copyright for the work?*	Choose an item.	Was the work subject to academic peer review?	Choose an item.

**If yes, please attach evidence of retention. If no, or if the work is being included in its published format, please attach evidence of permission from the copyright holder (publisher or other author) to include this work.*

SECTION C – Prepared for publication, but not yet published

Where is the work intended to be published?	Frontiers in Immunology
Please list the paper's authors in the intended authorship order:	Satria Arief Prabowo, Hannah Painter, Andrea Zelmer, Steven G. Smith, Karin Seifert, Merce Amat, Pere-Joan Cardona, Helen A. Fletcher
Stage of publication	Submitted, undergoing review

SECTION D – Multi-authored work

<p>For multi-authored work, give full details of your role in the research included in the paper and in the preparation of the paper. (Attach a further sheet if necessary)</p>	<p>I conceived the research idea, designed the experiments, performed laboratory works and analysed the results with advice from my supervisor and co-authors. I lead the preparation and wrote the draft of the manuscript, and implemented revisions following discussion and comments from my supervisor and co-authors.</p>
---	---

Student Signature:  _____

Date: 17/09/2018

Supervisor Signature:  _____

Date: 18/09/2018

Abstract

Tuberculosis (TB) is a major global health problem and there is a need for an improved treatment. A strategy to combine vaccination with drug treatment, termed therapeutic vaccination, is expected to provide benefit in shortening treatment duration and augmenting treatment success rate. RUTI candidate vaccine has been specifically developed as a therapeutic vaccine for TB. The vaccine is shown to reduce bacillary load when administered after chemotherapy in murine and guinea pig models, and is also immunogenic when given to healthy adults and individuals with latent TB. In the absence of a validated correlate of vaccine-induced protection for TB vaccine testing, the mycobacterial growth inhibition assay (MGIA) has been developed as a comprehensive tool to evaluate vaccine potency *ex vivo*.

In this study, we investigated the potential of RUTI vaccine to control mycobacterial growth *ex vivo* and demonstrated the capacity of MGIA to help the identification of essential immune mechanisms. We found an association between the peak response of vaccine-induced growth inhibition and a shift in monocyte phenotype following RUTI vaccination in healthy mice. The vaccination significantly increased the frequency of non-classical Ly6C⁻ monocytes in the spleen after two doses of RUTI. Furthermore, mRNA expressions of Ly6C⁻-related transcripts (Nr4a1, Itgax, Pparg, Bcl2) were upregulated at the RUTI peak response. This is the first time the impact of RUTI has been assessed on monocyte phenotype. Given that non-classical Ly6C⁻ monocytes are considered to play an anti-inflammatory role, our findings in conjunction with previous studies have demonstrated that RUTI could induce a balanced immune response, promoting an effective cell-mediated response whilst at the same time limiting an

excessive inflammation. On the other hand, the impact of RUTI on non-classical monocytes could also reflect its impact on trained innate immunity which warrants further investigation.

In summary, we have demonstrated a novel mechanism of action of the RUTI vaccine, which suggests the importance of a balanced M1/M2 monocyte function in controlling mycobacterial infection. The MGIA could be used as a screening tool for therapeutic TB vaccine candidates and may aid the development of therapeutic vaccination regimens for TB in the near future.

Keywords: RUTI, vaccine, tuberculosis, monocytes, mycobacteria, growth inhibition assay

Introduction

Tuberculosis (TB) remains a leading cause of death from infectious disease and is responsible for an estimated annual 1.6 million deaths globally¹. With the emergence of drug-resistant TB, there is a dire need for new therapy and for shorter, more effective, safer and better tolerated treatment regimens. Vaccination could help to achieve these objectives. TB vaccines are regarded to be equally effective against drug-sensitive and drug-resistant strains, due to the nature of drug-resistant mutations which are not considered to change the immunological profile of the organism². A strategy to combine vaccination with drug treatment, termed therapeutic vaccination, is expected to improve current treatments³. This concept was first introduced by Robert Koch upon the discovery of TB bacilli and his initial attempts to administer tuberculin⁴. Currently several therapeutic TB vaccines candidates are available in the vaccine pipeline.

The RUTI vaccine is among the few candidates currently in the clinical pipeline which has been specifically developed as a therapeutic TB vaccine. The vaccine is composed of purified cellular fragments of *Mycobacterium tuberculosis* (*Mtb*) bacilli in liposomes cultured under stress (to mimic intra-granulomatous conditions) to induce latency antigens which would typically be hidden from the immune system⁵. The immune response to RUTI has been studied in animal models and clinical studies and is characterised by a poly-antigenic response. Its main immunotherapeutic effect is thought to be through induction of a T helper-1 (Th1) response, not only against growth-related antigens but also structural antigens as shown in the murine model^{3,6}. RUTI vaccination generated a poly-antigenic response in healthy volunteers (phase I study), as well as in

HIV-positive and HIV-negative patients with latent TB after isoniazid treatment for 1 month in a phase II clinical trial^{7,8}.

The lack of an immune correlate of protection has been hampering the development of novel TB vaccines, as lengthy and expensive clinical trials with protracted follow-up periods are needed to demonstrate efficacy and proceed to licensure⁹. For a single vaccine candidate, it generally takes at least a decade to reach efficacy trials from discovery^{2,9}. If we are going to achieve the WHO target to eliminate TB by 2050, major progress is required to overcome the painstakingly slow progress. Such an immune correlate could also be used to help identify vaccine candidates with the greatest potential efficacy.

The mycobacterial growth inhibition assay (MGIA) has been developed as a simple and comprehensive tool to evaluate vaccine immunogenicity *ex vivo*^{10,11}. As an assay that measures the summative vaccine-mediated host capacity to control mycobacterial growth, the MGIA is proposed as a screening tool for TB vaccine candidates¹²⁻¹⁴. The nature of the *ex vivo* assay does not require that the vaccine-mediated immune mechanism which underlies growth control to be known in advance, while in turn the MGIA could help to determine immune mechanisms of protection through investigation of the cellular frequencies, phenotypes and cytokines that associate with enhanced growth inhibition¹⁵⁻¹⁷. Several variations of human and murine MGIA have been described in the literature (reviewed in¹¹). Here, we implemented the assay using direct co-culture of mouse splenocytes with mycobacteria, based on recent optimisation work¹⁴, to investigate the potential of the RUTI vaccine to control mycobacterial growth *ex vivo*.

Monocytes are highly plastic and heterogeneous circulating cells, which are known to change their functional phenotype in response to environmental stimulation^{18,19}. Two

distinct subpopulations of mouse monocytes have been identified, commonly referred to as Ly6C⁺ and Ly6C⁻ monocytes²⁰. Ly6C⁺ monocytes represent classical pro-inflammatory and phagocytic monocytes which could subsequently differentiate into M1 macrophages, while Ly6C⁻ monocytes are regarded as non-classical anti-inflammatory monocytes which could differentiate into M2 macrophages¹⁸. In addition to the induction of an antigen-specific Th1 response, evidence suggests the potential importance of a balanced M1/M2 monocyte function in controlling mycobacterial infection^{19,21}. In a previous murine study, the RUTI vaccine was shown to reduce intragranulomatous infiltration and decrease Tumour Necrosis Factor (TNF)- α expression in *Mtb* infected mice⁶. We hypothesise that immunisation with RUTI will lead to improved control of mycobacterial growth *ex vivo* and such observation will be used to gain insight into the mechanism of immune protection.

In this study, we investigated the impact of RUTI vaccination in mice using the *ex vivo* MGIA assay and found an association between peak response of vaccine-induced growth inhibition and a shift in monocyte phenotype. Our study demonstrates the benefit of the *ex vivo* MGIA to aid the identification of immune mechanisms of action for therapeutic TB vaccine candidates. The MGIA could be used as a tool for screening such vaccine candidates and might aid the development of therapeutic vaccine regimens for TB patients.

Materials and Methods

Animals

Six to seven week-old female C57Bl/6 mice (Charles River, UK) acclimatised for at least 5 days were housed and handled in the Biological Services Facility (BSF) at London School of Hygiene and Tropical Medicine (LSHTM), UK. Mice were provided standard sterilised food and water *ad libitum*. Animals were housed in specific pathogen-free individually vented cages with environmental enrichment, with equal day and light cycle, at temperature between 19° – 23°C and relative humidity of 45 – 65%. Mice were allocated to cages as groups of six. All animal work was carried out in accordance with the Animals (Scientific Procedures) Act 1986 under a license granted by the UK Home Office (PPL 70/8043), and approved locally by the LSHTM Animal Welfare and Ethics Review Body.

Immunisation

Seven experimental groups were established, with six mice per group (Figure 1). Mice in the treatment groups were vaccinated with RUTI, which is based on purified fragments of *Mtb* in liposomes cultured under stress conditions, manufactured by Archivel Farma (Badalona, Catalonia, Spain). Vaccination with RUTI (batch A14, 204 µg) was performed subcutaneously once or twice (three weeks apart), as has been described previously^{6,22}. Five groups of mice were vaccinated with RUTI at week 0, among which three groups were boosted at week 3. Mice were sacrificed at week 1, 3, 4, 6 and 9 as the designated time points of this experiment. Two groups of mice sacrificed at week 1 and 6 served as naïve controls.

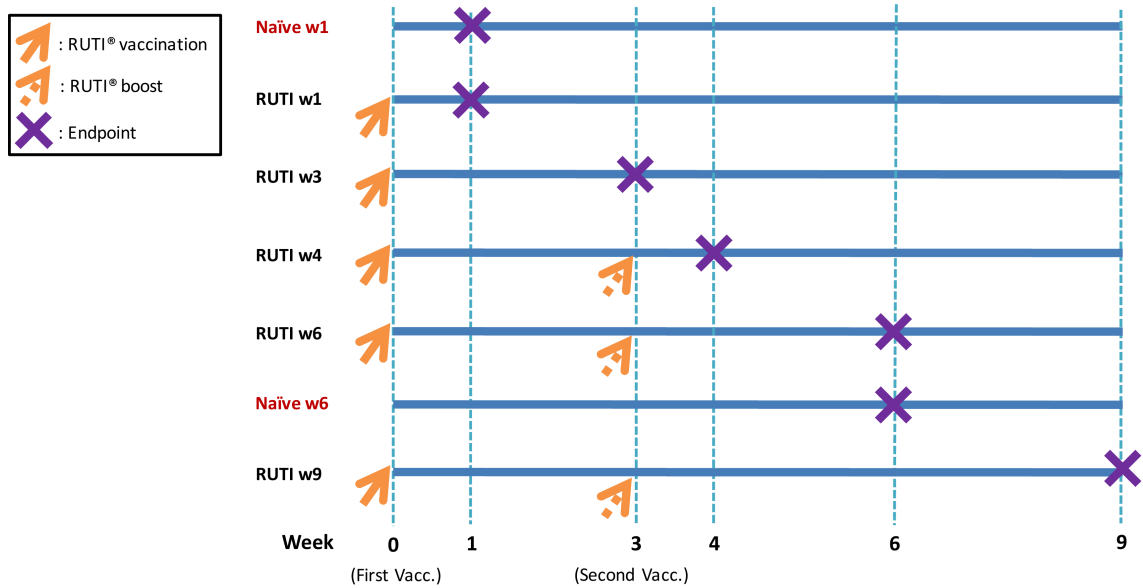


Figure 1. Experimental design and vaccination schedule. As indicated in the figure, orange arrows mean RUTI vaccination (dotted if boosting). The purple X represents endpoint (mice sacrifice). Enzyme-linked immunospot assay and mycobacterial growth inhibition assay were performed at each endpoint. In total, 42 mice were sacrificed at all time points (6 mice per group).

Mycobacteria and culture conditions

Bacillus Calmette-Guérin (BCG) Pasteur strain was obtained from Aeras (Rockville, MD, USA) as frozen aliquots. These were stored at -80°C until needed. Mycobacterial suspensions for infection inoculum and BACTEC MGIT standards were prepared in antibiotic-free media (described below). All work with cells pre-BCG infection and involving BCG infected samples were performed in Biosafety Level (BSL) 2 laboratory.

Ex vivo Mycobacterial Growth Inhibition Assay (MGIA)

At the determined time points, spleens were removed aseptically from mice and single splenocyte suspensions were prepared by homogenisation through 100 µm cell strainers

followed by lysis of red blood cells and washing. Cells were adjusted to 5×10^6 splenocytes per 300 μl in antibiotic-free media [RPMI-1640 (Sigma-Aldrich, Dorset, UK) + 10% heat-inactivated FBS (Labtech International Ltd, Uckfield, UK) + 2mM L-Glutamine (Fisher Scientific, Loughborough, UK)]. Mycobacteria were diluted in a sufficient volume for all samples in the same media to a concentration of 90 CFU per 300 μl . Aliquots of bacteria (300 μl) were added to the splenocytes, and the splenocytes-mycobacteria co-culture (600 μl) was then incubated in 48-well plates (Sigma-Aldrich, UK) at 37°C for 4 days.

After 4 days, splenocytes-mycobacteria mixtures were collected from the 48-well plates by pipetting up and down three times before transferring to 2 ml screw cap tubes. The tubes were centrifuged at 12,000 rpm in a bench top micro centrifuge and the supernatants were removed (500 μl) while ensuring the pellets remain intact. Sterile tissue culture grade water (500 μl) was added to the 48-well plates which were incubated at room temperature for 5 minutes, followed by pipetting up and down for five times before transferring to the 2 ml screw cap tubes with pellets. The pellets were dissolved by pipetting, and lysates containing mycobacteria were transferred to Bactec MGIT tubes supplemented with PANTA antibiotic and oleic acid-albumin-dextrose-catalase (OADC) enrichment broth (all from Becton Dickinson (BD), Oxford, UK). The MGIT tubes were incubated in a Bactec MGIT liquid culture system (BD) until registered positive. The resulting time to positivity (TTP) was converted to bacterial numbers (\log_{10} CFU) using a standard curve. The standard curve was obtained by a linear regression analysis of TTP values from inoculated BCG in 10-fold dilutions against CFUs obtained from plating aliquots of BCG onto 7H11 agar plates containing 10% OADC supplement (Yorlab, York, UK) and 0.5% glycerol. Direct-to-MGIT controls were included at each time point,

defined as 90 CFU BCG directly placed into Bactec MGIT system without any pre-incubation (at day 0). To compare the growth inhibition between time points, \log_{10} CFU values were normalised using the direct-to-MGIT controls by subtracting or adding the values based on the average TTP of direct-to-MGIT controls.

Interferon (IFN)- γ ELISpot

To measure antigen-specific responses towards mycobacterial antigen following RUTI vaccination over the time course, an IFN- γ ELISpot assay was performed. Single cell suspensions of mouse splenocytes were resuspended in RPMI-1640 media containing 10% heat-inactivated FBS and 2mM L-Glutamine. 96-well microtiter ELISpot plates (MAIPS4510, Millipore, Watford, UK) were coated with 10 $\mu\text{g/ml}$ rat anti-mouse IFN- γ (clone AN18, Mabtech, Nacka Strand, Sweden). Free binding sites were blocked with the above mentioned media. 2.5×10^5 of total splenocytes were added and incubated in duplicate with 10 $\mu\text{g/ml}$ Purified protein derivative (PPD) (Oxford Biosystem, Oxfordshire, UK), RPMI media as a negative control, or phytohemagglutinin (PHA) (1 $\mu\text{g/ml}$, Sigma-Aldrich) and phorbol myristate acetate (PMA) (0.1 $\mu\text{g/ml}$, Sigma-Aldrich) as a positive control. Cells were incubated overnight at 37°C with 5% CO₂. IFN- γ was detected with 1 $\mu\text{g/ml}$ biotin labelled rat anti-mouse antibody (clone R4-6A2, Mabtech) and 1 $\mu\text{g/ml}$ alkaline phosphatase-conjugated streptavidin (Mabtech). The enzyme reaction was developed with BCIP/NBT substrate (5-Bromo-4-chloro-3-indolyl phosphate/Nitro blue tetrazolium) (MP Biochemicals, UK) and stopped by washing the plates with tap water when individual spots could be visually detected (up to 3 minutes). Upon completion of the colour development stage, spots were quantified using an automated plate reader with ELISpot 5.0 software. IFN- γ -specific cells are expressed as

the number of spot forming cells (SFC) per million splenocytes after non-specific background was subtracted using negative control wells.

Flow Cytometry

Single splenocyte suspensions were fixed and red blood cells were lysed using PhosFlow lyse-fix solution (Becton Dickinson, Oxford, UK) for 30 minutes at 4°C prior to freezing. Fixed cells were then re-suspended in freezing media (FBS containing 10% DMSO) at the concentration of 10⁶ cells per ml and stored in a -40°C freezer from each time point. Frozen cells were thawed by adding FACS buffer (PBS containing 5% FBS) and pipetting up and down to encourage thawing. Cells were added to 10 ml of FACS buffer and centrifuged for 10 minutes at 1800 rpm. Cells were re-suspended in FACS buffer (concentration 10⁷ cells/ml) and were left for 15 minutes on ice for rehydration.

Fc block (anti-mouse CD16/32, eBioscience, Loughborough, UK) was added to cells and left for a further 10 minutes on ice prior to surface staining. Cells were aliquoted in FACS tubes (100µl each, 10⁶ cells) and stained with the following titrated antibody: 1.25 µl CD3-APC/Cy7 (clone 17A2), 2.5 µl CD45R/B220-BV510 (clone RA3-6B2), 1.25 µl CD11b-PerCP/Cy5.5 (clone M1/70), 2.5 µl Ly6G-BV711 (clone 1A8) and 5 µl Ly6C-BV421 (clone HK1.4). All antibodies were purchased from Biolegend (via Fisher Scientific).

Cells were incubated for 30 minutes at RT in the dark and washed prior to analysis. Fluorescence minus one (FMO) controls were set using cells for each antibody and used to guide gating. OneComp beads (eBioscience, Loughborough, UK) were used to calculate compensation by staining with single antibodies as per manufacturer's

instruction. Cells were acquired on a BD LSR II flow cytometer. Data was analysed with FlowJo software version 10.4 (Treestar Inc., USA).

Real-Time Quantitative PCR

To quantitatively analyse the mRNA expressions in splenocytes following RUTI vaccination, real-time quantitative reverse transcriptase PCR (qRT-PCR) assays were performed. 5×10^5 splenocytes were stimulated overnight with PPD (final concentration 10 $\mu\text{g/ml}$). Cells were pelleted, lysed in 200 μl RLT buffer containing 10 $\mu\text{l/ml}$ β -mercaptoethanol and stored in -40°C freezer from each time point. Cells were thawed and RNA was extracted using the RNeasy mini kit (Qiagen, Manchester, UK) according to the manufacturer's instructions. After a DNase treatment with RNase-free DNase set (Qiagen, UK), total RNA concentration was determined by spectrophotometry with a Nanodrop (Labtech International, Heathfield, UK). One microgram of each sample of total RNA was reverse-transcribed into complementary DNA (cDNA) using Omniscript[®] Reverse Transcription kit (Qiagen, UK) according to the manufacturer's recommendation, using oligo(dT) (Invitrogen, UK) to obtain cDNA. Each PCR was carried out in a 20 μl volume in the presence of 10 μl of 2x QuantiTect SYBR Green PCR Master Mix (Qiagen, UK), 1 μl of cDNA (or water as a negative control), MgCl_2 to a final concentration of 2.5 mM and primers to a final concentration of 0.5 μM . PCR was carried out for 10 minutes at 95°C denaturation, followed by 40 cycles at 95°C for 15 seconds and 60°C for 1 minute in Applied Biosystems 7500 (Applied Biosystems, CA, USA).

Analyses were performed for gene expressions of Nr4a1, Cebpb, Itgax, Pparg, Bcl2 (markers of Ly6C⁻), Ccr2, Sell, Ly6C2 (markers of Ly6C⁺) and β -actin (housekeeping gene). Primers used were listed in Table 1. mRNA expressions of β -actin was quantified for every target sample to normalise for efficiency in cDNA synthesis and RNA loading. A ratio based on the β -actin mRNA expression was obtained for each sample.

Table 1. Specific sets of primers of real-time PCR. F, forward primer; R, reverse primer.

Gene names	Primer Sequences (5' – 3')	Nucleotide position	Accession number
Ly6C⁻-related			
Nr4a1	(F) GCACAGCTTGGGTGTTGATG (R) CAGACGTGACAGGCAGCTG	1616-1635 1802-1784	NM_010444.2
Cebpb	(F) GCTGAGCGACGAGTACAAGA (R) TGCTCCACCTTCTTCTGCAG	767-786 916-897	NM_001287738.1
Itgax	(F) TTTGGGTGCCCATAGAGCTG (R) ATACCTGAGGGTGGGAGACC	2994-3013 3059-3040	NM_021334.2
Pparg	(F) TCTCTCCGTAATGGAAGACC (R) GCATTATGAGACATCCCCAC	550-569 1023-1004	NM_001127330.2
Bcl2	(F) AGGATTGTGGCCTTCTTTGA (R) CAGATGCCGGTTCAGGTACT	1837-1856 1956-1937	NM_009741.5
Ly6C⁺-related			
Ccr2	(F) AGAGAGCTGCAGCAAAAAGG (R) GGAAAGAGGCAGTTGCAAAG	2338-2357 2522-2503	NM_009915.2
Sell	(F) TCAGACTCCTTGCGCATAG (R) GTGGCTGTCACTCACAGATAG	1511-1529 1649-1629	NM_001164059.1
Ly6C2	(F) TGCCTCGGTCTTCCAAGTTC (R) ACTTCTTATGCAGGGGCCAC	416-435 545-526	NM_001252058.1
Housekeeping gene			
β -actin	(F) CATCCGTAAGACCTCTATGCCAAC (R) ATGGAGCCACCGATCCACA	973-997 1143-1125	NM_007393.5

Statistical analysis

Statistical analysis was carried out using GraphPad Prism version 7 (GraphPad, La Jolla, CA, USA). A p value of <0.05 was considered statistically significant. The specific tests used for each analysis are described in the figure legends.

Results

RUTI vaccination did not induce antigen-specific IFN- γ but did improve mycobacterial growth inhibition in murine splenocytes

To assess the immune response to mycobacterial antigens from mice vaccinated with RUTI, splenocytes were stimulated with PPD and the number of IFN- γ -producing cells was measured using the ELISpot assay (Figure 2, red line). We found a weak, non-significant response at one week following the second vaccination with RUTI (week 4, $p=0.08$). This response appeared to have decreased by week 6. Significant control of mycobacterial growth was observed 1 week after the first vaccination and 3 weeks after the second RUTI vaccination (week 6) when compared to the baseline control ($p<0.05$, Figure 2, blue line). A trend of reduction was still observed 6 weeks after the second vaccination (week 9), although it did not reach significance ($p=0.064$).

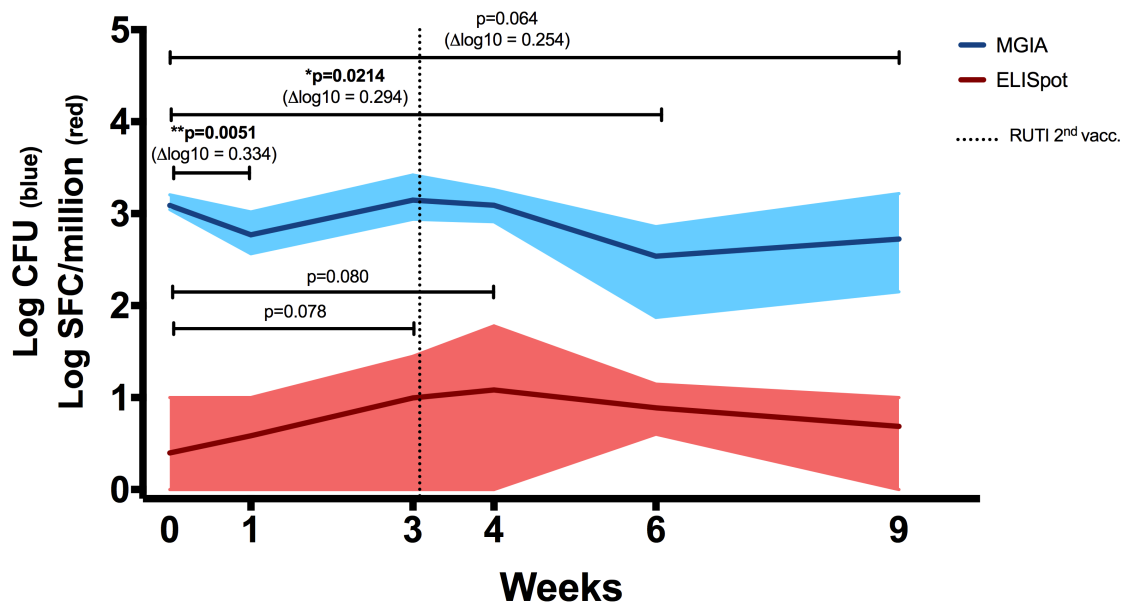


Figure 2. ELISpot (Red Line). IFN- γ response in mice receiving vaccination with RUTI was measured. Modest PPD antigen-specific responses were detected in splenocytes of healthy C57BL/6 mice across time points. The splenocytes were stimulated overnight with PPD, and the responses were detected using the IFN- γ ELISpot assay. SFC, spot-forming cells. Dark red line indicates mean response, and shading indicates range. Statistical significance was tested using Mann-Whitney test. **MGIA (Blue Line).** RUTI vaccination induced mycobacterial growth inhibition in murine splenocytes, performed *ex vivo* in a 48-well plate. Dark blue line indicates mean mycobacterial growth, and shading indicates range. One-way ANOVA was used to test for significance, followed by t-test. * $p < 0.05$; ** $p < 0.01$.

In a separate experiment performed in rotating tubes instead of 48 well plates (Figure S1A in Supplementary Material), RUTI-induced control of mycobacterial growth was superior to BCG-induced control when both vaccines were given six weeks prior to sacrifice ($p < 0.005$, Figure S1B). Therefore, week 6 appeared to be the peak response of RUTI in the *ex vivo* MGIA system. Growth control was also significant when compared to an age-matched control group ($p < 0.05$, Figure S2A in Supplementary Material).

RUTI vaccination led to control of mycobacterial growth as measured by the MGIA, despite a weak, non-significant antigen-specific IFN- γ response. This was consistent with

results of a separate experiment with RUTI and BCG, in which BCG induced IFN- γ -secreting cells whereas RUTI did not and yet cells from RUTI immunised mice were better able to control mycobacterial growth than cells from BCG vaccinated mice (Figure S1C and D in Supplementary Material). The lack of robust IFN- γ response following two doses of RUTI in healthy mice has been observed previously during potency testing for batch release (Archivel Farma, personal communication). Then, four doses of RUTI were required for induction of a detectable IFN- γ response. Although IFN- γ is associated with control of TB infection in mice and reduces the risk of TB disease in humans²³⁻²⁵, some studies suggested IFN- γ alone was not sufficient^{26,27}. As the MGIA measures the summative effect of immune responses from all cellular components, our data implied an alternative mechanism by which growth inhibition could be enhanced *ex vivo* following RUTI vaccination.

Shift of monocyte phenotype following RUTI vaccination in healthy mouse splenocytes

In this experiment, we investigated the impact of RUTI vaccination on the population of immune cells in the spleen using flow cytometry (Figure 3 and Figure S3 in Supplementary Material). RUTI did not alter the percentages of monocytes/macrophages, T-cells and B-cells in the spleen of healthy mice ($p > 0.05$, Figure S3 A, C, D). We also measured monocyte to lymphocyte (ML) ratio as a factor influencing mycobacterial growth inhibition^{28,29}, defined as the percentage of monocytes/macrophages divided by the percentage of T-cells and B-cells. We did not find a significant change of ML ratio following RUTI vaccination across time (Figure S3B).

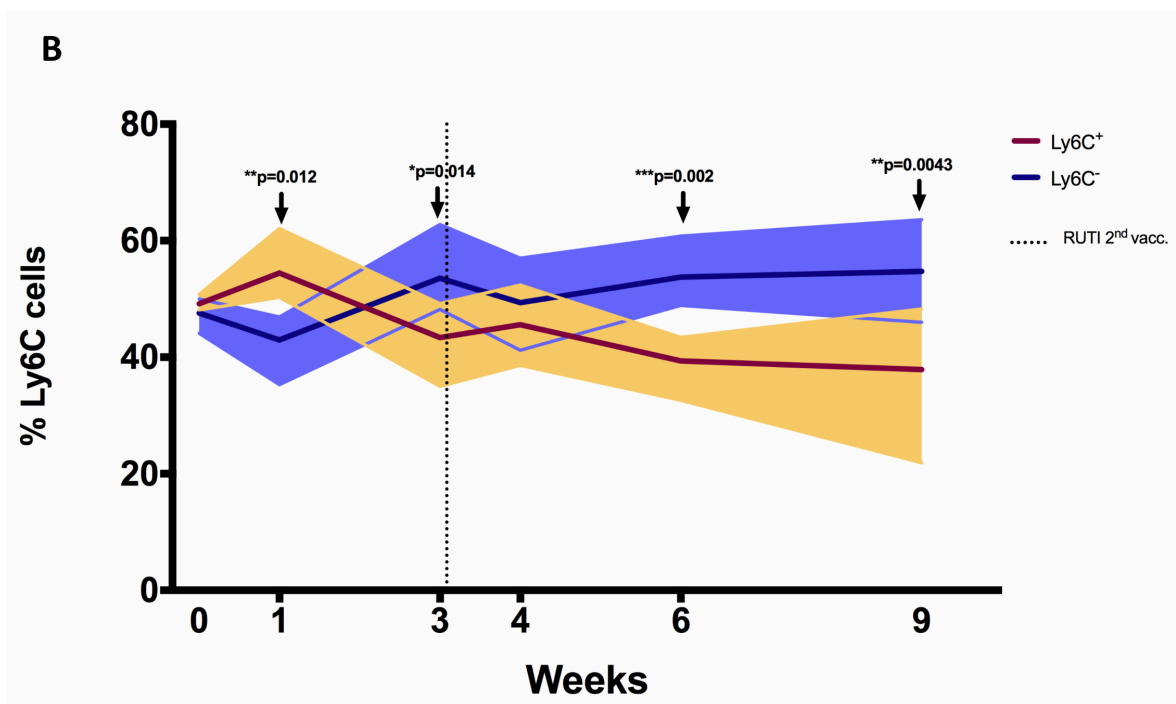
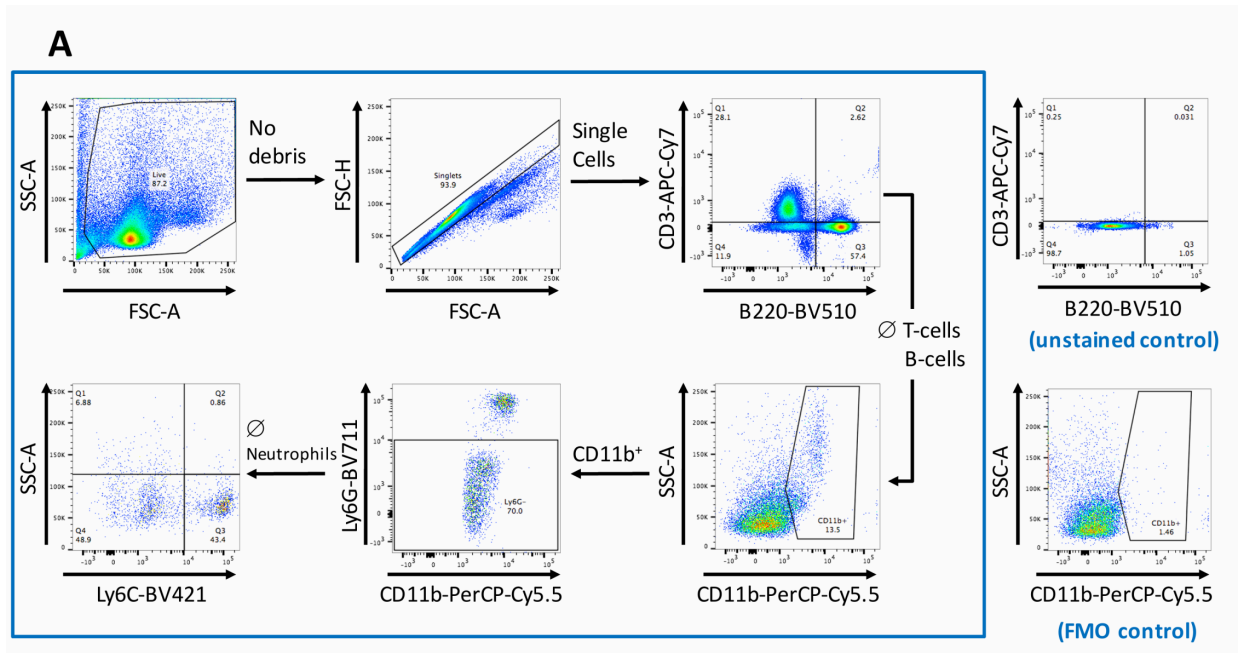


Figure 3. The shift of Ly6C⁺ and Ly6C⁻ monocytes/macrophages populations following RUTI vaccination in healthy mice. (A) Gating strategy for flow cytometric analysis. Splenocytes from C57BL/6 mice were fixed, stained and data acquired as described in Materials and Methods. Cell debris was gated out by use of FSC-SSC gate, followed by gating on single cells (FSC-A and FSC-H). A sequential gating strategy was then applied to determine the frequency of T-cells (CD3⁺), B cells (B220⁺),

monocytes/macrophages (CD11b⁺ Ly6G⁻ ssc^{low}) and the phenotypes of the monocytes/macrophages (Ly6C⁺ or Ly6C⁻) as a percentage of live cells. Plots shown are from a sample of a C57BL/6 spleen. **(B)** The frequencies of Ly6C⁺ and Ly6C⁻ monocytes/macrophages were compared at each time point following RUTI vaccination. Dark brown and dark purple lines represent mean percentages of Ly6C⁺ and Ly6C⁻ monocytes/macrophages, respectively and shading indicates range. Statistical significance was tested using unpaired t-test, *p < 0.05; **p < 0.01; ***p < 0.005.

We then further characterised monocyte phenotype based on the Ly6C marker, and observed a significant increase of Ly6C⁻ monocytes/macrophages (non-classical) at weeks 3, 6 and 9 following RUTI vaccination (p<0.05, Figure 3B). The peak increase of Ly6C⁻ cells was observed at week 6, with the shift being evident compared to both baseline and age-matched naïve control at week 6 (Figure S2B in Supplementary Material). The Ly6C⁺ monocytes/macrophages (classical) population appeared to be decreasing following vaccination, although there was an initial significant increase observed at week 1 (p<0.05, Figure 3). The shift of Ly6C⁺/Ly6C⁻ phenotype at week 6 was notably consistent with the peak response of the *ex vivo* mycobacterial growth inhibition assay, in which enhanced inhibition was observed following two doses of RUTI vaccination. We found no correlation between higher frequency of Ly6C⁻ monocytes/macrophages and lower growth of mycobacteria across time points (p=0.247, Spearman r = -0.20, data shown in Appendix 8B of this thesis).

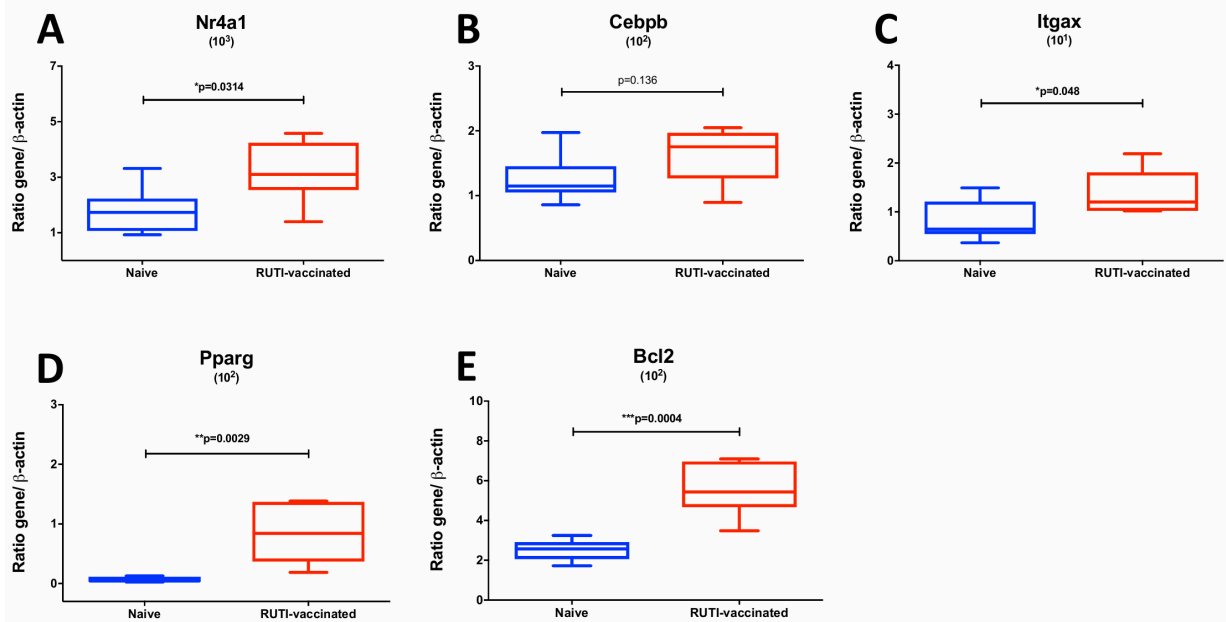
Gene expression of Ly6C⁺- and Ly6C⁻- related markers induced by RUTI vaccination

To confirm findings from the flow cytometry analysis described in the previous section, we performed real-time qRT-PCR looking at transcripts associated with Ly6C⁺ and Ly6C⁻ monocytes/macrophages. The selection of transcripts was based on a recent publication

by Mildner *et al.* (2017) regarding genomic characterisation of murine monocytes²⁰. We chose differentially expressed transcripts between the two monocyte subsets from several gene clusters of monocyte development. Three transcripts, namely *Nr4a1*, *Itgax* and *Pparg*, were selected from a cluster which was strongly upregulated in *Ly6C⁻* compared to *Ly6C⁺* monocytes. *Cebpb* was selected from a cluster that showed a gradual increase of expression from *Ly6C⁺* to *Ly6C⁻* monocytes. *Bcl2* belongs to a cluster characterised by transcripts associated with a progenitor phenotype of MDP (monocyte-macrophage DC progenitor), which was highly expressed in *Ly6C⁻* monocytes. In addition, transcripts associated with *Ly6C⁺* monocytes were selected from clusters involved in cell cycle (*Sell* and *Ly6C2*) as well as maturation of *Ly6C⁺* monocytes (*Ccr2*).

The mRNA expressions of *Ly6C⁻*-related transcripts, including *Nr4a1*, *Itgax*, *Pparg*, *Bcl2*, were significantly upregulated following the second RUTI vaccination at week 6 ($p < 0.05$, Figure 4A and C-E), with a trend of upregulation for *Cebpb* ($p = 0.136$, Figure 4B). While we did not observe a difference in expression of *Ccr2*, a *Ly6C⁺*-related gene, following RUTI vaccination at the peak time point, we saw significant upregulations of *Sell* and *Ly6C2* at week 6 ($p < 0.05$, Figure 4G-H). Quality control for the PCR assay was also performed (Figure S4 in Supplementary Materials).

Ly6C⁻ -related genes



Ly6C⁺ -related genes

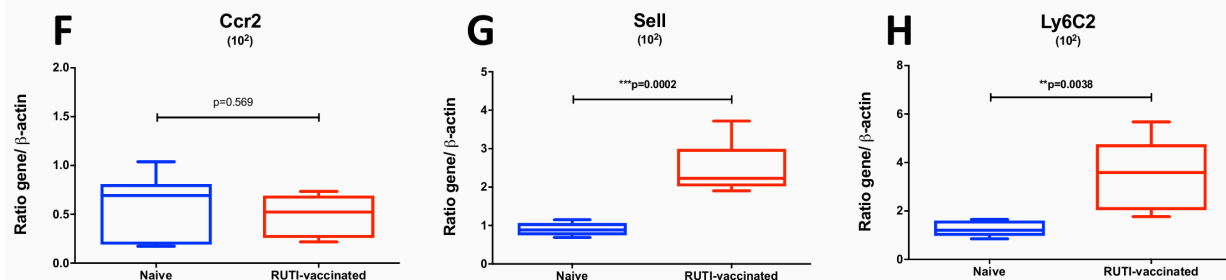


Figure 4. mRNA expressions of Ly6C⁻-related (A – E) and Ly6C⁺-related genes (F – H) in mice following vaccination with RUTI at week 6 compared to the age-matched naïve control group. Data are expressed as ratio obtained after dividing every value by the expression of β -actin in each sample and multiplying it by a factor (ranging from 10^1 to 10^3). The box plots show the minimum and maximum values (ends of the whiskers), the median (band near the middle of the box) and interquartile ranges. Statistical significance was tested using unpaired t-test, $*p < 0.05$; $**p < 0.01$; $***p < 0.005$.

Discussion

Vaccination with RUTI resulted in enhanced control of mycobacterial growth, notably at three weeks following the second vaccination (week 6), which was considered as the peak response of the vaccine observed in the *ex vivo* assay system. In addition, there was also a significant reduction of mycobacterial growth at one week after the first vaccination. There was no significant induction of antigen-specific IFN- γ as measured by ELISpot or ELISA. These observations were replicated in a separate experiment and support the notion that the two assays measure different aspects of immunity following vaccination, with the MGIA being reflective of the summative effect of host immune responses at the point of tissue harvest, compared to the IFN- γ -based assay which is an assessment of a T-cell mediated recall response following vaccination.

In this context, we argue that the *ex vivo* assay is more capable of measuring the direct, short-term effect of vaccination, while the IFN- γ response is more representative of the medium- to long-term protection conferred by vaccination. This was supported by a recent finding of Fletcher *et al.* in which PPD-specific IFN- γ response was associated with reduced risk of developing TB disease in BCG-vaccinated South African infants²⁵. In testing therapeutic vaccine candidates, it might be more relevant to measure the direct effect of vaccination, as it would represent the immediate and potentially synergistic impact of a vaccine during TB chemotherapy. This was depicted in the *ex vivo* assay, in which significant mycobacterial growth inhibition was observed at one week following the first RUTI vaccination, when there was no apparent increase of IFN- γ response at this time point.

The *ex vivo* MGIA was shown to be able to capture the impact of distinct aspects of protective immunity as a part of a summative measurement of cellular immune responses. In this experiment, we performed flow cytometry to characterise immune cells associated with enhanced growth inhibition across time. RNA was also isolated to investigate gene expression by RT-qPCR. The important finding in our present study was the impact of RUTI vaccination in shifting the phenotype of Ly6C⁺/Ly6C⁻ monocytes/macrophages in the spleen of healthy mice. This was the first time the impact of RUTI on monocyte phenotype has been assessed. In addition, while others have shown a lack of correlation between antigen-specific IFN- γ and mycobacterial growth inhibition, this is the first demonstration of vaccine induced mycobacterial growth inhibition in the absence of antigen-specific IFN- γ . Our results suggest that the enhanced control of mycobacterial growth *ex vivo* was associated with the increase of Ly6C⁻ monocytes (non-classical, anti-inflammatory), which were both observed three weeks after the second vaccination with RUTI (week 6).

We confirmed the flow cytometry finding by demonstrating the upregulation of transcripts associated with Ly6C⁻ cells at the peak time point (week 6), while the Ly6C⁺ gene transcript (*Ccr2*) remained unchanged. Among the significantly upregulated transcripts in our study was *Nr4a1*, which is obligatory for Ly6C⁻ monocytes development³⁰. Expression of *Nr4a1* as a monocyte survival factor is regulated by *Cebpb*^{20,31}, which was also elevated following RUTI vaccination. In addition, the expressions of all other Ly6C⁻-associated transcripts (*Itgax*, *Pparg*, *Bcl2*) were significantly upregulated following vaccination in our study. As Ly6C⁻ monocytes are known to mature from Ly6C⁺^{32,33}, the increased expression of some Ly6C⁺ transcripts (*Sell* and *Ly6C2*) at the peak time point was regarded as a consequence of transition from

Ly6C⁺ to Ly6C⁻. Ly6C⁻ monocytes do not represent a distinct lineage and instead arise from the conversion of Ly6C⁺ cells³⁴ and approximately 92% of expressed transcripts are shared between the two monocyte subsets³⁵. Our results suggest that RUTI could enhance Ly6C⁺ cell frequency and induce maturation of Ly6C⁺ to Ly6C⁻ monocytes. This was evidenced by our results in which an initial increase of Ly6C⁺ monocytes was observed at week 1 following the first RUTI vaccination, followed by the shift towards Ly6C⁻ and the decrease of Ly6C⁺ monocytes at the subsequent time points.

Ly6C⁻ monocytes secrete anti-inflammatory cytokine upon bacterial infection *in vivo* and when recruited to tissue, are more likely to differentiate into M2 macrophages³². This is in contrast to Ly6C⁺ monocytes, which are more likely to mature into pro-inflammatory M1 macrophages³³. In relation to our findings, the study by Guirado *et al.*⁶ demonstrated a decrease of intragranulomatous infiltration in the lungs upon administration of RUTI in infected mice after treatment. One of the notable findings in that study was a significant decrease of TNF- α at the earliest time point after RUTI administration, measured by mRNA expression in the lung. Among the producers of TNF- α during bacterial infection are Ly6C⁺ monocytes which will subsequently differentiate into M1 macrophages^{18,36}. Although our experiment differs with the one previously performed by Guirado and colleagues in several aspects (including the investigated target organ), the decrease of TNF- α observed in the previous study could be associated with the impact of RUTI on monocyte populations which has been discovered in our investigation.

RUTI is a poly-antigenic vaccine made from fragmented *Mtb* bacilli designed to induce the host immune response against latency epitopes, which is grown under stress, purified and delivered in liposomes. The part of RUTI formulation that could potentially influence

monocyte phenotype remains to be further explored. Nevertheless, our study has revealed an interesting mechanism of action of RUTI as a therapeutic vaccine for TB. As reviewed by Prabowo and colleagues³⁷, it is essential to prevent the occurrence of an exacerbated immune response for a successful therapeutic vaccination strategy in TB. This was exemplified in a recent study, in which an excessive inflammation from the T-cell compartment could also be deleterious in TB³⁸. The fact that RUTI vaccination could induce a shift towards an anti-inflammatory monocyte phenotype might be considered as an advantage in this context and such approach should be further investigated in future studies.

While this could imply that less inflammation might be beneficial for the *ex vivo* control of mycobacterial growth following RUTI vaccination in healthy mice, our results should be interpreted with prudence in relation to previous results of RUTI testing in *in vivo* animal models. The observed trend of correlation between the frequency of Ly6C⁻ monocytes/macrophages and growth of mycobacteria across time points hinted that this was only one aspect contributing to the enhanced *ex vivo* growth control and other factors might be playing roles. In a murine model infected with *Mtb*, RUTI has been shown to trigger a balanced Th1/Th2 response as well as Immunoglobulin (Ig)G1, IgG2a and IgG3 antibodies against 13 *Mtb* antigens, reflecting its broad immunogenicity³⁹. In addition, the vaccine was also shown to induce a Th3 response as a subset population of regulatory T-cells³⁹. In another mouse study, RUTI administration following drug therapy in infected mice stimulated stronger IFN- γ secretion by CD4⁺ and CD8⁺ T-cells compared to BCG against early secretory antigen target (ESAT)-6, Ag85B, and PPD and also induced an immune response against structural antigens Ag16 kDa and Ag38 kDa⁶. While immune responses in infected and drug-treated mice could be reasonably different in

comparison to healthy mice as was done in our *ex vivo* study, the fact that RUTI did not induce an exacerbated immune response in various animal studies could be linked to its impact on Ly6C⁻ monocytes which was discovered in our investigation. In the experimental animals immunised with RUTI, no elevated IgE levels were observed⁴⁰. In this study, histology also revealed no eosinophilia, necrosis or granulomatous infiltration, as well as allergic or hypersensitivity reactions. Taken together, these findings and observations suggest that RUTI could induce a balanced immune response, promoting an effective cell-mediated response whilst at the same time limiting an excessive inflammation, which could be beneficial for its implementation as a therapeutic vaccine for active TB patients undergoing treatment.

Intriguingly, a recent study by Joosten *et al.* demonstrated the protective effect of human nonclassical CD14^{dim} monocytes in inhibiting mycobacterial growth following recent *Mtb* exposure and BCG vaccination through the trained innate immunity mechanism⁴¹. As Ly6C⁻ monocyte is the equivalent of CD14^{dim} monocyte in mice¹⁸, our results could also suggest an impact of RUTI on trained innate immunity which has not been characterised before. BCG is known to induce trained immunity on human monocytes and such ability has been attributed to the non-specific protective effect conferred by the vaccine^{42,43}. A synthetic mycobacterial structure – muramyl tripeptide (MTP) – is also considered to induce trained immunity⁴⁴, and interestingly, both MTP and RUTI are delivered in liposomes. Further studies are required to elucidate downstream and upstream pathways related to the potential effect of RUTI on trained innate immunity.

In summary, we have demonstrated the benefit of the *ex vivo* MGIA assay to help streamlining and identifying immune mechanisms of a therapeutic TB vaccine candidate.

Our results could be complemented by further experiments, such as by using cells from infected mice. Depleting specific population of monocytes and using genetically deficient mice could also provide more insight on the mechanism of protection by Ly6C⁺ monocytes in the *ex vivo* assay system. Future investigation of the novel immune mechanism of RUTI observed in our study is also warranted in upcoming clinical trials of the vaccine and could potentially accelerate the development of a therapeutic vaccine regimen for TB patients in the near horizon.

Acknowledgements

We are very grateful to Archivel Farma S.L. for provision of RUTI vaccine vials used in this study. We would like to thank Ayad Eddaoudi and Stephanie Canning for expert technical assistance with flow cytometry. We are grateful to all staff at the Biological Service Facility at London School of Hygiene and Tropical Medicine for their assistance with animal work. We also thank Erni Marlina for technical advices with the qPCR assay. HAF has received support for this project from EC HORIZON2020 TBVAC2020 (grant no. 643381). SAP received a PhD scholarship from the Indonesian Endowment Fund for Education (LPDP). KS was supported by the UK Medical Research Council (MRC) and the UK Department for International Development (DFID) under the MRC/DFID Concordat agreement (grant reference MR/J008702/1).

Author Contributions

SAP and HAF conceived and planned the experiments. SAP performed the experiments, with HP and AZ participating in some of the qPCR and MGIA experiments. SAP, HAF, KS, MA and PJC contributed to the interpretation of the results. SAP took the lead in writing the manuscript. All authors reviewed, provided critical feedback and approved the final version of the manuscript.

Competing interest: Merce Amat is an employee of Archivel Farma S.L. Pere-Joan Cardona is a consultant of Archivel Farma S.L. and a co-inventor of the patent of RUTI as a therapeutic vaccine. All other authors declared no competing interest.

References

1. Tiberi S, du Plessis N, Walzl G, et al. Tuberculosis: progress and advances in development of new drugs, treatment regimens, and host-directed therapies. *Lancet Infect Dis* 2018; **S1473-3099**(18): 30110-5.
2. Fletcher HA, Schrager L. TB vaccine development and the End TB Strategy: importance and current status. *Trans R Soc Trop Med Hyg* 2016; **110**(4): 212-8.
3. Cardona PJ. The progress of therapeutic vaccination with regard to tuberculosis. *Front Microbiol* 2016; **7**: 1536.
4. Vilaplana C, Cardona PJ. Tuberculin immunotherapy: its history and lessons to be learned. *Microbes Infect* 2010; **12**(2): 99-105.
5. Cardona PJ. RUTI: a new chance to shorten the treatment of latent tuberculosis infection. *Tuberculosis (Edinb)* 2006; **86**(3-4): 273-89.
6. Guirado E, Gil O, Caceres N, Singh M, Vilaplana C, Cardona PJ. Induction of a specific strong polyantigenic cellular immune response after short-term chemotherapy controls bacillary reactivation in murine and guinea pig experimental models of tuberculosis. *Clin Vaccine Immunol* 2008; **15**(8): 1229-37.
7. Vilaplana C, Montane E, Pinto S, et al. Double-blind, randomized, placebo-controlled Phase I Clinical Trial of the therapeutical antituberculous vaccine RUTI. *Vaccine* 2010; **28**(4): 1106-16.
8. Nell AS, D'Lom E, Bouic P, et al. Safety, tolerability, and immunogenicity of the novel antituberculous vaccine RUTI: randomized, placebo-controlled phase II clinical trial in patients with latent tuberculosis infection. *PLoS One* 2014; **9**(2): e89612.
9. Dockrell HM. Towards new TB vaccines: what are the challenges? *Pathog Dis* 2016; **74**(2016): ftw016.
10. Zelmer AA, Tanner R, Stylianou E, et al. Ex vivo mycobacterial growth inhibition assay (MGIA) for tuberculosis vaccine testing - a protocol for mouse splenocytes. *bioRxiv* 2015: 020560.
11. Tanner R, O'Shea MK, Fletcher HA, McShane H. *In vitro* mycobacterial growth inhibition assays: A tool for the assessment of protective immunity and evaluation of tuberculosis vaccine efficacy. *Vaccine* 2016: 0264-410X.
12. Parra M, Yang AL, Lim J, et al. Development of a murine mycobacterial growth inhibition assay for evaluating vaccines against *Mycobacterium tuberculosis*. *Clin Vaccine Immunol* 2009; **16**(7): 1025-32.
13. Fletcher HA, Tanner R, Wallis RS, et al. Inhibition of mycobacterial growth in vitro following primary but not secondary vaccination with *Mycobacterium bovis* BCG. *Clin Vaccine Immunol* 2013; **20**(11): 1683-9.
14. Zelmer A, Tanner R, Stylianou E, et al. A new tool for tuberculosis vaccine screening: Ex vivo Mycobacterial Growth Inhibition Assay indicates BCG-mediated protection in a murine model of tuberculosis. *BMC Infect Dis* 2016; **16**: 412.

15. Marsay L, Matsumiya M, Tanner R, et al. Mycobacterial growth inhibition in murine splenocytes as a surrogate for protection against *Mycobacterium tuberculosis* (M. tb). *Tuberculosis (Edinb)* 2013; **93**(5): 551-7.
16. Smith SG, Zelmer A, Blitz R, Fletcher HA, Dockrell HM. Polyfunctional CD4 T-cells correlate with in vitro mycobacterial growth inhibition following *Mycobacterium bovis* BCG-vaccination of infants. *Vaccine* 2016; **34**(44): 5298-305.
17. Jensen C, Lindebo Holm L, Svensson E, Aagaard C, Ruhwald M. Optimisation of a murine splenocyte mycobacterial growth inhibition assay using virulent *Mycobacterium tuberculosis*. *Sci Rep* 2017; **7**(1): 2830.
18. Yang J, Zhang L, Yu C, Yang XF, Wang H. Monocyte and macrophage differentiation: circulation inflammatory monocyte as biomarker for inflammatory diseases. *Biomark Res* 2014; **2**(1): 1.
19. Mildner A, Marinkovic G, Jung S. Murine Monocytes: Origins, Subsets, Fates, and Functions. *Microbiol Spectr* 2016; **4**(5).
20. Mildner A, Schonheit J, Giladi A, et al. Genomic Characterization of Murine Monocytes Reveals C/EBPbeta Transcription Factor Dependence of Ly6C- Cells. *Immunity* 2017; **46**(5): 849-62 e7.
21. Sampath P, Moideen K, Ranganathan UD, Bethunaickan R. Monocyte Subsets: Phenotypes and Function in Tuberculosis Infection. *Front Immunol* 2018; **9**: 1726.
22. Vilaplana C, Gil O, Caceres N, Pinto S, Diaz J, Cardona PJ. Prophylactic effect of a therapeutic vaccine against TB based on fragments of *Mycobacterium tuberculosis*. *PLoS One* 2011; **6**(5): e20404.
23. Cooper AM, Dalton DK, Stewart TA, Griffin JP, Russell DG, Orme IM. Disseminated tuberculosis in interferon gamma gene-disrupted mice. *J Exp Med* 1993; **178**(6): 2243-7.
24. Bustamante J, Boisson-Dupuis S, Abel L, Casanova JL. Mendelian susceptibility to mycobacterial disease: genetic, immunological, and clinical features of inborn errors of IFN-gamma immunity. *Semin Immunol* 2014; **26**(6): 454-70.
25. Fletcher HA, Snowden MA, Landry B, et al. T-cell activation is an immune correlate of risk in BCG vaccinated infants. *Nat Commun* 2016; **7**: 11290.
26. Kagina BM, Abel B, Scriba TJ, et al. Specific T cell frequency and cytokine expression profile do not correlate with protection against tuberculosis after bacillus Calmette-Guerin vaccination of newborns. *Am J Respir Crit Care Med* 2010; **182**(8): 1073-9.
27. Abebe F. Is interferon-gamma the right marker for bacille Calmette-Guerin-induced immune protection? The missing link in our understanding of tuberculosis immunology. *Clin Exp Immunol* 2012; **169**(3): 213-9.
28. Naranbhai V, Fletcher HA, Tanner R, et al. Distinct Transcriptional and Anti-Mycobacterial Profiles of Peripheral Blood Monocytes Dependent on the Ratio of Monocytes: Lymphocytes. *EBioMedicine* 2015; **2**(11): 1619-26.

29. Brennan MJ, Tanner R, Morris S, et al. The Cross-Species Mycobacterial Growth Inhibition Assay (MGIA) Project, 2010-2014. *Clin Vaccine Immunol* 2017; **24**(9).
30. Hanna RN, Carlin LM, Hubbeling HG, et al. The transcription factor NR4A1 (Nur77) controls bone marrow differentiation and the survival of Ly6C- monocytes. *Nat Immunol* 2011; **12**(8): 778-85.
31. Thomas GD, Hanna RN, Vasudevan NT, et al. Deleting an Nr4a1 Super-Enhancer Subdomain Ablates Ly6Clow Monocytes while Preserving Macrophage Gene Function. *Immunity* 2016; **45**(5): 975-87.
32. Auffray C, Fogg D, Garfa M, et al. Monitoring of blood vessels and tissues by a population of monocytes with patrolling behavior. *Science* 2007; **317**(5838): 666-70.
33. Serbina NV, Jia T, Hohl TM, Pamer EG. Monocyte-mediated defense against microbial pathogens. *Annu Rev Immunol* 2008; **26**: 421-52.
34. Yona S, Kim KW, Wolf Y, et al. Fate mapping reveals origins and dynamics of monocytes and tissue macrophages under homeostasis. *Immunity* 2013; **38**(1): 79-91.
35. Polletti S, Natoli G. Understanding Spontaneous Conversion: The Case of the Ly6C-Monocyte. *Immunity* 2017; **46**(5): 764-6.
36. O'Garra A, Redford PS, McNab FW, Bloom CI, Wilkinson RJ, Berry MP. The immune response in tuberculosis. *Annu Rev Immunol* 2013; **31**: 475-527.
37. Prabowo SA, Groschel MI, Schmidt ED, et al. Targeting multidrug-resistant tuberculosis (MDR-TB) by therapeutic vaccines. *Med Microbiol Immunol* 2013; **202**(2): 95-104.
38. Tzelepis F, Blagih J, Khan N, et al. Mitochondrial cyclophilin D regulates T cell metabolic responses and disease tolerance to tuberculosis. *Sci Immunol* 2018; **3**(23).
39. Cardona PJ, Amat I, Gordillo S, et al. Immunotherapy with fragmented *Mycobacterium tuberculosis* cells increases the effectiveness of chemotherapy against a chronic infection in a murine model of tuberculosis. *Vaccine* 2005; **23**(11): 1393-8.
40. Gröschel MI, Prabowo SA, Cardona P-J, Stanford JL, Werf TSvd. Therapeutic vaccines for tuberculosis—A systematic review. *Vaccine* 2014; **32**(26): 3162-8.
41. Joosten SA, van Meijgaarden KE, Arend SM, et al. Mycobacterial growth inhibition is associated with trained innate immunity. *J Clin Invest* 2018; **128**(5): 1837-51.
42. Kleinnijenhuis J, Quintin J, Preijers F, et al. Bacille Calmette-Guerin induces NOD2-dependent nonspecific protection from reinfection via epigenetic reprogramming of monocytes. *Proc Natl Acad Sci U S A* 2012; **109**(43): 17537-42.
43. de Bree LCJ, Koeken V, Joosten LAB, et al. Non-specific effects of vaccines: Current evidence and potential implications. *Semin Immunol* 2018; **06**(002): 1044-5323.
44. Mourits VP, Wijkmans JC, Joosten LA, Netea MG. Trained immunity as a novel therapeutic strategy. *Curr Opin Pharmacol* 2018; **41**: 52-8.

Supplementary Figures

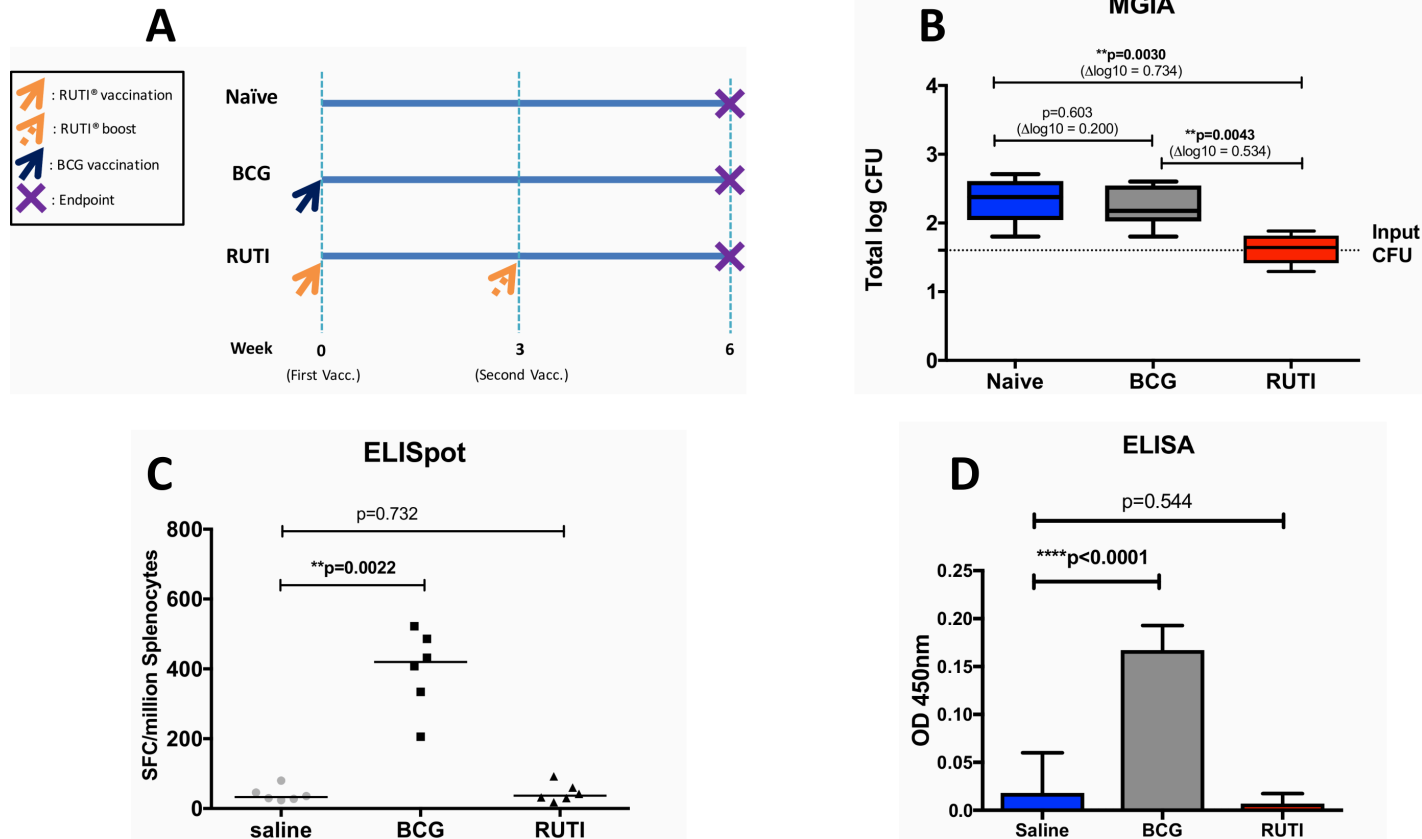


Figure S1. RUTI vaccination induced mycobacterial growth inhibition in murine splenocytes in comparison with BCG, performed in rotating tubes. Groups of mice were immunised with BCG, RUTI or placebo/ saline (A). RUTI vaccination enhanced mycobacterial growth inhibition which was superior to BCG (B). IFN- γ responses in mice receiving vaccination with RUTI and BCG were assessed using ELISpot and ELISA assays (C and D). Statistical significance was tested using t-test (B and D) and Mann-Whitney test (C). A p value <0.05 was considered statistically significant.

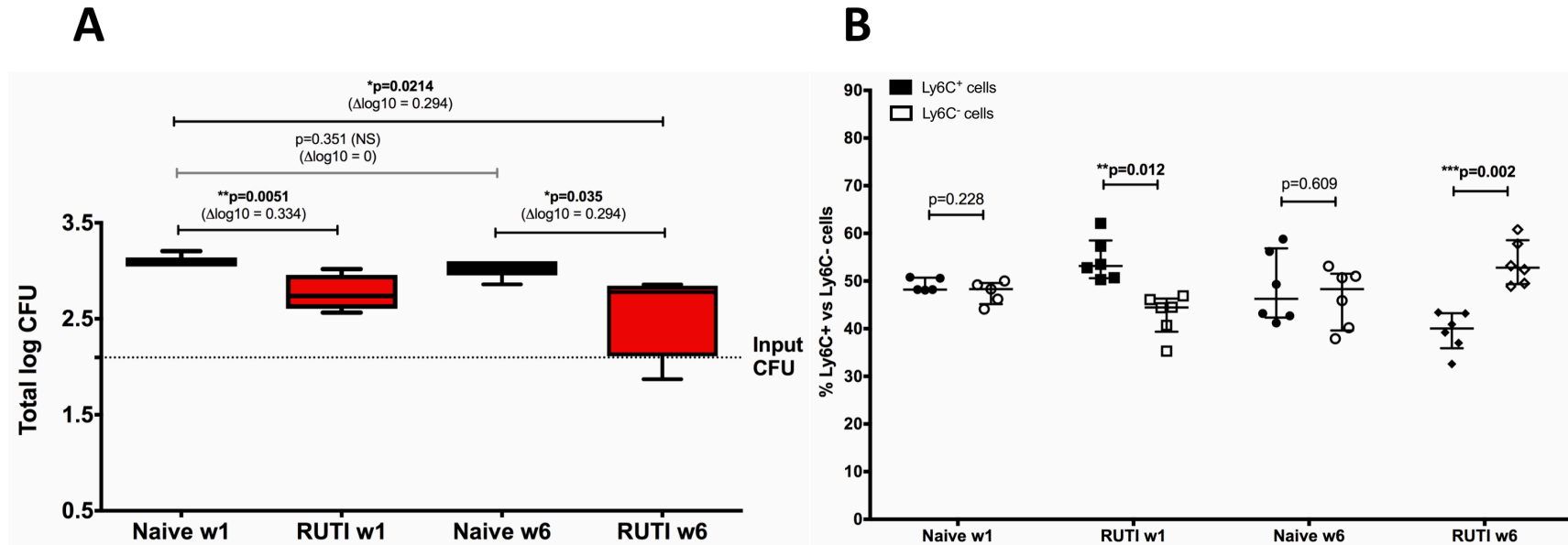


Figure S2. (A) An additional naïve group was set up at the peak time point (week 6). No difference in growth inhibition was observed between the naïve group at week 1 and week 6. The box plots show the minimum and maximum (ends of the whiskers), the median (band near the middle of the box) and interquartile ranges. **(B)** The proportion of Ly6C⁺ and Ly6C⁻ monocytes/macrophages was not shifted in the naïve groups on week 1 and week 6, in contrast to the RUTI-vaccinated groups. Error bars represent the median \pm interquartile range. Statistical significance was tested using t-test. A p value <0.05 was considered statistically significant. *p < 0.05 ; **p < 0.01 ; ***p < 0.005 .

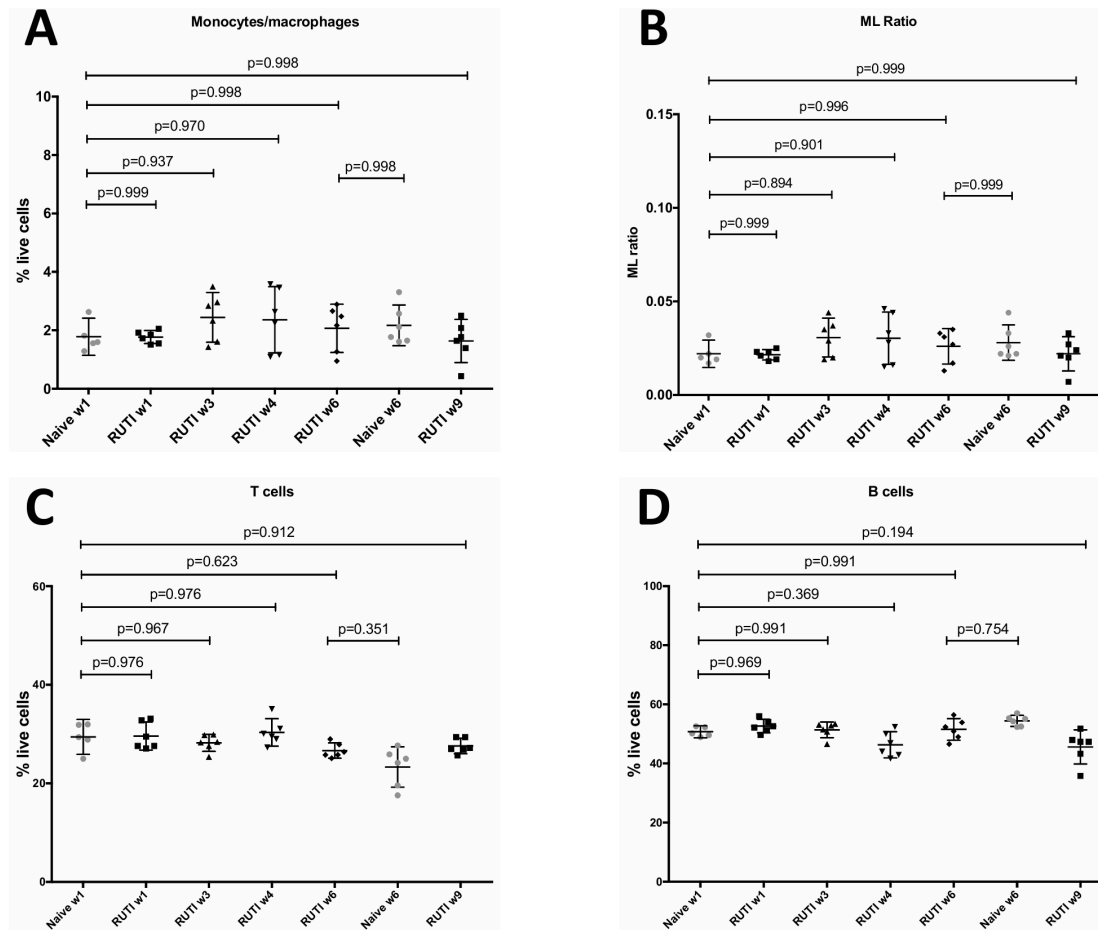


Figure S3. The frequency of monocytes/macrophages (A), ML ratio (B) as well as the frequency of T cells (C) and B cells (D) were determined in spleen using the gating strategy described in Figure 3. The frequencies of monocytes/macrophages ($CD11b^+ Ly6G^- ssc^{low}$), T cells ($CD3^+$) and B cells ($B220^+$) were used to calculate the ML ratio. The ML ratio was obtained by dividing the percentage of monocytes/macrophages by the sum of the percentages of T and B cells. Error bars represent the median \pm interquartile range. p values were determined using ordinary ANOVA. A p value <0.05 was considered statistically significant.

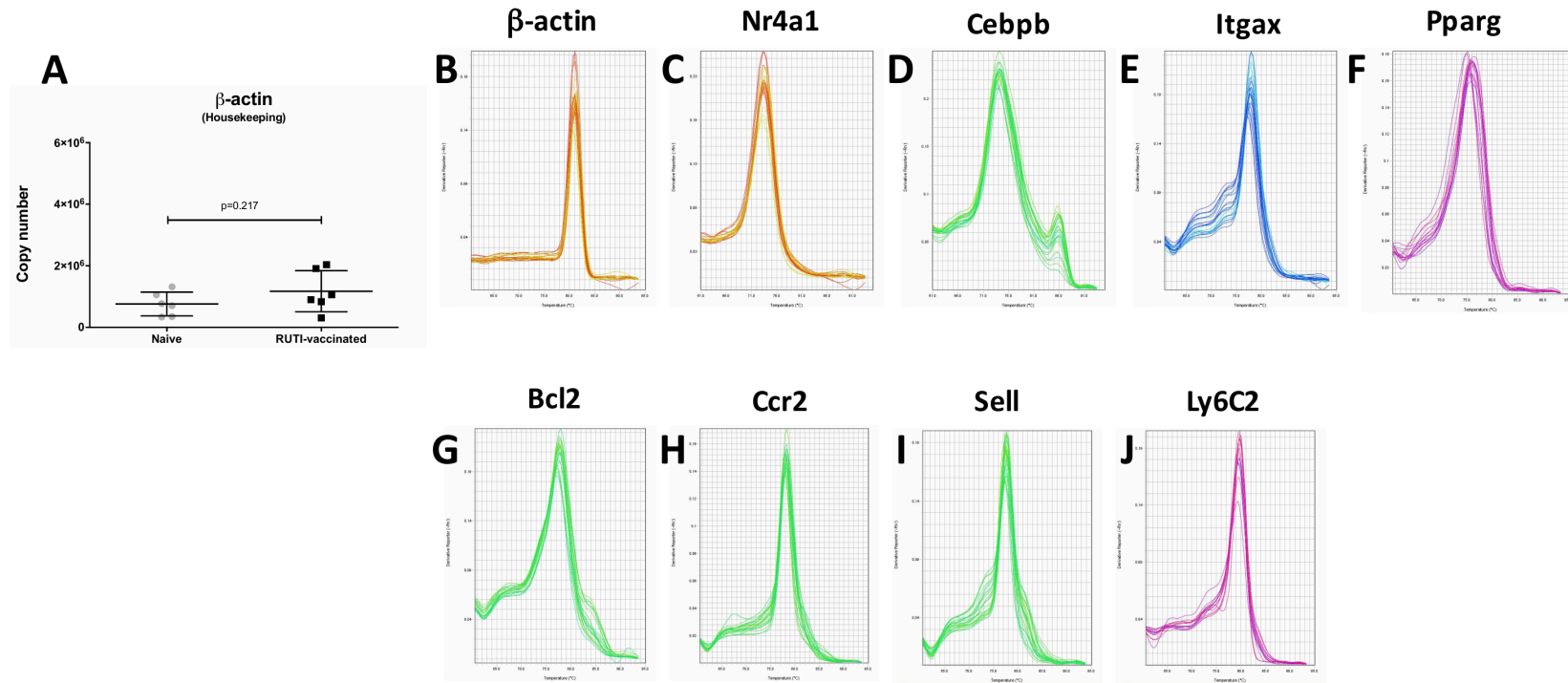


Figure S4. mRNA expressions of β -actin was analysed for every target sample (A) to normalise for efficiency in cDNA synthesis and RNA loading. A ratio based on the β -actin mRNA expression was obtained for each sample. Following qPCR, single peaks were present in the melting curve analysis for every target gene (B – J).

Title: Impact of individual-level factors on *ex vivo* mycobacterial growth inhibition: The influence of immune cells phenotype, cytomegalovirus-specific response and sex on immunity following BCG vaccination in humans

Author list:

Satria Arief Prabowo (1)(2), Steven G. Smith (1)(2), Karin Seifert (1)(3), Helen A. Fletcher (1)(2)

Affiliations:

- (1) Department of Immunology and Infection, Faculty of Infectious and Tropical Diseases, London School of Hygiene and Tropical Medicine, London, UK
- (2) Tuberculosis Centre, London School of Hygiene and Tropical Medicine, London, UK
- (3) Department of Pharmacovigilance, Federal Institute for Drugs and Medical Devices, Bonn, Germany

Correspondence to: Satria Arief Prabowo, Department of Immunology and Infection, Faculty of Infectious and Tropical Diseases, London School of Hygiene and Tropical Medicine, London, WC1E 7HT, UK. satria.prabowo@lshtm.ac.uk

Registry

T: +44(0)20 7299 4646

F: +44(0)20 7299 4656

E: registry@lshtm.ac.uk

RESEARCH PAPER COVER SHEET

PLEASE NOTE THAT A COVER SHEET MUST BE COMPLETED FOR EACH RESEARCH PAPER INCLUDED IN A THESIS.

SECTION A – Student Details

Student	Satria Arief Prabowo
Principal Supervisor	Prof Helen A. Fletcher
Thesis Title	Accelerating Development of Therapeutic Tuberculosis Vaccines using an <i>Ex Vivo</i> Immune Assay Platform

If the Research Paper has previously been published please complete Section B, if not please move to Section C

SECTION B – Paper already published

Where was the work published?	-		
When was the work published?	-		
If the work was published prior to registration for your research degree, give a brief rationale for its inclusion	-		
Have you retained the copyright for the work?*	Choose an item.	Was the work subject to academic peer review?	Choose an item.

**If yes, please attach evidence of retention. If no, or if the work is being included in its published format, please attach evidence of permission from the copyright holder (publisher or other author) to include this work.*

SECTION C – Prepared for publication, but not yet published


Where is the work intended to be published?	Tuberculosis (Edinb)
Please list the paper's authors in the intended authorship order:	Satria Arief Prabowo, Steven G. Smith, Karin Seifert, Helen A. Fletcher
Stage of publication	Submitted, undergoing review

SECTION D – Multi-authored work

<p>For multi-authored work, give full details of your role in the research included in the paper and in the preparation of the paper. (Attach a further sheet if necessary)</p>	<p>I conceived the research idea, designed the experiments, performed laboratory works and analysed the results with advice from my supervisor and co-authors. I lead the preparation and wrote the draft of the manuscript, and implemented revisions following discussion and comments from my supervisor and co-authors.</p>
---	---

Student Signature:  _____

Date: 25/09/2018

Supervisor Signature:  _____

Date: 05/10/2018

Abstract

Introduction: Understanding factors associated with varying protection from vaccination with Bacillus Calmette-Guérin (BCG) is essential to develop a new vaccine against tuberculosis (TB). Investigation of individual-level factors affecting mycobacterial-specific immune responses could provide insights for vaccine developers to understand what may confound their ability to observe a vaccine effect when testing candidates in clinical trials. The mycobacterial growth inhibition assay (MGIA) has been developed as a measure of vaccine immunogenicity *ex vivo* and may serve as a better correlate of vaccine-induced protection.

Aims: To assess the impact of immune cell phenotype, cytomegalovirus (CMV)-specific response and sex on *ex vivo* growth inhibition following historical BCG vaccination in a cohort of healthy individuals (n=100).

Methods: Peripheral blood mononuclear cells (PBMC) cryopreserved at the time of sample collection were thawed and incubated with live BCG for four days following which inhibition of BCG growth was determined. Essential immune mechanisms were investigated using ELISpot and ELISA to identify cytokine productions, as well as using flow cytometry with surface staining and intracellular cytokine staining to characterise immune cell phenotype and CMV-specific response.

Results: A higher frequency of cytokine-producing NK cells in peripheral blood was associated with enhanced *ex vivo* mycobacterial growth inhibition following historical BCG vaccination. We confirmed findings from previous studies regarding the role of T-cell activation associated with a CMV-specific response as a risk factor for TB disease

and our study is the first to show the association with *ex vivo* mycobacterial growth. Interestingly, BCG-vaccinated females in our cohort controlled mycobacterial growth better than males, which may provide an explanation to the higher number of TB cases in males worldwide, in addition to the sociocultural factors.

Conclusion: The present study has displayed the value of MGIA in assessing changes in the innate immune compartment as well as in adaptive immunity following BCG vaccination. Individual-level factors influence capacity to control mycobacterial growth and the MGIA tool could be used by vaccine developers to assess how their candidate may perform in different populations.

Keywords: BCG, tuberculosis vaccine, growth inhibition assay, cytomegalovirus, sex, NK cell

Introduction

Tuberculosis (TB) is the number one cause of death from infectious disease worldwide and it is currently estimated that a quarter of the world population is infected with *Mycobacterium tuberculosis* (*Mtb*)^{1,2}. The introduction of Bacillus Calmette-Guérin (BCG) vaccination and chemotherapy in the past century provided optimism to fight the disease. Despite this, drug-resistant TB is now a major risk to global health security, and BCG as the only licensed vaccine for TB is known to have variable efficacy against contagious adult pulmonary TB^{3,4}. BCG remains the most widely used vaccine worldwide, mainly because it provides good protection against TB in children³. BCG has been given to more than 4 billion individuals since its wide implementation in the 1970s with favourable safety records⁵. Understanding factors associated with varying BCG protection is essential to improve current vaccination practice as well as to develop new vaccines against TB.

It has been proposed that the observed variation in BCG efficacy is attributed to individual-level factors which influence host mycobacteria-specific immune responses⁶⁻⁸. In a recent systematic review, protection following BCG vaccination was shown to vary according to the geographical latitudes in which the vaccine was given. Protection was higher in trials further from the equator where exposure to environmental mycobacteria is lower, and this protection gradually decreases in the latitudes closer to the equator³. In some places with high exposure to environmental mycobacteria, BCG demonstrated limited evidence of efficacy against adult pulmonary TB when tested in large clinical trials^{7,9}. In the UK, a country where exposure to environmental mycobacteria is regarded to be minimum (latitude > 40°), BCG is known to provide protection up to 80% against

pulmonary TB¹⁰ and vaccination of school-aged children could protect until at least 20 years¹¹.

Another factor that may influence the mycobacteria-specific immune response is sex. Globally, TB case rates are much higher in men than in women, as reflected by a global male to female ratio (M:F) of 1.7 for case notifications in 2016¹². This difference is seen in all regions of the world, including Europe, and in some countries such as Vietnam, the M:F ratio is as high as 4.5¹². Males contribute to 65% of TB cases worldwide and although it has been alluded that socioeconomic and cultural factors are contributing to the observed sex bias, differences in the immune responses between the sexes also play a role^{13,14}. It is generally acknowledged that females exhibit more robust immune responses towards infection and vaccination compared to males¹⁵. In the context of susceptibility to TB, differences in immune cells frequencies and functions have been thought to contribute to higher TB rates in males¹⁶. With regard to BCG vaccination, there is currently limited evidence concerning the impact of sex on its protective effect against pulmonary TB in adults, although some studies reported higher tuberculin skin test response and larger BCG scar formation in males compared to females^{17,18}. Analysis from participants of clinical trials of a TB vaccine candidate in the UK showed that males exhibited a higher baseline response of interferon-gamma (IFN- γ)⁸. Interestingly, BCG is also thought to provide a non-specific protective effect against unrelated pathogens, thus contributing in reduction of overall cause of mortality, and this effect is more pronounced in females rather than males¹⁹⁻²¹.

In addition, several other factors have been proposed to explain the variable efficacy of BCG, such as genetic differences between trial populations, variable virulence of the

circulating *Mtb* strains as well differences between strains of the BCG vaccine itself, although in the latter case findings between studies have shown equivocal results^{3,22}. Recently, Fletcher *et al.* found that T-cell activation is an immune correlate of risk of TB disease in BCG-vaccinated infants in a study enrolling a large cohort of infants²³. Chronic exposure to antigen from persistent viral or bacterial infection is known to cause continuous T-cell activation which could lead to dysfunction of antigen specific T-cells²⁴. Further to the finding of the infant study, it was identified that cytomegalovirus (CMV)-specific IFN- γ responses were associated with T-cell activation and could have contributed to increased risk of developing TB disease²⁵.

The mycobacterial growth inhibition assay (MGIA) has been developed as a measure of vaccine immunogenicity *ex vivo*. Following optimisation works in the past few years²⁶⁻²⁸, the assay has gained attention for its potential ability to detect vaccine-mediated inhibition of growth following BCG vaccination in adults and infants²⁹⁻³¹. The assay described in the present study involves direct co-culture of peripheral blood mononuclear cells (PBMCs) with mycobacteria, and subsequent measurement of mycobacterial growth inhibition as a functional assessment of vaccine response. Several studies have demonstrated the ability of the MGIA to detect changes in the innate and adaptive compartment following vaccination. The frequency of polyfunctional T-helper-1 cells correlated with *ex vivo* inhibition of mycobacterial growth following BCG vaccination in UK infants³⁰. The ratio of host monocyte to lymphocyte cells (ML ratio) is associated with risk of TB disease³²⁻³⁴, and altering the ML ratio *in vitro* affects the control of mycobacterial growth, with a higher ML ratio associated with higher growth of mycobacteria³⁵. More recently, Joosten and colleagues (2018) found that the capacity to control mycobacterial growth following recent *Mtb* exposure and BCG vaccination is

associated with nonclassical monocytes, and this observation is reflective of the trained innate immune mechanism³¹. In a study by Jensen *et al.*, IFN- γ was associated with reduction of mycobacterial growth *ex vivo* following immunisation with a TB vaccine candidate in mice³⁶. However, in that study the source of IFN- γ was not found among the investigated vaccine-specific T-cells, suggesting potential contribution from other cells, such as NK cells.

Characterisation of immune cell phenotype which contributes to protection following BCG vaccination is crucial for augmenting vaccination strategies against TB. Moreover, investigating individual-level factors affecting mycobacterial-specific immune responses could provide insights for vaccine developers to understand what may confound their ability to observe a vaccine effect when testing candidates in clinical trials. In this study, the impacts of immune cell phenotype, CMV-specific response and sex on vaccine-specific mycobacterial growth inhibition following historical BCG vaccination were demonstrated in adult healthy volunteers. The findings further confirm evidences from previous studies regarding the role of T-cell activation associated with a CMV-specific response as a risk factor for TB disease^{23,25} using the *ex vivo* MGIA. The result presented in this study suggest that BCG vaccinated females control mycobacterial growth better than males, which is consistent with the observation of higher number of TB cases in males worldwide. A higher frequency of cytokine-producing NK cells in peripheral blood was also found to be associated with enhanced inhibition of mycobacterial growth *ex vivo* following historical BCG vaccination. Collectively, our data indicate that individual-level factors influence capacity to control mycobacterial growth and that the MGIA tool could be used by vaccine developers to assess how their candidate may perform in different populations.

Materials and Methods

Study participants and ethics statement

We recruited 100 healthy adult participants with (i) no history of BCG vaccination or (ii) a history of BCG vaccination more than 6 months before study enrolment. Verbal interviews were conducted to determine eligibility based on the absence of any major chronic illness, current medication administration or symptoms of infection. Participants were aged 18 to 80 years with no evidence of exposure or infection with TB. Participants were excluded if they were suffering from any persistent medical condition or infection. Written informed consent was obtained from all participants prior to enrolment in the study. Individuals were recruited under protocols approved by the LSHTM Observational Research Ethics Committee (ref 8762 and 10485). All procedures were conducted in accordance with the Declaration of Helsinki, as agreed by the World Medical Association General Assembly (Washington, 2002) and ICH Good Clinical Practice (GCP).

Blood sampling and PBMCs isolation

Peripheral blood was collected at the amount of 50 ml and processed within 6 hours. Blood samples were collected in tubes containing sodium heparin (Sigma-Aldrich, Dorset, UK). Peripheral blood mononuclear cells were isolated from heparinised whole blood by centrifugation over 15 ml LymphoPrep (Stemcell, Cambridge, UK) in a LeucoSep tube (Greiner Bio-One, Stonehouse, UK) according to the manufacturer's instruction. PBMCs were cryopreserved in FBS (Labtech International Ltd, Uckfield, UK) containing 10% DMSO (Sigma-Aldrich) and stored in -80 °C freezer using CoolCell

containers (VWR International, Lutterworth, UK). PBMCs were transferred to a cryobox after a minimum of an overnight in a CoolCell container.

IFN- γ Enzyme-linked immunospot (ELISpot) assay

PBMCs were thawed and an *ex vivo* IFN- γ ELISpot assay was performed to assess antigen-specific response. The ELISpot assay was performed using a human IFN- γ ELISpot kit (capture mAb 1-D1K, Mabtech, Nacka Strand, Sweden). Duplicate wells containing 3×10^5 PBMC were stimulated overnight for 18 hours with 20 $\mu\text{g/ml}$ purified protein derivative (PPD) (Oxford Biosystem, Oxfordshire, UK), Phytohemagglutinin (PHA) (10 $\mu\text{g/ml}$, Sigma-Aldrich) as a positive control or media alone as a negative control. IFN- γ was detected with 1 $\mu\text{g/ml}$ biotin labelled rat anti-mouse antibody (clone 7-B6-1, Mabtech) and 1 $\mu\text{g/ml}$ alkaline phosphatase-conjugated streptavidin (Mabtech). Results are reported as spot forming cells (SFC) per million PBMCs, calculated by subtracting the mean of the unstimulated wells from the mean of antigen wells and correcting for the numbers of PBMC in the wells. Spots were quantified using an automated plate reader with ELISpot 5.0 software as well as checked manually.

***Ex vivo* Mycobacterial Growth Inhibition Assay**

Cryopreserved PBMCs were thawed and rested for 2 hours at 37 °C in antibiotic-free medium [RPMI-1640 (Sigma-Aldrich) + 10% pooled human AB serum (Sigma-Aldrich) + 2 mM L-Glutamine (Fisher Scientific, Loughborough, UK)] containing 10 U/ml benzonase (Insight Biotechnology, Wembley, UK). After the rest, the cells were counted,

washed and re-suspended in the above-mentioned medium without benzonase. The percent viability of recovered cells was around 70 to 90% per vial. A 2-ml screw-cap tube containing 3×10^6 PBMCs in 300 μ l of medium was co-cultured with ~100 Colony Forming Units (CFU) of BCG in 300 μ l for 4 days (total volume 600 μ l) on a 360° rotator (VWR International, UK) at 37°C. BCG Pasteur Aeras strain was obtained from Aeras (Rockville, MD, USA) and used as the immune target in the MGIA.

After 4 days, the 2-ml tubes were centrifuged at 12,000 rpm for 10 minutes. The MGIA supernatants (500 μ l) were transferred to other 2 ml tubes and frozen at -80 °C for further analysis. The remaining cells were then lysed by addition of 400 μ l of sterile tissue culture grade water and vortexed 3 times with 5-minutes intervals. Lysate containing mycobacteria was transferred to a Bactec MGIT tube supplemented with PANTA antibiotics and oleic acid-albumin-dextrose-catalase (OADC) enrichment broth (all from Becton Dickinson, Oxford, UK). The tube was placed in a Bactec MGIT 960 and incubated until registered positive (measured as time to positivity [TTP]). Use of a standard curve enables conversion of the TTP of a sample tube into bacterial numbers (log CFU) (Supplementary Fig. S1). All work with cells pre-BCG infection and involving BCG infected samples was done in Biosafety Level (BSL) 2 laboratory.

Enzyme-linked immunosorbent assay (ELISA)

MGIA supernatants were analysed to assess cytokine concentrations by ELISA. The levels of following cytokines were measured: IFN- γ , tumor necrosis factor alpha (TNF- α), interleukin (IL)-12p40, IL-10, IL-17, IL-6, granulocyte-macrophage colony-stimulating factor (GM-CSF), interferon-gamma-induced protein 10 (IP-10), perforin,

granzyme, IL-32 and IL-22. The concentrations of IFN- γ , IL-12p40 and IL-6 were measured using BD OptiEIA kits (Becton Dickinson, UK), while TNF- α , GM-CSF, IP-10, granzyme B, IL-32 and IL-22 DuoSet ELISA kits were obtained from R&D Systems (Abingdon, UK), IL-10 ELISA MAX Standard and IL-17 ELISA MAX Deluxe from BioLegend (London, UK), and perforin ELISA kit from Abcam (Cambridge, UK). Assays were performed according to the manufacturers' instruction.

Flow cytometric immune phenotyping

Cryopreserved PBMCs were thawed and upon 2 hours resting at 37 °C, cell surface flow cytometry was performed. Cells were resuspended in FACS buffer (1% FBS in PBS with 0.02% sodium azide). Fc block (Becton Dickinson, UK) was added (2.5 μ g per million cells) and incubated for 10 minutes at room temperature prior to surface staining. Cells were aliquoted in FACS tubes (100 μ l each, 1x10⁶ cells) and stained with 1 μ l/ml Live Dead Blue Stain (Invitrogen), followed by staining with the following titrated antibody for the lymphocyte panel: 2.5 μ l CD3-AF700 (clone UCHT1, Ebioscience, Loughborough, UK), 1.25 μ l CD4-APC/Cy7 (clone RPA-T4, BioLegend), 1.25 μ l CD8-Superbright645 (clone RPA-T8, Ebioscience), 2.5 μ l CD19-FITC (clone HIB19, BioLegend), 2.5 μ l CD56-APC (clone HCD56, BioLegend), 2.5 μ l CD16-BV510 (clone 3G8, BioLegend), 5 μ l HLA-DR-PE (clone L243, BioLegend), 5 μ l LAG3-PE/Cy7 (clone 11C3C65, BioLegend) and 1.25 μ l PD1-BV421 (clone EH12.2H7, BioLegend).

For the monocyte panel, the cells were stained with the following titrated antibodies: 2.5 μ l CD3-AF700 (clone UCHT1, Ebioscience), 2.5 μ l CD19-FITC (clone HIB19,

BioLegend), 2.5 μ l CD14-BV421 (clone HCD14, BioLegend), 2.5 μ l CD16-BV510 (clone 3G8, BioLegend), 1.25 μ l CD86-APC/Cy7 (clone IT2.2, BioLegend), 5 μ l HLA-DR-PE (clone L243, BioLegend), 5 μ l CD206-APC (clone 15-2, BioLegend), 5 μ l CD163-BV605 (clone GHI/61, BioLegend), 2.5 μ l CD64-APC/Cy7 (clone 10.1, BioLegend) and 5 μ l CD123-BV650 (clone 6H6, BioLegend). Cells were incubated for 30 minutes at RT in the dark, washed and fixed prior to analysis. Fluorescence minus one (FMO) controls were set using cells for each antibody and used to guide gating. OneComp beads (eBioscience) were used to calculate compensation by staining with single antibodies as per manufacturer's instruction. Cells were acquired on a BD LSR II flow cytometer. Data was analysed with FlowJo software version 10.4 (Treestar Inc., USA).

Results are presented as percentages of cells after gating out of dead cells and doublets. CD4⁺ and CD8⁺ T-cells were identified from CD3⁺ CD19⁻ cells, whereas CD56⁺ NK cells were identified from CD3⁻ CD19⁻ cells. CD56^{dim} CD16⁺ and CD56^{bright} CD16^{+/-} cells were identified as cytotoxic and cytokine-producing NK cells, respectively (Supplementary Fig. S2A, lymphocyte gating). Furthermore, CD4⁺ and CD8⁺ T-cells were gated for T-cell activation markers: HLA-DR, LAG3 and PD1 using the FMO. Meanwhile, CD14⁺ monocytes were gated from CD3⁻ CD19⁻ cells, and CD14^{bright} CD16^{+/-} and CD14^{dim} CD16⁺ cells were identified as M1 and M2 monocytes, respectively (Supplementary Fig. S2B, monocyte gating). In addition, CD86 and HLA-DR markers were used to confirm M1 phenotype, while CD206 and CD163 markers were used to affirm M2 phenotype³⁷. CD64⁺ and CD123⁺ cells were also gated from CD14⁺ monocytes as activated monocytes³⁸.

Intracellular cytokine staining (ICS) flow cytometry

PBMCs were thawed and rested for 2 hours in a 37°C incubator with 5% CO₂ after addition of 10 U/ml of benzonase. PBMCs were then incubated alone (medium only) as a negative control, with 5 µg/ml *Staphylococcus enterotoxin B* (SEB; Sigma, UK) as a positive control, with ~100 CFU BCG (as per the MGIA protocol) and with 10 µg/ml CMV peptide pool (5 peptides, 2 µg/ml/peptides, ANASPEC, Fremont, CA, USA). The CMV peptide pool used is the same as the previous study²⁵. The incubation with BCG was performed for 4 days and the addition of SEB and CMV was performed on Day 3. Two hours after the addition of SEB and CMV to the respective tubes, brefeldin A (Sigma, UK) was added to all tubes which were then incubated for 18 hours at 37°C until Day 4.

Following incubation, cells were washed with ICS FACS buffer (0.1% BSA in PBS, with 0.01% sodium azide) and stained with Vivid live/dead reagent (Invitrogen) for 10 minutes at 4°C in the dark. Cells were then surface stained with anti-CD4-APC (BD Biosciences), anti-CD19-eFluor450 and anti-CD14-eFluor450 (eBiosciences) for 30 minutes at 4°C in the dark. After washing with ICS FACS buffer, cells were permeabilised with Cytofix/Cytoperm reagent (BD Biosciences) at 4°C for 20 min, washed in Perm Wash buffer (BD Biosciences) and stained with anti-CD3-Horizon-BV510, anti-IL-2-FITC, anti-TNFα-PE-Cy7 (BD Biosciences), anti-CD8-PE (eBiosciences) and anti-IFNγ-PerCP-Cy5.5 (Biolegend) for 30 min at room temperature in the dark. Cells were finally resuspended in 250 µL 1% paraformaldehyde (Sigma, UK) and filtered prior to acquisition.

Data was acquired using an LSRII flow cytometer (BD Biosciences) and FACSDiva acquisition software (BD Biosciences). Compensation was performed using tubes of OneComp eBeads (ThermoFisher, UK) individually stained with each fluorophor and compensation matrices were calculated with FACSDiva. ICS flow cytometry data was analysed using FlowJo software version 10.4 (TreeStar Inc., Ashland, OR, USA). Samples were gated sequentially on singlet, live, CD14⁻CD19⁻, CD3⁺ (lymphoid), CD4⁺, CD8⁺ cells and negative control stimulation tubes were used to set cytokine gates (see Supplementary Fig. S3, ICS gating). Median cytokine responses in negative control tubes, as a percentage of the gated CD4⁺ T-cell population, were as follows: IFN- γ – 0.07%; IL-2 – 0.09%; TNF- α – 0.40%. Median cytokine responses in positive control tubes (SEB-stimulated) were as follows: IFN- γ – 3.16%; IL-2 – 4.24%; TNF- α – 24.35%. Cytokine responses analysed for all stimuli (BCG and CMV) were after subtraction of background values measured in un-stimulated tubes.

Statistical analysis

To identify statistical significance of *ex vivo* growth inhibition (log CFU values) and ELISA responses, students *t*-test were used. Mann-Whitney *U* Test was performed to identify significant differences of the ELISpot, cell surface flow cytometry and ICS responses between groups. Spearman's correlation coefficient was used to test for correlations between growth inhibition and immune responses. A multiple comparison correction was included (Bonferroni), as indicated in each figure legend. Statistical analyses were performed in GraphPad Prism 7 (GraphPad, La Jolla, CA, USA).

Results

Demographics of enrolled participants

One hundred participants were enrolled in the study; 37 vaccine-naïve volunteers with no history of BCG vaccination and 63 volunteers previously-vaccinated with BCG (average time since vaccination 29.4 years prior to enrolment). Table 1 summarises the characteristics of the study participants. Almost 70% of the BCG-vaccinated participants were from the UK.

Characteristic	Total Participants : 100	
	Naïve (n = 37)	BCG Vaccinated (n = 63)
Female [no. (%)]	28 (75.7 %)	42 (66.7 %)
Median age [yr (range)]	31 (23 – 70)	39 (24 – 80)
Average time since BCG vaccination [yr (range)]	-	29.4 (10 – 58)
Country of Origin UK [no. (%)]	8 (21.6 %)	44 (69.8 %)

Table 1. Characteristics of study participants.

Assessment of *ex vivo* growth inhibition and cytokine responses

The growth inhibition assay was performed to assess the impact of historical BCG vaccination on *ex vivo* mycobacterial growth control. Using cryopreserved PBMCs, enhanced growth inhibition in PBMCs from BCG-vaccinated individuals was observed compared to vaccine-naïve individuals (median log CFU 1.680 and 2.027, $p < 0.0001$, Figure 1A). There was no correlation between the age of participants and time since vaccination with *ex vivo* mycobacterial growth ($p > 0.1$, Spearman's correlation, data shown in Appendix 8C of this thesis). The IFN- γ ELISpot assay was performed to

measure the magnitude of the mycobacteria-specific response. The secretion of IFN- γ in response to PPD was elevated in samples from vaccinated individuals in comparison to unvaccinated individuals (median SFC 109.5 and 48, $p < 0.0001$, Figure 1B). There was a significant inverse correlation between higher IFN- γ ELISpot response and lower mycobacterial growth ($p = 0.022$, Spearman $r = -0.23$, Figure 1C), although the association was not significant when the correlation was performed in the BCG-vaccinated group only ($p = 0.836$, Spearman $r = 0.027$, data shown in Appendix 8D of this thesis).

ELISA assays were performed using the MGIA supernatant to investigate cytokine production which may be associated with *ex vivo* growth inhibition. Trends for higher production of Th1-type cytokines (IFN- γ , IP-10, TNF- α , IL-12) as well as GM-CSF ($p = 0.0512$) were observed in the BCG-vaccinated group compared to the vaccine-naïve group (Table 2). There was a statistically significant correlation between higher IL-10 production and higher mycobacterial growth (Spearman $r = 0.37$, $p = 0.0003$, Table 2), with a trend of higher TNF- α production with reduced mycobacterial growth (Spearman $r = -0.35$, $p = 0.0558$). Meanwhile, historical BCG-vaccination significantly increased the frequency of IL-2⁺ CD4 T-cells in the BCG-vaccinated group upon 4 days of stimulation with BCG in the MGIA system ($p = 0.0077$, Supplementary Figure S4). Similar trends were observed with the frequencies of IFN- γ ⁺ as well as TNF- α ⁺ CD4 T-cells, and to a lesser extent with Th1-cytokine⁺ CD8 T-cells (Supplementary Figure S4). There were no significant correlations between the frequencies of BCG-specific CD4 and CD8 T-cells and mycobacterial growth, although the observed trends suggest that these cells may contribute to control of growth (Supplementary Table S1).

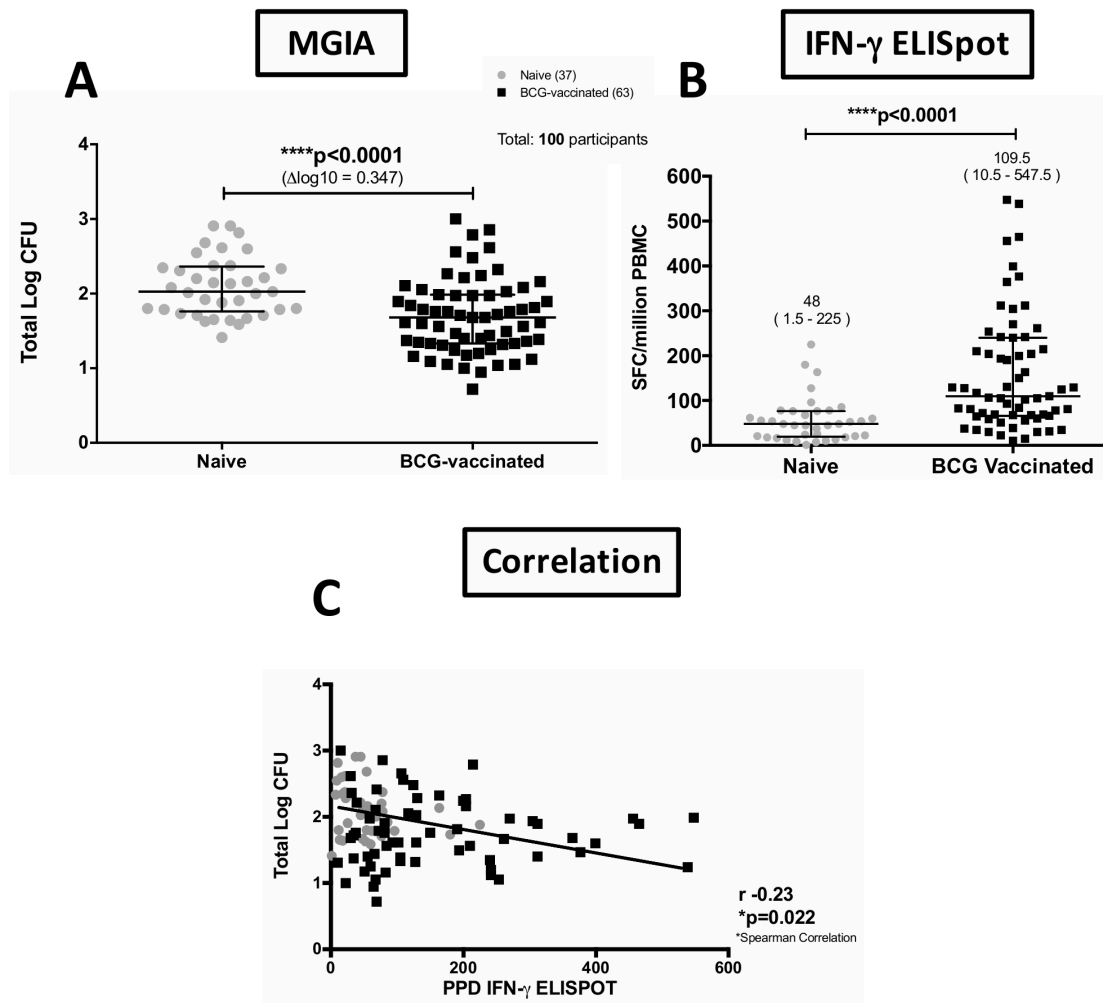


Figure 1. Growth inhibition and immune responses following historical BCG vaccination. Assessment was performed from 37 BCG-naïve and 63 BCG-vaccinated participants. **(A)** Growth inhibition was compared using BCG input ~ 100 CFU as immune target (unpaired t-test). Data is presented as total number of log CFUs per sample, which was determined by use of a standard curve. **(B)** IFN- γ production from PBMC following stimulation with PPD was compared (Mann-Whitney test). Numbers above each group represent median (range). SFC, spot forming cells. **(C)** The correlation between *ex vivo* growth inhibition and PPD-specific IFN- γ response was assessed (Spearman's correlation). A p value <0.05 was considered statistically significant. Dots and squares represent individual data points, and the central lines indicate the median response with inter-quartile range (IQR). ****p<0.0001.

Cytokine (pg/ml)	Comparison			Correlation with <i>ex vivo</i> mycobacterial growth	
	Naïve	BCG-vaccinated	p-value	r	p-value
IFN- γ	12.47 [8.245-16.69]	23.37 [10.8-35.94]	0.1962	-0.027	0.8432
IP-10	111.7 [55.42-168]	204.5 [112.1-297]	0.1505	0.19	0.1158
TNF- α	37.97 [2.547-73.4]	97.98 [38.61-157.4]	0.1471	-0.35	0.0558
IL-12	27.6 [3.033-52.17]	63.61 [20.83-106.4]	0.2299	-0.23	0.3158
IL-10	52.55 [31.07-74.03]	59.99 [36.56-83.41]	0.6688	<u>0.37***</u>	0.0003
GM-CSF	7.729 [-1.688-17.15]	88.54 [26.19-150.9]	0.0512	-0.37	0.1552
IL-6	356.7 [246.1-467.3]	315 [236.5-393.4]	0.5293	0.071	0.5449
IL-17	0.00 [0.00-0.00]	0.1596 [0.00-0.4083]	0.3291	-0.13	0.2141

Table 2. Summary of mean cytokine responses measured with ELISA assays, assessed from MGIA supernatant samples after 4 days of co-culture. Comparisons were made between naïve and BCG-vaccinated groups (unpaired t-test), the values indicate mean of concentration in pg/ml [95% CI]. Correlations were assessed with *ex vivo* mycobacterial growth among responders (Spearman's correlation). A p value <0.05 was considered statistically significant (in bold), and after a multiple testing correction only values with p <0.0063 were considered significant (underlined). n= 37 BCG-naïve and n=63 BCG-vaccinated participants. ***p<0.001.

Effects of the historical BCG vaccination on the frequencies of circulating leukocyte subsets

Historical BCG vaccination did not influence the frequencies of circulating leukocytes in T-cell, NK cell and monocyte compartments (Supplementary Table S2). However, significant correlations were observed between the frequencies of NK cells and enhanced control of mycobacterial growth *ex vivo* in the naïve and BCG-vaccinated groups (p<0.05, Spearman's correlations, Table 3). In the BCG-vaccinated group, the higher frequency of cytokine-producing NK cells was associated with reduced mycobacterial growth (Spearman r = -0.41, p=0.015, Figure 2A). A higher production of perforin was observed from the cells of BCG-vaccinated participants compared to naïve (p=0.018, Figure 2B). The production of perforin significantly correlated with enhanced growth inhibition (Spearman r = -0.44, p=0.013, Figure 2C and Supplementary Table S3), and the

association was still significant when the correlation was performed in the BCG-vaccinated group only (Spearman $r = -0.36$, $p=0.037$, data shown in Appendix 8E of this thesis). Correlations with other measured NK cells products and cytokines (granzyme, IL-32, IL-22) did not reach significance (Supplementary Table S3). There was also a non-significant trend of T-cell frequency in peripheral blood being protective against mycobacterial growth in cells from BCG-vaccinated participants (Spearman $r = -0.30$, $p=0.087$, Table 3).

Leukocyte subsets	Correlation with <i>ex vivo</i> mycobacterial growth					
	All participants		Naïve		BCG-vaccinated	
	r	p-value	r	p-value	r	p-value
T-cells	-0.068	0.6367	0.29	0.2708	-0.30	0.0866
CD4 T-cells	-0.041	0.7764	0.17	0.5172	-0.091	0.6080
CD8 T-cells	0.24	0.0938	0.36	0.1714	0.093	0.6011
CD4/CD8 ratio	-0.16	0.2718	-0.20	0.4579	-0.058	0.7448
NK cells	-0.27	0.0593	<u>-0.71**</u>	0.0028	-0.19	0.2833
Cytokine NK cell	-0.26	0.0702	-0.47	0.0679	-0.41*	0.0147
Cytotoxic NK cell	-0.25	0.0814	-0.64**	0.0093	-0.19	0.2699
NK cell ratio	-0.2	0.1602	-0.35	0.1866	-0.087	0.6241
Monocytes	0.12	0.4244	-0.0088	0.9758	0.13	0.4638
ML ratio	0.064	0.6609	-0.044	0.8714	0.083	0.6390
M1 monocytes	-0.076	0.5993	-0.28	0.2867	-0.031	0.8610
M2 monocytes	-0.16	0.2784	-0.16	0.5458	-0.12	0.4978
M1/M2 ratio	0.059	0.6831	-0.17	0.5283	0.15	0.3939
CD64 ⁺ monocytes	-0.063	0.6659	-0.29	0.2664	0.028	0.8759
CD123 ⁺ monocytes	-0.072	0.6169	-0.27	0.3025	0.015	0.9313
Suppressor monocytes	0.21	0.1414	0.31	0.2381	0.089	0.6149

Table 3. Correlation of immune cell frequencies in peripheral blood and *ex vivo* mycobacterial growth inhibition. Assessment was performed from 16 BCG-naïve and 34 BCG-vaccinated participants. Correlations were performed from a total of 50 participants, as well as from each naïve and BCG-vaccinated groups respectively (Spearman's correlation). A p value <0.05 was considered statistically significant (in bold), and after a multiple testing correction only values with $p < 0.0031$ were considered significant (underlined). Note: The ML ratio was obtained by dividing the percentage of monocytes by the sum of the percentages of T- and B-cells. The NK cell ratio was obtained by dividing the percentage of cytokine-producing by cytotoxic NK cells. * $p < 0.05$, ** $p < 0.01$.

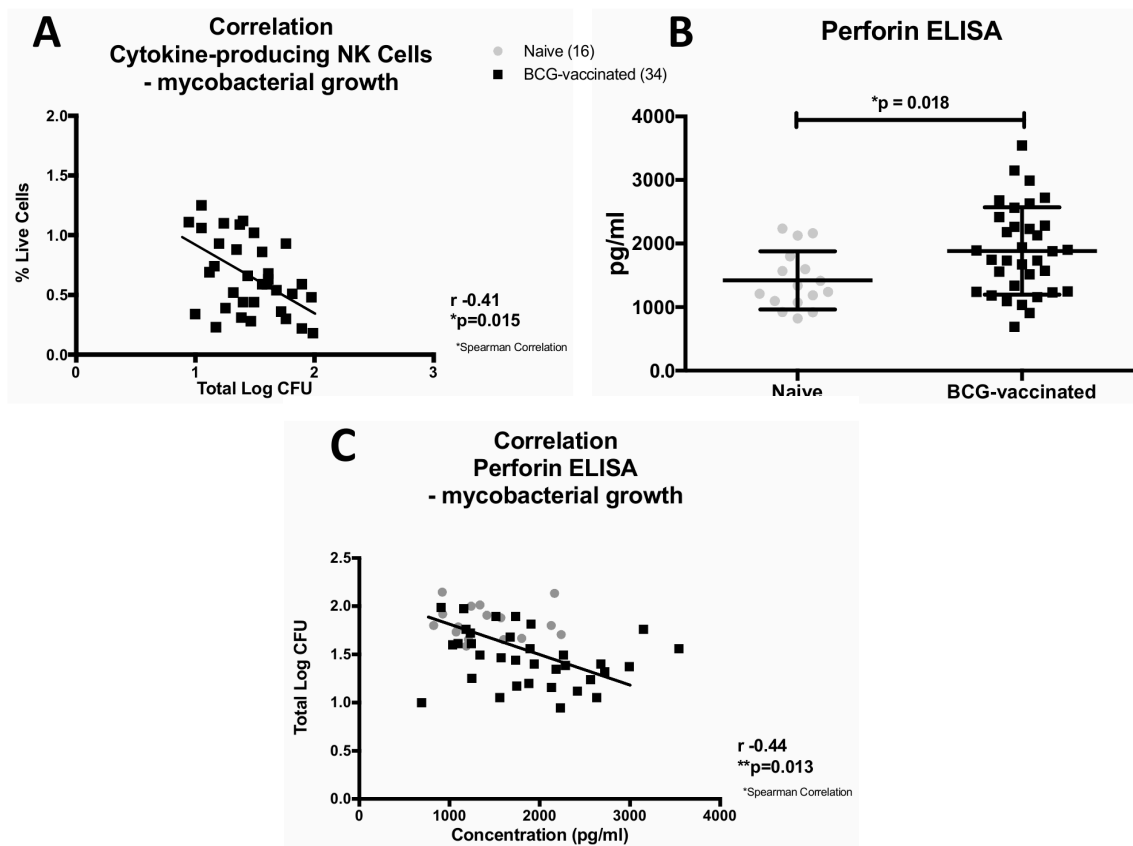


Figure 2. NK cells correlations. A higher frequency of cytokine-producing NK cells ($CD56^{\text{bright}} CD16^{+/-}$) correlated with enhanced *ex vivo* mycobacterial growth inhibition (Spearman's correlation) (A). A perforin ELISA was performed from MGIA supernatants and the response was compared between vaccination groups (unpaired t-test) (B). The production of perforin was associated with enhanced *ex vivo* growth inhibition (Spearman's) (C). A p value <0.05 was considered statistically significant. $*p < 0.05$, $**p < 0.01$.

Impacts of CMV-specific T-cell response and T-cell activation on *ex vivo* mycobacterial growth inhibition

CMV-specific T-cells producing $IFN-\gamma^+$ and $TNF-\alpha^+$, notably in the CD8 compartment, were significantly associated with frequency of T-cells expressing LAG3 and PD1 markers ($p < 0.05$, Spearman's correlations, Table 4 and Figure 3 A-D). Historical BCG-vaccination did not appear to influence CMV-specific response nor T-cell activation

between groups (Supplementary Table S2 and S4). Furthermore, T-cell activation was shown to correlate with higher growth of mycobacteria *ex vivo*, particularly in the naïve group (Figure 3 and Supplementary Table S5). LAG3⁺ CD4 T-cells were significantly associated with growth of mycobacteria (p=0.047), with a similar trend for LAG3⁺ CD8 T-cells (p=0.072) (Figure 3 F and I). There was no correlation between the CMV-specific T-cell response and the frequency of BCG-specific cytokine⁺ T-cells (p>0.05, Spearman's correlations, data shown in Appendix 8F of this thesis).

CMV-specific cytokine ⁺ T-cells	Correlation with activated T-cells					
	HLA-DR ⁺ CD4 T-cells		LAG3 ⁺ CD4 T-cells		PD1 ⁺ CD4 T-cells	
	r	p-value	r	p-value	r	p-value
IFN- γ ⁺ CD4 T-cells	0.026	0.8748	-0.004	0.9805	0.20	0.2112
IL-2 ⁺ CD4 T-cells	-0.045	0.7823	-0.056	0.7310	-0.0082	0.9601
TNF- α ⁺ CD4 T-cells	0.054	0.7401	0.058	0.7239	0.091	0.5757
	HLA-DR ⁺ CD8 T-cells		LAG3 ⁺ CD8 T-cells		PD1 ⁺ CD8 T-cells	
IFN- γ ⁺ CD8 T-cells	0.31	0.0552	0.39*	0.0140	<u>0.44**</u>	0.0049
IL-2 ⁺ CD8 T-cells	-0.087	0.5917	0.0024	0.9885	-0.15	0.3609
TNF- α ⁺ CD8 T-cells	0.28	0.0799	0.35*	0.0281	0.33*	0.0375

Table 4. Correlation of CMV-specific T-cell responses and T-cell activation. Associations were investigated from 3 different subsets of CMV-specific cytokine⁺ T-cells producing IFN- γ ⁺, IL-2⁺ or TNF- α ⁺, respectively. Three markers were used for T-cell activation: HLA-DR, LAG3 and PD1. A p value <0.05 was considered statistically significant (in bold), and after a multiple testing correction only values with p <0.0083 were considered significant (underlined) (Spearman's correlation). n=50 participants, consisted of 16 BCG-naïve and n=34 BCG-vaccinated participants. *p<0.05, **p<0.01.

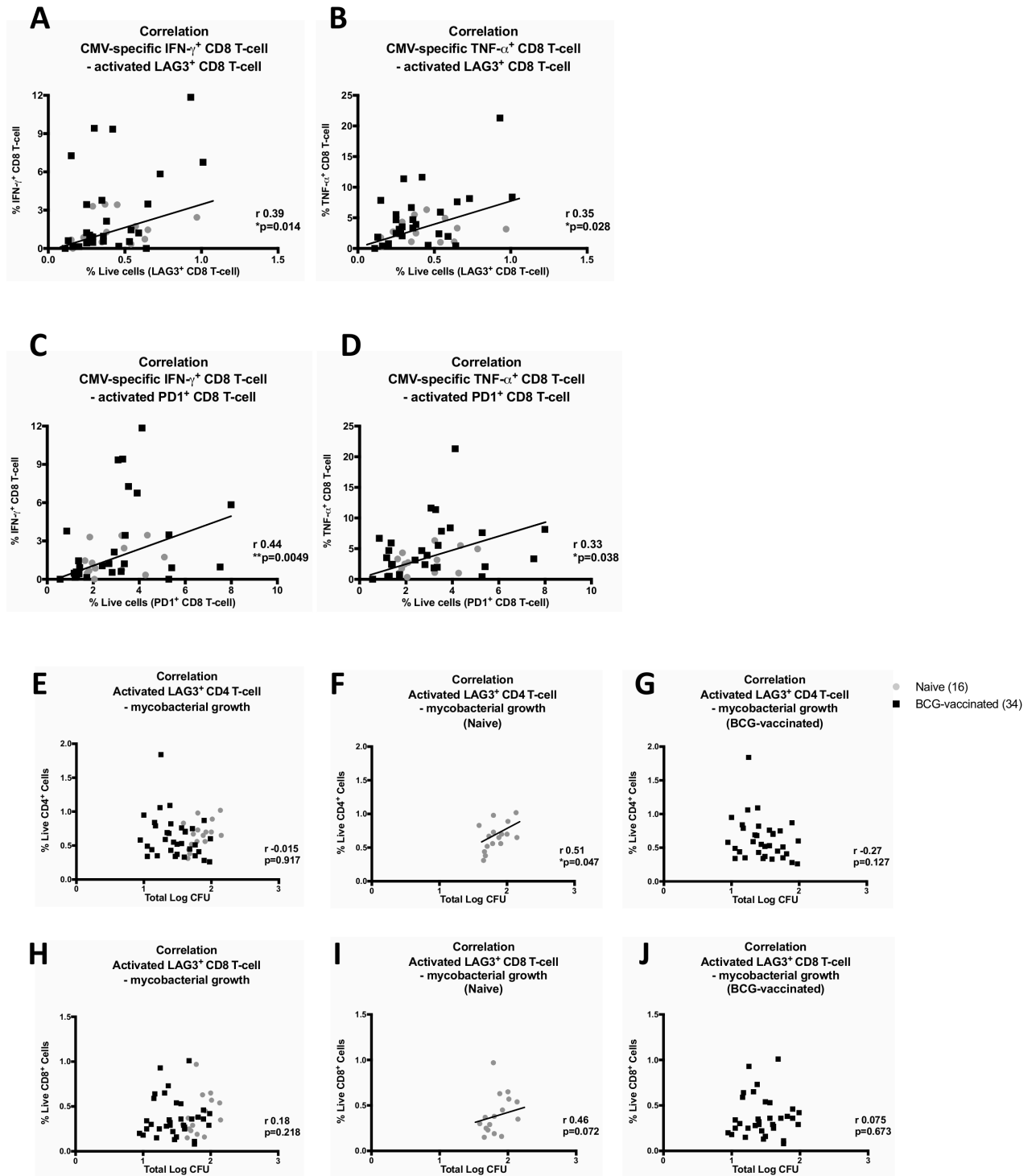


Figure 3. CMV-specific responses were associated with higher CD8 T-cell activation, expressing markers LAG3 (A-B) and PD1 (C-D) respectively. Activated CD4 and CD8 T-cells (E-J) were correlated with higher growth of mycobacteria, notably in the naïve groups (F, I). A p value <0.05 was considered statistically significant (Spearman's correlation). n=50 participants, consisted of 16 BCG-naïve and 34 BCG-vaccinated participants. *p<0.05, **p<0.01.

Impact of sex on *ex vivo* mycobacterial growth inhibition and cytokine responses

In this study, it was demonstrated that sex was associated with several differences in immune responses following historical BCG vaccination. First, BCG-vaccinated females were shown to exhibit superior capacity to control mycobacterial growth when compared to males ($p=0.029$, Figure 4B). In contrast, males appear to have a higher IFN- γ response from PPD-stimulated PBMCs as well as higher IP-10 production in the MGIA supernatant, both in naïve and BCG-vaccinated groups (Figure 4 C-F). Supplementary Table S6 summarises the sex comparisons of all measured cytokines from the MGIA supernatants.

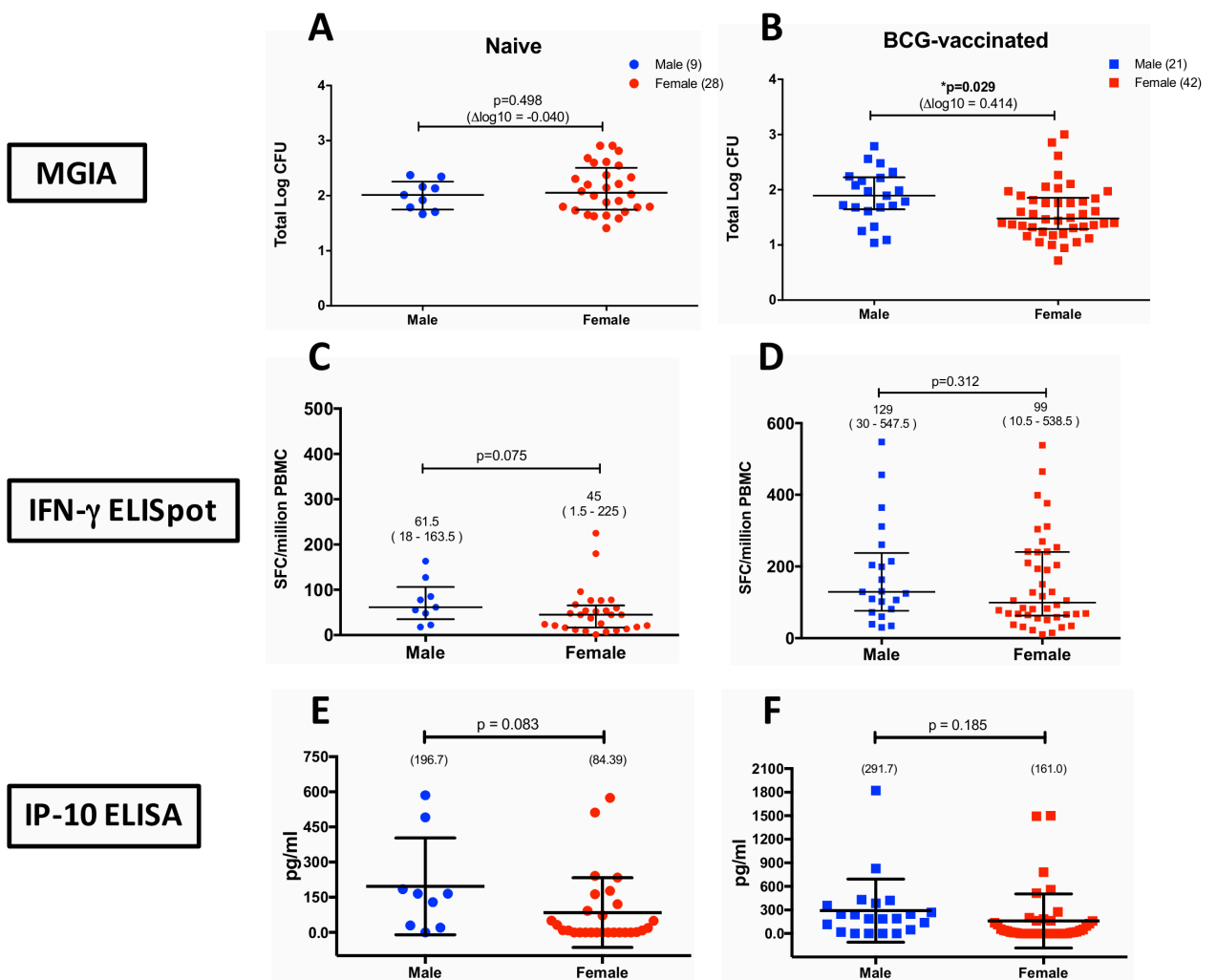


Figure 4. Sex impact on growth inhibition and immune responses following historical BCG vaccination. Assessment was performed from 37 BCG-naïve (**A, C, E**) and 63 BCG-vaccinated participants (**B, D, F**). (A-B) Growth inhibition was compared between sex and data was presented as total number of log CFUs per sample (unpaired t-test). (C-D) IFN- γ production from PBMC following stimulation with PPD was compared (Mann-Whitney test). Numbers above each group represent median (range). SFC, spot forming cells. (E-F) IP-10 was measured from MGIA supernatants using ELISA assay (mean, unpaired t-test). Dots and squares represent individual data points, and the central lines indicate the median response with IQR. * $p < 0.05$.

Impact of sex on immune cells phenotype

In the BCG-vaccinated group, females had a higher frequency of cytokine-producing NK cells ($p=0.018$, Figure 5A). There was also a higher CD4/CD8 ratio in females compared to males in the naïve group ($p=0.028$, Figure 5B). Interestingly, there was a higher frequency of monocytes in males in the BCG-vaccinated group ($p=0.049$, Figure 5C). There was also a trend of higher ML ratio in BCG-vaccinated males compared to females ($p=0.08$, Supplementary Table S7). In terms of T-cell activation, BCG-vaccinated females exhibited a lower frequency of LAG3⁺ CD8 T-cells ($p=0.0297$, Figure 5D). While in the naïve group, females also had lower frequencies of activated CD8 T-cells expressing HLA-DR, LAG3 and PD1 ($p < 0.05$, Supplementary Table S7). The lower frequencies of activated T-cells in females may be a consequence of lower CMV-specific CD8 T-cells response (Figure 5E and Supplementary Table S7).

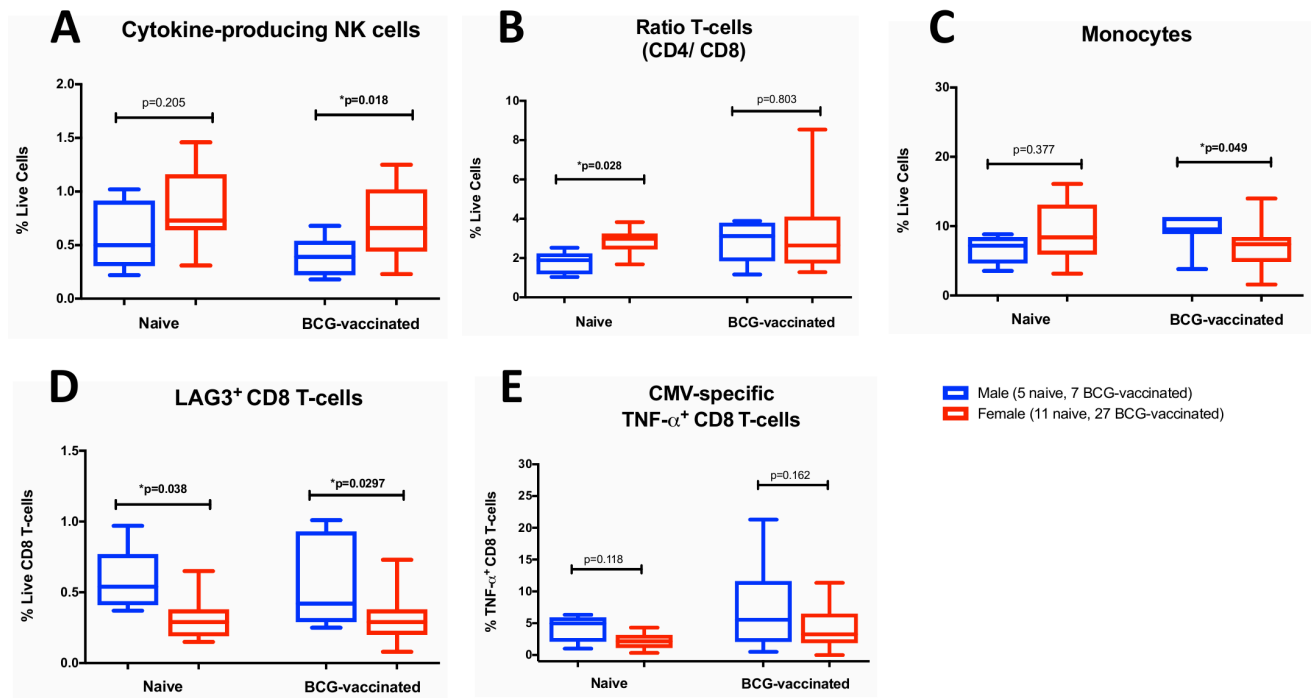


Figure 5. Comparison by sex of immune cells phenotype (A-C), T-cell activation (D) and CMV-specific T-cell response (E). Assessment was performed from 16 BCG-naïve and 34 BCG-vaccinated participants. The box plots show the minimum and maximum values (ends of the whiskers), the median (band near the middle of the box) and interquartile ranges. Blue and red colour represent males and females, respectively. A p value <0.05 was considered statistically significant (Mann-Whitney). *p<0.05, **p<0.01, ****p<0.0001.

Discussion

The present study reports that mycobacterial growth inhibition can be detected *ex vivo* following historical BCG vaccination in adult healthy volunteers. In this study, the average time since BCG vaccination was 29.4 years prior to enrolment. Our results are in line with previous studies such as Fletcher *et al.*²⁹ which detected the impact of historical BCG vaccination after more than 20 years using the same PBMC-based MGIA. Most vaccinated individuals enrolled in our study are UK participants immunised with BCG

during their school age (12-13 years old), which has been shown in a recent study by Mangtani *et al.* to provide protection for over 20 years¹¹. A higher IFN- γ response was also observed in the BCG-vaccinated group compared to the naïve group using the ELISpot assay, reflecting the presence of BCG-specific memory cells. Moreover, there was a significant correlation between IFN- γ response and lower mycobacterial growth in all cohort participants, although the association did not reach significance in the BCG-vaccinated group only. Several published MGIA studies reported increased IFN- γ production following BCG vaccination^{29,39,40}, and BCG-specific IFN- γ response measured with the ELISpot assay is known to be associated with reduced TB disease risk following BCG vaccination in infants²³. The ELISpot assay measures all cells that secrete IFN- γ in response to antigen stimulation, including NK cells and $\gamma\delta$ T-cells in addition to conventional T-cells. Focusing on the conventional T-cells response, in this study, we did not observe a significant association between Th1-type cytokine-expressing T-cells and *ex vivo* mycobacterial growth inhibition, although the data suggest that they may be protective. This finding was in contrast with the study of Smith *et al.*³⁰ which showed an association between MGIA control capacity and the frequency of polyfunctional CD4 T-cells when studying a small cohort of BCG-vaccinated infants, but was consistent with the finding of Joosten *et al.*³¹ using the same PBMC-based MGIA, as well as with a study by Kagina *et al.*⁴¹ which showed no association between polyfunctional T-cells and the risk to develop TB disease following BCG vaccination.

We also observed higher Th1-type cytokines in the MGIA supernatants from BCG-vaccinated participants compared to the naïve, although statistical significance was not arrived at. Interestingly, there was a strong significant correlation between IL-10 production and reduced control of mycobacterial growth. This observation replicates an

earlier finding using PBMC from the MVA85A trial participants cohort, in which IL-10 was associated with reduced *ex vivo* growth inhibition, and was significantly predictive of mycobacterial growth through inhibition of other pro-inflammatory cytokines⁴². Addition of recombinant IL-10 to the *ex vivo* MGIA system has been shown previously to promote mycobacterial growth^{42,43}. IL-10 is known to have immunosuppressive activity by inhibiting T-cell proliferation and IFN- γ production, leading to reduced macrophage activation⁴⁴. The capacity of individuals to produce IL-10 may need to be considered when assessing TB vaccine effects in clinical trials.

In this study, the frequency of NK cells – in particular cytokine-producing NK cells – is notably associated with enhanced *ex vivo* mycobacterial growth inhibition following historical BCG vaccination. This may account for the correlation between IFN- γ ELISpot response and control of mycobacterial growth. The results again support a recent finding, in which a greater frequency of putative cytokine-producing CD16⁺ NK cells was associated with reduced mycobacterial growth in the multiple regression analysis of MVA85A correlate of risk study^{42,45}. Cytokine-producing NK cells are the main source of NK-cell derived cytokines such as IFN- γ , TNF- α and GM-CSF⁴⁶, which were modestly increased in the MGIA supernatants of the BCG-vaccinated group in this study. Initially, cytotoxicity and cytokine-producing functions of NK cells are often regarded as two distinct functions with little synergy between them as a result of early association of the two distinct subsets of NK populations^{46,47}. However, it was recently shown that IFN- γ and TNF- α synergistically enhance NK cell cytotoxicity through NF- κ B-dependent up-regulation of intracellular adhesion molecule-1 expression in target cells, hence rendering the cells more sensitive to cytolysis activities⁴⁸. In the present study, BCG-vaccinated

participants produced a higher level of perforin and the secretion of these lytic granules was associated with enhanced growth inhibition.

Although considered a component of innate immune system, an emerging body of evidence has revealed that NK cells can also behave in a memory-like manner following infection or vaccination (reviewed in^{49,50}). NK cells isolated from pleural fluid express the memory marker CD45RO and produce higher amounts of IFN- γ and IL-22 in response to stimulation with IL-12, IL-15 and BCG when compared with CD45RO⁻ cells^{51,52}. Even though NK cells do not have antigen receptors generated by genetic rearrangement, they possess receptors which allow direct antigenic contact, resulting in subsequent cellular activation⁵⁰. Moreover, NK cells can also undergo secondary responses following activation by cytokines, such as IL-12, IL-15 and IL-18^{53,54}. This process will generate antigen-specific NK cells, which lead to an enhanced response following re-exposure with the same stimulus. In addition, work by Kleinnijenhuis *et al.* also unveil that BCG vaccination promotes augmented secondary responses towards the same and unrelated stimulus through the trained innate immunity mechanism⁵⁵. The growth inhibition assay has recently been shown to be able to detect contribution from the trained innate immune compartment, following *Mtb* exposure and BCG vaccination, by the role of nonclassical monocytes³¹. Our present study has shown the additional contribution of NK cells to *ex vivo* mycobacterial growth control, and in line with this, recent clinical trials also reported that immune cells associated with protection from TB disease and after BCG vaccination were not T-cells, but IFN- γ -producing NK cells^{56,57}.

Furthermore, it was demonstrated that a CMV-specific response may be associated with T-cell activation, in particular in the CD8 compartment, and this activation is correlated

with mycobacterial growth *ex vivo*. In HIV infection, T-cell activation has been established as a risk factor for acquisition of infection as well as progression from infection to disease⁵⁸⁻⁶⁰. In TB, evidence has emerged denoting the role of CMV and T-cell activation on TB disease risk^{23,25}, and our study is the first to show such association with *ex vivo* mycobacterial growth. In this study, we chose to measure CMV-specific T-cell cytokine response with ICS flow cytometry rather than with serology, as evidence in the literature showed that CMV-antibody levels do not correlate with the size of the T-cell response against CMV and the ICS method is more sensitive for detection of CMV-specific cytokine-producing T-cells^{61,62}. The previous study by Muller *et al.* reported that CMV positive infants who developed TB disease had lower frequency of putative NK cells and lower expression of genes associated with NK cells²⁵. In the present study, we did not observe a significant correlation between the CMV-specific T-cell response and NK-cell frequency (data shown in Appendix 8G of this thesis). However, CMV infection is recognised to drive the expansion of NKG2C⁺ NK cells⁶³, which do not respond well to IL-12 and IL-18 stimulation discussed above, although they may still degranulate and produce cytokine in response to direct contact stimulation^{64,65}. Further studies are required to better understand the interplay between CMV-specific responses, T-cell activation and NK cells in the context of BCG vaccination.

Differences in TB disease notification rates between the sexes are well documented and thought to be a result of biological factors, in addition to social factors^{13,16,66}. Therefore, it is of interest that our study demonstrated a higher capacity of BCG-vaccinated females to control mycobacterial growth *ex vivo* compared to males. In conjunction with this data, we found that females had a higher frequency of cytokine-producing NK cells, and lower frequency of activated T-cells as well as CMV-specific response. In addition, females also

had a lower monocyte frequency, with a trend of a lower ML ratio compared to males. Altogether, these individual-level factors appear to contribute to the enhanced growth inhibition in females following BCG vaccination. The only contrasting finding was the trend of higher IFN- γ production in males compared to females, which has been observed previously^{8,18,67}. A balanced immune response is required to protect against TB disease and perhaps, in males, stronger immune responses may lead to detrimental exaggerated inflammatory responses⁶⁸.

Such a sex specific effect has also been observed with measles and smallpox vaccines, where females are more protected than males following vaccination^{69,70}. The epidemiological observation that the sex bias in TB does not arise until puberty has suggested the important role of sex hormones¹³. Sex hormones have diverse effects on many immune cell types, including T-cells, B-cells, neutrophils, dendritic cells, macrophages and NK cells (reviewed in¹⁶). In general, testosterone is considered to downregulate the Th1 response, whereas estrogen is believed to enhance it¹⁶. Males have also been shown in a previous study to display a higher ML ratio compared to females³². Moreover, genetic or epigenetic differences between sex may play a role as well in the observed sex-differential protective effect¹⁵, aside from sex hormones.

In summary, we have demonstrated the impact of individual-level factors on *ex vivo* mycobacterial growth inhibition in a cohort of healthy, adult volunteers. Our results indicate that immune cell phenotype, cytomegalovirus-specific response and sex have impacts on immunity following BCG vaccination. These *ex vivo* observations are reflective of epidemiological data and published human studies, and such impacts may need to be considered when testing TB vaccine candidates in trial populations.

Importantly, researchers should consider routinely stratifying the trial population for analysis by sex in clinical vaccine studies, as the impact of sex in infectious diseases is common but often neglected⁷¹. The MGIA assay offers an *ex vivo* testing platform for assessment of a wide range of candidate TB vaccines, with the ability to reflect inter-individual variation which may be important for vaccine effectiveness. This present study has displayed the value of MGIA in assessing changes in the innate immune compartment as well as the adaptive immunity following BCG vaccination. The *ex vivo* MGIA is therefore an important additional tool for the TB vaccine community and should continue to be assessed for its ability to act as a correlate of vaccine-induced protection.

Acknowledgements

We would like to thank Carolynne Stanley for participant recruitment and blood sample collection, and Ayad Eddaoudi and Stephanie Canning for assistance with flow cytometry. H.A.F. has received support for this project from EC HORIZON2020 TBVAC2020 (grant no. 643381). S.A.P. received a PhD scholarship from the Indonesian Endowment Fund for Education (LPDP). K.S. was supported by the UK Medical Research Council (MRC) and the UK Department for International Development (DFID) under the MRC/DFID Concordat agreement (grant reference MR/J008702/1).

Author Contributions

S.A.P. conceived and planned the experiments, supervised by H.A.F. S.A.P. performed laboratory work and analysed the results supervised by H.A.F., K.S. and S.G.S. S.A.P.

wrote the first draft of the manuscript. All authors reviewed and approved the final version of the manuscript.

Competing interest: All authors declare no competing interests.

References

1. Houben RMGJ, Dodd PJ. The global burden of latent tuberculosis infection: A re-estimation using mathematical modelling. *PLoS Med* 2016; **13**(10): e1002152.
2. Floyd K, Glaziou P, Zumla A, Raviglione M. The global tuberculosis epidemic and progress in care, prevention, and research: an overview in year 3 of the End TB era. *Lancet Respir Med* 2018; **6**(4): 299-314.
3. Mangtani P, Abubakar I, Ariti C, et al. Protection by BCG vaccine against tuberculosis: a systematic review of randomized controlled trials. *Clin Infect Dis* 2014; **58**(4): 470-80.
4. Pai M, Behr MA, Dowdy D, et al. Tuberculosis. *Nat Rev Dis Primers* 2016; **2**: 16076.
5. Pitt JM, Blankley S, McShane H, O'Garra A. Vaccination against tuberculosis: how can we better BCG? *Microb Pathog* 2013; **58**: 2-16.
6. Fine PE. Variation in protection by BCG: implications of and for heterologous immunity. *Lancet* 1995; **346**(8986): 1339-45.
7. Black GF, Weir RE, Floyd S, et al. BCG-induced increase in interferon-gamma response to mycobacterial antigens and efficacy of BCG vaccination in Malawi and the UK: two randomised controlled studies. *Lancet* 2002; **359**(9315): 1393-401.
8. Rhodes SJ, Knight GM, Fielding K, et al. Individual-level factors associated with variation in mycobacterial-specific immune response: Gender and previous BCG vaccination status. *Tuberculosis (Edinb)* 2016; **96**: 37-43.
9. Baily GV. Tuberculosis prevention Trial, Madras. *Indian J Med Res* 1980; **72 Suppl**: 1-74.
10. B.C.G. AND vole bacillus vaccines in the prevention of tuberculosis in adolescents; first (progress) report to the Medical Research Council by their Tuberculosis Vaccines Clinical Trials Committee. *Br Med J* 1956; **1**(4964): 413-27.
11. Mangtani P, Nguipdop-Djomo P, Keogh RH, et al. The duration of protection of school-aged BCG vaccination in England: a population -based case-control study. *Int J Epidemiol* 2017: 1-9.
12. World Health Organization. Global Tuberculosis Report. *WHO, Geneva*, 2017.
13. Neyrolles O, Quintana-Murci L. Sexual inequality in tuberculosis. *PLoS Med* 2009; **6**(12): e1000199.
14. Horton KC, MacPherson P, Houben RM, White RG, Corbett EL. Sex differences in tuberculosis burden and notifications in low- and middle-income countries: A systematic review and meta-analysis. *PLoS Med* 2016; **13**(9): e1002119.
15. Fish EN. The X-files in immunity: sex-based differences predispose immune responses. *Nat Rev Immunol* 2008; **8**(9): 737-44.

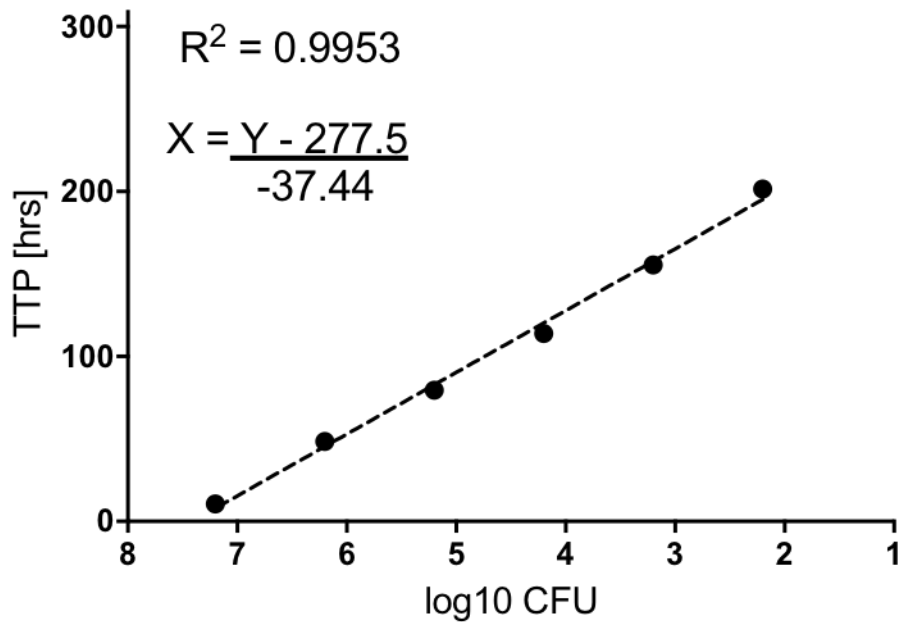
16. Nhamoye-bonde S, Leslie A. Biological differences between the sexes and susceptibility to tuberculosis. *J Infect Dis* 2014; **209**(Suppl 3): S100-6.
17. Roth A, Sodemann M, Jensen H, et al. Vaccination technique, PPD reaction and BCG scarring in a cohort of children born in Guinea-Bissau 2000-2002. *Vaccine* 2005; **23**(30): 3991-8.
18. Burl S, Adetifa UJ, Cox M, et al. The tuberculin skin test (TST) is affected by recent BCG vaccination but not by exposure to non-tuberculosis mycobacteria (NTM) during early life. *PLoS One* 2010; **5**(8): e12287.
19. Stensballe LG, Nante E, Jensen IP, et al. Acute lower respiratory tract infections and respiratory syncytial virus in infants in Guinea-Bissau: a beneficial effect of BCG vaccination for girls community based case-control study. *Vaccine* 2005; **23**(10): 1251-7.
20. Roth A, Sodemann M, Jensen H, et al. Tuberculin reaction, BCG scar, and lower female mortality. *Epidemiology* 2006; **17**(5): 562-8.
21. Stensballe LG, Sorup S, Aaby P, et al. BCG vaccination at birth and early childhood hospitalisation: a randomised clinical multicentre trial. *Arch Dis Child* 2017; **102**(3): 224-31.
22. Ritz N, Dutta B, Donath S, et al. The influence of bacille Calmette-Guerin vaccine strain on the immune response against tuberculosis: a randomized trial. *Am J Respir Crit Care Med* 2012; **185**(2): 213-22.
23. Fletcher HA, Snowden MA, Landry B, et al. T-cell activation is an immune correlate of risk in BCG vaccinated infants. *Nat Commun* 2016; **7**: 11290.
24. Klenerman P, Hill A. T cells and viral persistence: lessons from diverse infections. *Nat Immunol* 2005; **6**(9): 873-9.
25. Muller J, Matsumiya M, Snowden MA, et al. Cytomegalovirus infection is a risk factor for TB disease in Infants. *bioRxiv* 2017: 222646.
26. Tanner R, O'Shea MK, Fletcher HA, McShane H. *In vitro* mycobacterial growth inhibition assays: A tool for the assessment of protective immunity and evaluation of tuberculosis vaccine efficacy. *Vaccine* 2016: 0264-410X.
27. Brennan MJ, Tanner R, Morris S, et al. The Cross-Species Mycobacterial Growth Inhibition Assay (MGIA) Project, 2010-2014. *Clin Vaccine Immunol* 2017; **24**(9).
28. Tanner R, O'Shea MK, White AD, et al. The influence of haemoglobin and iron on *in vitro* mycobacterial growth inhibition assays. *Sci Rep* 2017; **7**: 43478.
29. Fletcher HA, Tanner R, Wallis RS, et al. Inhibition of mycobacterial growth *in vitro* following primary but not secondary vaccination with *Mycobacterium bovis* BCG. *Clin Vaccine Immunol* 2013; **20**(11): 1683-9.
30. Smith SG, Zelmer A, Blitz R, Fletcher HA, Dockrell HM. Polyfunctional CD4 T-cells correlate with *in vitro* mycobacterial growth inhibition following *Mycobacterium bovis* BCG-vaccination of infants. *Vaccine* 2016; **34**(44): 5298-305.

31. Joosten SA, van Meijgaarden KE, Arend SM, et al. Mycobacterial growth inhibition is associated with trained innate immunity. *J Clin Invest* 2018; **128**(5): 1837-51.
32. Naranbhai V, Hill AV, Abdool Karim SS, et al. Ratio of monocytes to lymphocytes in peripheral blood identifies adults at risk of incident tuberculosis among HIV-infected adults initiating antiretroviral therapy. *J Infect Dis* 2014; **209**(4): 500-9.
33. Naranbhai V, Kim S, Fletcher H, et al. The association between the ratio of monocytes:lymphocytes at age 3 months and risk of tuberculosis (TB) in the first two years of life. *BMC Med* 2014; **12**: 120.
34. Naranbhai V, Moodley D, Chipato T, et al. The association between the ratio of monocytes: lymphocytes and risk of tuberculosis among HIV-infected postpartum women. *J Acquir Immune Defic Syndr* 2014; **67**(5): 573-5.
35. Naranbhai V, Fletcher HA, Tanner R, et al. Distinct Transcriptional and Anti-Mycobacterial Profiles of Peripheral Blood Monocytes Dependent on the Ratio of Monocytes: Lymphocytes. *EBioMedicine* 2015; **2**(11): 1619-26.
36. Jensen C, Lindebo Holm L, Svensson E, Aagaard C, Ruhwald M. Optimisation of a murine splenocyte mycobacterial growth inhibition assay using virulent *Mycobacterium tuberculosis*. *Sci Rep* 2017; **7**(1): 2830.
37. Kewcharoenwong C, Prabowo SA, Bancroft GJ, Fletcher HA, Lertmemongkolchai G. Glibenclamide Reduces Primary Human Monocyte Functions Against Tuberculosis Infection by Enhancing M2 Polarization. *Frontiers in Immunology* 2018; **9**(2109).
38. La Manna MP, Orlando V, Dieli F, et al. Quantitative and qualitative profiles of circulating monocytes may help identifying tuberculosis infection and disease stages. *PLoS One* 2017; **12**(2): e0171358.
39. Hoft DF, Worku S, Kampmann B, et al. Investigation of the relationships between immune-mediated inhibition of mycobacterial growth and other potential surrogate markers of protective *Mycobacterium tuberculosis* immunity. *J Infect Dis* 2002; **186**(10): 1448-57.
40. Kampmann B, Tena GN, Mzazi S, Eley B, Young DB, Levin M. Novel human in vitro system for evaluating antimycobacterial vaccines. *Infect Immun* 2004; **72**(11): 6401-7.
41. Kagina BM, Abel B, Scriba TJ, et al. Specific T cell frequency and cytokine expression profile do not correlate with protection against tuberculosis after bacillus Calmette-Guerin vaccination of newborns. *Am J Respir Crit Care Med* 2010; **182**(8): 1073-9.
42. Tanner R. Development of mycobacterial growth inhibition assays for the early evaluation and gating of novel TB vaccine candidates [Doctoral Thesis]: University of Oxford; 2015.
43. Anwar S. Impact of Helminth Infection on Antimycobacterial Immune Responses in UK Migrants [Doctoral Thesis]: London School of Hygiene & Tropical Medicine; 2017.
44. Redford PS, Murray PJ, O'Garra A. The role of IL-10 in immune regulation during M. tuberculosis infection. *Mucosal Immunol* 2011; **4**(3): 261-70.

45. Tameris MD, Hatherill M, Landry BS, et al. Safety and efficacy of MVA85A, a new tuberculosis vaccine, in infants previously vaccinated with BCG: a randomised, placebo-controlled phase 2b trial. *Lancet* 2013; **381**(9871): 1021-8.
46. Cooper MA, Fehniger TA, Caligiuri MA. The biology of human natural killer-cell subsets. *Trends Immunol* 2001; **22**(11): 633-40.
47. Barcelos W, Sathler-Avelar R, Martins-Filho OA, et al. Natural killer cell subpopulations in putative resistant individuals and patients with active Mycobacterium tuberculosis infection. *Scand J Immunol* 2008; **68**(1): 92-102.
48. Wang R, Jaw JJ, Stutzman NC, Zou Z, Sun PD. Natural killer cell-produced IFN-gamma and TNF-alpha induce target cell cytolysis through up-regulation of ICAM-1. *J Leukoc Biol* 2012; **91**(2): 299-309.
49. Paust S, von Andrian UH. Natural killer cell memory. *Nat Immunol* 2011; **13**(6): 500-8.
50. Chorenno Parra JA, Martinez Zuniga N, Jimenez Zamudio LA, Jimenez Alvarez LA, Salinas Lara C, Zuniga J. Memory of Natural Killer Cells: A New Chance against Mycobacterium tuberculosis? *Front Immunol* 2017; **8**: 967.
51. Fu X, Liu Y, Li L, et al. Human natural killer cells expressing the memory-associated marker CD45RO from tuberculous pleurisy respond more strongly and rapidly than CD45RO- natural killer cells following stimulation with interleukin-12. *Immunology* 2011; **134**(1): 41-9.
52. Fu X, Yu S, Yang B, Lao S, Li B, Wu C. Memory-Like Antigen-Specific Human NK Cells from TB Pleural Fluids Produced IL-22 in Response to IL-15 or Mycobacterium tuberculosis Antigens. *PLoS One* 2016; **11**(3): e0151721.
53. Sun JC, Beilke JN, Lanier LL. Adaptive immune features of natural killer cells. *Nature* 2009; **457**(7229): 557-61.
54. Sun JC, Madera S, Bezman NA, Beilke JN, Kaplan MH, Lanier LL. Proinflammatory cytokine signaling required for the generation of natural killer cell memory. *J Exp Med* 2012; **209**(5): 947-54.
55. Kleinnijenhuis J, Quintin J, Preijers F, et al. BCG-induced trained immunity in NK cells: Role for non-specific protection to infection. *Clin Immunol* 2014; **155**(2): 213-9.
56. Suliman S, Geldenhuys H, Johnson JL, et al. Bacillus Calmette-Guerin (BCG) Revaccination of Adults with Latent Mycobacterium tuberculosis Infection Induces Long-Lived BCG-Reactive NK Cell Responses. *J Immunol* 2016; **197**(4): 1100-10.
57. Roy Chowdhury R, Vallania F, Yang Q, et al. A multi-cohort study of the immune factors associated with M. tuberculosis infection outcomes. *Nature* 2018; **s41586**: 018-0439-x.
58. Appay V, Sauce D. Immune activation and inflammation in HIV-1 infection: causes and consequences. *J Pathol* 2008; **214**(2): 231-41.

59. Wittkop L, Bitard J, Lazaro E, et al. Effect of cytomegalovirus-induced immune response, self antigen-induced immune response, and microbial translocation on chronic immune activation in successfully treated HIV type 1-infected patients: the ANRS CO3 Aquitaine Cohort. *J Infect Dis* 2013; **207**(4): 622-7.
60. Gronborg HL, Jespersen S, Hønge BL, Jensen-Fangel S, Wejse C. Review of cytomegalovirus coinfection in HIV-infected individuals in Africa. *Rev Med Virol* 2017; **27**(1).
61. Clari MA, Munoz-Cobo B, Solano C, et al. Performance of the QuantiFERON-cytomegalovirus (CMV) assay for detection and estimation of the magnitude and functionality of the CMV-specific gamma interferon-producing CD8(+) T-cell response in allogeneic stem cell transplant recipients. *Clin Vaccine Immunol* 2012; **19**(5): 791-6.
62. Terrazzini N, Bajwa M, Vita S, et al. Cytomegalovirus infection modulates the phenotype and functional profile of the T-cell immune response to mycobacterial antigens in older life. *Exp Gerontol* 2014; **54**: 94-100.
63. Guma M, Angulo A, Vilches C, Gomez-Lozano N, Malats N, Lopez-Botet M. Imprint of human cytomegalovirus infection on the NK cell receptor repertoire. *Blood* 2004; **104**(12): 3664-71.
64. Beziat V, Dalgard O, Asselah T, et al. CMV drives clonal expansion of NKG2C+ NK cells expressing self-specific KIRs in chronic hepatitis patients. *Eur J Immunol* 2012; **42**(2): 447-57.
65. Wu Z, Sinzger C, Frascaroli G, et al. Human cytomegalovirus-induced NKG2C(hi) CD57(hi) natural killer cells are effectors dependent on humoral antiviral immunity. *J Virol* 2013; **87**(13): 7717-25.
66. Rhines AS. The role of sex differences in the prevalence and transmission of tuberculosis. *Tuberculosis (Edinb)* 2013; **93**(1): 104-7.
67. Nielsen NO, Soborg B, Borresen M, Andersson M, Koch A. Cytokine responses in relation to age, gender, body mass index, Mycobacterium tuberculosis infection, and otitis media among Inuit in Greenland. *Am J Hum Biol* 2013; **25**(1): 20-8.
68. Orme IM, Robinson RT, Cooper AM. The balance between protective and pathogenic immune responses in the TB-infected lung. *Nat Immunol* 2015; **16**(1): 57-63.
69. Haralambieva IH, Ovsyannikova IG, Kennedy RB, Larrabee BR, Shane Pankratz V, Poland GA. Race and sex-based differences in cytokine immune responses to smallpox vaccine in healthy individuals. *Hum Immunol* 2013; **74**(10): 1263-6.
70. de Bree LCJ, Koeken V, Joosten LAB, et al. Non-specific effects of vaccines: Current evidence and potential implications. *Semin Immunol* 2018; **06**(002): 1044-5323.
71. van Lunzen J, Altfeld M. Sex differences in infectious diseases-common but neglected. *J Infect Dis* 2014; **209**(Suppl 3): S79-80.

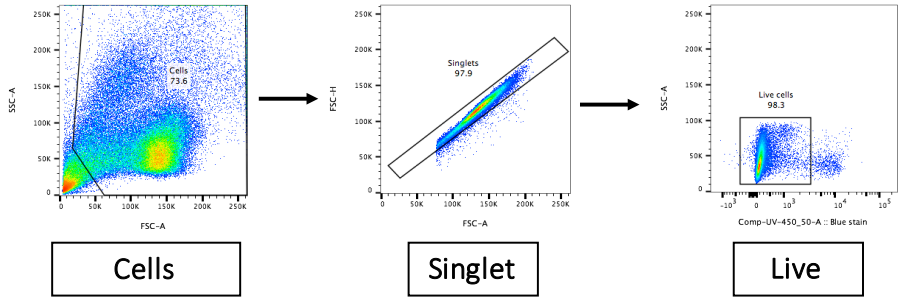
Supplementary Figures



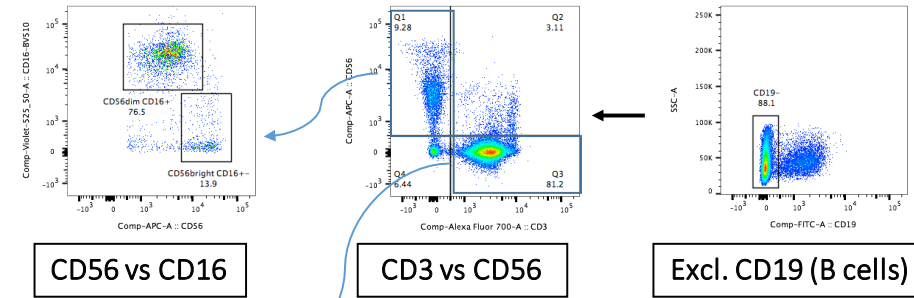
Supplementary Figure S1. Standard curve of BCG Pasteur Aeras used to convert TTP to CFU. A titration experiment was conducted to establish the relationship between log₁₀ CFU and MGIT time to positivity (TTP). Linear regression analysis was carried out in GraphPad Prism. The resulting equation was used to calculate log₁₀ CFU.

[A]

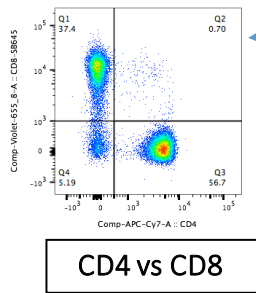
Lymphocyte Gating



NK Cells

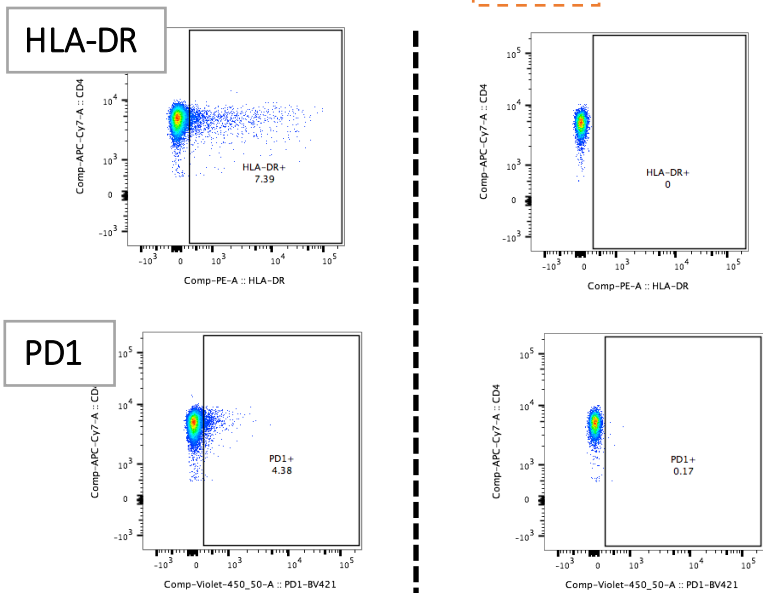


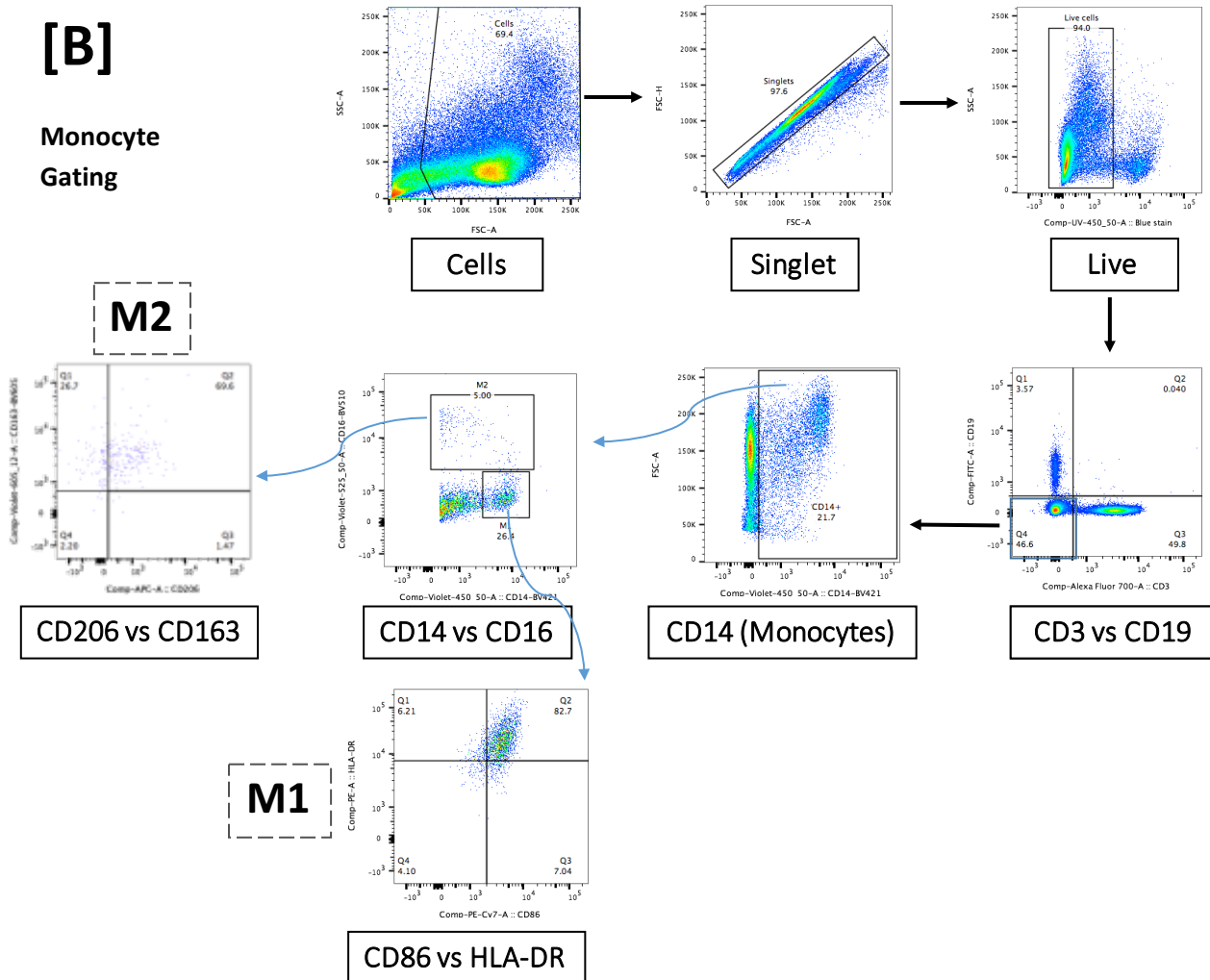
T Cells



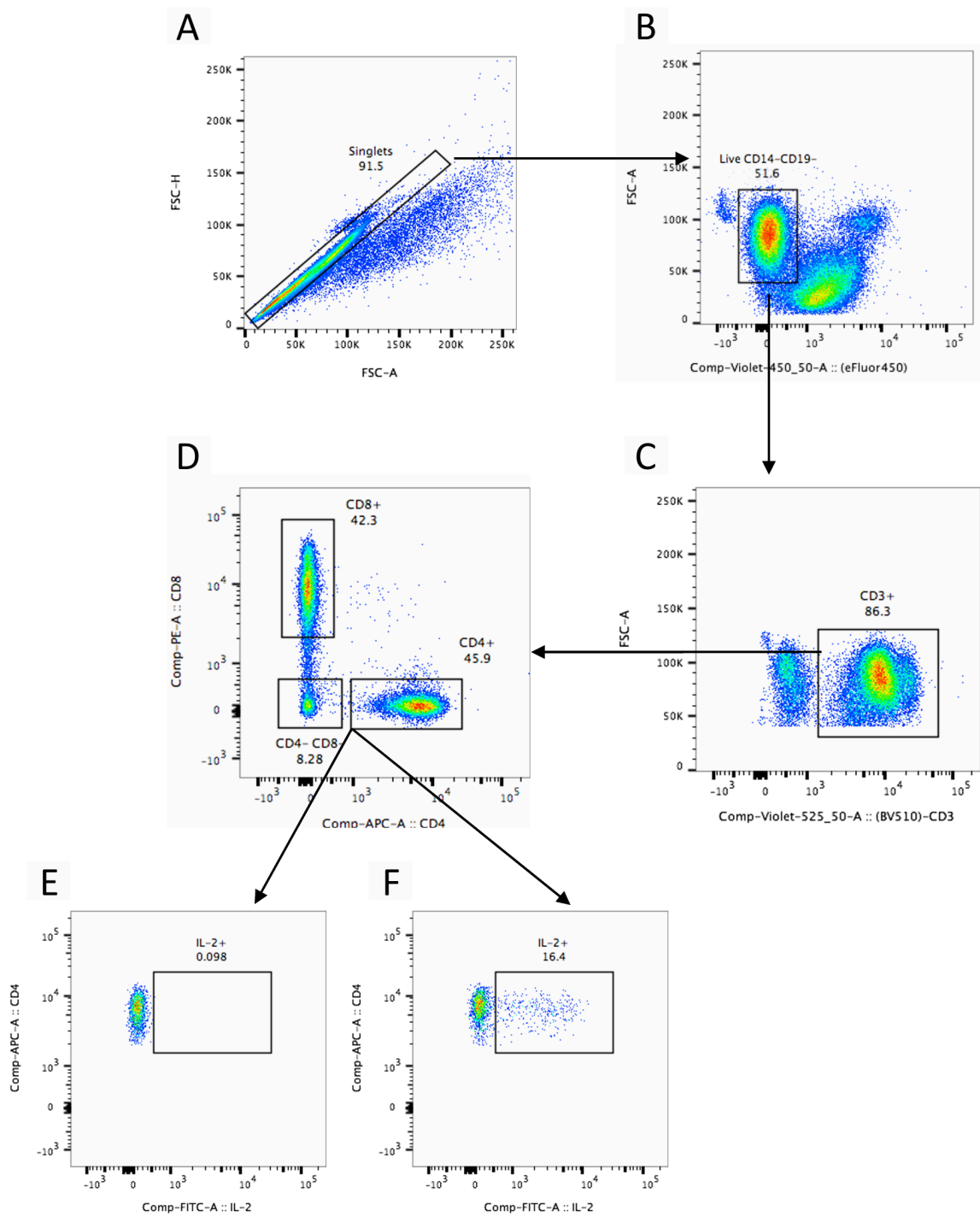
T-cell Activation

FMO

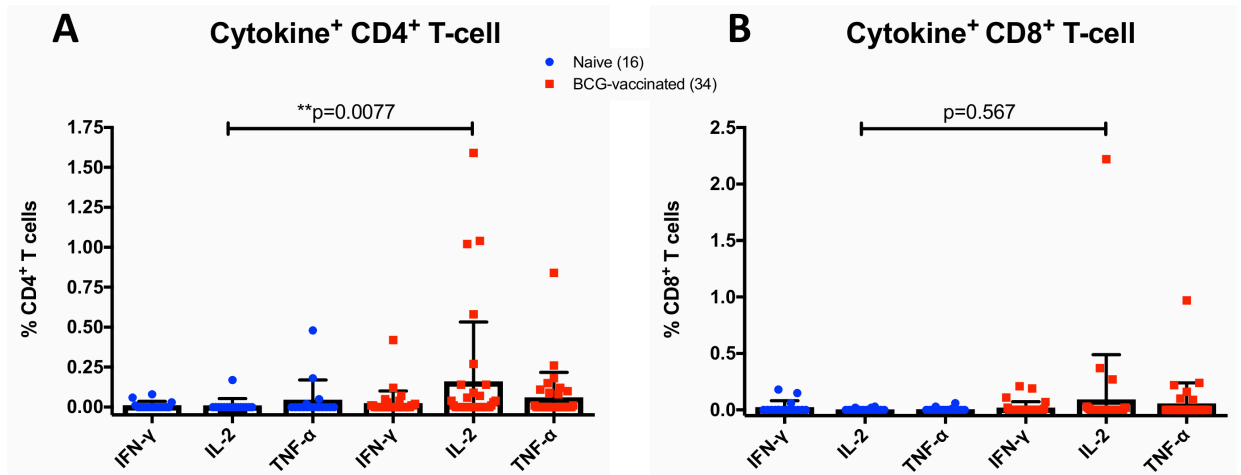




Supplementary Figure S2. Cell surface flow cytometry gating strategies. (A) Lymphocyte gating. For each sample, gating of singlet, live cells, CD19⁻, CD3⁺ (T-cells) and CD56⁺ (NK cells) was performed in sequence. Subsequently, CD4 or CD8 T-cells as well as CD56^{dim} CD16⁺ or CD56^{bright} CD16^{+/-} NK cell were also gated. Furthermore, CD4 and CD8 T-cells were gated for T-cell activation markers. Gating for the following markers were performed: LAG3, HLA-DR and PD1, with above examples represent the latter two. **(B) Monocyte gating.** Gating of singlet, live cells, CD3⁻CD19⁻ and CD14⁺ (monocytes) was performed in sequence for each sample. Next, CD14^{bright} CD16^{+/-} (M1) or CD14^{dim} CD16⁺ (M2) monocytes were gated. M1 was further defined by CD86 and HLA-DR markers, while M2 was confirmed by CD206 and CD163 markers. CD64⁺ and CD123⁺ activated monocytes were also gated from CD14⁺ monocytes using the FMO controls.



Supplementary Figure S3. ICS flow cytometry gating strategy. Gating of singlet (A), dump negative (live, CD14⁻, CD19⁻) (B), CD3⁺ lymphocytes (C) and CD4⁺, CD8⁺ as well as CD4⁻ CD8⁻ T-cells (D) was performed in sequence for each sample. Cytokine gates were then set on unstimulated tubes (E) and copied to stimulated tubes (F). Gating for the following cytokines were set: IFN- γ , TNF- α and IL-2, with E & F represent an example of IL-2.



Supplementary Figure S4. Frequencies of Th1 cytokine-expressing T-cells. Expressions were measured from PBMCs after stimulation with ~100 CFU BCG for 4 days. Among CD4 and CD8 T-cells (**A** and **B**), comparisons were made between the naïve (blue) and historically BCG-vaccinated (red) groups. Data is displayed as bar graphs and error bars represent mean \pm SD. The Mann-Whitney *U* test was used to determine significance and p value <0.05 was considered statistically significant. n=16 naïve and 34 historically BCG-vaccinated participants.

Supplementary Tables

BCG-specific cytokine ⁺ T-cells	Correlation with <i>ex vivo</i> mycobacterial growth					
	All participants		Naïve		BCG-vaccinated	
	r	p-value	r	p-value	r	p-value
IFN- γ ⁺ CD4 T-cells	-0.0055	0.9703	0.031	0.9098	0.005	0.9784
IL-2 ⁺ CD4 T-cells	-0.23	0.1196	-0.25	0.5000	0.038	0.8377
TNF- α ⁺ CD4 T-cells	-0.2	0.1673	-0.21	0.4241	-0.14	0.4413
IFN- γ ⁺ CD8 T-cells	-0.16	0.2674	-0.063	0.8167	-0.23	0.2030
IL-2 ⁺ CD8 T-cells	0.11	0.4658	0.64	0.0060	0.045	0.8058
TNF- α ⁺ CD8 T-cells	-0.038	0.7964	0.071	0.7940	0.079	0.6670

Table S1. Correlation of BCG-specific T-cell response and *ex vivo* mycobacterial growth. Associations were assessed from total 50 participants, as well as from each naïve and BCG-vaccinated groups respectively (Spearman's correlation). A p value <0.05 was considered statistically significant (not corrected for multiple comparisons).

Leukocyte subsets (% live cells)	Naïve	BCG-vaccinated	p-value
T-cells	67.84 [63.53-72.15]	66.12 [62.96-69.28]	0.7537
CD4 T-cells	43.76 [39.48-48.04]	44.69 [41.31-48.08]	0.7149
CD8 T-cells	18.98 [16.02-21.94]	16.48 [14.49-18.46]	0.1396
CD4/CD8 ratio	2.502 [2.066-2.939]	3.142 [2.596-3.688]	0.2428
NK cells	5.933 [4.176-7.691]	6.699 [5.122-8.277]	0.7970
Cytokine NK cell	0.765 [0.5785-0.9515]	0.6488 [0.5412-0.7565]	0.2202
Cytotoxic NK cell	3.99 [2.636-5.344]	4.905 [3.503-6.307]	0.8736
NK cell ratio	5.275 [3.899-6.65]	7.314 [5.395-9.233]	0.4154
Monocytes	8.541 [6.512-10.57]	7.571 [6.47-8.672]	0.5468
ML ratio	0.1116 [0.08108-0.1422]	0.09897 [0.08217-0.1158]	0.6175
M1 monocytes	3.489 [2.196-4.781]	3.192 [2.514-3.871]	0.8571
M2 monocytes	0.2256 [0.1648-0.2865]	0.2812 [0.2083-0.3541]	0.6616
M1/M2 ratio	18.7 [10.38-27.01]	15.01 [11.46-18.55]	0.7812
CD64 ⁺ monocytes	4.303 [2.515-6.092]	4.069 [3.183-4.955]	0.8774
CD123 ⁺ monocytes	4.00 [2.457-5.543]	3.838 [3.015-4.661]	0.9221
Suppressor monocytes	0.2356 [0.1402-0.331]	0.1673 [0.1313-0.2034]	0.0888
Activated T-cells			
HLA-DR ⁺ CD4 T-cells	7.381 [5.656-9.106]	7.291 [5.57-9.013]	0.4615
LAG3 ⁺ CD4 T-cells	0.6619 [0.5543-0.7694]	0.6256 [0.5179-0.7332]	0.3450
PD1 ⁺ CD4 T-cells	3.263 [2.712-3.813]	3.647 [3.066-4.228]	0.5399
HLA-DR ⁺ CD8 T-cells	6.043 [3.853-8.232]	6.135 [4.564-7.707]	0.6285
LAG3 ⁺ CD8 T-cells	0.405 [0.2873-0.5227]	0.3726 [0.2959-0.4494]	0.5466
PD1 ⁺ CD8 T-cells	2.643 [2.029-3.256]	2.985 [2.34-3.631]	0.8094

Table S2. Impact of historical BCG vaccination on immune cell frequencies. Comparisons were made between naïve and BCG-vaccinated groups (Mann-Whitney), the values indicate mean of live cells percentage [95% CI]. Assessment was performed from 16 BCG-naïve and 34 BCG-vaccinated participants. A p value <0.05 was considered statistically significant (not corrected for multiple comparisons).

Cytokine (pg/ml)	Comparison			Correlation with <i>ex vivo</i> mycobacterial growth	
	Naïve	BCG-vaccinated	p-value	r	p-value
Perforin	1421 [1177-1664]	1884 [1645-2124]*	0.0179	-0.44**	0.0013
Granzyme	33.63 [2.33-64.94]	60.11 [2.283-117.9]	0.5394	-0.023	0.8738
IL-32	26.75 [22.83-30.67]	28 [24.47-31.52]	0.6611	-0.073	0.6160
IL-22	0.00 [0.00-0.00]	7.607 [-7.357-22.57]	0.4839	-0.064	0.6595

Table S3. Summary of mean NK cells cytokine responses measured with ELISA assays. Comparisons were made between naïve and BCG-vaccinated groups (unpaired t-test), the values indicate mean of concentration in pg/ml [95% CI]. Correlations were assessed with *ex vivo* mycobacterial growth (Spearman's correlation). A p value <0.05 was considered statistically significant. n=16 BCG-naïve and n=34 BCG-vaccinated participants. *p<0.05, **p<0.01.

CMV-specific cytokine ⁺ T-cells (% live cells)	Naïve	BCG-vaccinated	p-value
IFN- γ ⁺ CD4 T-cells	0.6446 [0.3842-0.905]	1.319 [0.4458-2.191]	0.9829
IL-2 ⁺ CD4 T-cells	1.009 [0.4506-1.568]	1.652 [0.8894-2.414]	0.7056
TNF- α ⁺ CD4 T-cells	3.255 [2.164-4.346]	3.982 [2.344-5.62]	0.7812
IFN- γ ⁺ CD8 T-cells	1.555 [0.8136-2.297]	2.744 [1.403-4.086]	0.7924
IL-2 ⁺ CD8 T-cells	0.3308 [0.09425-0.5673]	0.6881 [0.3361-1.04]	0.4612
TNF- α ⁺ CD8 T-cells	2.934 [1.788-4.079]	4.924 [3.1-6.748]	0.2490

Table S4. CMV-specific T-cell responses. Comparisons were made between naïve and BCG-vaccinated groups (Mann-Whitney), the values indicate mean of live cells percentage [95% CI]. A p value <0.05 was considered statistically significant (not corrected for multiple comparisons). n=16 BCG-naïve and n=34 BCG-vaccinated participants.

Activated T-cells	Correlation with <i>ex vivo</i> mycobacterial growth					
	All participants		Naïve		BCG-vaccinated	
	r	p-value	r	p-value	r	p-value
HLA-DR ⁺ CD4 T-cells	-0.029	0.8399	0.35	0.1809	-0.14	0.4220
LAG3 ⁺ CD4 T-cells	-0.015	0.9165	0.51*	0.0466	-0.27	0.1274
PD1 ⁺ CD4 T-cells	-0.052	0.7197	0.15	0.5757	-0.053	0.7660
HLA-DR ⁺ CD8 T-cells	0.13	0.3748	0.3	0.2566	0.071	0.6902
LAG3 ⁺ CD8 T-cells	0.18	0.2184	0.46	0.0721	0.075	0.6734
PD1 ⁺ CD8 T-cells	0.025	0.8610	0.11	0.6817	0.0069	0.9692

Table S5. Correlation of activated T-cells and *ex vivo* mycobacterial growth. Associations were assessed from total 50 participants, as well as from each naïve and BCG-vaccinated groups respectively (Spearman's correlation). A p value <0.05 was considered statistically significant (not corrected for multiple comparisons). *p<0.05.

Cytokine (pg/ml)	Naïve-Male	Naïve-Female	p-value	BCG-vaccinated - Male	BCG-vaccinated - Female	p-value
IFN- γ	10.39 [3.976-16.8]	13.14 [7.772-18.5]	0.5785	20.37 [8.289-32.46]	24.87 [6.65-43.09]	0.7392
IP-10	196.7 [37.72-355.6]	84.39 [26.68-142.1]	0.0825	291.7 [108.4-474.9]	161 [53.55-268.4]	0.1849
TNF- α	35.07 [-5.432-75.57]	38.91 [-7.344-85.16]	0.9265	107.3 [-9.475-224]	93.33 [22.35-164.3]	0.8268
IL-12	42.96 [-32.43-118.4]	67.7 [-28.17-163.6]	0.7731	40.64 [-19.23-100.5]	75.1 [16.97-133.2]	0.4523
IL-10	67.05 [29.53-104.6]	47.89 [21.21-74.57]	0.4454	62.27 [19.76-104.8]	58.84 [29.57-88.12]	0.8916
GM-CSF	15.2 [-12.24-42.65]	5.327 [-4.645-15.3]	0.3689	35.59 [-10.84-82.02]	115 [23.92-206.1]	0.2330
IL-6	463.5 [201.8-725.2]	322.3 [195.3-449.4]	0.2726	319.9 [177.2-462.7]	312.5 [214.6-410.4]	0.9295
IL-17	0.00 [0.00-0.00]	0.00 [0.00-0.00]	n/a	0.00 [0.00-0.00]	0.2394 [-0.1366-0.6154]	0.3687

Table S6. Comparison by sex of mean cytokine responses measured with ELISA assays, assessed from MGIA supernatant samples after 4 days of co-culture. Assessment was performed from 37 BCG-naïve (9 males, 28 females) and 63 BCG-vaccinated participants (21 males, 42 females). Comparisons were made between males and females in each group (unpaired t-test), the values indicate mean of concentration in pg/ml [95% CI]. A p value <0.05 was considered statistically significant (not corrected for multiple comparisons).

Leukocyte subsets (% live cells)	Naïve – Male	Naïve – Female	p-value	BCG-vaccinated – Male	BCG-vaccinated – Female	p-value
T-cells	69.62 [62.53-76.71]	67.03 [60.91-73.14]	0.4922	65.44 [58.02-72.87]	66.3 [62.57-70.02]	0.4995
CD4 T-cells	39.78 [31.7-47.86]	45.57 [40.02-51.13]	0.1804	43.59 [35.39-51.79]	44.98 [41.01-48.96]	0.8427
CD8 T-cells	24.18 [17.33-31.03]**	16.62 [14.06-19.18]	0.0087	16.56 [11.52-21.6]	16.46 [14.14-18.77]	0.9394
CD4/CD8 ratio	1.741 [1.018-2.465]	2.848 [2.397-3.299]*	0.0275	2.876 [1.944-3.808]	3.211 [2.543-3.879]	0.8027
NK cells	3.824 [0.2743-7.374]	6.892 [4.787-8.997]	0.1451	5.82 [0.7967-10.84]	6.927 [5.209-8.646]	0.4269
Cytokine NK cell	0.588 [0.1865-0.9895]	0.8455 [0.6135-1.077]	0.2051	0.4071 [0.2441-0.5702]	0.7115 [0.5903-0.8326]*	0.0183
Cytotoxic NK cell	2.55 [-0.3777-5.478]	4.645 [3.005-6.284]	0.2674	4.183 [-0.4383-8.804]	5.092 [3.582-6.602]	0.3987
NK cell ratio	4.323 [1.705-6.942]	5.707 [3.86-7.554]	0.4409	8.197 [1.091-15.3]	7.085 [5.127-9.044]	0.6410
Monocytes	6.652 [4.059-9.245]	9.4 [6.597-12.2]	0.3773	9.204 [6.842-11.57]*	7.148 [5.883-8.413]	0.0494
ML ratio	0.083 [0.04796-0.118]	0.1246 [0.08207-0.1672]	0.3773	0.1187 [0.08337-0.1541]	0.09385 [0.07418-0.1135]	0.0824
M1 monocytes	2.772 [0.924-4.62]	3.815 [1.967-5.663]	0.5833	3.539 [2.244-4.833]	3.103 [2.282-3.924]	0.5248
M2 monocytes	0.254 [0.01668-0.4913]	0.2127 [0.1684-0.2571]	0.8926	0.2514 [0.1121-0.3907]	0.2889 [0.2006-0.3772]	0.8270
M1/M2 ratio	15.57 [-2.966-34.11]	20.11 [9.089-31.14]	0.7427	16.83 [8.988-24.68]	14.53 [10.32-18.74]	0.4027
CD64 ⁺ monocytes	3.082 [1.316-4.848]	4.858 [2.256-7.46]	0.6612	4.781 [3.108-6.455]	3.884 [2.819-4.95]	0.2941
CD123 ⁺ monocytes	3.044 [1.272-4.816]	4.435 [2.197-6.672]	0.6612	4.393 [2.796-5.99]	3.694 [2.704-4.685]	0.3755
Suppressor monocytes	0.196 [0.1374-0.2546]	0.2536 [0.1095-0.3978]	0.8938	0.1921 [0.03059-0.3537]	0.1609 [0.1295-0.1923]	0.8759
Activated T-cells						
HLA-DR ⁺ CD4 T-cells	8.306 [3.852-12.76]	6.961 [4.842-9.08]	0.3773	8.776 [1.51-16.04]	6.907 [5.329-8.485]	0.7651
LAG3 ⁺ CD4 T-cells	0.722 [0.4286-1.015]	0.6345 [0.5068-0.7623]	0.4906	0.7814 [0.3113-1.252]	0.5852 [0.4942-0.6762]	0.3517
PD1 ⁺ CD4 T-cells	3.41 [2.022-4.798]	3.195 [2.495-3.896]	0.7624	3.981 [2.014-5.949]	3.561 [2.943-4.178]	0.6844
HLA-DR ⁺ CD8 T-cells	9.738 [2.882-16.59]	4.363 [3.161-5.564]**	0.0032	6.787 [3.03-10.54]	5.966 [4.119-7.813]	0.5312
LAG3 ⁺ CD8 T-cells	0.58 [0.2923-0.8677]	0.3255 [0.2101-0.4408]*	0.0380	0.5314 [0.2458-0.8171]	0.3315 [0.262-0.4009]*	0.0297
PD1 ⁺ CD8 T-cells	4.058 [3.1-5.016]	1.999 [1.634-2.364]***	0.0007	3.207 [1.808-4.606]	2.928 [2.157-3.699]	0.4027
CMV-specific cytokine⁺ T-cells						
IFN- γ ⁺ CD4 T-cells	0.522 [-0.01317-1.057]	0.7213 [0.3524-1.09]	0.4351	2.831 [-0.7875-6.45]	0.789 [0.4012-1.177]	0.4554
IL-2 ⁺ CD4 T-cells	0.674 [-0.004646-1.353]	1.219 [0.3168-2.121]	0.5237	2.099 [0.03712-4.16]	1.496 [0.6306-2.36]	0.4890
TNF- α ⁺ CD4 T-cells	3.068 [1.063-5.073]	3.373 [1.688-5.057]	0.7242	5.836 [0.07525-11.6]	3.334 [1.891-4.776]	0.4247
IFN- γ ⁺ CD8 T-cells	2.282 [0.6636-3.9]	1.101 [0.2655-1.937]	0.1274	4.72 [0.4053-9.035]	2.053 [0.8223-3.284]	0.2581
IL-2 ⁺ CD8 T-cells	0.222 [-0.02421-0.4682]	0.3988 [0.0009476-0.7966]	0.4584	0.9314 [0.1728-1.69]	0.603 [0.1736-1.032]	0.2026
TNF- α ⁺ CD8 T-cells	4.192 [1.553-6.831]	2.148 [1.044-3.251]	0.1181	7.73 [1.209-14.25]	3.942 [2.501-5.383]	0.1618

Table S7. Impact of sex on immune cell frequency, T-cell activation and CMV-specific T-cell response. Comparisons were made between males and females in each group (Mann-Whitney), the values indicate mean of live cells percentage [95% CI]. Assessment was performed from 16 BCG-naïve (5 males, 11 females) and 34 BCG-vaccinated participants (7 males, 27 females). A p value <0.05 was considered statistically significant. *p<0.05, **p<0.01, ****p<0.0001.

5.1 Impact of BCG vaccination in mice on MGIA in the presence of TB drugs**5.1.1 Introduction**

As described in Chapter 2, historical BCG vaccination in humans was shown to enhance the *ex vivo* drug-mediated killing of INH, and this was reflective of previously published *in vivo* human observational and animal studies. It was not attainable to access PBMC from recently BCG immunised participants during this study. Therefore, it was of interest to see if recent BCG vaccination in mice could enhance the efficacy of INH or RIF. Moreover, PZA and EMB as additional first-line TB drugs were also tested *ex vivo* using splenocyte samples of BCG-vaccinated mice. In this chapter, the impact of BCG-vaccination on *ex vivo* drug-mediated killing in mouse splenocytes has been observed and the related immune mechanisms were also explored by measuring cytokine production.

5.1.2 Materials and Methods**Animal procedure and vaccination**

Female C57Bl/6 mice aged between 6-7 weeks were supplied commercially from Charles River Laboratories, UK. Mice were kept in an individual cage in LSHTM Biological Service Facility (BSF) supplied with bedding, nesting material and enrichment. A maximum number of 6 mice per cage was applied. Autoclaved water and food pellets were provided. Procedures were performed under a personal licence issued by United

Kingdom Home Office under the Animals (Scientific Procedure) Act and under project licence number 70/8043. In two separate experiments, 5-6 female C57Bl/6 mice aged 6-7 weeks were vaccinated with BCG Pasteur Aeras and another 5-6 mice were injected with saline. Mice were immunised subcutaneously in the skin fold lateral of the abdomen with 4×10^5 CFU BCG in 100 μ l of saline and left for 6 weeks to mount a sufficient immune response prior to sacrifice.

Splenocytes harvesting from mice

Mice were sacrificed and spleens were dissected aseptically inside a sterile cabinet and placed in 5 ml of antibiotic-free media (RPMI+10% FBS+L-Glutamine) in 15 ml falcon tubes. Spleens were poured with the media into a 100 μ m nylon mesh cell strainer (BD) in a small petri dish. Spleens were then mashed through the strainer using the plunger from a 5 ml syringe. Using a Pasteur pipette, cells were transferred to 15 ml Falcon tubes and were spun at 1500 rpm for 5 minutes. Supernatants were discarded by decanting and pellets were loosened by tapping the bottom of the tube. Erythrocytes were lysed by adding 3 ml of RBC lysis buffer (Sigma) for 2 minutes at room temperature. To dilute the lysis buffer, up to 15 ml of media was added and the cells were pelleted again. Cells were resuspended in 10 ml of media for counting.

Interferon- γ ELISpot

Ex vivo ELISPOT assay was performed to measure IFN- γ secretion from mouse splenocytes. The assay was conducted in a 96-well plate coated with antibody to capture the production of IFN- γ . Mouse splenocytes were resuspended in media to yield the cell concentration of 0.3×10^6 cells / 100 μ l. Coating solution was prepared by adding anti-

IFN- γ antibody to carbonate-bicarbonate buffer (Sigma) to produce a final concentration of 15 $\mu\text{g/ml}$. To each well, 50 μl of coating solution was added until the entire surface of the well was covered. The plate was then incubated overnight at 4 $^{\circ}\text{C}$ on a flat surface. After incubation, the plate was washed 5 times with sterile PBS (200 μl per well) and blocked by adding 100 μl of media to each well. The plate was further incubated at 37 $^{\circ}\text{C}$ for 2-5 hours. Without washing the plate, the blocking solution was flicked out and 100 μl of cell suspension was added to each well. Six wells were set up for each sample, with a duplicate of wells stimulated with PHA as positive control, a duplicate of wells stimulated with PPD to measure antigen-specific response, and a duplicate of wells added with media as negative control. Mabtech kit (Nacka Strand, Sweden) was used and the rest of the procedure was performed as described in Chapter 3.

Bacterial strain for vaccination and growth inhibition assay

BCG Pasteur Aeras, an early passage Pasteur strain, was used for vaccination as well as for an immune target of the growth inhibition assay. BCG stocks were prepared and distributed by Aeras for this project. BCG stocks were kept as aliquots at -70 $^{\circ}\text{C}$. Each stock was equivalent to 2×10^8 CFU/ml. Prior to usage, a stock was thawed and kept on ice before being diluted with appropriate media to a desired concentration. The same BCG stock was used throughout this project (including data presented in Chapter 2, 3 and 4).

Generation of a standard curve

An experiment had been conducted in our group to correlate the TTP data from the MGIT to \log_{10} CFU of BCG Pasteur Aeras suspension using plate counting (Figure 1). In brief, BCG stock was serially diluted 7 times (10^{-1} – 10^{-7}) in tubes containing 1.08 ml of 7H9

broth. Duplicate MGIT tubes were set for each dilution and 500 µl of dilution was added to the respective MGIT tubes. Each dilution was plated on 7H11 agar plates and incubated for 1.5 - 2 weeks. Colonies were counted and plotted against the TTP values. The same standard curve was used throughout this project (as has been described in Chapter 2, 3 and 4).

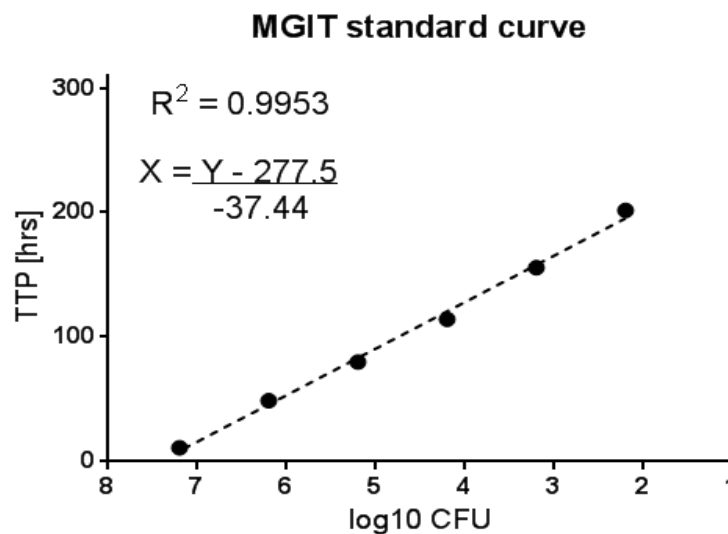


Figure 1. Correlation between TTP and log₁₀ CFU as MGIT standard curve.

Determination of drug concentrations

Optimum drug concentration was determined based on a dilution in which there was a decrease in bacterial growth, but sufficient bacterial load to identify synergistic effect of vaccination in addition to the drugs. Different BCG strains have been shown to possess different susceptibility towards anti-TB drugs¹. In this mouse study we aimed to test four first-line TB drugs: INH, RIF, PZA and EMB. Previous studies have identified the minimum inhibitory concentration of INH and RIF towards BCG Pasteur to be 0.1 and 0.063-0.125 µg/ml respectively, with no previous data for PZA and EMB¹. Thus, drug

concentrations of 1; 0.1 and 0.01 $\mu\text{g/ml}$ for all 4 drugs were chosen in this study. The concentration of 0.01 $\mu\text{g/ml}$ was introduced to identify whether the vaccine will enhance the drugs effect when used at a lower concentration. For RIF, the concentration of 1 $\mu\text{g/ml}$ was replaced with 0.5 $\mu\text{g/ml}$ in concordance to a preliminary titration experiment in which the earlier concentration resulted in very minimum growth that is not detected by the MGIT system. Drugs were diluted in sterile tissue culture grade water for INH, PZA and EMB and in DMSO for RIF (final DMSO concentration in cell culture < 0.001%).

Ex vivo MGIA

Day 1: Mouse splenocytes were resuspended in antibiotic-free media (RPMI+10% FBS+L-Glutamine) to be co-cultured with BCG and TB drugs *ex vivo*. Control tubes containing no drugs were also established for each mouse. The co-culture was performed in 2 ml screw cap tubes placed on a rotator in a CO₂ controlled incubator. For each tube, 300 μl of mouse splenocytes (5×10^6) and 300 μl of BCG input (~100 CFU) as well as 6 μl of TB drug dilution (except for control) were added. The tubes were continuously spun at 37 °C for 4 days. The tubes were labelled with sample ID, date and the added drug concentration accordingly.

Day 4: After 4 days, the 2 ml tubes were removed from the incubator. MGIT tubes were supplemented on the day of specimen inoculation. MGIT PANTA (Polymyxin B, Amphotericin B, Nalidixic Acid, Trimethoprim, Azlocillin) was prepared by pouring 15 ml MGIT OADC (Oleic acid, Albumin, Dextrose and Catalase) supplement into a bottle of lyophilized MGIT PANTA. To each respective MGIT tube, 0.8 ml of this enrichment was added. MGIT tubes were labelled to match the 2 ml tubes and then supplemented. The 2 ml tubes were centrifuged at 12,000 rpm for 10 minutes. The supernatants (500 μl)

were transferred to other 2 ml tubes and frozen at -80 °C for further analysis. The remaining cells were then lysed by the addition of 400 µl of sterile tissue culture grade water and vortexed 3 times in 5 minutes intervals. 500 µl of sample was added to the respective MGIT tubes. Tubes were placed in the MGIT machine and TTP values were recorded.

ELISA

MGIA supernatants were analysed to assess cytokine concentrations by ELISA. The levels of following cytokines were measured: IFN- γ , TNF- α , IL-12p40, IL-10, IL-17, IL-6, GM-CSF and IP-10. The concentrations of IFN- γ , IL-12p40 and IL-6 were measured using BD OptiEIA kits (Becton Dickinson, UK), while TNF- α , GM-CSF and IP-10 DuoSet ELISA kits were obtained from R&D Systems (Abingdon, UK), and IL-10 ELISA MAX Standard and IL-17 ELISA MAX Deluxe kits were sourced from BioLegend (London, UK). Assays were performed as described by the manufacturers.

Statistical analysis

Statistical analyses were performed in Graphad Prism 7 (GraphPad, La Jolla, CA, USA). To identify statistical significance of *ex vivo* growth inhibition (log CFU values) and ELISA responses, one-way analysis of variance (ANOVA) and students *t*-test were used. Mann-Whitney *U* Test was performed to identify significant differences of the ELISpot response between groups. Spearman's correlation coefficient was used to test for correlations between growth inhibition and immune responses.

5.1.3 Results

Measurement of IFN- γ ELISpot response and growth inhibition

To assess the impact of BCG vaccination on induction of antigen-specific cells in mice, the ELISpot assay was performed to measure the production of IFN- γ following stimulation with PPD antigen. BCG vaccination significantly enhanced the production of PPD antigen-specific IFN- γ response in BCG-vaccinated mice compared to the naïve group ($p < 0.0001$, Figure 2A). BCG-vaccinated mice also significantly controlled the growth of mycobacteria when compared to saline-injected mice ($p < 0.05$, Figure 2B).

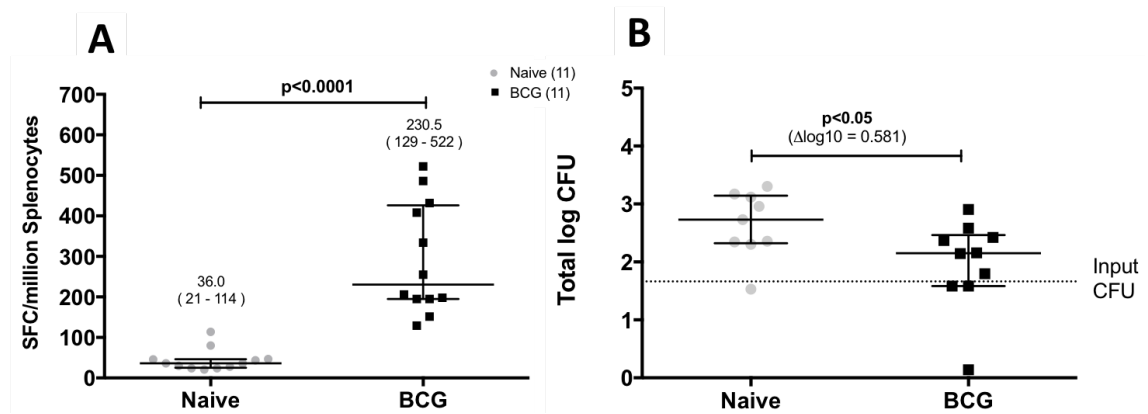


Figure 2. (A) Production of antigen-specific IFN- γ response measured with ELISpot. PPD antigen-specific cells were measured in mice splenocytes from BCG-vaccinated and naïve groups (Mann-Whitney test). Numbers above each group represent median (range). **(B) *Ex vivo* control of mycobacterial growth between naïve and vaccinated mice.** Inhibition of growth was compared using splenocytes from naïve ($n=11$) and vaccinated mice ($n=11$, unpaired t-test). Data is displayed as median with IQR. Presented data is pooled from two experiments.

Drug titration curve and impact of BCG vaccination on drug-mediated growth inhibition

In addition to INH and RIF as tested in the human study, two additional drugs PZA and EMB were also tested in the mouse experiment. This was possible due to the large number of cells obtained from a mouse spleen, double the number that can be obtained from 50 ml of human blood. Due to the lack of previous data regarding the susceptibility of BCG Pasteur Aeras towards PZA and EMB in the MGIT system, drug concentrations in the range selected for INH were used.

There was a significant reduction in mycobacterial growth when BCG was co-cultured with mouse splenocytes at an INH concentration of 0.1 and 1 $\mu\text{g/ml}$ (Figure 3 A and B) and RIF concentration of 0.1 and 0.5 $\mu\text{g/ml}$ (Figure 4 A and B) in both saline-injected and BCG-vaccinated mice. No significant reduction of bacterial growth was observed with 0.01 $\mu\text{g/ml}$ of INH and RIF. The slope of the titration curve was similar to the one observed in the experiment with human PBMCs as described in Chapter 2, with the curve of RIF being steeper compared to that of INH. In this explorative experiment with PZA and EMB, no dose – response relationship was observed in any of the drug concentrations tested (Figure 5 and 6).

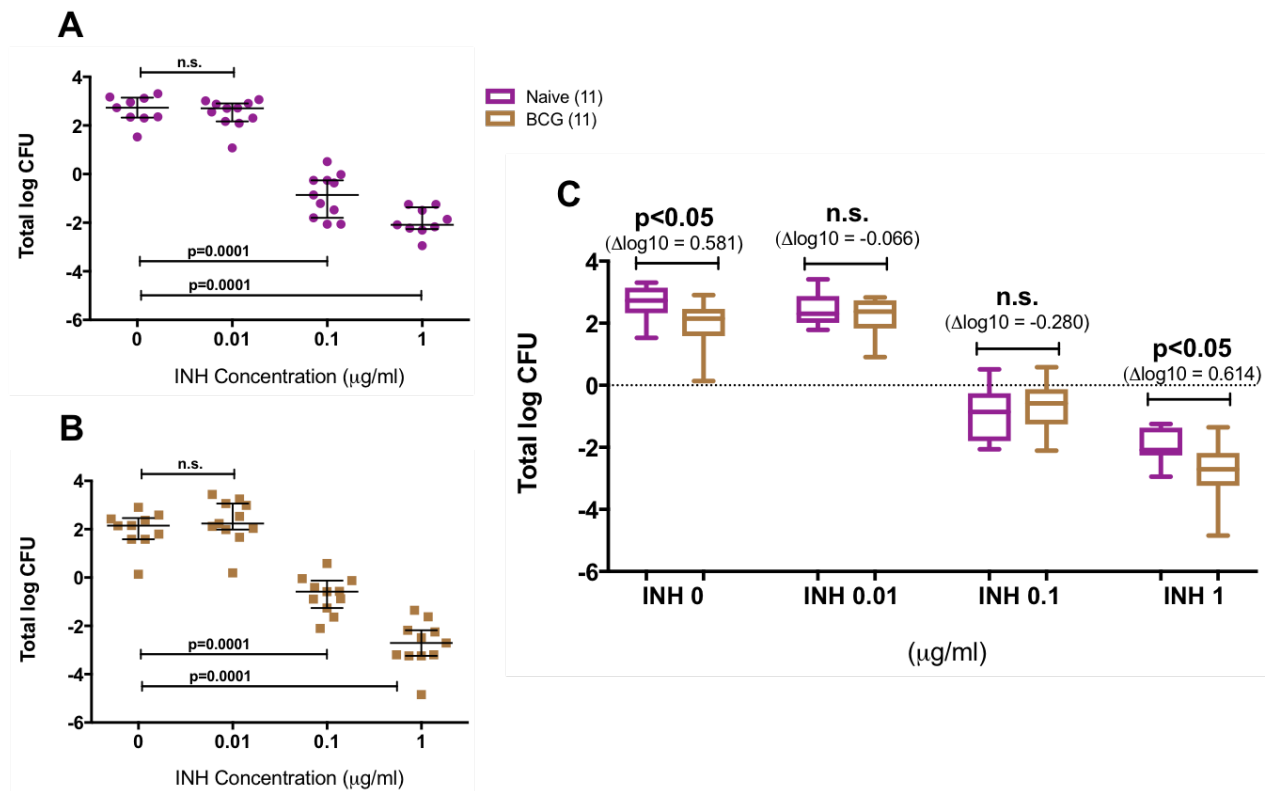


Figure 3. Growth inhibition in BCG-vaccinated and saline-injected mice, in the absence and presence of INH. The ability of drug to inhibit mycobacterial growth was assessed in a titration curve. INH inhibited mycobacterial growth in a dose-dependent manner in the naïve (A) and BCG-vaccinated (B) mice. Data from both groups was compiled in a dose-response box plots to identify the vaccine effect in the presence of drug (C). Dots and squares represent individual data point in the titration curves (A and B) and data is displayed as median with IQR. Each group of is represented in a single box plot with range in the dose-response analysis (C). Presented data is pooled from two experiments. Statistical significances were tested using one-way ANOVA (A and B) and unpaired t-test (C).

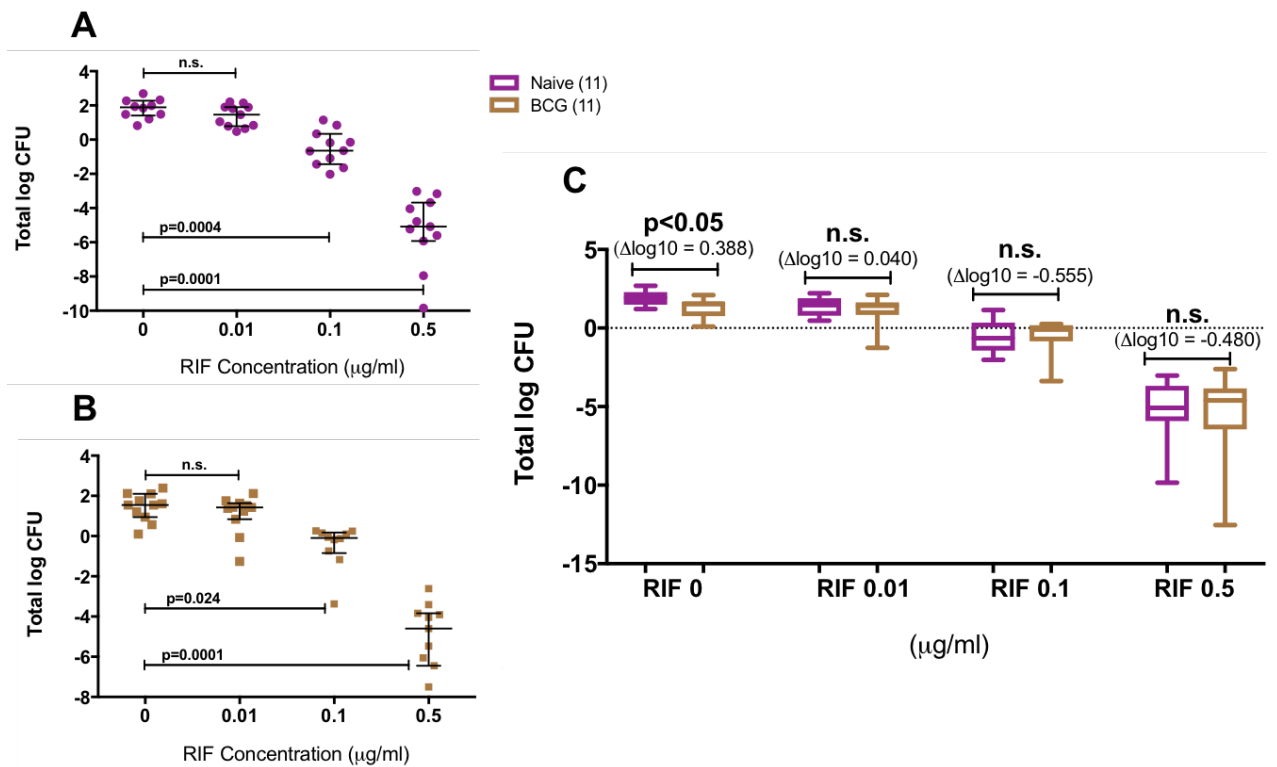


Figure 4. Growth inhibition in BCG-vaccinated and saline-injected mice, in the absence and presence of RIF. The ability of drug to inhibit mycobacterial growth was assessed in a titration curve. RIF inhibited mycobacterial growth in a dose-dependent manner in the naïve (A) and BCG-vaccinated (B) mice. Data from both groups was compiled in a dose-response box plots to identify the vaccine effect in the presence of drug (C). Dots and squares represent individual data point in the titration curves (A and B) and data is displayed as median with IQR. Each group of is represented in a single box plot with range in the dose-response analysis (C). Presented data is pooled from two experiments. Statistical significances were tested using one-way ANOVA (A and B) and unpaired t-test (C).

To determine if BCG vaccination could enhance the drug effect, data from each naïve and vaccinated group were plotted in a dose response analysis to observe the vaccine impact at various drug concentrations. BCG vaccination enhanced the ability of INH to control mycobacterial growth at the concentration of 1 $\mu\text{g/ml}$ ($p < 0.05$) but the differences did not reach significance at other drug concentrations (Figure 3C). Meanwhile, BCG vaccination did not significantly influence control of mycobacterial growth at any RIF concentrations

tested (Figure 4C). As there was no dose-response relationship observed between PZA and EMB in the chosen concentrations, no vaccine impact towards PZA and EMB could be assessed in this experiment (Figure 5C and 6C).

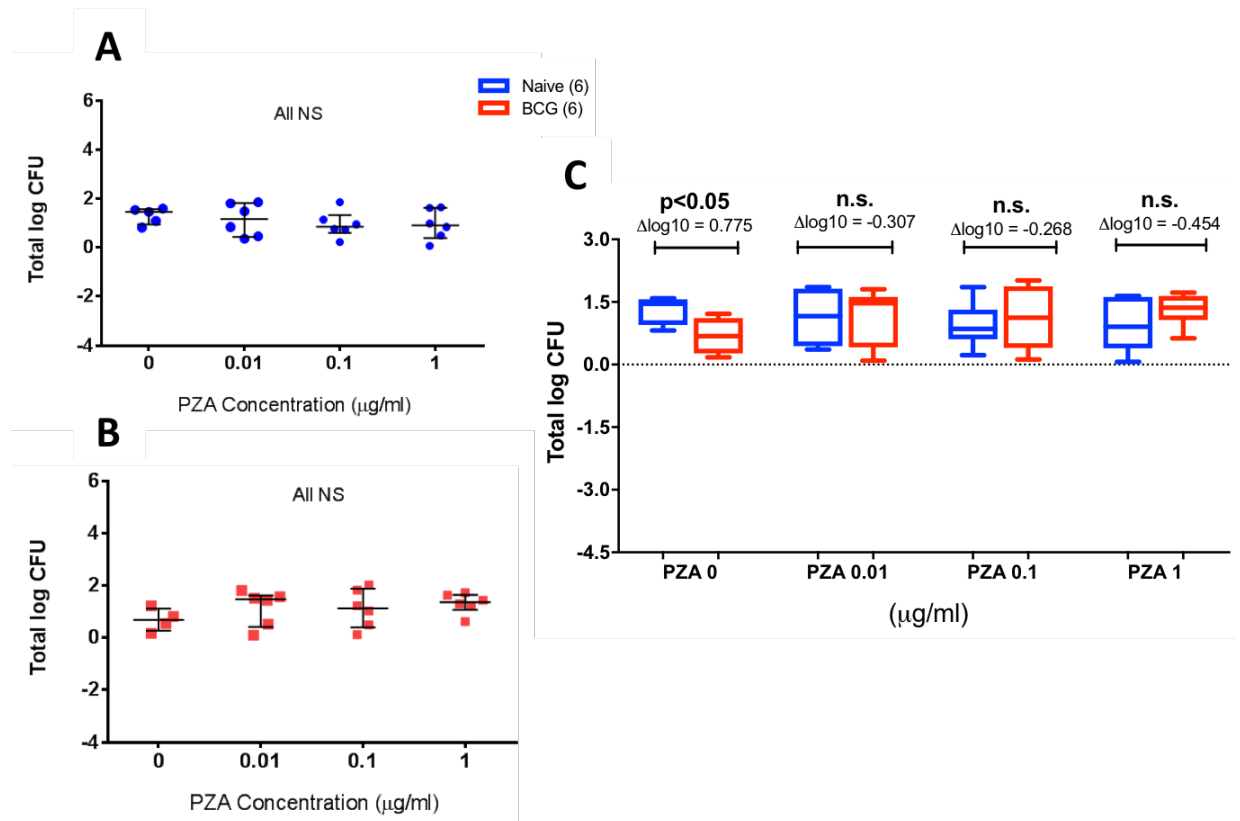


Figure 5. Growth inhibition in BCG-vaccinated and saline-injected mice, in the absence and presence of PZA. The ability of drug to inhibit mycobacterial growth was assessed in a titration curve. Addition of PZA did not result in dose-dependent inhibition of mycobacterial growth in both naïve (A) and BCG-vaccinated (B) groups, as also shown in the dose-response analysis (C). Dots and squares represent individual data point in the titration curves (A and B) and data is displayed as median with IQR. Each group of is represented in a single box plot with range in the dose-response analysis (C). Statistical significances were tested using one-way ANOVA (A and B) and unpaired t-test (C).

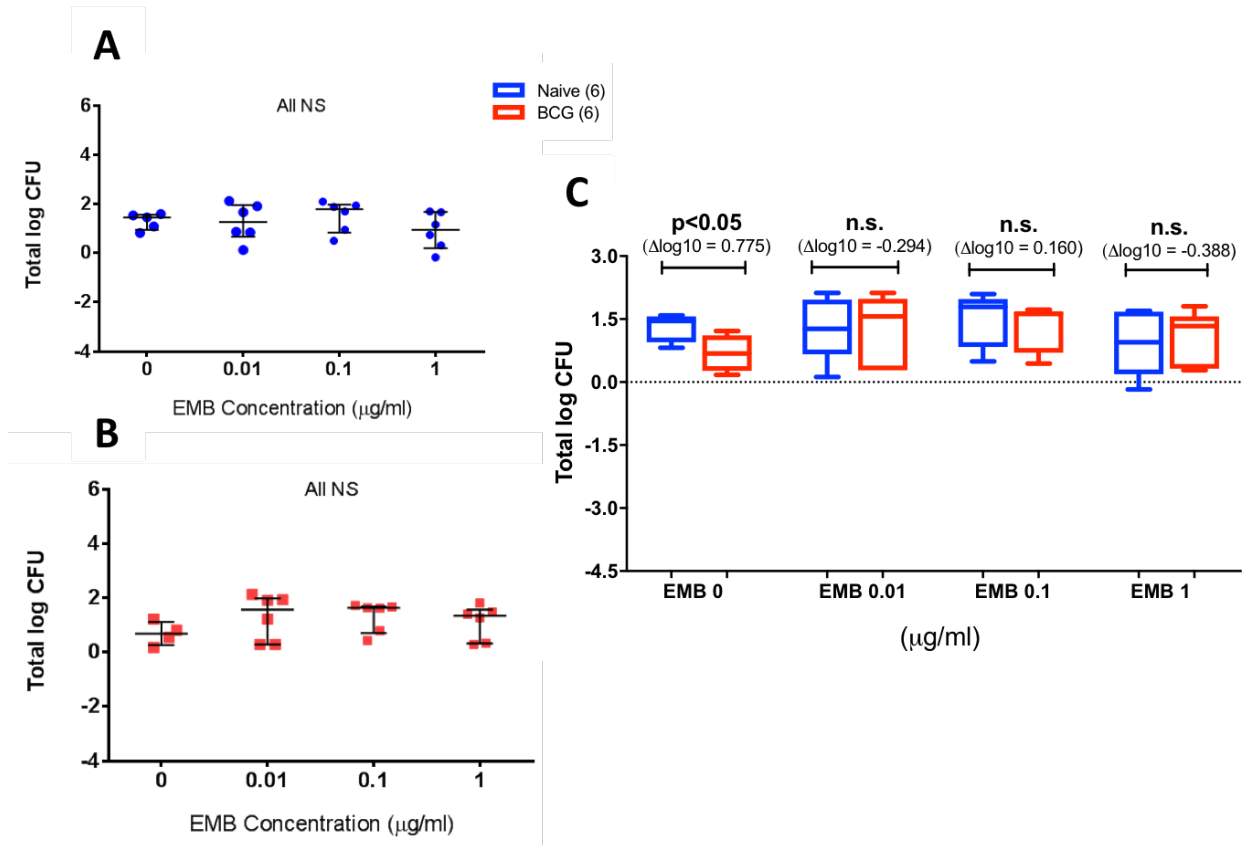


Figure 6. Growth inhibition in BCG-vaccinated and saline-injected mice, in the absence and presence of EMB. The ability of drug to inhibit mycobacterial growth was assessed in a titration curve. Addition of EMB did not result in dose-dependent inhibition of mycobacterial growth in both naïve (A) and BCG-vaccinated (B) groups, as also shown in the dose-response analysis (C). Dots and squares represent individual data point in the titration curves (A and B) and data is displayed as median with IQR. Each group of is represented in a single box plot with range in the dose-response analysis (C). Statistical significances were tested using one-way ANOVA (A and B) and unpaired t-test (C).

Cytokine production associated with *ex vivo* growth inhibition

ELISA assays were performed using the MGIA supernatant to investigate cytokine production which may be associated with *ex vivo* growth inhibition at all drug concentrations (INH and RIF). There was significantly higher IP-10 and TNF- α production at INH concentration of 0.1 and 0.01 $\mu\text{g/ml}$, respectively ($p < 0.05$, Figure 7),

but this did not correspond with enhanced growth inhibition, which was observed at 1 $\mu\text{g/ml}$ INH (Figure 3). There were also non-significant trends for higher production of IL-6 in the BCG-vaccinated group compared to the vaccine-naïve group when splenocytes were co-cultured with INH (Figure 7), which was not observed in humans. With RIF, we did not see any significantly enhanced cytokine production in the presence of drug (Figure 8), which could be due to the lack of impact of BCG towards *ex vivo* drug killing of RIF in this experiment (Figure 4). Interestingly, in the absence of drug, there was a trend of correlation between higher IL-10 production and higher growth of mycobacteria ($p=0.09$, Figure 9A), as has been demonstrated in humans. We did not observe robust IFN- γ production in mice in the presence and absence of drugs (Figure 8 and 9), which was in contrast to humans. At an INH concentration of 1 $\mu\text{g/ml}$, there was a significant correlation between higher production of IL-6 and lower growth of mycobacteria (Spearman $r = -0.59$, $p=0.0059$, Figure 9B). Notably, this was also where we observed a significant difference in the MGIA assay with mouse splenocytes.

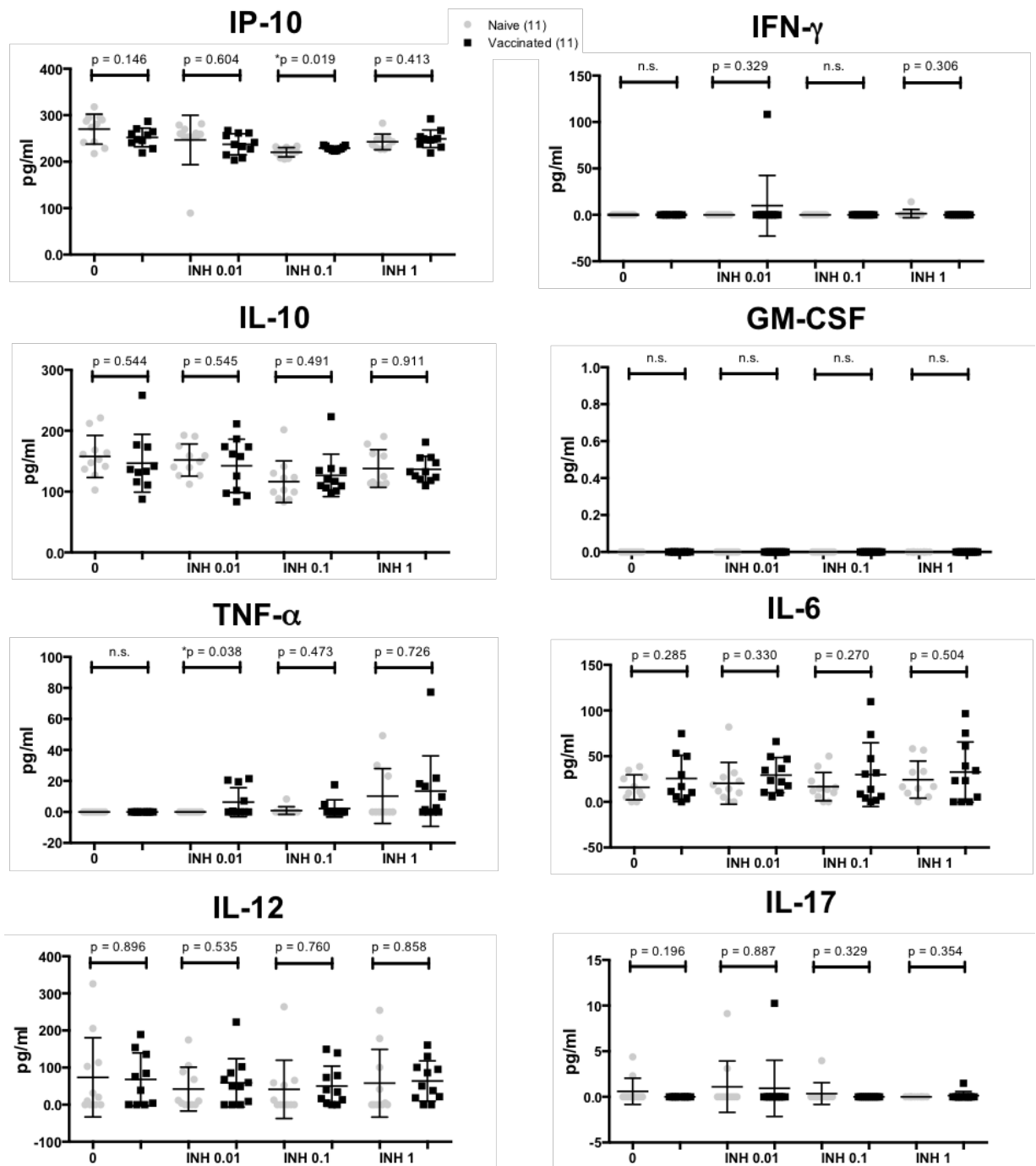


Figure 7. Cytokine responses from co-culture with INH. MGIA supernatants were analysed for the released cytokines IP-10, IFN- γ , IL-10, GM-CSF, TNF- α , IL-6, IL-12 and IL-17. Comparison of responses between BCG-vaccinated and BCG-naïve groups at different drug concentrations were performed using unpaired *t*-test. A p value <0.05 is considered statistically significant. Data is displayed as median with IQR.

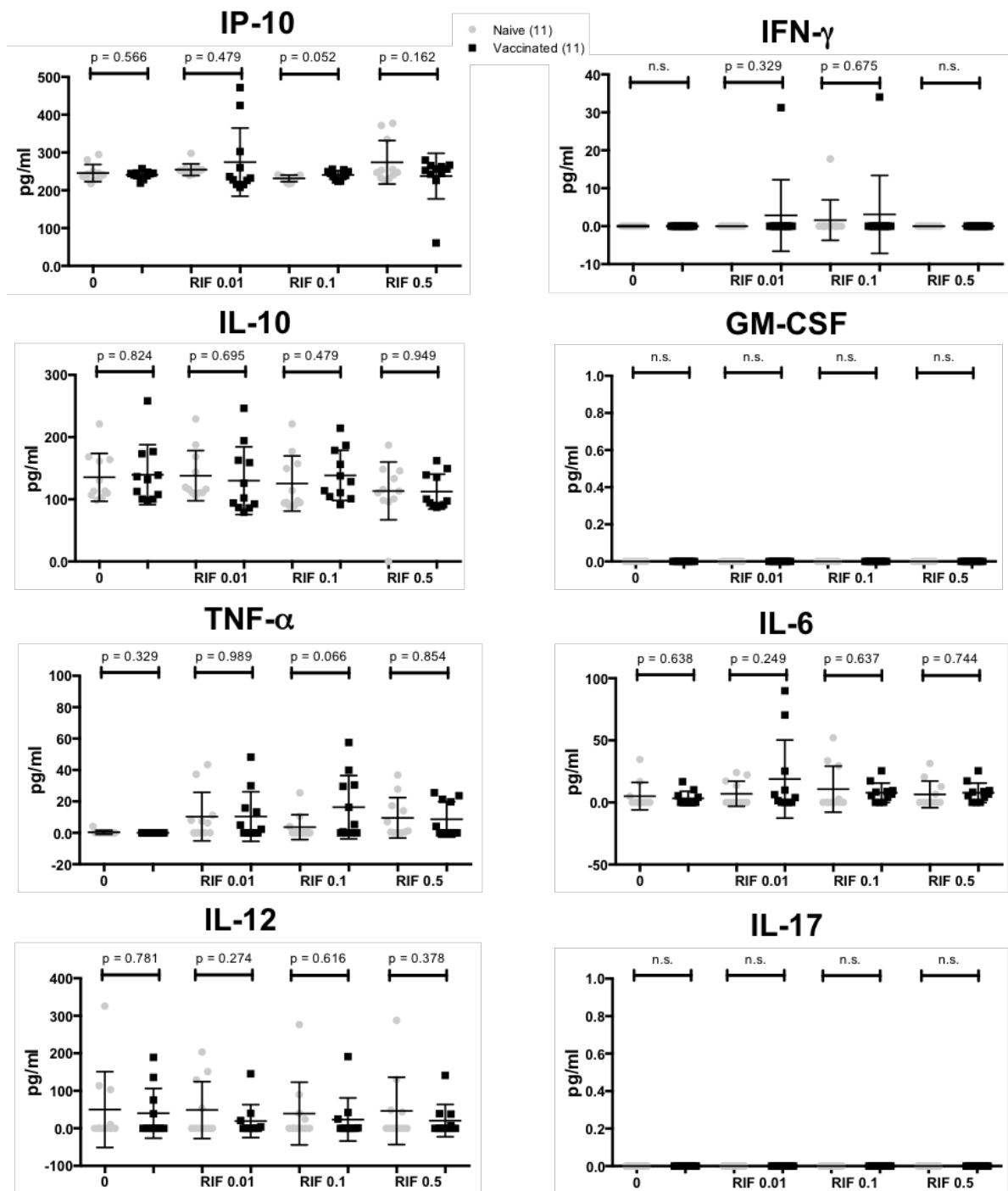


Figure 8. Cytokine responses from co-culture with RIF. MGIA supernatants were analysed for the released cytokines IP-10, IFN- γ , IL-10, GM-CSF, TNF- α , IL-6, IL-12 and IL-17. Comparison of responses between BCG-vaccinated and BCG-naïve groups at different drug concentrations were performed using unpaired *t*-test. A p value <0.05 is considered statistically significant. Data is displayed as median with IQR.

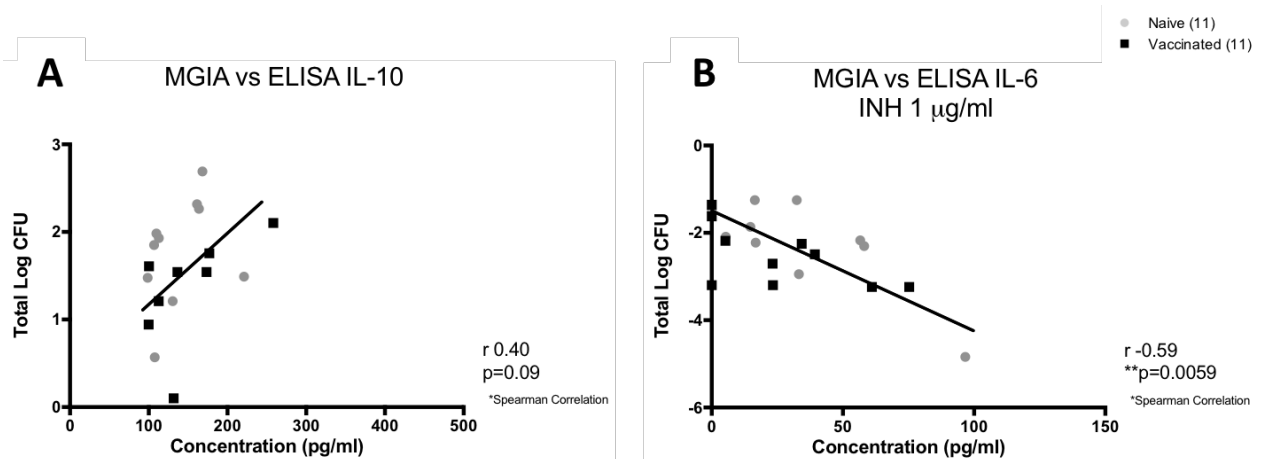


Figure 9. Correlation between cytokine productions and growth inhibition. The production of IL-10 was associated with higher growth of mycobacteria in the absence of drug (**A**) and the production of IL-6 was associated with lower mycobacterial growth at INH concentration 1 µg/ml (**B**). Correlations between cytokine production and mycobacterial growth were assessed using Spearman's correlation. Dots and squares represent individual data points.

5.1.4 Discussion

In the present study, a higher IFN- γ response was observed in the BCG-vaccinated mice compared to naïve mice. BCG-vaccinated mice also demonstrated improved capacity to control the growth of mycobacteria *ex vivo*. The magnitude of difference between vaccinated and naïve groups was higher in mice (~0.6 log) compared to historically BCG-vaccinated humans, as described in Chapter 2 and 4. These results further supported our findings from the human study, as BCG vaccination given at a determined time point in mice (6 weeks prior to sacrifice) resulted in a similar enhanced killing with INH *ex vivo*, but no notable effect on RIF. Our results were also consistent with an earlier murine study by Marsay *et al.*², which found enhanced *ex vivo* growth inhibition using mouse splenocytes following BCG vaccination in mice in the absence of drug. In our study, the magnitude of mycobacterial growth difference was higher (0.6 log) compared to the

Marsay study (0.2 log), as we adopted an optimised protocol based on the study of Zelmer *et al.*³. The study by Marsay *et al.* and Zelmer *et al.* also showed that the *ex vivo* growth inhibition using BCG as immune target was correlated with an *in vivo* challenge experiment in mice using *Mtb* Erdman^{2,3}. Moreover, the study by Marsay *et al.* also demonstrated the protective effect of IFN- γ towards *ex vivo* mycobacterial growth using gene expression analysis², similar to our finding using the ELISpot assay as well as Zelmer *et al.* using the IFN- γ knockout mice³.

This study, using spleen cells from BCG immunised mice, was performed in year one of my PhD. The objective was to refine my laboratory techniques including the microbiological and immunological assays required for this project and to ensure that the author was proficient in all assays before handling samples from my human BCG cohort. In addition, these experiments, although not conclusive, gave the author sufficient confidence in the approach to proceed with analysis of human samples. Murine cell viability was lower and the standard deviation within groups was significantly higher than what can now be achieved with this assay using murine cells. As viability was low and standard deviation was high, data from these experiments must be interpreted with prudence.

In this study, cell viability from mouse splenocytes was relatively lower as the assay was performed in rotating tubes rather than culture plates. It was later identified that optimising assay conditions, including the use of culture plates instead of tubes, could substantially increase viability of splenocytes (viability increase from 21% to 46% at day 4 of culture)⁴. This impacted our ability to observe significant growth inhibition and to observe secretion of cytokine from splenocytes, as they are less robust than PBMC. The author has since optimised the procedures to better preserve cell viability, including by

the use of culture plates rather than rotating tubes in the 4 day MGIA culture, as was performed in Chapter 3. Nevertheless, this study was the first to assess the impact of recent BCG vaccination in mice towards *ex vivo* killing of first-line tuberculosis drugs using the MGIA assay. It was found that BCG enhanced the capacity of INH to control mycobacterial growth *ex vivo* at the concentration of 1 µg/ml, and this gave confidence to proceed with our experiments using human PBMC. We did not find an impact of BCG on RIF effect in mice, as RIF is the most active drug in the regimen and significantly decrease the bacterial growth in the MGIA system⁵, therefore no additional impact of BCG was observed on top of RIF.

With regard to PZA, we did not observe a drug effect using the *ex vivo* assay as BCG Pasteur is known to be resistant towards this drug. This result was consistent with the literature as most of the vaccine strains of *Mycobacterium bovis* BCG are resistant towards PZA¹. In the case of EMB, a higher dose is required in future studies as BCG Pasteur maybe sensitive towards EMB if a higher concentration is used. Some BCG vaccine strains are shown to be sensitive to 5 µg/ml of EMB¹. Alternatively, it may be preferable to use *Mtb* when assessing growth inhibition in the presence of TB drugs in the future. This data was important in guiding our choice of INH and RIF only for the human study. Our preliminary data also suggest that the assay can be implemented in a murine model using splenocytes samples to assess vaccine impact on drug-mediated killing of mycobacteria.

Data from our mouse experiment suggested that BCG vaccination may enhance the killing effect of INH. A similar phenomenon has been observed by Dhillon and Mitchison, in which BCG vaccination was shown to enhance the effect of INH and RIF in guinea-pig⁶. More recently, Shang *et al.* also showed that BCG vaccination improved

the effectiveness of combined therapy in prolonging survival following *in vivo* infection with *Mtb*⁷. In the latter study, administration of BCG in adjunct to therapy was superior compared to therapy alone. The combined therapy consisted of INH, RIF and PZA but the author did not assess the impact of BCG towards individual drugs. The MGIA assay could provide an advantage in this regard, as the *ex vivo* nature of the assay makes it flexible to test various conditions of different drugs and vaccine combinations, hence allowing an easier assessment of vaccine effect at an individual drug level.

Furthermore, the *ex vivo* MGIA assay could also help in identifying immune mechanisms of vaccine-induced growth inhibition. The protective effect of IFN- γ (ELISpot) and negative effect of IL-10 were also demonstrated following BCG vaccination using the murine assay. When measuring the MGIA supernatant for cytokine production using ELISA, we noticed that the secretions of certain cytokines such as IFN- γ and GM-CSF were less robust in mice compared to humans. As elaborated above, this may be due to the fact that after 4 days of culture, mouse splenocytes are less viable compared to human PBMCs⁴. Indeed, the author explored this and did find lower assay variability when using plates for splenocyte cell culture. Another possible explanation would be the different kinetics between cytokines over 4 days of culture i.e. some cytokine responses might peak at day 2 or 3 instead of day 4, and this has been observed by Tanner *et al.* using human PBMCs⁸. In order to allow periodic cytokine assessment without disturbing the *ex vivo* assay system, only a small amount of supernatant is allowed to be obtained in between the 4 days culture and this would be possible using a highly-sensitive Multiplex assay (Luminex) for cytokine measurement. For this project, cytokine assessment could only be performed with ELISA which requires a large amount of supernatant and this can only be collected at day 4.

Interestingly, the data showed trends of higher IL-6 production in the BCG-vaccinated mice at day 4 and this correlates with enhanced mycobacterial growth inhibition in the presence of 1 µg/ml INH. IL-6 is a cytokine which has been previously associated with trained innate immunity^{9,10} and this observation in murine study is consistent with our notion in the human studies discussed in the previous chapters. Unfortunately, it was not possible to perform immune cell phenotyping with flow cytometry in this murine study as the cells were not of sufficient viability, thus the cells which produce these cytokines measured in the MGIA supernatant remain elusive. Nevertheless, this experiment has demonstrated that the murine MGIA assay could be used to assess vaccine-mediated killing of mycobacteria *ex vivo* in the presence of TB drugs. Our study described in this section acts as a proof-of-principle that the MGIA assay can be used to screen different vaccine and drug combinations in the mouse model.

5.2 Impact of RUTI vaccination in mice on MGIA in the presence of INH and RIF

5.2.1 Introduction

RUTI is a leading therapeutic TB vaccine candidate which has been studied in various animal models and in several clinical trials¹¹. In mice, the vaccine has been previously shown to augment the efficacy of INH and RIF treatment following TB infection *in vivo*^{12,13}. This study sought to investigate whether this finding could be recapitulated using the *ex vivo* MGIA assay. The impact of RUTI vaccination on *ex vivo* mycobacterial growth control in the absence of drug has been elaborated in Chapter 3. In this chapter, it was found that RUTI vaccination also enhanced the *ex vivo* killing of INH and RIF using mouse splenocyte samples, although the effect appears to be dependent on the age of the

vaccinated mice. Again, this experiment was performed at an early stage in my PhD to determine if it was possible to detect growth inhibition with a vaccine other than BCG. The assay was performed in rotating tubes so cell viability was low and the standard deviation within the group was high and data should be interpreted with care. Nevertheless, our data suggested that the MGIA could be further developed as a screening tool for therapeutic TB vaccine candidates using mouse splenocytes samples. The developers of the RUTI vaccine were sufficiently interested in this data to allow us to proceed with further experiments with RUTI as reported in Chapter 3 before.

5.2.2 Materials and Methods

Animal procedure and vaccination

In the first experiment, female C57Bl/6 mice aged between 6-7 weeks supplied commercially from Charles River Laboratories (UK) were used. Twenty mice were divided into four groups (five mice per group, Figure 10). Mice in two treatment groups were injected subcutaneously with 204 µg of RUTI vaccine twice in a three-week interval (week 0 and week 3). Two different batches of RUTI (A12 and A14) were tested. Mice in another treatment group were injected with 4×10^5 CFU BCG at week 0 and saline at week 3. The last group of mice were injected with saline at weeks 0 and 3. All mice in this experiment were sacrificed six weeks after commencing the study.

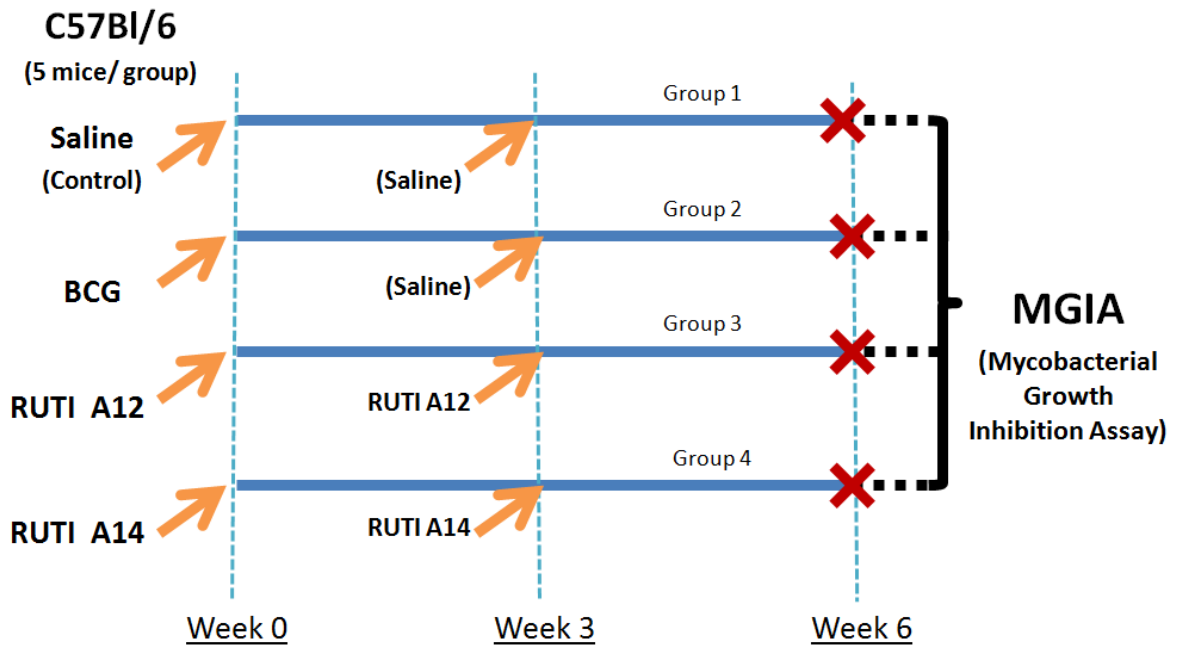


Figure 10. Experiment design of first RUTI experiment. Two different batches of RUTI vaccine were tested (A12 and A14).

For the second experiment, female C57Bl/6 mice aged between 13-14 weeks (Charles River, UK) were used. Eighteen mice were divided into three groups (six mice per group, Figure 11). Mice in the RUTI-treated group were injected subcutaneously with 204 μg of RUTI A14 twice in a three-week interval (week 0 and week 3). Mice in the BCG-treated group were injected with 4×10^5 CFU BCG at week 0 and saline at week 3. The mice in the control group were injected with saline at weeks 0 and 3. All mice in this experiment were also sacrificed six weeks after commencing the study.



Figure 11. Experiment design of second RUTI experiment. RUTI vaccine (batch A14) was tested in comparison to BCG.

Splenocytes harvesting, *ex vivo* growth inhibition assay and statistical analysis

Upon mice sacrificed in both experiments, the subsequent procedures were conducted as described in section 5.1.2. Spleens were processed to obtain single cell suspensions and 5×10^6 splenocytes were used as the cellular input for the *ex vivo* MGIA assay. BCG Pasteur Aeras (~100 CFU) was used as the immune target, and INH was added in the following concentrations 0.01, 0.1 or 1 $\mu\text{g/ml}$. For RIF, the tested concentration was 0.01, 0.1, 0.25 or 0.5 $\mu\text{g/ml}$. Statistical analysis was performed in Graphad Prism 7. To identify statistical significance of *ex vivo* growth inhibition (log CFU values), students *t*-test were used and a p value <0.05 was considered significant.

5.2.3 Results

Impact of RUTI vaccination on mycobacterial growth inhibition in the absence of drug

In the first experiment, vaccination with RUTI reduced the growth of mycobacteria *ex vivo* compared to the saline-injected mice ($p < 0.01$ and $p = 0.06$ for RUTI batch A12 and A14 respectively, Figure 12A). An enhanced growth inhibition appeared to be also observed with BCG, although it did not reach significance. The reduction of mycobacterial growth conferred by RUTI was superior compared to BCG. There was no statistically significant difference of growth inhibition between two RUTI batches tested ($p > 0.1$, Figure 12A).

Mycobacterial growth inhibition following RUTI vaccination was also compared in the second experiment. Vaccination with RUTI significantly reduced the growth of mycobacteria *ex vivo* compared to the saline-injected mice ($p < 0.005$, Figure 12B). A similar non-significant reduction of growth was also observed with BCG. The growth reduction in the RUTI-vaccinated group was superior compared to the BCG ($p < 0.005$, Figure 12B). The magnitude of difference was lesser for both RUTI and BCG in the second experiment, in which older mice were used.

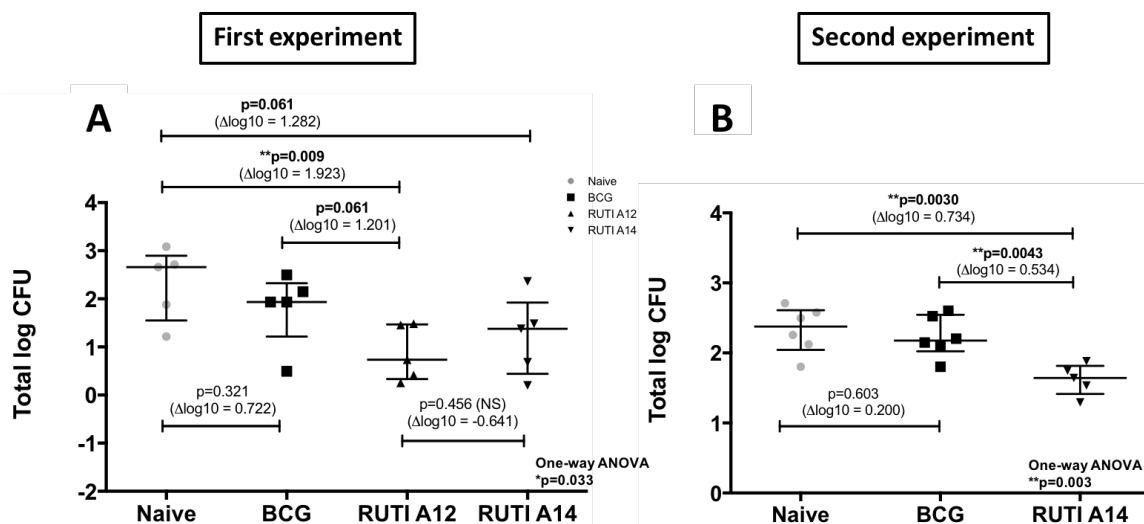


Figure 12. *Ex vivo* control of mycobacterial growth between RUTI-vaccinated groups in the absence of drug. In the first experiment, two different batches of RUTI vaccine were tested (A). In the second experiment, older mice were used and only RUTI batch A14 was tested (B). Significant difference between treatment groups was observed ($p < 0.05$, one-way ANOVA). Unpaired t-test was used for pairwise comparison and p value < 0.05 was considered statistically significant. Each symbols represents individual data point. Data is displayed as median with IQR.

Impact of RUTI vaccination on drug-mediated growth inhibition (first experiment)

A dose-dependent decrease of bacterial load was observed in the *ex vivo* system at the INH concentration of 0.1 and 1 $\mu\text{g/ml}$, but not at 0.01 $\mu\text{g/ml}$ (Figure 13A). This was consistent with the previously known MIC of INH towards BCG Pasteur. In the presence of drugs, there was a significant reduction of bacterial growth when RUTI-vaccinated splenocytes were co-cultured with all concentration of INH compared to saline-injected naïve control ($p < 0.05$, Figure 13 B-D). Difference in RUTI batches tested (A12 and A14) did not result in a significant difference in the ability of mycobacterial growth control in the presence of INH ($p > 0.1$). BCG vaccination provided a similar beneficial effect in the presence of INH compared to RUTI, although the magnitude of difference was lower and did not reach significance in this experiment with only 5 mice per group.

A similar dose-dependent decrease of bacterial load with RIF was observed, and the curve was steeper compared to INH (Figure 14A). This was also consistent with the previously known MIC of RIF towards BCG Pasteur. In the presence of drugs, there were significant reductions of bacterial growth when RUTI-vaccinated splenocytes were co-cultured with all concentrations of RIF compared to control ($p < 0.05$, Figure 14 B-D). Vaccination with RUTI A14 displayed a similar trend with RUTI A12, although at the RIF concentration 0.01 $\mu\text{g/ml}$ RUTI A14 was less able to control mycobacterial growth *ex vivo* compared to RUTI A12 ($p < 0.05$, Figure 14B).

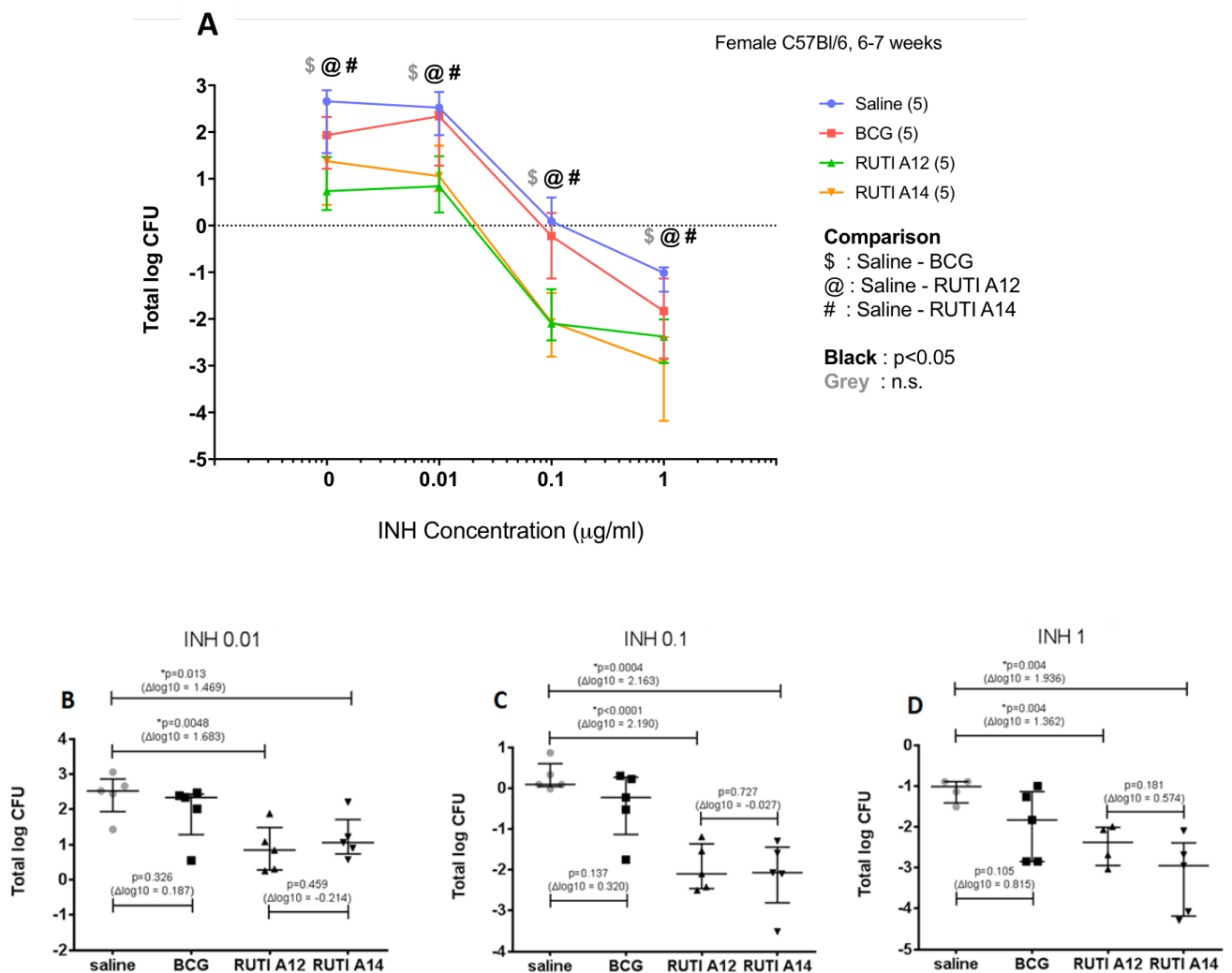


Figure 13. *Ex vivo* control of mycobacterial growth following RUTI vaccination in the presence of INH. Vaccine effects were assessed in a dose-response curve (A). Differences between drug concentrations were described in separate graphs, with INH 0.01 $\mu\text{g}/\text{ml}$ (B), INH 0.1 $\mu\text{g}/\text{ml}$ (C) and INH 1 $\mu\text{g}/\text{ml}$ (D), respectively. Refer to Figure 12A for similar graph in the absence of drugs. Each symbols represents individual data point in the graphs (B-D) and each group of data in a same condition is represented in a single symbol in the dose-response curve (A). Data is displayed as median with IQR.

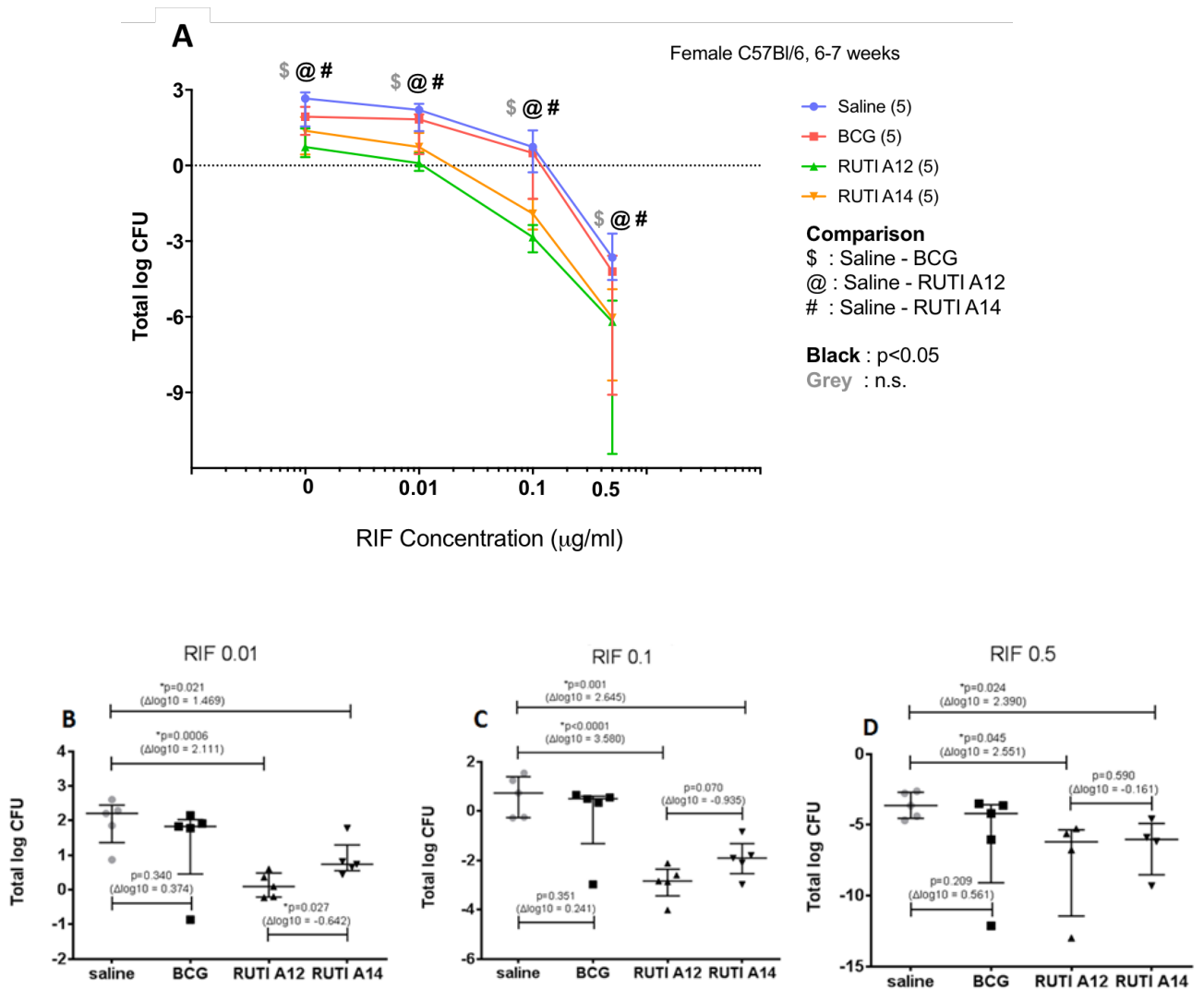


Figure 14. *Ex vivo* control mycobacterial growth following RUTI vaccination in the presence of RIF. Vaccine effects were assessed in a dose-response curve (A). Differences between drug concentrations were described in separate graphs, with RIF 0.01 $\mu\text{g}/\text{ml}$ (B), RIF 0.1 $\mu\text{g}/\text{ml}$ (C) and RIF 0.5 $\mu\text{g}/\text{ml}$ (D), respectively. Refer to Figure 12A for similar graph in the absence of drugs. Each symbols represents individual data

point in the graphs (B-D) and each group of data in a same condition is represented in a single symbol in the dose-response curve (A). Data is displayed as median with IQR.

Impact of RUTI vaccination on drug-mediated growth inhibition (second experiment)

In this repeat experiment, older mice were used due to a technical consideration. A dose-dependent decrease of bacterial load was observed in the presence of INH (Figure 15A). There was a significant reduction of bacterial growth when RUTI-vaccinated splenocytes were co-cultured with INH concentration 0.01 $\mu\text{g/ml}$ compared to saline-injected naïve control ($p < 0.001$, Figure 15B). In this experiment, we observed different trends of growth inhibition at higher INH concentrations compared to the previous experiment, despite the similar mycobacterial input and other experiment conditions. At INH concentration 0.1 $\mu\text{g/ml}$, the RUTI effect appeared to diminish compared to control (Figure 15C), while a reversed effect of increased mycobacterial growth was observed at the highest INH concentration ($p < 0.05$, Figure 15D). BCG vaccination provided trends of beneficial effect towards increased control of mycobacteria growth in the presence of INH, being significant at the concentration of 1 $\mu\text{g/ml}$ ($p < 0.005$, Figure 15D).

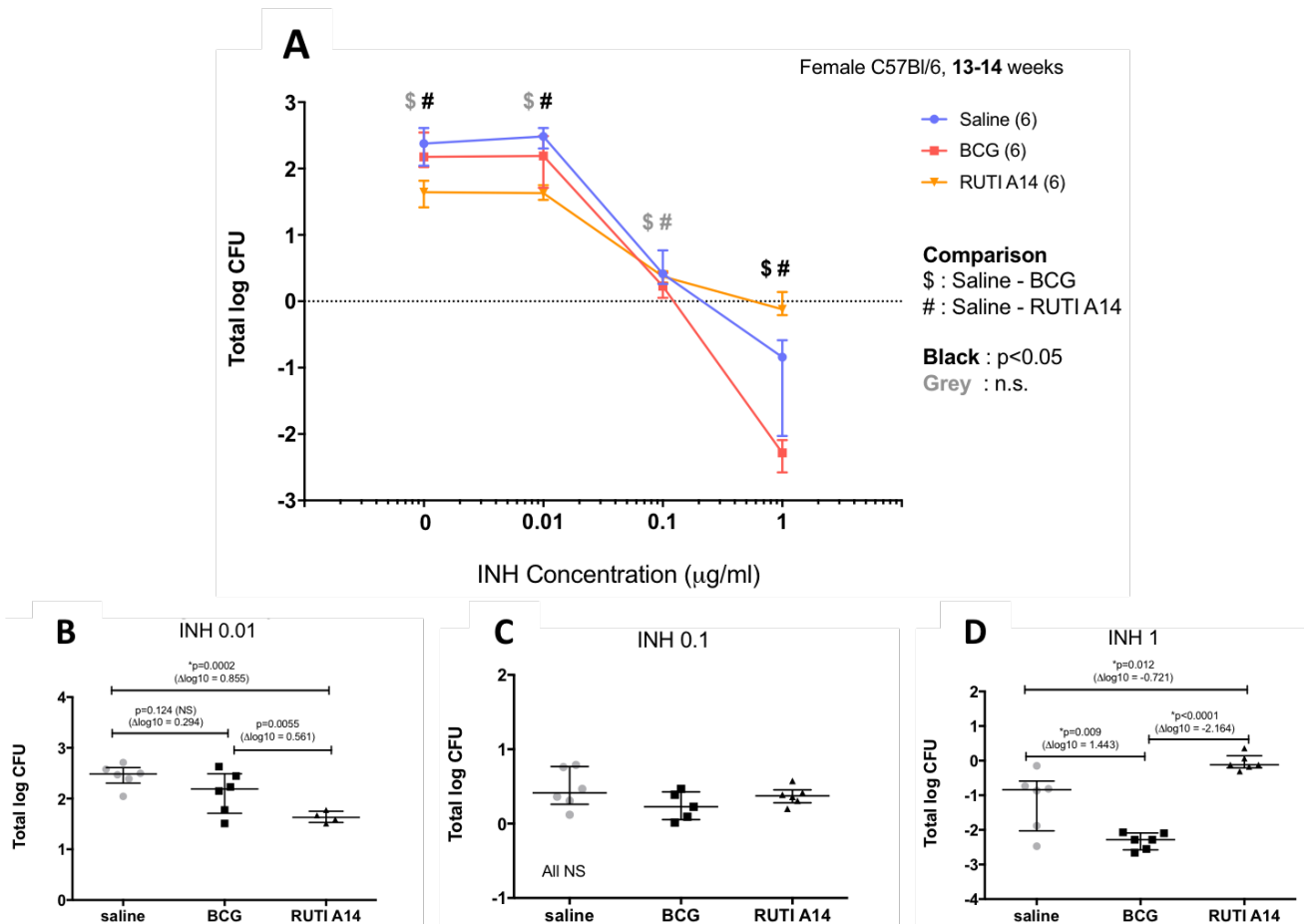


Figure 15. Ex vivo control of mycobacterial growth following RUTI vaccination in the presence of INH. Vaccine effects were assessed in a dose-response curve (A). Differences between drug concentrations were described in separate graphs, with INH 0.01 $\mu\text{g/ml}$ (B), INH 0.1 $\mu\text{g/ml}$ (C) and INH 1 $\mu\text{g/ml}$ (D), respectively. Refer to Figure 12B for a similar graph in the absence of drugs. Each symbols represents individual data point in the graphs (B-D) and each group of data in a same condition is represented in a single symbol in the dose-response curve (A). Data is displayed as median with IQR.

In the presence of RIF, a dose-dependent decrease of bacterial load was also observed (Figure 16A). There was a significant reduction of bacterial growth when RUTI-vaccinated splenocytes were co-cultured with RIF concentration of 0.01 $\mu\text{g/ml}$ compared to control ($p < 0.001$, Figure 16B). We also observed different trends of growth inhibition at higher RIF concentrations compared to our first experiment. At RIF concentration of 0.1 $\mu\text{g/ml}$, the RUTI effect appeared to diminish (Figure 16C), while a reversed effect of

increased mycobacterial growth was also observed at the highest RIF concentration ($p < 0.05$, Figure 16D). BCG vaccination did not provide statistically significant impact towards control of mycobacteria growth in the presence of RIF (Figure 16).

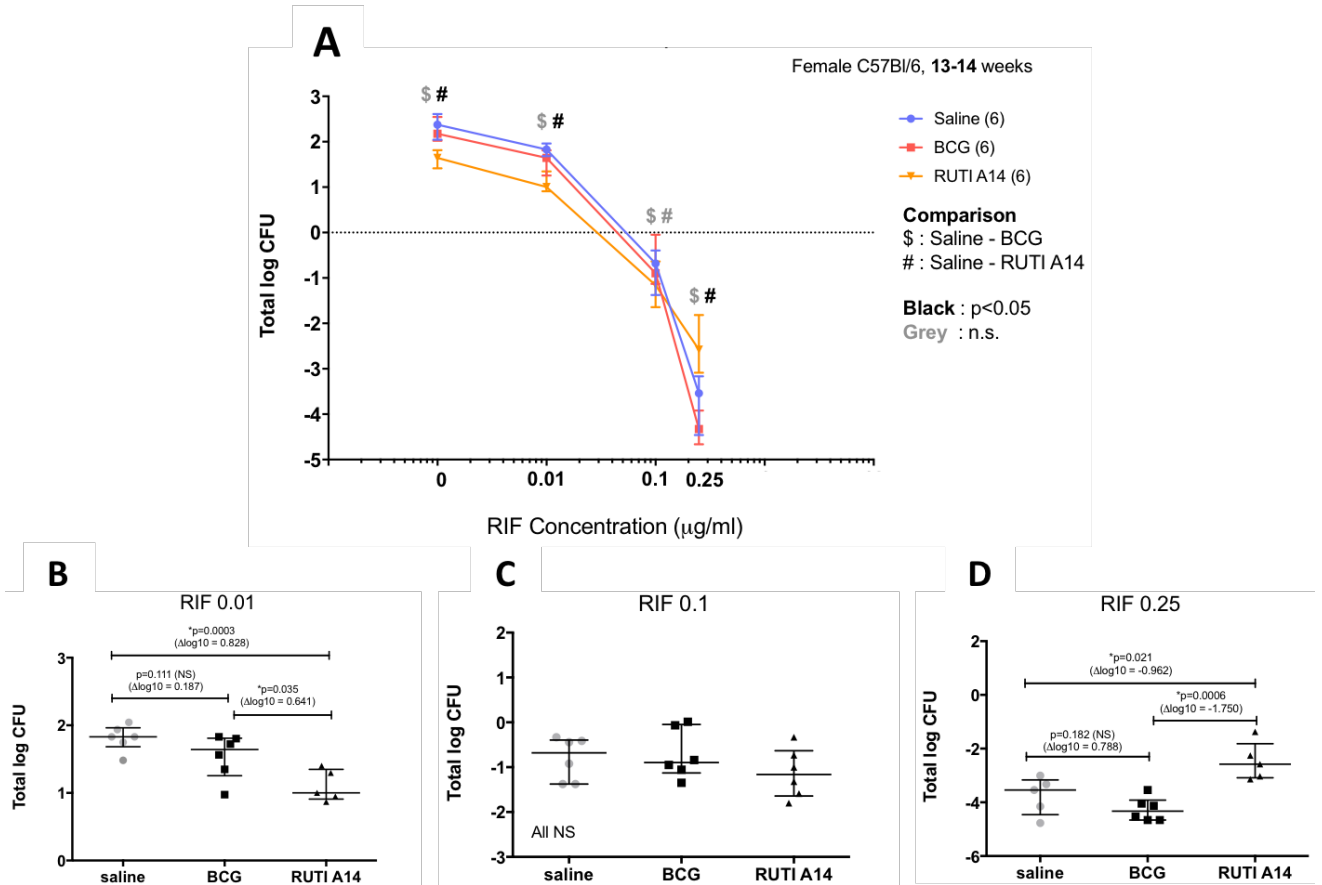


Figure 16. *Ex vivo* control mycobacterial growth following RUTI vaccination in the presence of RIF. Vaccine effects were assessed in a dose-response curve (A). Differences between drug concentrations were described in separate graphs, with RIF 0.01 $\mu\text{g/ml}$ (B), RIF 0.1 $\mu\text{g/ml}$ (C) and RIF 0.25 $\mu\text{g/ml}$ (D), respectively. Refer to Figure 12B for a similar graph in the absence of drugs. Each symbols represents individual data point in the graphs (B-D) and each group of data in a same condition is represented in a single symbol in the dose-response curve (A). Data is displayed as median with IQR.

5.2.4 Discussion

Vaccination with RUTI resulted in enhanced control of mycobacterial growth *ex vivo* compared to both naïve and BCG-vaccinated mice in the absence of drug. This observation replicates findings from the *in vivo* challenge experiment with RUTI, in which the vaccine was given in untreated infected mice and was shown to reduce bacillary load in both lung and spleen¹⁴. The impact of RUTI on mycobacterial growth control was better than BCG in the *ex vivo* mouse study, while in the *in vivo* challenge experiment, BCG appeared to provide a slightly better protection than the candidate vaccine¹⁴. This might be due to the fact that in the *in vivo* study, RUTI was given in infected mice. In the context of the MGIA assay, the vaccine was given in healthy mice to be challenged with mycobacteria *ex vivo*. Giving RUTI in healthy mice might help the identification of essential immune mechanisms prior to its administration in infected mice. This has been demonstrated in Chapter 3 of this thesis, in which such an approach has unraveled a valuable immune mechanism which was not identified before during *in vivo* testing in infected mice. When tested in a survival study in guinea pigs, both RUTI and BCG improved survival in *Mtb* infected animal up to 50 weeks, in which 60-80% of the vaccinated animals survived, while only less than 20% of the unvaccinated animals survived at week 50¹⁴. In the *ex vivo* MGIA experiment, there was mostly no significant difference between the two RUTI batches tested.

In the presence of drugs, RUTI vaccination in C57Bl/6 mice aged 6-7 weeks resulted in enhanced capacity of INH and RIF to control mycobacterial growth *ex vivo* at all tested drug concentrations. The benefit of RUTI vaccination when administered after chemotherapy *in vivo* in *Mtb*-infected C57Bl/6 mice aged 6-7 weeks have been demonstrated previously, in which the vaccine reduced bacillary load in lung and spleen

further than what was conferred by the chemotherapy alone^{12,13}. However, when the impact of RUTI was tested in the presence of drugs *ex vivo* in older mice (strain C57Bl/6 aged 13-14 weeks), we saw different observations at higher drug concentrations, in which vaccination with RUTI resulted in a reversed effect in promoting mycobacterial growth at the highest INH and RIF concentrations. Given the very similar conditions of these two experiments, except the mouse age, it was speculated that the reverse effect in the latter experiment could be due to a reduced capacity of the older mice to mount sufficient immunity against mycobacterial infection. This was also supported by the fact that the magnitude of mycobacterial growth reduction in the absence of drug was lower in the older mice. Alternatively, as this experiment was performed at an early stage in my PhD, while the author was still optimising the techniques, it is probable that low cell viability confounded results and led to higher standard deviation within the groups and between experiments and this data should therefore be interpreted with discretion. Several *in vivo* studies have demonstrated the impaired capacity of older mice to develop effective immune responses against TB¹⁵⁻¹⁷, and in future experiments it would be important to explore if this impact of mouse age on MGIA was real.

Nevertheless, it was encouraging to observe in this study that the MGIA assay was able to assess the effects of a therapeutic vaccine towards *ex vivo* mycobacterial growth control and this supported our further studies with the RUTI vaccine. With BCG, we have demonstrated consistent results of the *ex vivo* assay using mouse and human samples. Implementation of the *ex vivo* assay using PBMCs from participants vaccinated with investigational vaccine candidates in clinical trials could be pursued to assess the association with clinical protection during treatment. The RUTI clinical trial in MDR-TB patients receiving chemotherapy which is currently ongoing (NCT02711735) would

provide an opportunity for this purpose. In summary, the MGIA assay has been shown to be able to assess a therapeutic effect on mycobacterial growth control and may be useful for the screening of immune therapeutic compounds in both a pre-clinical and clinical samples.

5.3 Optimisation of the murine and human MGIA assays

5.3.1 Introduction

Several optimisation attempts were performed during the course of this project with the murine MGIA utilising splenocyte samples and the PBMC-based human MGIA. The main purposes of the optimisation efforts are to minimise variability and maximise the discriminant ability of the MGIA assays. Optimisation measures included determination of optimum cell number and bacterial input to be used in the assay. Identification of optimum bacterial input is crucial as too high bacterial input can overwhelm the vaccine effect¹⁸. Moreover, the impact of different culture method (rotating tubes vs 48-well plate) as well as culture medium (for human PBMC) were also investigated.

5.3.2 Materials and Methods

Initially, the murine MGIA assay as described in section 5.1.2 was performed with the following varying conditions: different bacterial inputs were chosen that represented the TTP value of 7.5 or 8.5 days using the standard curve (equal to approximately 500 CFU or 100 CFU, respectively). Moreover, different cellular numbers of splenocytes to be used as an input for the *ex vivo* MGIA assay were also investigated (1, 3 or 5 million,

respectively). Subsequently, a head-to-head comparison between culture method in rotating tubes or 48-well plate was performed in the RUTI time course study, leading to an optimised protocol as described in Chapter 3. Similar optimisation efforts were also performed for human PBMC, with the following varying conditions: cellular input 1 million vs 3 million and culture medium containing 10% FBS vs 10% pooled human AB serum. Furthermore, a comparison between cultures in rotating tubes and 48-well plate was also performed for PBMC. This has led to an optimised protocol as described in Chapter 2 and 4.

5.3.3 Results and Discussion

With regard to mycobacterial input, the CFU input equivalent to TTP 8.5 days was shown to be superior in distinguishing mycobacterial growth control between naïve and vaccinated mice groups (Figure 17). Subsequent comparison had also been performed in this project to identify optimum cellular input, with higher cellular concentration resulting in less variability and better differences between the two groups (Figure 18). This study further showed a better magnitude of difference between naïve and vaccinated group with less variability when the culture was performed in 48-well plate instead of rotating tubes for mouse splenocytes (Figure 19). These findings have led us to implement the following optimised conditions for the murine MGIA utilising mouse splenocytes: culture performed in a 48-well plate, with cellular input 5 million splenocytes and BCG target TTP 8.5 days (~ 100 CFU), as described in Chapter 3.

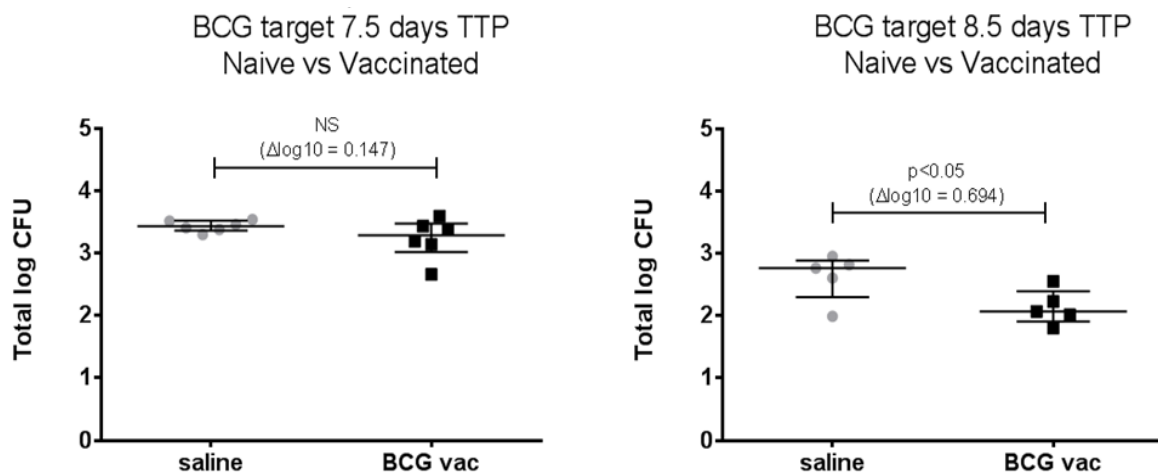


Figure 17. Comparison of different mycobacterial input to identify optimum condition for investigation of vaccine effect in mice. Each symbols represents individual data point. Data is displayed as median with IQR.

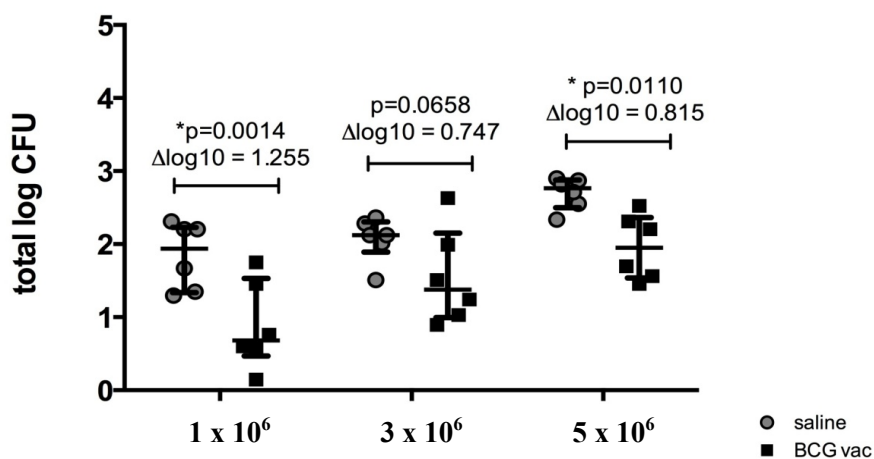


Figure 18. Comparison of different cellular input to identify optimum condition for investigation of vaccine effect in mice. Each symbols represents individual data point. Data is displayed as median with IQR. (Data was obtained from published literature³ with permission from Dr Andrea Zelmer).

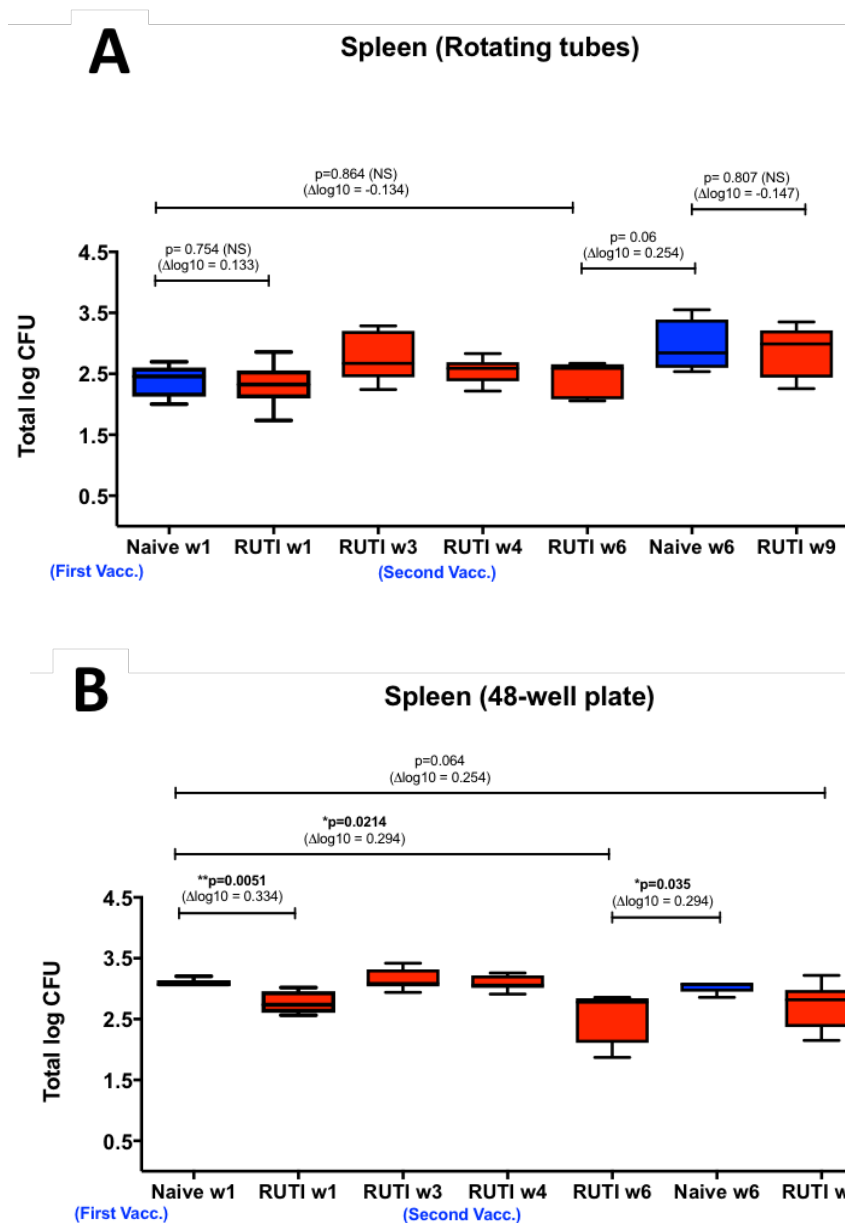


Figure 19. Comparison of different culture method in rotating tubes (A) or 48-well plate (B) to identify optimum condition for investigation of vaccine effect in mice. The box plots show the minimum and maximum values (ends of the whiskers), the median (band near the middle of the box) and interquartile ranges.

For the human PBMC-based MGIA, an INH titration experiment was initially performed in different experiment conditions to better identify the impact of vaccine on top of the drug. When two different culture media were compared, it was found there was less

growth of mycobacteria during PBMC co-culture with media containing 10% FBS compared to 10% pooled human AB serum, and this effect was more notable when 1 million cellular PBMC input was used (Figure 20A). With 3 million cellular input, less variability within group was observed and the effect of FBS on reducing mycobacterial growth was also less notable (Figure 20B). The use of pooled human AB serum is considered to represent a more natural environment for human PBMC compared to FBS⁸. It was found that a higher growth of mycobacteria with BCG input TTP 7.5 days (Figure 21) and the author decided to use input TTP 8.5 days in order not to overwhelm the vaccine effect. In contrast to our finding with mouse splenocytes, a better magnitude of difference between naïve and vaccinated groups was observed when PBMC was cultured in rotating tubes instead of 48-well plate (Figure 22). These findings have led the author to implement the following optimised conditions for the PBMC-based MGIA: culture performed in rotating tubes, with cellular input 3 million PBMC and BCG target TTP 8.5 days (~ 100 CFU), as described in Chapter 2 and Chapter 4.

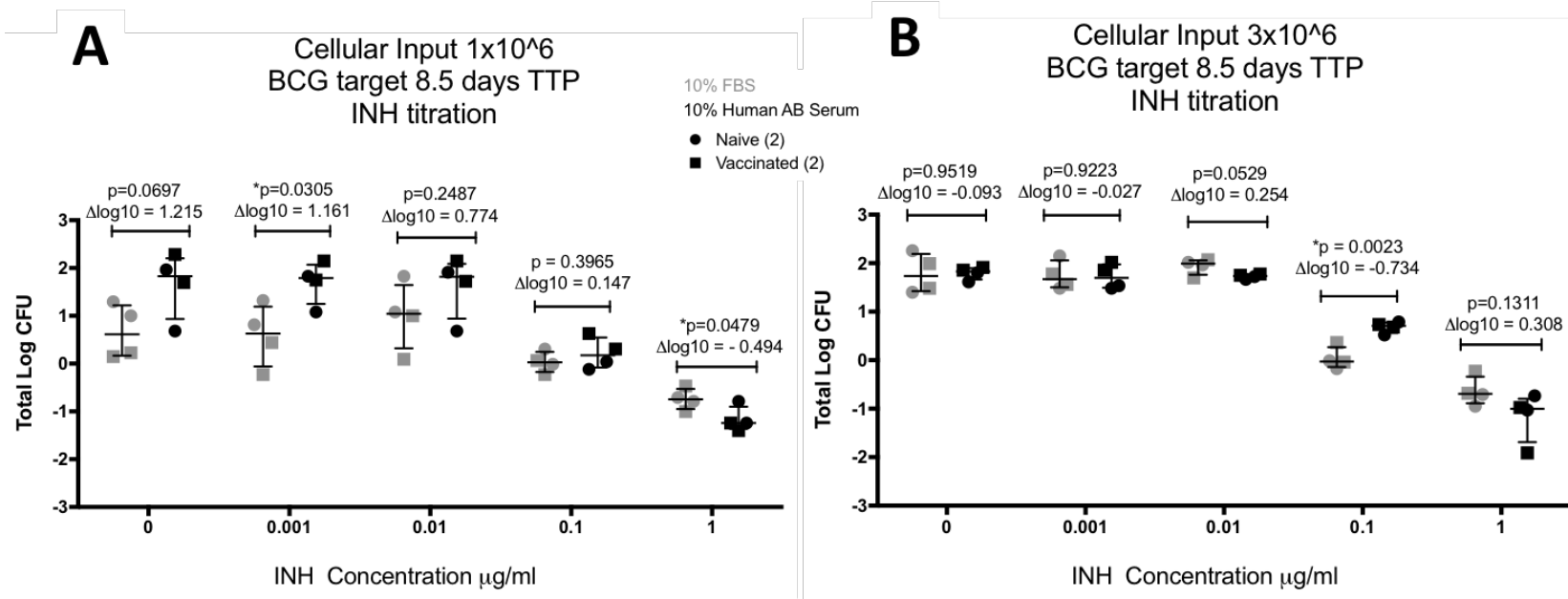


Figure 20. Comparison of different cellular input and culture media to identify optimum condition for investigation of vaccine effect in human. Titration experiments using different concentrations of INH were performed with two different cellular inputs: 1 million (A) or 3 million (B). In addition, two different culture media were also tested: containing 10% FBS (grey) or 10% pooled human AB serum (black). Each symbols represents individual data point. Data is displayed as median with IQR.

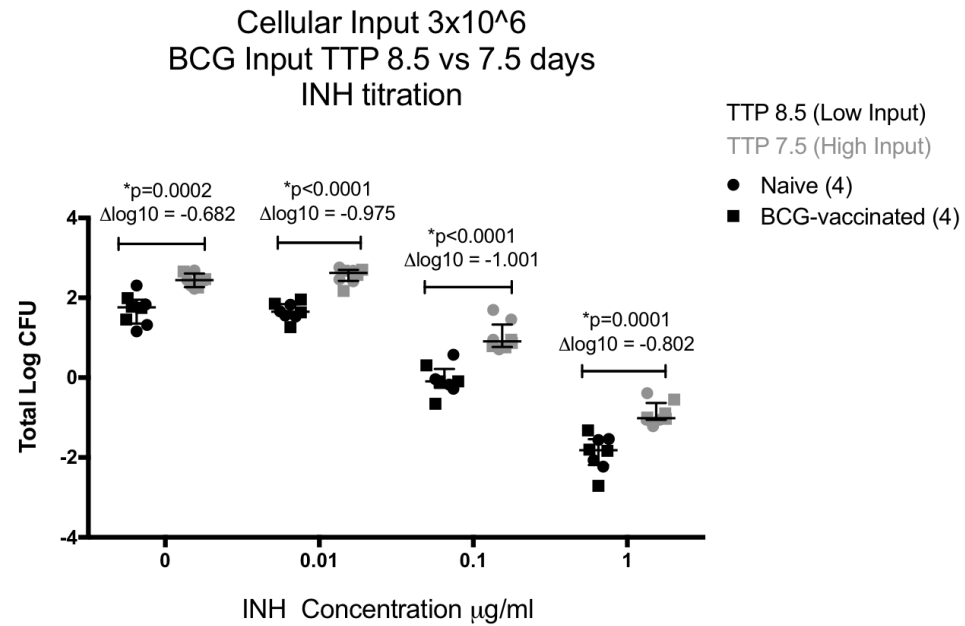


Figure 21. Comparison of different mycobacterial input to identify optimum condition for investigation of vaccine effect in human. A titration experiment with different concentrations of INH was performed with two different mycobacterial inputs: TTP 8.5 days (black) or TTP 7.5 days (grey). Each symbols represents individual data point. Data is displayed as median with IQR.

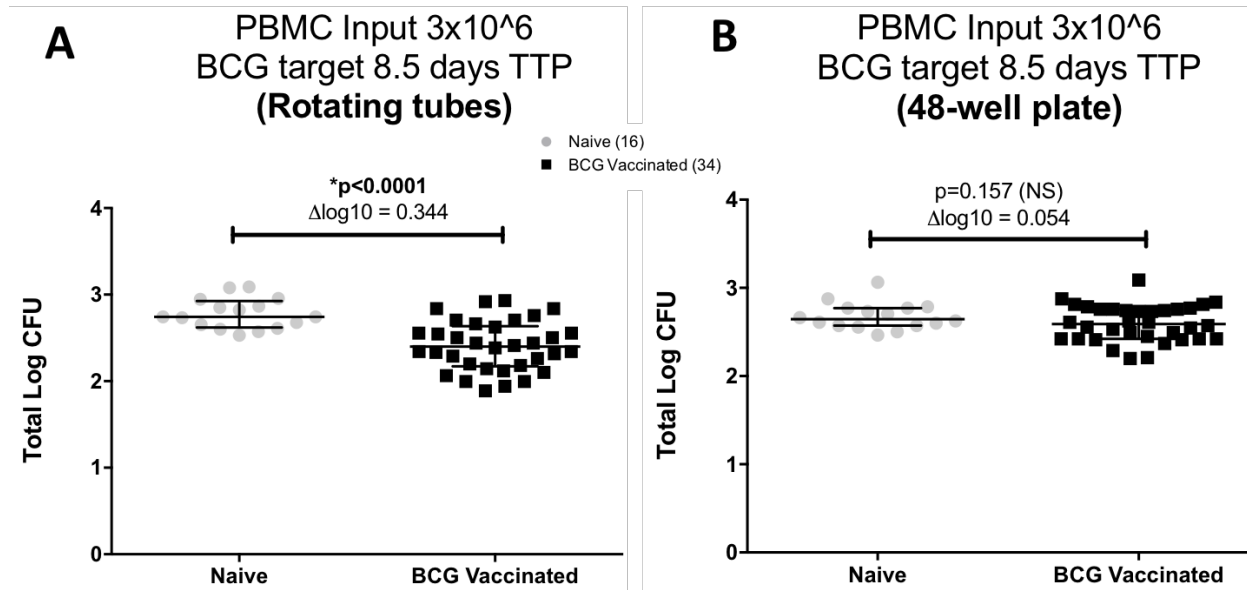


Figure 22. Comparison of different culture method to identify optimum condition for investigation of vaccine effect in human. Culture was performed either in rotating tubes (A) or 48-well plate (B) in the absence of drug. Each symbols represents individual data point. Data is displayed as median with IQR.

References

1. Ritz N, Tebruegge M, Connell TG, Sievers A, Robins-Browne R, Curtis N. Susceptibility of *Mycobacterium bovis* BCG vaccine strains to antituberculous antibiotics. *Antimicrob Agents Chemother* 2009; **53**(1): 316-8.
2. Marsay L, Matsumiya M, Tanner R, et al. Mycobacterial growth inhibition in murine splenocytes as a surrogate for protection against *Mycobacterium tuberculosis* (M. tb). *Tuberculosis (Edinb)* 2013; **93**(5): 551-7.
3. Zelmer A, Tanner R, Stylianou E, et al. A new tool for tuberculosis vaccine screening: Ex vivo Mycobacterial Growth Inhibition Assay indicates BCG-mediated protection in a murine model of tuberculosis. *BMC Infect Dis* 2016; **16**: 412.
4. Jensen C, Lindebo Holm L, Svensson E, Aagaard C, Ruhwald M. Optimisation of a murine splenocyte mycobacterial growth inhibition assay using virulent *Mycobacterium tuberculosis*. *Sci Rep* 2017; **7**(1): 2830.
5. Wallis RS, Palaci M, Vinhas S, et al. A whole blood bactericidal assay for tuberculosis. *J Infect Dis* 2001; **183**(8): 1300-3.
6. Dhillon J, Mitchison DA. Influence of BCG-induced immunity on the bactericidal activity of isoniazid and rifampicin in experimental tuberculosis of the mouse and guinea-pig. *Br J Exp Pathol* 1989; **70**(1): 103-10.
7. Shang S, Shanley CA, Caraway ML, et al. Drug treatment combined with BCG vaccination reduces disease reactivation in guinea pigs infected with *Mycobacterium tuberculosis*. *Vaccine* 2012; **30**(9): 1572-82.
8. Tanner R. Development of mycobacterial growth inhibition assays for the early evaluation and gating of novel TB vaccine candidates [Doctoral Thesis]: University of Oxford; 2015.
9. Kleinnijenhuis J, Quintin J, Preijers F, et al. Bacille Calmette-Guerin induces NOD2-dependent nonspecific protection from reinfection via epigenetic reprogramming of monocytes. *Proc Natl Acad Sci U S A* 2012; **109**(43): 17537-42.
10. Joosten SA, van Meijgaarden KE, Arend SM, et al. Mycobacterial growth inhibition is associated with trained innate immunity. *J Clin Invest* 2018; **128**(5): 1837-51.
11. Cardona PJ. The progress of therapeutic vaccination with regard to tuberculosis. *Front Microbiol* 2016; **7**: 1536.
12. Cardona PJ, Amat I, Gordillo S, et al. Immunotherapy with fragmented *Mycobacterium tuberculosis* cells increases the effectiveness of chemotherapy against a chronic infection in a murine model of tuberculosis. *Vaccine* 2005; **23**(11): 1393-8.
13. Guirado E, Gil O, Caceres N, Singh M, Vilaplana C, Cardona PJ. Induction of a specific strong polyantigenic cellular immune response after short-term chemotherapy controls bacillary reactivation in murine and guinea pig experimental models of tuberculosis. *Clin Vaccine Immunol* 2008; **15**(8): 1229-37.

14. Vilaplana C, Gil O, Caceres N, Pinto S, Diaz J, Cardona PJ. Prophylactic effect of a therapeutic vaccine against TB based on fragments of *Mycobacterium tuberculosis*. *PLoS One* 2011; **6**(5): e20404.
15. Vesosky B, Turner J. The influence of age on immunity to infection with *Mycobacterium tuberculosis*. *Immunol Rev* 2005; **205**: 229-43.
16. Friedman A, Turner J, Szomolay B. A model on the influence of age on immunity to infection with *Mycobacterium tuberculosis*. *Exp Gerontol* 2008; **43**(4): 275-85.
17. Kato C, Mikami M. Effect of aging on BCG immunostimulation of *Porphyromonas gingivalis* infection in mice. *Biomed Res* 2011; **32**(1): 45-54.
18. Fletcher HA, Tanner R, Wallis RS, et al. Inhibition of mycobacterial growth in vitro following primary but not secondary vaccination with *Mycobacterium bovis* BCG. *Clin Vaccine Immunol* 2013; **20**(11): 1683-9.

6.1 Overall Discussion and Key Findings

A major problem in tuberculosis control is the long duration of drug treatment, both in the context of active and latent TB¹. Moreover, the effectiveness of current treatment is challenged by drug-resistant TB, which although only contributes to a lesser proportion of cases compared to drug-sensitive TB, is difficult to cure and requires prolonged and more expensive treatment^{2,3}. Therapeutic vaccination as an approach has been proposed to enhance efficacy and reduce duration of treatment, and several candidates have been developed and are currently progressing through the TB vaccine pipeline⁴. The lack of correlates of protection has hampered the development of novel TB vaccines, as it will take at least a decade from discovery before the efficacy of a vaccine can be demonstrated in advanced phase 3 clinical trials⁵. Moreover, there is currently inadequate funding for TB vaccine research as well as limited field trial sites with sufficient capacity to conduct robust TB vaccine trials⁶. Therefore, vaccine candidates need to be screened at an early stage in order to narrow down which candidates should be prioritised for more advanced animal studies and clinical trials.

The MGIA as a functional assay has been developed to directly measure the ability of heterogeneous populations of host lymphocytes and other immune cells to inhibit the growth of mycobacteria *ex vivo*. The use of a validated and robust surrogate of vaccine-induced protection could reduce the number or even replace the need of animal challenge experiments and accelerate vaccine development by potentially shortening clinical trials. The growth inhibition assay could be used to gain insight into the immune pathways

essential for the control of mycobacterial growth. This could help provide a better understanding of the TB immune control, as well as directing future design of more effective vaccines.

In the present PhD project described in this thesis, an optimised human PBMC-based MGIA as well as murine MGIA using splenocyte samples were implemented to investigate the potential of MGIA as a tool for screening therapeutic TB vaccines. The first objective of this thesis was to establish a human cohort of healthy, previously BCG immunised and BCG naïve individuals in order to assess the impact of historical BCG vaccination on mycobacterial growth inhibition in the absence and presence of drugs. During the course of this project, a total 100 participants was enrolled, of which samples from 50 participants were used to investigate the impact of BCG vaccination on two major first-line TB drugs (INH and RIF), as discussed in Chapter 2. In this chapter, historical BCG vaccination was shown to enhance the ability of INH (but not RIF) to inhibit the growth of mycobacteria *ex vivo*. This finding reflects human epidemiological data and published animal studies, and therefore demonstrates the capacity of the MGIA as a potential screening tool for therapeutic TB vaccines. Importantly, the presence of drugs did not interfere with our ability to measure immune mediated mycobacterial growth inhibition. In addition, potential immune mechanisms were also identified. With regard to the combined effect between BCG vaccination and INH, increased IFN- γ and IP-10 in the MGIA supernatants were observed in participants with superior growth control. Interestingly, the source of IFN- γ did not appear to be from CD4 or CD8 T-cells, but rather from NK cells. This is consistent with emerging evidences from clinical studies denoting the essential protective role of NK cells in TB infection and vaccination^{7,8}.

The role of NK cells was further characterised in Chapter 4, in which growth inhibition was assessed in the absence of drug with the cohort of 100 participants. Enhanced *ex vivo* mycobacterial growth control was attributed to the cytokine-producing NK cells, and an association was also observed between the production of perforin in MGIA supernatants and inhibition of growth. NK cells have lately been discovered to be able to act in a memory-like manner⁹, which could be under the direction of T-cells (Figure 23). In addition, NK cells are a component of the innate system in which the trained immunity phenomenon has been observed¹⁰.

Furthermore, several other immune cell phenotypes and cytokines were demonstrated to be correlated with mycobacterial growth control, such as activated T-cells, monocyte frequency and IL-10 production. CMV-specific responses were associated with T-cell activation and these were associated with increased mycobacterial growth *ex vivo* in our cohort. These findings have emphasised the value of the MGIA as a summative measure of host immune responses which could serve as a better correlate of protection (Figure 23), rather than just measuring one cytokine such as IFN- γ . Intriguingly, we found that BCG-vaccinated females responded better than males when assessed using the *ex vivo* MGIA assay in the cohort of 100 participants. This is the first time such a large cohort has been examined using MGIA with sufficient statistical power to assess the impact of sex. As globally, males are more affected by TB when compared to females and immune differences are thought to play a role, our findings suggest that females might be better protected from BCG vaccination. Further in this regard, investigating individual-level factors affecting mycobacterial-specific immune responses could help vaccine developers to understand what may influence their ability to observe a vaccine effect when testing candidates in clinical trials.

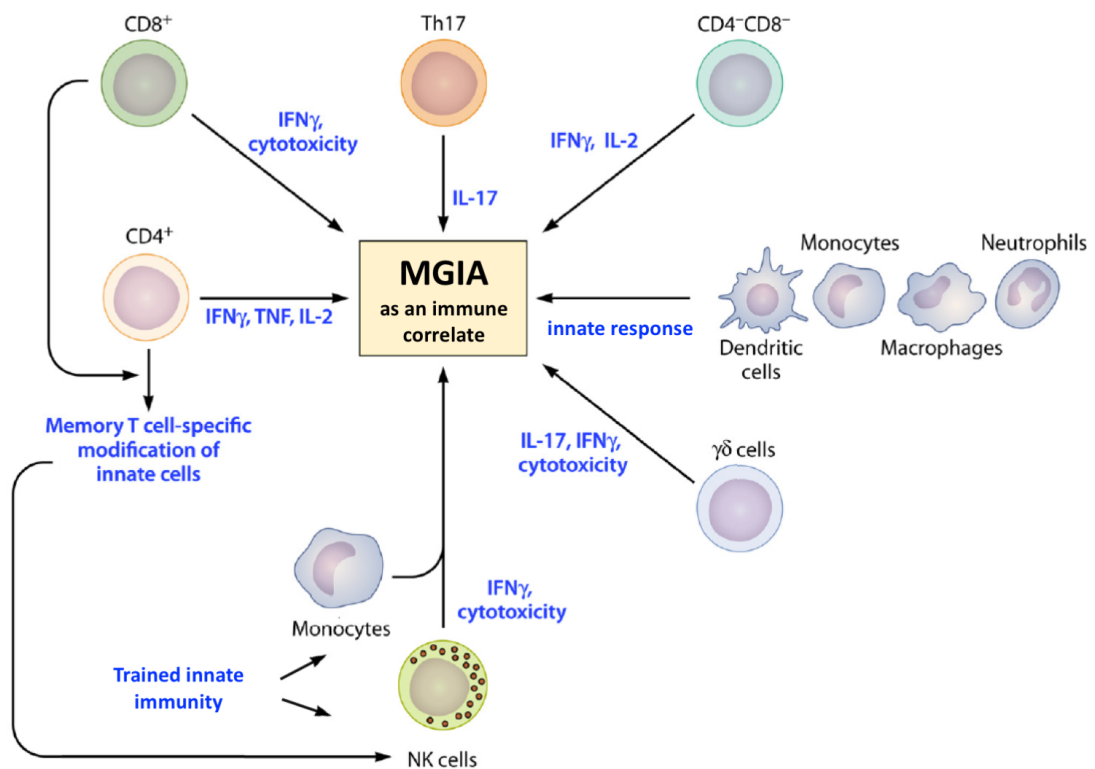


Figure 23. Illustration of the contribution of immune cells from various compartments on the *ex vivo* mycobacterial growth inhibition assay system (adapted with modification from¹¹).

Our finding in historically BCG-vaccinated humans is also supported by the mouse model, in which recent BCG vaccination is shown to enhance the *ex vivo* efficacy of INH, as discussed in Chapter 5. In this context, the murine MGIA assay could be implemented as well to screen therapeutic TB vaccine candidates in pre-clinical testing stage. In the same chapter, the impact of RUTI in enhancing the *ex vivo* efficacy of INH and RIF has also been demonstrated in one of the experiments, although we could not fully replicate this result in a repeat experiment. Regardless of this issue, we observed a consistent impact of RUTI vaccine in both experiments in the absence of drug and decided to proceed with further experiments using an optimised protocol (culture performed in 48-

well plate instead of rotating tubes for mouse splenocytes). In Chapter 3, a time course experiment was performed to characterise the kinetic of the immune response to RUTI in the murine MGIA assay in the absence of drug. A peak vaccine response measured by growth inhibition was observed at week 6 after two doses of RUTI. Compellingly, the results also showed a shift of monocyte phenotype in the spleen in this experiment and such shift concurred with the peak response of RUTI in the MGIA assay.

In this study, RUTI vaccination was shown to induce nonclassical Ly6C⁻ monocytes in the spleen of healthy mice, characterised using flow cytometry and further confirmed using qPCR. Most evidence in the literature propose the role of Ly6C⁻ monocytes as anti-inflammatory and the fact that their increase is associated with enhanced *ex vivo* growth control has further supported the importance of a balanced immune response in the context of mycobacterial containment¹². On the other hand, the finding by Joosten *et al.*¹³ regarding the role of nonclassical monocytes in trained innate immunity should also be taken into consideration when interpreting the RUTI data as this might represent a novel mechanism of action by the vaccine. Altogether, the present investigations in humans and mice using the *ex vivo* MGIA assays have demonstrated its benefit in identifying immune mechanisms following immunisation with TB vaccines.

6.2 Strengths and Limitations of the Research Presented

During the course of this PhD project, 100 healthy adult volunteers were enrolled and this sample size gives sufficient statistical power to assess the impact of historical BCG vaccination and sex on mycobacterial growth inhibition. Moreover, this study was conducted in the UK, enrolling mostly UK BCG-vaccinated participants, where BCG is

known to provide a high level of protection. With this study characteristic, we were able to demonstrate the impact of individual-level factors on *ex vivo* mycobacterial growth inhibition. Our study is also the first to demonstrate the impact of vaccination on top of drug treatment using the *ex vivo* MGIA assay and this serves as an important proof-of-principle to implement the MGIA as a screening tool for therapeutic TB vaccines. With regard to the mouse study, the author was privileged to be able to test the RUTI vaccine in my project as a promising therapeutic TB vaccine candidate.

For this project, the LSHTM blood donation system for research purposes was utilised, in which only 50 ml of blood could be taken from each participant in accordance to the ethical permission given to this study. With the amount of PBMCs isolated from the restricted volume of blood, this study can only test two major first-line TB drugs with several different concentrations as well as without drug. Stored PBMC samples from participants of this study have all been used for early optimisation work, MGIA, ELISpot and cell surface as well as ICS flow cytometry. In addition, there was also a budget consideration which could only allow us to perform the MGIA assay with drugs in 50 participants. For this project, cytokine production can only be measured from the MGIA supernatant by ELISA, in which a large volume of sample is required and this can only be done at day 4 in order not to disturb the MGIA culture system. Moreover, the MGIA system is very sensitive to contamination and requires intensive training in order to master the technique. In addition, some of the results presented in this study were only reaching non-significant trends, albeit close to statistical significance. In future studies, significance may be achieved with larger sample size or further optimised assay with less variability.

In relation to the murine MGIA assay, it was found that cell viability was a notable issue as mouse splenocytes are less robust compared to human PBMCs during the 4 day culture. This issue has been addressed in this study, by switching culture conditions in 48-well plates instead of rotating tubes, where we subsequently observed more consistent results with less variability in the optimised conditions. Finally, in the future it would be important to compare the control of *Mtb* growth alongside the control of BCG growth. We could not do that in this study as we wished to process a large number of samples with a wide range of immune assays and did not have the ability to perform many of these immune assays in the BSL3 laboratory.

6.3 Conclusion

In conclusion, this thesis has demonstrated that immunisation with therapeutic tuberculosis vaccines can enhance the ability of immune cells to control the growth of mycobacteria, in the absence and in the presence of TB drugs, and this effect can be measured *ex vivo* with the growth inhibition assay. Specifically, it has been shown that BCG vaccination in humans and mice, and RUTI vaccination in mice could enhance *ex vivo* control of mycobacterial growth. Further, the growth inhibition assay can be used to gain insight into the immune pathways important for the mycobacterial growth control. Indeed, although more work is needed, MGIA has the potential to be further implemented in pre-clinical and clinical vaccine testing, as an endeavour to accelerate the development of therapeutic tuberculosis vaccines.

6.4 Future Directions

The thesis described above has extended our understanding of immune mechanisms as well as the value of the *ex vivo* MGIA assay in testing therapeutic TB vaccine candidates. Nevertheless, the findings raise further questions which will need to be addressed in future studies. Using the human cohort, the impact of historical BCG vaccination towards *ex vivo* drug-mediated killing of INH and RIF has been demonstrated. While the effectiveness of these two drugs are unequivocally challenged by MDR-TB, it will be important in the future to investigate the impact of BCG and other therapeutic vaccines towards second-line TB drugs, which are less effective than the first-line drugs. Given the current treatment success rate of MDR-TB ranging only around 50% in many service conditions worldwide, there is certainly a room for improvement by introducing therapeutic vaccination in order to maximise benefit for patients in the clinical setting.

Various cellular components, as well as cytokines, and their role in the MGIA have been demonstrated in this study. In particular, IL-10 has been shown to be an influential immunoregulatory cytokine in the MGIA, which is in line with previous studies. It will be interesting to characterise which cells are the major producers of this cytokine and to further demonstrate its importance by the use of splenocytes from IL-10 knockout mice. Unfortunately, due to time and capital constraints, this could not be achieved in this project. Furthermore and importantly, our study has highlighted the role of NK cells for *ex vivo* control of mycobacterial growth in the presence and absence of drug. Therefore, NK cells could be further explored as a target for a novel therapeutic vaccine against TB. In this regard, the exact mechanism of NK cell protection following BCG vaccination on *ex vivo* mycobacterial growth remains to be further elucidated. It may be that its role is

through antigen-specific memory-like response of NK cells, or through the trained innate immunity mechanism.

The observed impact of sex following BCG vaccination in our cohort of 100 participants warrants further investigation in larger epidemiological studies. To our knowledge, no study has identified a differential protection between sex following BCG vaccination against adult pulmonary TB, despite the abundance of TB cases in males worldwide. Nevertheless, the non-specific protective effect of BCG on overall mortality and reduced incidence of respiratory infections – not related to TB – is more pronounced in young females compared to males¹⁴⁻¹⁶. In this context, it is speculated that the notable BCG-induced enhanced growth inhibition in females could be more reflective of the non-specific protective effect conferred by the vaccine, which has been linked to the trained innate immune mechanism^{13,17}. Therefore, it will be fascinating in the future to investigate downstream and upstream pathways related to this mechanism, such as by looking at DNA methylation. A recent study did not find an association between *in vitro* addition of sex hormones and BCG-induced trained innate immunity on adult monocytes¹⁸. However, considering the results of the our present study, it will be worth looking at such impact on another cell population in which trained innate immunity has been described¹⁰, that is the NK cells.

The importance of trained innate immunity mechanism may also be attributed to impact of RUTI in driving nonclassical monocytes in mice. Nonetheless, our *ex vivo* data still needs to be confirmed by *in vivo* studies with *Mtb* to better demonstrate the impact of RUTI on trained innate immunity. In our study, splenocyte samples were used in the murine MGIA as it is considered to be the most practical tissue to use. Development of

MGIA with mouse lung cells is currently underway in our group (Hannah Painter, personal communication), as an attempt to better reflect the natural infection site of the mycobacteria. Furthermore, studies are required to better understand the interplay between CMV-specific response, T-cell activation and NK cells in the context of BCG vaccination, in which the mouse model could serve as a platform for mechanistic exploration.

References

1. Schon T, Lerm M, Stendahl O. Shortening the 'short-course' therapy- insights into host immunity may contribute to new treatment strategies for tuberculosis. *J Intern Med* 2013; **273**(4): 368-82.
2. Maeurer M, Schito M, Zumla A. Totally-drug-resistant tuberculosis: hype versus hope. *Lancet Respir Med* 2014; **2**(4): 256-7.
3. Millard J, Ugarte-Gil C, Moore DA. Multidrug resistant tuberculosis. *BMJ* 2015; **350**: h882.
4. Gröschel MI, Prabowo SA, Cardona P-J, Stanford JL, Werf TSvd. Therapeutic vaccines for tuberculosis—A systematic review. *Vaccine* 2014; **32**(26): 3162-8.
5. Fletcher HA, Dockrell HM. Human biomarkers: can they help us to develop a new tuberculosis vaccine? *Future Microbiol* 2016; **11**: 781-7.
6. Kaufmann SH, Evans TG, Hanekom WA. Tuberculosis vaccines: Time for a global strategy. *Sci Transl Med* 2015; **7**(276): 276fs8.
7. Suliman S, Geldenhuys H, Johnson JL, et al. Bacillus Calmette-Guerin (BCG) Revaccination of Adults with Latent Mycobacterium tuberculosis Infection Induces Long-Lived BCG-Reactive NK Cell Responses. *J Immunol* 2016; **197**(4): 1100-10.
8. Roy Chowdhury R, Vallania F, Yang Q, et al. A multi-cohort study of the immune factors associated with M. tuberculosis infection outcomes. *Nature* 2018; **s41586**: 018-0439-x.
9. Choreno Parra JA, Martinez Zuniga N, Jimenez Zamudio LA, Jimenez Alvarez LA, Salinas Lara C, Zuniga J. Memory of Natural Killer Cells: A New Chance against Mycobacterium tuberculosis? *Front Immunol* 2017; **8**: 967.
10. Kleinnijenhuis J, Quintin J, Preijers F, et al. BCG-induced trained immunity in NK cells: Role for non-specific protection to infection. *Clin Immunol* 2014; **155**(2): 213-9.
11. Bhatt K, Verma S, Ellner JJ, Salgame P. Quest for correlates of protection against tuberculosis. *Clin Vaccine Immunol* 2015; **22**(3): 258-66.
12. Orme IM, Robinson RT, Cooper AM. The balance between protective and pathogenic immune responses in the TB-infected lung. *Nat Immunol* 2015; **16**(1): 57-63.
13. Joosten SA, van Meijgaarden KE, Arend SM, et al. Mycobacterial growth inhibition is associated with trained innate immunity. *J Clin Invest* 2018; **128**(5): 1837-51.
14. Stensballe LG, Nante E, Jensen IP, et al. Acute lower respiratory tract infections and respiratory syncytial virus in infants in Guinea-Bissau: a beneficial effect of BCG vaccination for girls community based case-control study. *Vaccine* 2005; **23**(10): 1251-7.
15. Roth A, Sodemann M, Jensen H, et al. Tuberculin reaction, BCG scar, and lower female mortality. *Epidemiology* 2006; **17**(5): 562-8.

16. Biering-Sorensen S, Jensen KJ, Monterio I, Ravn H, Aaby P, Benn CS. Rapid Protective Effects of Early BCG on Neonatal Mortality Among Low Birth Weight Boys: Observations From Randomized Trials. *J Infect Dis* 2018; **217**(5): 759-66.
17. Netea MG, Joosten LA, Latz E, et al. Trained immunity: A program of innate immune memory in health and disease. *Science* 2016; **352**(6284): aaf1098.
18. de Bree C, Janssen R, Aaby P, et al. The impact of sex hormones on BCG-induced trained immunity. *J Leukoc Biol* 2018; **104**(3): 573-8.

APPENDIX 1. Ethical approval 1 for human study

London School of Hygiene & Tropical Medicine

Keppel Street, London WC1E 7HT
United Kingdom
Switchboard: +44 (0)20 7636 8636

www.lshtm.ac.uk

LONDON
SCHOOL of
HYGIENE
& TROPICAL
MEDICINE



Observational / Interventions Research Ethics Committee

Satria Probowo
LSHTM

30 January 2015

Dear Satria

Study Title: Assessment of Therapeutic Tuberculosis Vaccine Strategies Using In Vitro Mycobacterial Growth Inhibition Assay In Human Blood

LSHTM Ethics Ref: 8762

Thank you for responding to the Observational Committee's request for further information on the above research and submitting revised documentation.

The further information has been considered on behalf of the Committee by the Chair.

Confirmation of ethical opinion

On behalf of the Committee, I am pleased to confirm a favourable ethical opinion for the above research on the basis described in the application form, protocol and supporting documentation as revised, subject to the conditions specified below.

Conditions of the favourable opinion

Approval is dependent on local ethical approval having been received, where relevant.

Approved documents

The final list of documents reviewed and approved by the Committee is as follows:

Document Type	File Name	Date	Version
Investigator CV	Curriculum Vitae - Satria A. Prabowo.pdf	23/10/2014	1
Information Sheet	Blood collection for research.doc	23/10/2014	1
Information Sheet	Consent form extra questions.doc	23/10/2014	1
Investigator CV	CV HFletcher Sept2014.doc	24/10/2014	1
Investigator CV	CV HFletcher Sept2014.doc	24/10/2014	1
Information Sheet	Blood collection for research	18/12/2014	1
Information Sheet	Consent form extra questions	18/12/2014	1
Information Sheet	Specific Information Sheet	18/12/2014	1
Covering Letter	Covering Letter	18/12/2014	1
Covering Letter	Covering Letter 8762_rev210115	21/01/2015	1
Protocol / Proposal	Study Protocol 8762_rev210115	21/01/2015	1

After ethical review

The Chief Investigator (CI) or delegate is responsible for informing the ethics committee of any subsequent changes to the application. These must be submitted to the Committee for review using an Amendment form. Amendments must not be initiated before receipt of written favourable opinion from the committee.

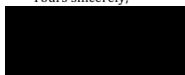
The CI or delegate is also required to notify the ethics committee of any protocol violations and/or Suspected Unexpected Serious Adverse Reactions (SUSARs) which occur during the project by submitting a Serious Adverse Event form.

At the end of the study, the CI or delegate must notify the committee using an End of Study form.

All aforementioned forms are available on the ethics online applications website and can only be submitted to the committee via the website at: <http://leo.lshtm.ac.uk>

Additional information is available at: www.lshtm.ac.uk/ethics

Yours sincerely,



Professor John DH Porter
Chair

ethics@lshtm.ac.uk
<http://www.lshtm.ac.uk/ethics/>

APPENDIX 2. Ethical approval 2 for human study

London School of Hygiene & Tropical Medicine

Keppel Street, London WC1E 7HT
United Kingdom
Switchboard: +44 (0)20 7636 8636

www.lshtm.ac.uk

LONDON
SCHOOL of
HYGIENE
& TROPICAL
MEDICINE



Observational / Interventions Research Ethics Committee

Mr Satria Arief Prabowo
LSHTM

14 April 2016

Dear Satria

Study Title: Investigation of Therapeutic Vaccination Strategies for Tuberculosis Using an Ex-vivo Mycobacterial Growth Inhibition Assay

LSHTM Ethics Ref: 10485

Thank you for responding to the Observational Committee's request for further information on the above research and submitting revised documentation.

The further information has been considered on behalf of the Committee by the Chair.

Confirmation of ethical opinion

On behalf of the Committee, I am pleased to confirm a favourable ethical opinion for the above research on the basis described in the application form, protocol and supporting documentation as revised, subject to the conditions specified below.

Conditions of the favourable opinion

Approval is dependent on local ethical approval having been received, where relevant.

Approved documents

The final list of documents reviewed and approved by the Committee is as follows:

Document Type	File Name	Date	Version
Investigator CV	Curriculum Vitae - Satria A. Prabowo	25/11/2015	1.0
Investigator CV	CV HFletcher Sept2014	25/11/2015	1.0
Protocol / Proposal	Study Protocol 10485	23/12/2015	1.0
Information Sheet	Information Sheet and Consent Form	11/04/2016	2.0
Information Sheet	Previous Information Sheet and Consent Form (8762)	11/04/2016	1.0
Covering Letter	Covering Letter 10485	11/04/2016	1.0

After ethical review

The Chief Investigator (CI) or delegate is responsible for informing the ethics committee of any subsequent changes to the application. These must be submitted to the Committee for review using an Amendment form. Amendments must not be initiated before receipt of written favourable opinion from the committee.

The CI or delegate is also required to notify the ethics committee of any protocol violations and/or Suspected Unexpected Serious Adverse Reactions (SUSARs) which occur during the project by submitting a Serious Adverse Event form.

At the end of the study, the CI or delegate must notify the committee using an End of Study form.

All aforementioned forms are available on the ethics online applications website and can only be submitted to the committee via the website at: <http://leo.lshtm.ac.uk>

Additional information is available at: www.lshtm.ac.uk/ethics

Yours sincerely,



Professor John DH Porter
Chair

ethics@lshtm.ac.uk



Collection of Normal Human Blood for Research Use

The Faculty of Infectious and Tropical Diseases conducts epidemiological and laboratory research on a number of important human pathogens. The research aims to give us a better understanding of the epidemiology and pathogenesis of certain infectious diseases and to assist in the development of new vaccines and drugs or diagnostic tests. As part of this research, there is a continuing need to obtain samples of human blood, from people who have not been exposed to or infected with the pathogen of interest. On occasion, it is also very helpful to obtain blood from people who know they *have* been exposed to certain pathogens (such as malaria, leishmaniasis, tuberculosis etc). These samples either act as negative and positive controls for comparison with samples taken from infected or immune individuals or are used to develop and validate new techniques prior to commencing new projects in disease endemic areas. For some types of work, samples obtained from the Blood Transfusion Service are sufficient. But for other projects, freshly obtained samples are needed and it is helpful if the researcher can obtain repeat samples from the same donors (for example where tissue-typing data is required).

The staff and students of LSHTM represent a potentially invaluable resource for this research. Although many staff and students are entirely based in the UK or Europe, others come to the School from a wide variety of different backgrounds and may have been exposed to a variety of different pathogens. The School's Research Ethics Committee has therefore agreed that all incoming staff and research students will be asked whether they would like to volunteer to take part in these research projects.

Volunteers will be asked to fill out a simple form indicating their country of origin and other countries where they have lived. This information will be held on a confidential database. An anonymised version of the database (where names have been replaced by code numbers) will be available to individual researchers in order to identify potential blood donors for their particular project. Volunteers will then be contacted, given details of the project and asked whether they would like to take part. If they agree, they will sign a consent form and a blood sample – of between 1 and 100mls depending on the project – will be collected by a clinician or qualified phlebotomist.

It is unlikely that any of the data collected will have any direct clinical relevance to the donor, but if this is the case it will be made clear on the consent form and any relevant data will be fed back to the donors. Any donor who wishes to see the results of any tests performed on his/her blood will be allowed to do so. By agreeing to go on the register of potential donors, volunteers do not commit themselves to take part in any particular project and may withdraw their name from the list at any time. There are no direct benefits to joining the register (donors will not be paid or receive any other benefit in kind) and no record will be kept of those who decide not to join. Blood samples will *not* be screened for evidence of current viral infections (such as HIV, hepatitis viruses etc) but people who know they have been exposed or infected are requested not to volunteer.

For more information on the blood donor scheme and a consent form, please contact Ms Carolynne Stanley, Faculty of Infectious and Tropical Diseases (carolyn.stanley@lshtm.ac.uk).

APPENDIX 4. Consent form for study participants

**Collection of normal human
blood for research use:
Consent Form**

LONDON
SCHOOL of
HYGIENE
& TROPICAL
MEDICINE



Name:	
Date of birth:	
Department \ Unit:	
Keppel Street or Tavistock Place Office\room no:	
Work telephone number:	
Email address:	
Are you: Staff Student	YES\NO YES\NO
If student: when are you due to complete your studies?	
Are you a regular blood donor in: The UK Elsewhere	YES\NO YES\NO
Have you had a Tetanus inoculation?	YES\NO
Have you had a Rabies vaccination?	YES\NO
Have you been BCG-vaccinated?	YES\NO
Do you still have a visible scar from this BCG vaccination?	YES\NO\NA
Country of origin	
Have you lived in any countries apart from your country of origin and the UK?	YES\NO
If YES, please list the countries and the dates when you lived there	
Blood group if known.	

Have you ever visited a malarious zone?	YES\NO
Have you ever had malaria?	YES\NO
Have you had a Hep B vaccination?	YES\NO

I would like my name to be added to the register of potential blood donors for research projects within LSHTM.

I understand that I may be asked to donate blood as part of a research project conducted by LSHTM staff or research students. I will be free to take part, or refuse to take part, in any of these projects.

All projects will have received ethical approval from the LSHTM Research Ethics Committee and individual informed consent will be required for each project.

Blood will be collected only by clinically qualified staff or a qualified phlebotomist whose name is held on a register of phlebotomists.

I will be entitled to see all data arising from the use of my blood, on request.

My blood will not be screened for HIV, Hepatitis B, Hepatitis C or any other persistent virus infection unless this it is specifically stated on the consent form for the project(s) for which I volunteer.

I am not aware that I suffer from any persistent medical condition or infection which affects my suitability to be a blood donor.

I understand that, in order to maintain confidentiality, information arising from research projects will be kept on an anonymised database and that individual researchers will not normally be aware of my identity. The database containing my name will be securely maintained and will not be made available to researchers.

Name (in capitals)

Signature

Date

APPENDIX 5. Material transfer agreement for RUTI vaccine study

CONFIDENTIAL

Materials Transfer Agreement effective as of 19th February 2015

This Agreement is made and entered into between

ARCHIVEL FARMA, S.L.
c/ Fogars de Tordera, 61
Badalona CP 08916
Spain

("ARCHIVEL")

and

LONDON SCHOOL OF HYGIENE AND TROPICAL MEDICINE
Keppel Street
London WC1E 7HT
United Kingdom

("RECIPIENT")

Background

RECIPIENT has requested that ARCHIVEL supply certain BIOLOGICAL MATERIALS that are identified in the Request for BIOLOGICAL MATERIALS ("Request"). The Request is attached hereto as Annex A (as may be updated from time to time by mutual agreement of the Parties), and which shall be deemed as an integral part of the Agreement.

The BIOLOGICAL MATERIALS requested are considered by ARCHIVEL to be highly valuable, confidential and proprietary biological materials and/or products of ARCHIVEL research development as well as license rights belonging to ARCHIVEL.

ARCHIVEL is willing to provide RECIPIENT with the requested quantities of the BIOLOGICAL MATERIALS specified in the Request upon the following terms:

1. Definitions.

- (a) "BIOLOGICAL MATERIALS" means all materials transferred by ARCHIVEL to RECIPIENT hereunder, and any replicates, progeny and derivatives of the BIOLOGICAL MATERIALS, as described in Annex A.

Date: 19 February 2015

Page 1 of 8

CONFIDENTIAL

- (b) "RECIPIENT Materials" means all materials provided by RECIPIENT but not necessarily covered by RECIPIENT's industrial and intellectual property rights.
 - (c) "Joint Materials" means all materials incorporating all or a portion of any BIOLOGICAL MATERIALS and all or a portion of any RECIPIENT Materials.
 - (d) "Authorized Use" shall mean use in strict accordance with the Development Plan set forth in the Annex B attached.
2. Title to BIOLOGICAL MATERIALS. ARCHIVEL shall retain all title and interest in and to the BIOLOGICAL MATERIALS. RECIPIENT shall not imply or represent to any person that it is the owner of the BIOLOGICAL MATERIALS.
 3. Delivery of BIOLOGICAL MATERIALS. ARCHIVEL shall have the requested BIOLOGICAL MATERIALS delivered to RECIPIENT as set forth in Annex A, but in no event prior to the execution of this Agreement.
 4. Use of BIOLOGICAL MATERIALS. As of the date that this Agreement is executed by ARCHIVEL, ARCHIVEL grants RECIPIENT a non-exclusive, royalty free, limited to the territory of United Kingdom, license to the use the BIOLOGICAL MATERIALS solely for the Authorized Use for research and development purposes and not for any other purpose, which other purpose include but is not limited to, any direct or indirect use for patent applications, commercial use or profit making purposes or any other purpose which final aim is commercial such as consultation, provision of services, production, sale or sponsored researches. To avoid any doubt, this research and development license excludes the right to sublicense or subcontract without the prior explicit written approval of ARCHIVEL. RECIPIENT shall not use the BIOLOGICAL MATERIALS in humans or in contact with any cells or other materials to be infused into humans. RECIPIENT shall use the BIOLOGICAL MATERIALS in compliance with all applicable national, federal, state and local laws and regulations. RECIPIENT shall not transfer the BIOLOGICAL MATERIALS or any information related to those materials to any person who is not an employee of the RECIPIENT who have a "need to know" for the purpose of conducting the Development Plan or a third person assigned to perform certain or all parts of the Development Plan in accordance with a legally binding agreement with RECIPIENT which agreement protects and maintains all of ARCHIVEL's rights under this Agreement, nor use the BIOLOGICAL MATERIALS in development that is subject to consulting or licensing obligations to another corporation or a government agency, unless prior written permission is obtained from ARCHIVEL.
 5. Reports and publications. RECIPIENT shall keep ARCHIVEL on a monthly basis informed of the progress of the Development Plan and, no later than thirty (30) business days after the conclusion of the Development Plan as set forth under this Agreement, RECIPIENT shall promptly provide ARCHIVEL a written report summarizing the results, data and information arising out of performance of the Development Plan and of the Authorized Use of the BIOLOGICAL MATERIALS. Neither party shall publish or disclose the terms and conditions of this Agreement without the prior written consent of the other party.

CONFIDENTIAL

RECIPIENT shall not publish or present any scientific information relating to any aspect of the BIOLOGICAL MATERIALS, including, but not limited to, the development or manufacture of the BIOLOGICAL MATERIALS, without providing ARCHIVEL the opportunity for prior review. RECIPIENT shall provide to ARCHIVEL at least (i) forty five (45) calendar days prior to each submission for publication of any detailed proposed publication such as manuscripts or other articles and (ii) forty five (45) days prior to each submission of publication of any proposed limited publication such as abstracts, posters or revised submissions, relating to any aspect of the BIOLOGICAL MATERIALS and RECIPIENT shall not proceed with such publication or presentation (a) to the extent ARCHIVEL demonstrates that ARCHIVEL's Confidential Information would be disclosed and (b) until ARCHIVEL has had the opportunity to secure any necessary patent protection for a period of no more than ninety (90) days from RECIPIENT's notice. In addition hereto RECIPIENT shall otherwise comply with all reasonable requests from ARCHIVEL for modifications and/or deletions in order to protect the confidential nature of non-patentable information.

RECIPIENT shall offer ARCHIVEL the opportunity to participate as co-author.

6. Inventions.

- (a) All rights, title and interest in ARCHIVEL patents or patent applications, including but not limited to patents or patent applications licensed by ARCHIVEL, of or related to the BIOLOGICAL MATERIALS as well as in which does not involve the use of any RECIPIENT Materials are and shall be exclusively ARCHIVEL's. In the event that use of the BIOLOGICAL MATERIALS or the Joint Materials results in any ideas, concepts, discoveries, inventions, developments, know-how, applications, techniques, methodologies, modifications, innovations, improvements, documentation, information and any other intellectual and industrial property rights (whether or not any of the foregoing are patentable under applicable law) or an invention or discovery involving a new use, methodology, process, improvement or enhancement ("Invention") of the BIOLOGICAL MATERIALS that are conceived, developed, created or obtained by RECIPIENT while executing the Development Plan, which Invention does not involve the use of any RECIPIENT Materials, RECIPIENT shall disclose such Invention to ARCHIVEL, and RECIPIENT hereby assigns all right and title to such Invention to ARCHIVEL. ARCHIVEL shall be responsible for all costs of obtaining patent coverage. ARCHIVEL shall have the right to commercially exploit such Inventions.

RECIPIENT shall not attempt to reverse engineer, develop, disassemble, manipulate, replicate or otherwise perform analyses directed or intended at learning the methodology, components, formulae, processes or other information pertaining to the make-up or production of the BIOLOGICAL MATERIALS or at purifying, cloning or generating additional material from the BIOLOGICAL MATERIALS, unless expressly authorized in writing by ARCHIVEL. If so authorized, RECIPIENT shall furnish copies of any such analyses to ARCHIVEL and RECIPIENT shall make no use thereof except as previously agreed in writing by ARCHIVEL. If no further agreement is reached by the Parties as to the BIOLOGICAL MATERIALS, RECIPIENT shall at ARCHIVEL's request either furnish all copies of such analyses to ARCHIVEL or destroy all copies thereof.

- (b) RECIPIENT shall remain the sole and exclusive owner of all rights, title and interest in and to patents or patent applications of or related to the RECIPIENT Materials. In the event RECIPIENT develops any Invention in relation to Development Plan which Invention does not involve the use of any BIOLOGICAL MATERIALS provided by

CONFIDENTIAL

ARCHIVEL, such Invention shall be solely owned by RECIPIENT. RECIPIENT shall be responsible for obtaining patent coverage, if it so desires, and shall bear all costs in this respect.

- (c) Any Invention made arising from the Authorized Use, other than the Inventions the ownership of which is described in subsections (a) and (b) hereof, shall be owned by ARCHIVEL. ARCHIVEL shall have the right to commercially exploit such Inventions.
- (d) Notwithstanding the foregoing, composition of matter inventions or discoveries (a) related to a vaccine use of the BIOLOGICAL MATERIALS and (b) that are modifications to the nucleic acid or amino acid sequence of the BIOLOGICAL MATERIALS shall be subject to 6.a.

Notwithstanding the foregoing each party shall maintain all rights and title to any patent or patent application granted or submitted before the date of this Agreement and pertaining to that party.

In case the Parties are interested in research and development activities in which the BIOLOGICAL MATERIAL is to be combined, coupled, joint, or used as an adjuvant or co-adjuvant with RECIPIENT Materials in any form or matter, totally or partially, the parties will engage in good faith negotiations to enter into a separate agreement to be agreed between the parties for the purposes of regulating such matters.

7. No Conflicts. RECIPIENT represents that it is authorized to enter into this Agreement and that no other contract or other obligation conflicts with the obligations to be assumed by RECIPIENT under this Agreement.

8. Disclaimer. The BIOLOGICAL MATERIALS are provided to RECIPIENT without warranty of merchantability or fitness for a particular purpose or any other warranty, express or implied or any warranty that the BIOLOGICAL MATERIALS will not infringe or violate any patent or other proprietary right of any third party. ARCHIVEL shall not be liable for any use of the BIOLOGICAL MATERIALS by RECIPIENT, or for any loss, claim, damage or liability, of any kind or nature, which may arise from or in connection with this Agreement or from the use, handling or storage of the BIOLOGICAL MATERIALS. No indemnification for any loss, claim, damage or liability is intended or shall be provided by ARCHIVEL under this Agreement.

9. "Confidential Information" shall mean any proprietary information that is specifically designated as such and that is disclosed by either party to the other in any form in connection with this Agreement. For the term of this Agreement and five (5) years from the date of expiration or termination, each party (a) shall treat as confidential all Confidential Information provided by the other party, (b) shall not use such Confidential Information except as expressly permitted under the terms of this Agreement, or as otherwise authorized in writing by the disclosing party, (c) shall implement reasonable procedures to prohibit the disclosure, unauthorized duplication, misuse or removal of such Confidential Information, and (d) shall not disclose such Confidential Information to any third party. Without limiting the foregoing, each of the parties shall use at least the same procedures and degree of care to prevent the disclosure of Confidential Information as it uses to prevent the disclosure of its own confidential information of like importance, and shall in any event use no less than reasonable procedures and a reasonable degree of care.

Both parties agree to disclose Confidential Information only to its employees who have a "need to know" for the purpose of conducting of the Development Plan under each party

CONFIDENTIAL

respective continuous supervision and control and who are bound by similar confidentiality obligations as contained herein.

Exceptions. Notwithstanding the above, neither party shall have liability to the other with regard to any Confidential Information that:

- (a) was generally known and available to the public domain at the time it was disclosed, or becomes generally known and available to the public domain through no fault of the receiver;
- (b) was known to the receiver at the time of disclosure as shown by the written records in existence at the time of disclosure
- (c) is disclosed with the prior written approval of the disclosing party;
- (d) becomes known to the receiving party from a source other than the disclosing party without breach of this Agreement by the receiving party and in a manner which is otherwise not in violation of the disclosing party's rights; or
- (e) is disclosed by Law or pursuant to the order or requirement of a court's decision, arbitration award, administrative agency, or other governmental or administrative body; provided, that the receiving party shall provide reasonable advance notice to enable the disclosing party to seek a protective order or otherwise prevent or limit such disclosure.

10. Term and Termination. This Agreement shall be effective as of the date of execution of this Agreement and shall terminate 24 months thereafter. This Agreement may be earlier terminated by either party upon a material breach of this agreement by the other party and upon thirty (30) days' written notice. All unused BIOLOGICAL MATERIALS shall be returned to ARCHIVEL or destroyed, at the sole option of ARCHIVEL, within ten (10) days following termination of this Agreement. Termination shall not affect any rights of any party under paragraphs 5 through 10 above.

11. Assignability. The rights and obligations of RECIPIENT under this Agreement shall not be assignable without the prior written consent of ARCHIVEL. ARCHIVEL may assign this Agreement, partially or in its entirety, without the prior written consent of RECIPIENT provided that ARCHIVEL serves notice of the identity of the assignee.

12. No Implied License. No right or license, title or interest is granted to RECIPIENT hereunder by implication, estoppel, or otherwise to any know-how, patent or other industrial or intellectual property right owned or controlled by ARCHIVEL. Except as otherwise stated herein, nothing in the Agreement shall constitute or create an obligation for any party to enter into any subsequent agreement, business arrangement or otherwise. Nothing in this Agreement is intended or shall be deemed, for financial, tax, legal or other purposes, to constitute a partnership, agency, joint venture or employer-employee relationship between the parties.

13. Applicable Law. This Agreement and the rights of the parties shall be governed by and interpreted in accordance with the laws of the Kingdom of Spain in force from time to time. In the event of actual or threatened disclosure or transfer of the BIOLOGICAL MATERIALS by RECIPIENT to a third party without the prior written consent of ARCHIVEL, ARCHIVEL is likely to suffer irreparable harm, and shall be entitled to specific performance of the obligations of RECIPIENT under this Agreement, with or without

CONFIDENTIAL

bond, at the discretion of ARCHIVEL, as well as all necessary injunctive relief against unauthorized disclosure or transfer.

14. Competent Jurisdiction. The Parties agree that any discrepancy in connection with the interpretation, performance, and execution of this Agreement will be subject to the exclusive jurisdiction of the courts of competent jurisdiction located in the city of Barcelona (Spain).

15. Amendments. No modification of this Agreement shall be effective unless the modification is in writing and signed by the authorized representatives of both parties.

IN WITNESS WHEREOF, duly authorized representatives of each party have executed this Agreement as of the date first above written.

ARCHIVEL FARMA, S.L.:

LONDON SCHOOL OF HYGIENE
AND TROPICAL MEDICINE:

Date: 25 February 2015

Date: 19 February 2015



Olga Rué Clarós
CEO

Chris Andrews
Research Operations Manager

LONDON
SCHOOL of
HYGIENE
& TROPICAL
MEDICINE



Date: 19 February 2015

Page 6 of 8

CONFIDENTIAL

ANNEX A

Request for ARCHIVEL BIOLOGICAL MATERIALS

This Request must be completed and signed by an authorized representative of RECIPIENT and will be subject to the express approval in writing of ARCHIVEL.

Biological Material Requested:

RUTI® vaccine developed by ARCHIVEL under good manufacturing practice consisted of fragmented *Mycobacterium tuberculosis* cells (FMtbC) would be requested. The 200µg dose of RUTI® vaccine composed of detoxified and liposomed FMtbC cultured under stress condition would be used. There will be two different formulations tested in the form of an older and a newer batch. In total, 120 vials comprising of 60 vials for each batch would be required. Twenty vials will be administered in each experiment and we aim to conduct the experiment three times.

ARCHIVEL shall have the requested BIOLOGICAL MATERIALS delivered to RECIPIENT no later than 90 days after this Materials Transfer Agreement has been signed at the RECIPIENT's premises located at London School of Hygiene and Tropical Medicine. If there is any delay, ARCHIVEL shall inform the RECIPIENT at least one month in advance. ARCHIVEL shall assume the costs of handling and transportation from ARCHIVEL's premises to the RECIPIENT's premises.

If the BIOLOGICAL MATERIALS have been delivered to RECIPIENT prior to the execution of this Materials Transfer Agreement, the provisions of the Materials Transfer Agreement shall apply retroactively from the actual date of receipt of BIOLOGICAL MATERIALS by RECIPIENT.

ARCHIVEL FARMA, S.L.

LONDON SCHOOL OF HYGIENE
AND TROPICAL MEDICINE

Date: 25 February 2015

Date: 19/02/15

[Redacted Signature]
Olga Rué Clarós
CEO

[Redacted Signature]
Chris Andrews
Research Operations Manager



Date: 19 February 2015

Page 7 of 8

CONFIDENTIAL

ANNEX B

Development Plan

The BIOLOGICAL MATERIALS requested will be used for:

RUTI® vaccine will be tested in a head-to-head comparison with Bacille Calmette-Gue´rin (BCG) vaccine in the proposed study. Using mouse model, four groups of animals each consisted of ten C57BL/6 mice will be used. The mice in two treatment groups will be injected subcutaneously with 200µg RUTI® vaccine twice in three weeks interval (week 0 and week 3). Two different batches of RUTI® will be tested in the two different groups. Mice in another treatment group will be injected with 1×10^6 CFU BCG at week 0 and phosphate buffered saline (PBS) at week 3. Last group of mice acts as control and will be injected with PBS at week 0 and 3. Six week after the commencing of the study, all mice will be sacrificed and splenocytes will be obtained for mycobacterial growth inhibition assay as an endpoint of the study. The experiment will be repeated at least 1 time to confirm initial findings. In the laboratory, samples will be combined with anti-mycobacterial drugs such as isoniazid, rifampicin, pyrazinamide, and ethambutol. The aim of this study is to identify optimum vaccine and drug combinations for the development of therapeutic vaccination strategies in tuberculosis (TB). The obtained result of this study is expected to act as a proof-of-principle in supporting the development of an in-vitro assay as a rapid screening tool for assessing therapeutic TB vaccine candidates. Such tool is currently needed to prioritize which candidate should be tested in a larger clinical trial considering limited study sites and funding.

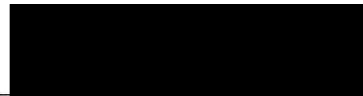
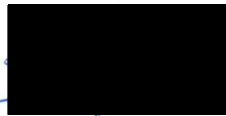
[Clarification Note: this Development Plan will not include the combination of the BIOLOGICAL MATERIAL with RECIPIENT Materials as any such combination in any form will be the subject matter of a separate agreement to be agreed between the parties]

ARCHIVEL FARMA, S.L.

LONDON SCHOOL OF HYGIENE
AND TROPICAL MEDICINE

Date: 28 February 2015

Date: 19/02/15



Olga Rué Clarós
CEO

Chris Andrews
Research Operations Manager



Date: 19 February 2015

Page 8 of 8

APPENDIX 6. Conference papers

I. Keystone Symposia: New Approaches to Vaccines for Human and Veterinary Tropical Diseases, Cape Town, South Africa, 22 – 26 May 2016.

The impact of immunotherapeutic tuberculosis vaccination towards drugs control of mycobacterial growth *ex-vivo*

Satria Arief Prabowo¹, Andrea Zelmer¹, Lisa Stockdale¹, Merce Amat², Pere-Joan Cardona^{2,3}, Helen Fletcher¹

¹ Department of Immunology and Infection, London School of Hygiene & Tropical Medicine, London, United Kingdom

² Archivel Farma SL, Barcelona, Spain

³ Unitat de Tuberculosi Experimental, Health Sciences Research Institute “Germans Trias i Pujol” Foundation (IGTP), Barcelona, Spain

Background: Current effort to effectively control tuberculosis (TB) is hindered by lengthy treatment and the emergence of drug resistance. Combining vaccination with drug therapy will enhance host immune response and improve the effectiveness of current treatment. Identification of optimum regimens is needed. Mycobacterial growth inhibition assay (MGIA) is a functional assay that measures the summative ability of host immune cells to inhibit the growth of mycobacteria *ex-vivo*. Recent evidence suggests that the assay might be a better correlate of protection following vaccination.

Methods: The ability of BCG and RUTI[®], a therapeutic TB vaccine candidate, to enhance drug killing of isoniazid (INH) and rifampicin (RIF) were assessed. Splenocytes of vaccinated mouse (n=6) and PBMC of historically BCG-vaccinated human (n=20) were co-cultured *ex-vivo* for 4 days with drugs and *Mycobacterium bovis* BCG as an immune target.

Results: Vaccination with RUTI[®] in mouse resulted in significant decrease of bacterial load *ex-vivo* in the presence of INH and RIF compared to naïve (p<0.05, 2 log magnitude), with a similar trend with BCG but to a lesser extent. Historical vaccination with BCG in human also exerted enhanced control of drugs killing *ex-vivo* (p<0.05, 0.5-1 log magnitude). *Ex-vivo* control of mycobacterial growth was not correlated with IFN-gamma response in human (p>0.05).

Conclusion: This study provided evidence regarding the benefit of therapeutic TB vaccination in enhancing drug efficacy. *Ex-vivo* MGIA could potentially be applied to identify optimum regimen in early phase clinical trials. Immune mechanisms responsible for enhanced *ex-vivo* growth control warrant further investigation.

II. 47th Union World Conference on Lung Health, International Union Against Tuberculosis and Lung Diseases, Liverpool, United Kingdom, 26-29 October 2016.

The impact of previous BCG vaccination in enhancing the effectiveness of tuberculosis drugs to control mycobacterial growth *ex-vivo*

Satria Arief Prabowo¹, Andrea Zelmer¹, Lisa Stockdale¹, Steven Smith¹, Karin Seifert¹, Helen Fletcher¹

¹ Department of Immunology and Infection, London School of Hygiene & Tropical Medicine, London, United Kingdom

Background: Current effort to effectively control tuberculosis (TB) is hindered by lengthy treatment and the emergence of drug resistance. Combining vaccination with drug therapy will enhance host immune response and improve the effectiveness of current treatment. Bacillus Calmette–Guerin (BCG) remains the only licensed TB vaccine to date. Several pre-clinical animal studies have suggested the benefit of BCG vaccination in adjunct to current treatment. A proof-of-principle study using human samples as well as identification of optimum regimens are needed before such concept can be further advanced. Mycobacterial growth inhibition assay (MGIA) is a functional assay that measures the summative ability of host immune cells to inhibit the growth of mycobacteria *ex-vivo*. There is a recent interest as the assay has been shown to better reflect epidemiological data in distinguishing protection and might be a better correlate of protection following TB vaccination.

Methods: We developed an *ex-vivo* MGIA to assess the ability of isoniazid (INH) and rifampicin (RIF) to inhibit the growth of mycobacteria using peripheral blood mononuclear cell (PBMC) from historically BCG-vaccinated and naïve volunteers (n=20, respectively). PBMCs were co-cultured for 4 days with *Mycobacterium bovis* BCG as an immune target in the presence of drugs.

Results: BCG-vaccinated participants were superiorly capable of inhibiting mycobacterial growth *ex-vivo* compared to the naïve (p< 0.005). The average time since BCG vaccination in this study was 23.8 years. There was a trend towards lesser inhibition of growth in BCG-vaccinated participants originated from regions closer to the equator. BCG vaccination enhanced the ability of INH to control mycobacterial growth at the drug concentrations of 0.01 and 1 ug/ml (p< 0.05). In the presence of RIF, improved drug killing by vaccination was observed at the concentration of 0.01 ug/ml (p< 0.005). *Ex-vivo* control of mycobacterial growth was not correlated with IFN-gamma response measured with ELISpot (p>0.5).

Conclusions: This study provided evidences regarding the benefit of BCG in enhancing drugs effectiveness *ex-vivo*. Immune mechanisms responsible for such enhanced drug killing remains to be elucidated. Implementation of the assay to screen optimum combinations of drugs and TB vaccine candidates in early phase clinical trials worth further consideration.

The author receives a PhD scholarship from the Indonesian Endowment Fund for Education (LPDP).

III. 35th Annual Meeting of European Society for Paediatric Infectious Diseases (ESPID), Madrid, Spain, 23 – 27 May 2017.

The impact of previous BCG vaccination in enhancing the effectiveness of tuberculosis drugs to control mycobacterial growth *ex-vivo*

Satria Arief Prabowo^{1,2}, Andrea Zelmer^{1,2}, Lisa Stockdale^{1,2}, Steven Smith^{1,2}, Karin Seifert¹, Helen Fletcher^{1,2}

¹ Department of Immunology and Infection, London School of Hygiene & Tropical Medicine, London, United Kingdom

² Tuberculosis Centre, London School of Hygiene & Tropical Medicine, London, United Kingdom

Background: Current effort to effectively control tuberculosis (TB) is hindered by lengthy treatment and the emergence of drug resistance. Combining vaccination with drug therapy will enhance host immune responses and improve the effectiveness of current treatment. Several pre-clinical animal studies suggest the benefit of Bacillus Calmette–Guerin (BCG) vaccination in adjunct to treatment. A proof-of-principle study is needed to identify optimum regimens prior to clinical investigation in children and adults.

Methods: We implemented an *ex-vivo* mycobacterial growth inhibition assay (MGIA) to assess the ability of isoniazid (INH) and rifampicin (RIF) in inhibiting the growth of mycobacteria when co-cultured with peripheral blood mononuclear cells (PBMCs). PBMCs were obtained from historically BCG-vaccinated and naïve participants (n=100), and were co-cultured for 4 days with *Mycobacterium bovis* BCG as an immune target.

Results: BCG-vaccinated participants were superiorly capable of inhibiting mycobacterial growth *ex-vivo* compared to the naïve ($p < 0.0001$). BCG-vaccinated females were better abler to control mycobacterial growth than males ($p < 0.05$), which could explain the epidemiological abundance of TB cases in male worldwide. BCG

vaccination enhanced the ability of INH to control mycobacterial growth at the drug concentrations of 0.01 and 1 ug/ml ($p < 0.05$), and RIF at the concentration of 0.01 ug/ml ($p < 0.005$). BCG-induced inhibition of mycobacterial growth was associated with increased IFN- γ and IP-10 production in the presence of drugs ($p < 0.05$), with correlations observed towards the increase of TNF- α and GM-CSF and the reduction of IL-10 in the absence of drugs ($p < 0.05$).

Conclusions: This study provided preliminary evidences regarding the benefit of BCG in enhancing TB drug effectiveness *ex-vivo*. Clinical studies are warranted in children and adults to further elucidate the benefit of BCG in adjunct to TB treatment.

IV. Cell-Weizmann Institute of Science Symposium: Next Generation Immunology, Rehovot, Israel, 11 – 14 February 2018.

Historical BCG vaccination combined with drug treatment enhances inhibition of mycobacterial growth *ex vivo* in human peripheral blood cells

Satria Arief Prabowo^{1,2}, Andrea Zelmer^{1,2}, Lisa Stockdale^{1,2}, Steven Smith^{1,2}, Karin Seifert¹, Helen Fletcher^{1,2}

¹ Department of Immunology and Infection, London School of Hygiene & Tropical Medicine, London, United Kingdom

² Tuberculosis Centre, London School of Hygiene & Tropical Medicine, London, United Kingdom

Current effort to effectively control tuberculosis (TB) is hindered by lengthy treatment. Combining vaccination with drug therapy will enhance host immune responses and improve the effectiveness of current treatment. Mycobacterial growth inhibition assay (MGIA) is a functional assay which measures the summative ability of host immune cells to inhibit the growth of mycobacteria *ex-vivo*. The impact of historical Bacille Calmette-Guerin (BCG) vaccination towards the *ex-vivo* drugs killing of isoniazid (INH) and rifampicin (RIF) were assessed (n=100). BCG vaccination enhanced the ability of INH and RIF to control mycobacterial growth ($p < 0.05$). BCG-induced inhibition of mycobacterial growth was associated with increased IFN- γ and IP-10 production in the presence of drugs ($p < 0.05$). This study provides evidence regarding the benefit of BCG vaccination in enhancing effectiveness of TB drugs *ex-vivo*. Implementation of the MGIA assay to screen optimum combinations of drugs and TB vaccine candidates in early phase clinical trials worth further consideration.

V. 5th Global Forum on Tuberculosis Vaccines, New Delhi, India, 20 – 23 February 2018.

Historical BCG vaccination combined with drug treatment enhances inhibition of mycobacterial growth *ex vivo* in human peripheral blood cells

Satria Arief Prabowo^{1,2}, Andrea Zelmer^{1,2}, Lisa Stockdale^{1,2}, Steven Smith^{1,2}, Karin Seifert¹, Helen Fletcher^{1,2}

¹ Department of Immunology and Infection, London School of Hygiene & Tropical Medicine, London, United Kingdom

² Tuberculosis Centre, London School of Hygiene & Tropical Medicine, London, United Kingdom

Background: Current effort to effectively control tuberculosis (TB) is hindered by lengthy treatment and the emergence of drug resistance. Combining vaccination with drug therapy will enhance host immune responses and improve the effectiveness of current treatment. Several pre-clinical animal studies suggest the benefit of Bacillus Calmette–Guérin (BCG) vaccination in adjunct to treatment. A proof-of-principle study is needed to identify optimum regimens. Mycobacterial growth inhibition assay (MGIA) is a functional assay that measures the summative ability of host immune cells to inhibit the growth of mycobacteria *ex-vivo*.

Methods: We implemented an *ex-vivo* MGIA to assess the ability of isoniazid (INH) and rifampicin (RIF) to inhibit the growth of mycobacteria using peripheral blood mononuclear cell (PBMC) from historically BCG-vaccinated and naïve volunteers (n=100). The average time since BCG vaccination was 23.8 years. PBMCs were co-cultured for 4 days with *Mycobacterium bovis* BCG as an immune target.

Results: BCG-vaccinated participants were superiorly capable of inhibiting mycobacterial growth *ex-vivo* compared to the naïve (p< 0.0001). BCG-vaccinated females were better able to control mycobacterial growth than males (p< 0.05). BCG vaccination enhanced the ability of INH to control mycobacterial growth at the drug concentrations of 0.01 and 1 ug/ml (p< 0.05), and RIF at the concentration of 0.01 ug/ml (p< 0.005). BCG-induced inhibition of mycobacterial growth was associated with increased IFN- γ and IP-10 production in the presence of drugs (p< 0.05).

Discussion and Conclusion: This study provides evidence regarding the benefit of BCG vaccination in enhancing effectiveness of TB drugs *ex-vivo*. Clinical studies might be warranted to further elucidate the benefit of BCG in adjunct to treatment. Implementation of the MGIA assay to screen optimum combinations of drugs and TB vaccine candidates in early phase clinical trials worth further consideration.

Key words: growth inhibition, BCG, therapeutic vaccine, MGIA

Conflict of interest: none

VI. 62nd Acid Fast Club Summer Meeting, Jenner Institute, University of Oxford, Oxford, United Kingdom, 5 – 6 July 2018.

Historical BCG vaccination combined with drug treatment enhances inhibition of mycobacterial growth *ex vivo* in human peripheral blood cells

Satria Arief Prabowo^{1,2}, Andrea Zelmer^{1,2}, Lisa Stockdale^{1,2}, Steven Smith^{1,2}, Karin Seifert¹, Helen Fletcher^{1,2}

¹ Department of Immunology and Infection, London School of Hygiene & Tropical Medicine, London, United Kingdom

² Tuberculosis Centre, London School of Hygiene & Tropical Medicine, London, United Kingdom

Vaccination and chemotherapy remain the main strategies to control tuberculosis (TB), while combination of both could provide a greater therapeutic value. We implemented an *ex vivo* mycobacterial growth inhibition assay (MGIA) to measure vaccine-induced inhibition following historical BCG vaccination in human volunteers towards the drug effect of isoniazid (INH) and rifampicin (RIF). BCG vaccination enhanced the ability of INH to control mycobacterial growth *ex vivo* by increased IFN- γ and IP-10 production. A higher frequency of IFN- γ ⁺ and TNF- α ⁺ CD3⁻ CD4⁻ CD8⁻ cells was observed, suggesting the role of Natural Killer (NK) cells. Our *ex vivo* data are consistent and support findings from previous observational and animal studies.



Glibenclamide Reduces Primary Human Monocyte Functions Against Tuberculosis Infection by Enhancing M2 Polarization

Chidchamai Kewcharoenwong^{1,2}, Satria A. Prabowo^{3,4}, Gregory J. Bancroft^{3,4}, Helen A. Fletcher^{3,4*} and Ganjana Lertmemongkolchai^{1,2*}

¹ Mekong Health Science Research Institute, Khon Kaen, Thailand, ² Faculty of Associated Medical Sciences, The Centre for Research and Development of Medical Diagnostic Laboratories, Khon Kaen University, Khon Kaen, Thailand, ³ Department of Immunology and Infection, Faculty of Infectious and Tropical Diseases, London School of Hygiene and Tropical Medicine, London, United Kingdom, ⁴ Tuberculosis Centre, London School of Hygiene and Tropical Medicine, London, United Kingdom

OPEN ACCESS

Edited by:

Uday Kishore,
Brunel University London,
United Kingdom

Reviewed by:

Anthony George Tsolaki,
Brunel University London,
United Kingdom
Paola Italiani,
Consiglio Nazionale Delle Ricerche
(CNR), Italy

*Correspondence:

Helen A. Fletcher
Helen.Fletcher@lshtm.ac.uk
Ganjana Lertmemongkolchai
ganja_le@kku.ac.th

Specialty section:

This article was submitted to
Molecular Innate Immunity,
a section of the journal
Frontiers in Immunology

Received: 11 May 2018

Accepted: 28 August 2018

Published: 19 September 2018

Citation:

Kewcharoenwong C, Prabowo SA,
Bancroft GJ, Fletcher HA and
Lertmemongkolchai G (2018)
Glibenclamide Reduces Primary
Human Monocyte Functions Against
Tuberculosis Infection by Enhancing
M2 Polarization.
Front. Immunol. 9:2109.
doi: 10.3389/fimmu.2018.02109

Tuberculosis (TB) is a global public health problem, which is caused by *Mycobacterium tuberculosis* (Mtb). Type 2 diabetes mellitus (T2DM) is one of the leading predisposing factors for development of TB after HIV/AIDS. Glibenclamide is a widely used anti-diabetic drug in low and middle-income countries where the incidence of TB is very high. In a human macrophage cell line, glibenclamide, a K⁺ATP-channel blocker, promoted alternative activation of macrophages by enhancing expression of the M2 marker CD206 during M2 polarization. M2 macrophages are considered poorly microbicidal and associated with TB susceptibility. Here, we investigated the effect of glibenclamide on M1 and M2 phenotypes of primary human monocytes and further determined whether specific drug treatment for T2DM individuals influences the antibacterial function of monocytes in response to mycobacterial infection. We found that glibenclamide significantly reduced M1 (HLA-DR⁺ and CD86⁺) surface markers and TNF- α production on primary human monocytes against mycobacterial infection. In contrast, M2 (CD163⁺ and CD206⁺) surface markers and IL-10 production were enhanced by pretreatment with glibenclamide. Additionally, reduction of bactericidal activity also occurred when primary human monocytes from T2DM individuals who were being treated with glibenclamide were infected with Mtb *in vitro*, consistent with the cytokine responses. We conclude that glibenclamide reduces M1 and promotes M2 polarization leading to impaired bactericidal ability of primary human monocytes of T2DM individuals in response to Mtb and may lead to increased susceptibility of T2DM individuals to TB and other bacterial infectious diseases.

Keywords: glibenclamide, *Mycobacterium tuberculosis*, monocyte, diabetes mellitus, M2 polarization, anti-diabetic drug

INTRODUCTION

Tuberculosis (TB) is a global public health problem, which is the leading cause of death due to a single infectious agent, *Mycobacterium tuberculosis* (Mtb). In 2016, TB resulted in 1.3 million deaths and 6.3 million new cases, and it is estimated that about one-quarter of the human population is latently infected (1, 2). In many tropical countries, such as Thailand, TB is an

important cause of death and primarily a disease of the lung, which serves as a port of entry and a site of disease manifestation. Type 2 diabetes mellitus (T2DM) is an important risk factor for development of TB (3). A global overview focusing specifically on Asian countries with a high TB-DM burden indicates a TB prevalence 1.8–9.5 times higher among DM patients when compared to the general population (4). The predictive factors for TB among those with DM are HIV co-infection, age (older than 45), overweight, poor glycemic control, and being male (5, 6). However, these underlying immunological mechanisms are still poorly understood. Given the lack of an effective vaccine to protect adults against TB in the tropics, the problems of antibiotic resistance and the predictions that the global burden of T2DM could reach almost 600 million people in the next 20 years (7), understanding the mechanisms by which diabetes predisposes to this infection is essential. Glibenclamide rINN (glyburide USAN, sulfonylurea group) is a widely commonly used anti-diabetic drug in low and middle-income countries where the incidence of TB is high (1). The drug acts by binding to and inhibiting the ATP-sensitive potassium channel (K_{ATP}) inhibitory regulatory subunit sulfonylurea receptor 1 (SUR1) in pancreatic beta cells, then increases the plasma insulin concentrations (8). This drug lowers blood glucose concentrations by about 20% and HbA1c by 1–2% (9). However, glibenclamide has side effects such as hypoglycemia and reduced immune functions through inhibition of inflammasome (8) and ATP binding cassette transporter (10). Our previous study showed that glibenclamide has potent and wide-ranging effects on cell-mediated immune responses including reduced neutrophil pro-inflammatory cytokine production, migration, and killing in response to another intracellular bacteria, *Burkholderia pseudomallei* (11, 12).

Monocytes and macrophages are the primary target of *Mtb*, and their innate capacity to control *Mtb* defines the early progression of the infection (13). In peripheral blood, monocyte numbers expand during active TB disease (14). *In vitro* study on diabetic cells found reduced level of *Mtb* phagocytosis possibly due to alteration in diabetic monocytes and complement system (15). Monocytes can differentiate into M1 or M2 macrophages with pro- or anti-inflammatory functional phenotypes, respectively (16). An M1 phenotype is associated with the up-regulation of MHC-II molecules (such as HLA-DR) (17) and a co-stimulatory receptor, CD86 and the ability to produce pro-inflammatory cytokines such as TNF- α and IL-1 β (16, 18, 19). Alternatively, the M2 phenotype can be characterized by the upregulation of the scavenger receptors, CD163 and the mannose receptor, CD206, as well as the ability to release anti-inflammatory cytokines, such as IL-10 (16, 20). Generally, M1 macrophages are considered part of the common host response against intracellular bacteria and involved in killing of mycobacteria, while M2 macrophages are associated with tissue repair and bacterial persistence (13, 21). The polarization state of monocytes is likely important for maintenance of a balanced inflammatory response in TB disease. In a human macrophage cell line, glibenclamide promoted alternative activation of macrophages by enhancing the expression of the M2 marker CD206 during M2 polarization (22). However, to date, there is

no information as to how glibenclamide affects primary human monocyte phenotype and function in response to mycobacterial infection. Here, we demonstrated the effect of glibenclamide on M1 and M2 phenotypes of primary human monocytes against BCG and *Mtb in vitro* and also investigated whether drug treatment for T2DM individuals influences cytokine production and killing activity by monocytes in response to mycobacterial infection. We conclude that glibenclamide reduces M1 markers and enhances M2 markers on primary human monocytes, which leads to reduced killing activity against *Mtb*. Our findings suggest that treatment with glibenclamide impairs the anti-bacterial defense functions of human monocytes in DM individuals.

MATERIALS AND METHODS

Participants

We collected whole blood from 10 healthy individuals at LSHTM, UK and 41 diabetic, and 15 healthy control Thai individuals enrolled at Yang Lum Health Promoting Hospital, Ubon Ratchathani, Thailand. All individuals had no signs of acute infectious disease in the 3 months prior to enrollment. We classified diabetic individuals according to drug treatment, divided into three groups: (1) glibenclamide alone or both glibenclamide and metformin, (2) glipizide alone, and (3) metformin alone. Diabetic individuals from each group exhibited impaired glycemic control based on HbA1c levels (>6.5%). Exclusion criteria for both healthy and diabetic volunteers included impaired renal function, defined by a serum creatinine level of ≥ 2.2 mg/dl.

Ethics Statement

This study was carried out in accordance with the recommendations of UK and Thailand guidelines for human research and the protocol was approved by LSHTM Research Ethics Committee and Nakhon Phanom Hospital Ethical Review Committee for Human Research. All subjects gave written informed consent in accordance with the Declaration of Helsinki.

Microorganisms

Stocks of *Mtb* H37Rv or *Mycobacterium bovis* Bacille Calmette-Guerin (BCG) Pasteur-Aeras were cultured in 7H9-OADC-Tween-Glycerol for 14 days. Bacterial growth was assessed by measuring the optical density at 600 nm and the number of viable bacteria (colony-forming units) in inocula determined by retrospective plating of serial ten-fold dilutions on 7H11 agar, and then frozen at -80°C . Live *Mtb* was handled under Advisory Committee on Dangerous Pathogens (UK) bio-containment level 3 conditions at LSHTM and Khon Kaen University.

Monocyte Isolation

We isolated human peripheral blood mononuclear cells (PBMCs) from heparinized venous blood by Ficoll-Paque centrifugation. PBMC suspensions at 10^7 cells/ml were plated 300 μl in each

respective well of a 48-well plate and incubated for 2 h. The non-adherent cells were removed by repeated pipetting and washed with 10% FBS in RPMI 1640 culture medium for three times. Fresh medium was added to the adherent cells. The resulting cell preparation was confirmed to consist of >95% monocytes by Giemsa staining and microscopy.

Monocyte Stimulation and Cytokine Measurement

Unless stated otherwise, purified monocytes at a concentration 2.5×10^5 cells/ml in RPMI 1640 culture medium were pretreated with 50 μ M glibenclamide (Sigma) [comparable to the peak human plasma concentration achieved following a 20 mg oral dose (23)] for 30 min and then infected with live Mtb or BCG at 10^2 or 10^5 CFU per well or activated with 10 μ g/ml of LPS (from *Escherichia coli*, Sigma) at 37°C for 96 h. The supernatants were stored at -80°C until cytokines were measured. TNF- α , IL-10, and IL-6 concentrations were tested in duplicate by ELISA (Invitrogen and BD Biosciences) according to the manufacturer's instructions. IL-1 β concentration was measured using Quantikine HS ELISA (R and D system). IL-8, MCP-1, RANTES, IP-10, and MIG were determined using a cytometric bead array multiplex assay (CBA) in accordance with the manufacturer's instructions (BD Biosciences). All cytokine data in response to Mtb, BCG, or LPS were subtracted from the medium control of each sample.

Cell Surface Marker Staining

Following incubations, the plate was incubated in 4°C for 30 min and rubbed gently by pipette. Then, suspended monocytes were collected and transferred to FACS tubes. Then, cells were centrifuged and washed with 1 ml FACS buffer. Pelleted cells were surface stained with anti-CD14-BV421, anti-CD16-BV510, anti-CD86-PE-Cy7, anti-HLA-DR-PE, anti-CD206-APC, and anti-CD163-BV605 (BioLegend) for 30 min at 4°C. After washing with FACS buffer, cells were fixed by 4% paraformaldehyde (Sigma, UK) for 10 min at 4°C and then washed by FACS buffer. Finally, cells were resuspended in 250 μ l FACS buffer and kept in 4°C until analysis. Data was acquired using an LSRII flow cytometer (BD Biosciences) configured with three lasers and 10 detectors and FACSDiva acquisition software (BD Biosciences). Compensation was performed using tubes of CompBeads (BD Biosciences) individually stained with each fluorophore and compensation matrices were calculated with Flowjo version 10 (TreeStar Inc., Ashland, OR, USA).

In vitro Mycobacterial Growth Inhibition Assay (MGIA)

Purified monocytes were pretreated with or without glibenclamide for 30 min as described and then infected with live Mtb or live BCG at 10^2 CFU for 96 h with glibenclamide in the condition. Following incubations, cells and remaining Mtb or BCG were pelleted and cells were lysed by incubation in sterile water with vortexing three times in between. Mtb or BCG from each individual tube were then transferred into a corresponding MGIT tube and time to positivity was determined using a MGIT 960 (Becton Dickinson). Direct-to-MGIT controls were used

for the calculation of relative growth. All mycobacteria growth inhibition assays were carried out in duplicate. For each tube, time to positivity in hours was converted to log CFU of bacteria using a previously determined standard curve for the stock of Mtb or BCG used (24).

Statistics

Statistical analysis (One way ANOVA and paired t-test) was performed by using Graphpad PRISM statistical software (Graphpad). P-values ≤ 0.05 were considered significant. The statistical power of the study was calculated by *post-hoc* power analysis for all experiments measuring cytokine production in diabetic individuals and there we have >80% power with 95% confidence to detect differences between groups.

RESULTS

Glibenclamide Reduces M1 While Enhancing M2 Surface Marker Expression on Primary Human Monocytes

Because the peripheral lipid portion of the cell wall is very similar between BCG and Mtb (25), it is predicted that their ability to infect peripheral monocytes or macrophages is similar. Firstly, to determine the effect of glibenclamide on M1 and M2 marker expression, purified primary monocytes from healthy control individuals were pretreated with the drug at doses comparable to the range of glibenclamide given during oral therapy to human patients (26, 27), prior to infection with BCG. In this study, we refer only to two major subsets, terming classical monocytes simply as CD14⁺CD16⁻, and non-classical as CD14⁺CD16⁺ (28). Cultured monocytes were analyzed with M1 (HLA-DR⁺ and CD86⁺) and M2 (CD163⁺ and CD206⁺) surface markers on CD14⁺CD16⁻ and CD14⁺CD16⁺, respectively (Figure 1A and Figure S1). Here, we found that glibenclamide significantly reduced M1 surface markers on CD14⁺CD16⁻ and enhanced M2 surface markers on CD14⁺CD16⁺ with or without BCG infection (Figure 1), regardless of the concentration of BCG (Figure S2). M2 surface markers were not detected on CD14⁺CD16⁻ and no difference was found with glibenclamide-pretreatment of M2 and M1 surface markers on CD14⁺CD16⁻ and CD14⁺CD16⁺ monocytes, respectively (Figure S3). To determine whether glibenclamide alters M1 and M2 surface markers in an M2 macrophage polarization model, we activated primary human monocytes with IL-4 to obtain M2 phenotype cells in the presence or absence of glibenclamide (Figure S4). With glibenclamide, M1 surface markers of CD14⁺CD16⁻ cells were significantly reduced, while an upward trend was observed in the expression of M2 surface markers (Figure S4B). Glibenclamide also clearly enhanced M2 surface marker expression (CD206) in CD14⁺CD16⁻ cells during M2 polarization (Figure S4A), consistent with the published data on human macrophage cell lines (22). We also performed an M1 macrophage polarization model, but no significant difference was found (data not shown). Nevertheless, we provide evidence that glibenclamide reduces M1

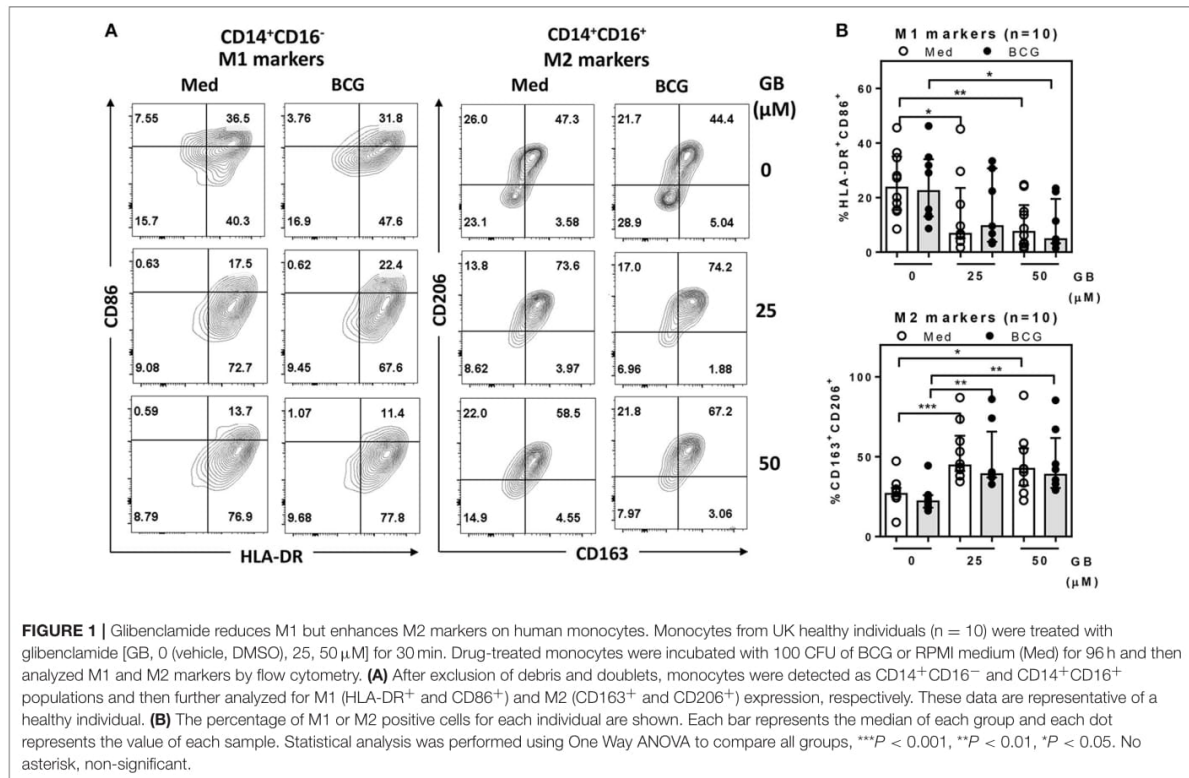


FIGURE 1 | Glibenclamide reduces M1 but enhances M2 markers on human monocytes. Monocytes from UK healthy individuals ($n = 10$) were treated with glibenclamide [GB, 0 (vehicle, DMSO), 25, 50 μM] for 30 min. Drug-treated monocytes were incubated with 100 CFU of BCG or RPMI medium (Med) for 96 h and then analyzed M1 and M2 markers by flow cytometry. **(A)** After exclusion of debris and doublets, monocytes were detected as $\text{CD14}^+\text{CD16}^-$ and $\text{CD14}^+\text{CD16}^+$ populations and then further analyzed for M1 (HLA-DR^+ and CD86^+) and M2 (CD163^+ and CD206^+) expression, respectively. These data are representative of a healthy individual. **(B)** The percentage of M1 or M2 positive cells for each individual are shown. Each bar represents the median of each group and each dot represents the value of each sample. Statistical analysis was performed using One Way ANOVA to compare all groups, $***P < 0.001$, $**P < 0.01$, $*P < 0.05$. No asterisk, non-significant.

and increases M2 surface marker expression on primary human monocytes.

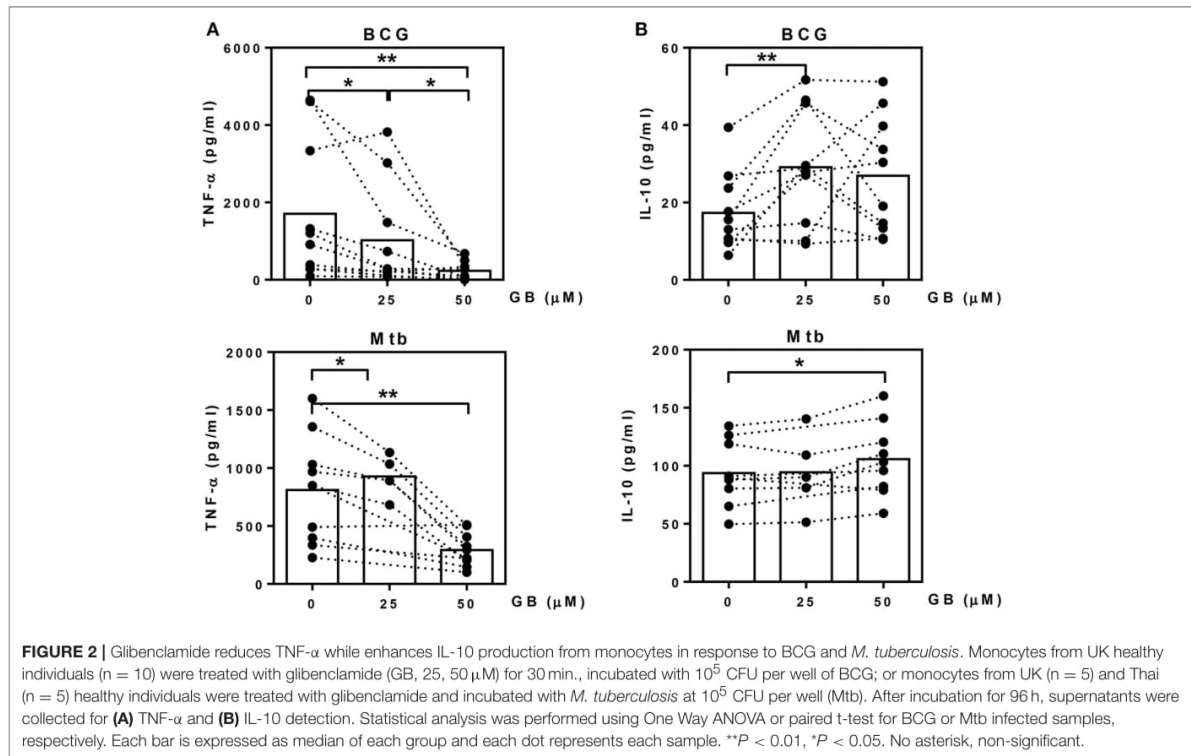
Glibenclamide Reduces $\text{TNF-}\alpha$ While Enhancing IL-10 Production From Primary Human Monocytes in Response to BCG and *M. tuberculosis*

We next evaluated whether glibenclamide alters the ability of primary human monocytes to release pro- and anti-inflammatory cytokines in response to BCG and *Mtb* infection by detecting $\text{TNF-}\alpha$ (M1 phenotype) and IL-10 (M2 phenotype), respectively. Purified primary monocytes from healthy individuals were pretreated with glibenclamide, infected with BCG or *Mtb* for 96 h and cytokine concentrations measured in supernatants. Consistent with its impact on macrophage polarization, glibenclamide significantly reduced $\text{TNF-}\alpha$ in a concentration-dependent manner (Figure 2A). Secretion of IL-1 β was significantly reduced when cells were pretreated with glibenclamide (Figure S5). In contrast, glibenclamide significantly enhanced IL-10 production in response to both BCG and *Mtb* from the same cell cultures (Figure 2B). Together, we conclude that glibenclamide reduces the expression of cytokines associated with M1 phenotype and enhances expression of M2 associated cytokines in

primary human monocytes in response to mycobacterial infection.

Broad Cytokine Production in Response to *M. tuberculosis* Is Associated With the Choice of Drug Treatment in Individuals With Diabetes Mellitus

Currently, not only glibenclamide and metformin but glipizide, a partial potassium channel blocker, is also one of the main drugs being used to control blood glucose levels in TB endemic areas (29). To investigate whether different drugs involved in the management of T2DM, vary in their effects on innate immune function, we compared the broad cytokine production including $\text{TNF-}\alpha$, IL-10, IL-8, IL-6, MCP-1, RANTES, IP-10, and MIG of monocytes purified from T2DM individuals under different drug regimens (see Table 1 for characteristic of individuals). These T2DM individuals had similar levels of BMI, fasting blood glucose and markers of glycemic control (HbA1c), regardless of anti-diabetic drug treatment used (Table 1). We found that T2DM individuals who were being treated with glibenclamide had significantly lower $\text{TNF-}\alpha$ and IL-8 but increased IL-6 when compared to monocytes from healthy control groups in response to *Mtb* infection (Figure 3A). A similar effect of glibenclamide was observed upon LPS stimulation of cells, with lower levels of $\text{TNF-}\alpha$ produced from glibenclamide treated cells (Figure 3B).



However, we only observed a trend toward increased IL-10 from monocytes from T2DM individuals who were being treated with glibenclamide against Mtb infection with or without LPS activation (Figures 3A,B). Moreover, T2DM individuals who were being treated with metformin had significantly reduced IL-8, IL-6, MCP-1, and RANTES in the presence of Mtb (Figure 3A) and reduced TNF- α and IL-6 in response to LPS (Figure 3B). IP-10 and MIG levels were lower than the limit of detection in this experiment. Our data suggests that in T2DM individuals, glibenclamide reduces an M1 phenotype, especially TNF- α and IL-8 production in primary human monocytes in response to Mtb and LPS. Moreover, metformin reduces IL-6 and chemokines which are involved with macrophage polarization.

Glibenclamide Treatment Impairs Killing of *M. tuberculosis* by Primary Human Monocytes

Our previous data suggested that glibenclamide promotes an M2 phenotype in T2DM individuals. Moreover, in other studies, the shift of polarization toward M2 is associated with poor microbicidal activity and parallels with TB susceptibility (21). We further investigated the effect of glibenclamide on the killing function of primary human monocytes using a mycobacterial growth inhibition assay (MGIA) (24). Bacterial growth, which was measured after culture with primary monocytes for

TABLE 1 | General characteristics of diabetic and healthy control individuals.

Individual groups	Diabetic ($n = 41$)			
	Healthy	Glibenclamide ^c	Glipizide	Metformin
Total ($n = 56$)	15	12	13	16
Sex (female: male)	13:2	5:7	8:5	11:5
Average age (year) ^a	47 \pm 7	59 \pm 9 ^b	64 \pm 10 ^b	61 \pm 10 ^b
BMI (kg/m^2) ^a	24.5 \pm 3.1	24.5 \pm 2.6 ^b	24.6 \pm 2.4 ^b	24.4 \pm 2.6 ^b
Fasting blood sugar ($\text{mg}\%$) ^a	ND	169.9 \pm 52.4 ^b	141.7 \pm 27.2 ^b	145.0 \pm 37.2 ^b
HbA1c ($\%$) ^a	5.3 \pm 0.4	8.4 \pm 2.3 ^b	7.8 \pm 1.9 ^b	7.5 \pm 2.1 ^b

ND, not determined.

^a The values are means \pm SD.

^b No statistically significant differences ($P \geq 0.05$) compared across all diabetic individuals using One Way ANOVA.

^c Glibenclamide alone, $n = 6$ and combination with metformin, $n = 6$.

96 h, showed that glibenclamide significantly reduced the ability of monocytes to eliminate Mtb and also BCG in a concentration-dependent manner (Figure 4A). Furthermore, to examine whether specific drug treatment for T2DM individuals influenced the antimicrobial functions of monocytes, purified monocytes from either healthy or T2DM individuals (see Table 1 for details of individuals) were exposed to Mtb and

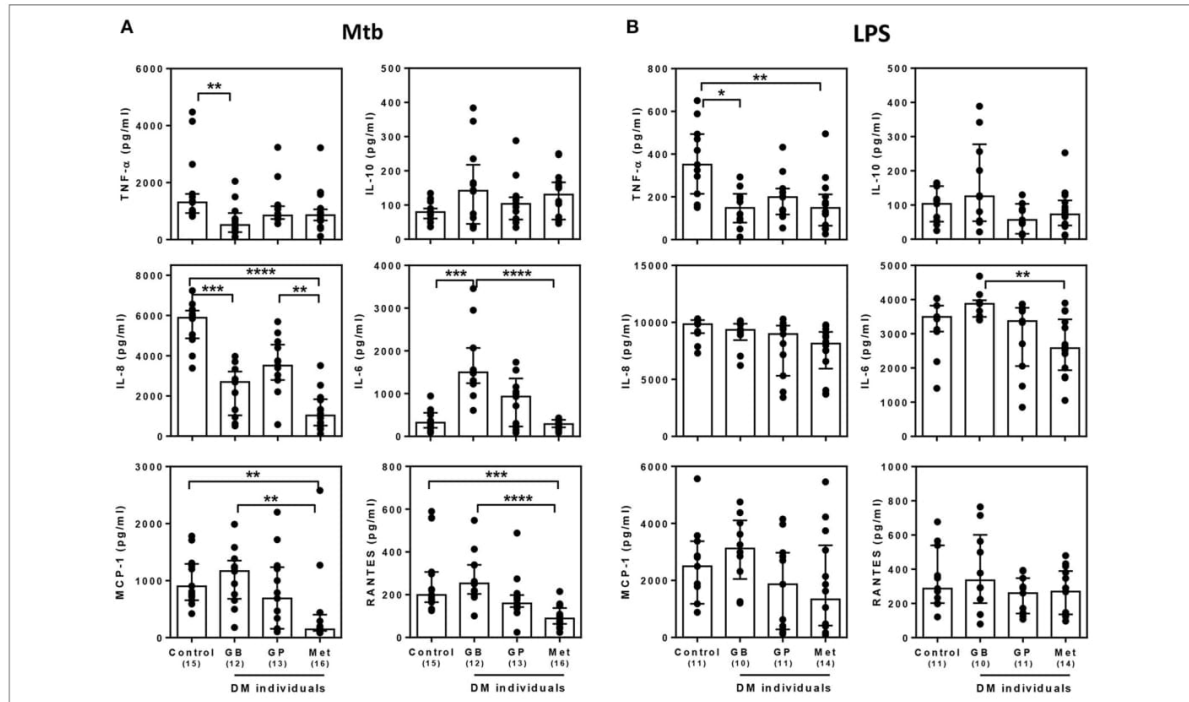


FIGURE 3 | Effect of different DM treatment regimens on broad cytokine production in response to *M. tuberculosis*. Four Thai groups are shown including healthy controls and diabetic individuals who have been treated with glibenclamide (GB), glipizide (GP), or metformin (Met). Purified monocytes from each group were infected with **(A)** *M. tuberculosis* at 10^5 CFU per well (Mtb) or stimulated with **(B)** $10 \mu\text{g/ml}$ of *E. coli* LPS. Due to limited blood volume, some samples were not stimulated with LPS. After incubated at 96 h, supernatants were collected and kept in -80°C prior to cytokine detection. TNF- α , IL-10, and IL-6 were detected by ELISA and IL-8, MCP-1 and RANTES were detected by CBA. Each bar is expressed as median with interquartile range of each group and each dot represents each sample. The number of individuals tested are shown in parentheses. Asterisks indicate significant differences between all individual groups by One Way ANOVA. **** $P < 0.0001$, *** $P < 0.001$, ** $P < 0.01$, * $P < 0.05$. No asterisk, non-significant.

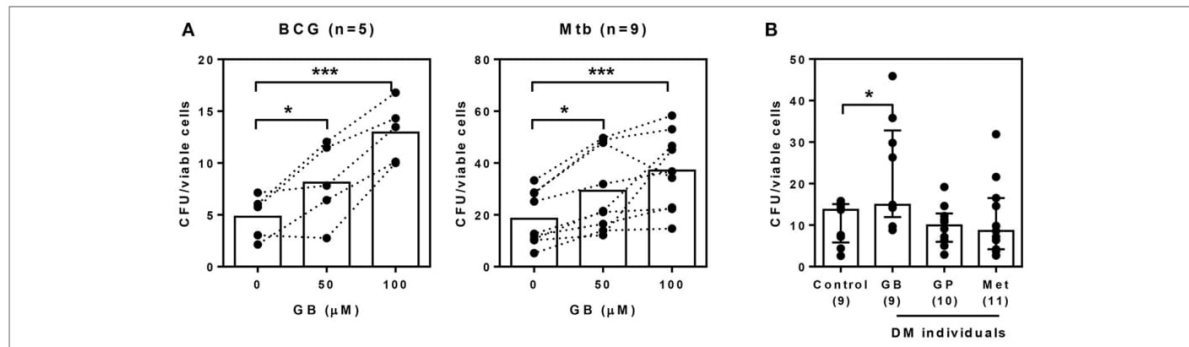


FIGURE 4 | Glibenclamide treatment impairs killing of *M. tuberculosis* by monocytes. **(A)** Monocytes from UK healthy individuals were treated with glibenclamide (GB, 50, 100 μM) for 30 min. Drug-treated monocytes were incubated with 10^2 CFU per well of *M. tuberculosis* (Mtb, $n = 9$) or BCG ($n = 5$) for 96 h and then the total bacteria were collected for MGIA. **(B)** Purified monocytes from four Thai individual groups shown as healthy control ($n = 9$) and diabetic individuals who have been treated with glibenclamide (GB, $n = 9$), glipizide (GP, $n = 10$), or metformin (Met, $n = 11$) were infected with 10^2 CFU of *M. tuberculosis* for 96 h and total bacteria were determined by MGIA. Statistical analysis was performed using One Way ANOVA to compare between control and other groups. Data are expressed as median with interquartile range. *** $P < 0.001$, * $P < 0.05$. No asterisk, non-significant.

the bacterial growth was assessed by MGIA. Monocytes of T2DM individuals who were being treated with glibenclamide had impaired killing activity compared to monocytes from healthy controls as well as other anti-diabetic drug treatment groups (Figure 4B). These data implied that glibenclamide impairs the antimycobacterial function of primary human monocytes.

DISCUSSION

Individuals with T2DM have an increased risk of developing infections and sepsis (30, 31). Previous studies show that phagocyte function is compromised (32) and that antioxidant systems and adaptive immunity may be depressed in individuals with T2DM (31). Many conditions are strongly associated with T2DM, including malignant otitis externa, emphysematous pyelonephritis, emphysematous cholecystitis, *Klebsiella* liver abscesses, rhinocerebral mucormycosis (33), urinary tract infection by *E. coli* (34), salmonellosis (35), TB (3), and melioidosis (36). Our previous studies show that not only T2DM physiology itself, but also anti-diabetic drug treatment reduced neutrophil functions of diabetic individuals in response to *B. pseudomallei* infection, which caused melioidosis (11, 12). These *Mtb* and *B. pseudomallei* infections share many features including the importance of cell mediated immunity for immune defense, generation of granulomatous pathology in infected tissues, prolonged periods of clinical latency, an interferon dominant host transcriptional profile and difficulty in generating sterilizing immunity (36–38). This is of particular relevance to increased risk of TB in individuals with T2DM, yet the understanding of the immunological changes, which underlie this susceptibility are still not defined.

In this study, we focus on the possible impact of anti-diabetic drugs on monocytes from diabetic individuals against mycobacterial infection as monocytes are key mediators of *Mtb* infection and resistance (13). Many studies indicate that human monocytes subsets respond differentially to *Mtb* infection (39–43). $CD14^+CD16^+$ monocytes have recently been shown to support *Mtb* replication as and there is a correlation between the abundance of $CD14^+CD16^+$ cells and the progression of TB disease (13, 39, 40). Although, binding and ingestion of microorganisms during non-opsonic phagocytosis had been reported through the mannose receptor, CD206 (43), our data showed that glibenclamide enhances CD206 (M2 marker) on $CD14^+CD16^+$ monocytes and this was associated with a reduction in mycobacterial killing. At the transcriptome level, M2 macrophages displayed a diminished inflammatory response to *Mtb* as reflected by reduced nitric oxide (NO) production and increased iron availability, suggesting these monocytes offer a permissible intracellular environment for bacterial replication (44). Moreover, our data also showed that glibenclamide reduced MHC-II molecules, HLA-DR, and a co-stimulatory receptor, CD86 which are involved in antigen presentation and T cell co-stimulation (21), implying that monocytes treated with glibenclamide are less efficient in

triggering T cell responses compared to non-treated monocytes. These data are consistent with a study in HIV negative TB patients with T2DM in Tanzania. They found that hyperglycemia was inversely correlated with live BCG-specific $CD4^+$ T cell responses in patients with latent or active TB and that half of these diabetic patients were prescribed with glibenclamide alone in combination with other anti-diabetic drugs (45). On the other hand, the novel monosubstituted sulfonylureas could inhibit *Mtb* replication of both H37Rv and extensively drug-resistant strains in lungs of mice through targeting acetoacetyl synthase (46). This latter study suggests that modified sulfonylureas may be effective as potential drug candidates against TB.

Since our previous data in human neutrophils from diabetic individuals who have been treated with glibenclamide alone and in combination with metformin showed a similar cytokine pattern against *B. pseudomallei* infection (11), and the majority of diabetic individuals who have been treated with sulfonylureas are also treated with metformin [as recommended by the American Diabetes Association's (47)], data from those diabetic individuals treated with glibenclamide alone or in combination were combined for immune analysis, unless stated otherwise. $TNF-\alpha$ is a major cytokine of the M1 pathway (14) and depletion of $TNF-\alpha$ causes a relative increase in M2 gene expression, thereby favoring the M2 pathway (exemplified by the presence of IL-14 or IL-13) (48, 49). In an *Mtb* infection model, $TNF-\alpha$ depletion resulted in increased susceptibility, with mice succumbing to infection within 2–3 weeks, while harboring a high bacterial burden (50). Also, chemokines such as IL-8 (CXCL8), MCP-1 (CCL2), and RANTES (CCL5) are produced at high levels in M1 macrophages (51). In this study, we not only observed a reduction of $TNF-\alpha$ but also IL-8 production from monocytes of T2DM individuals who were being treated with glibenclamide. Surprisingly, we also found that IL-6 was significantly enhanced in monocytes of the glibenclamide treatment group. IL-6 exerts a pro-inflammatory (52) or an anti-inflammatory (53) effect dependent on the local immune microenvironment. IL-6 can induce M2 macrophage differentiation through STAT3 activation and can enhance infiltration of $CD163^+CD206^+$ macrophages in gastric tumor tissue (54). Moreover, IL-6 production by *Mtb*-infected macrophages inhibited uninfected macrophage responses to $IFN-\gamma$ (55). These previous reports support our data significantly showing that T2DM individuals who were being treated with glibenclamide have reduced $TNF-\alpha$ and IL-8 while it enhances IL-6 production and M2 surface markers on primary human monocytes, leading to impair mycobacterial killing (even though some of DM individuals who were being treated with glibenclamide were also being treated with metformin in combination).

In contrast, IL-10 is a hallmark M2 cytokine in both mice and human (21). However, we only observed a trend of IL-10 increase in T2DM individuals who have been treated with glibenclamide. The reason that we could not clearly see a significant enhancement of IL-10 could be due to (1) length of culture as IL-10 might be used by monocytes after 96 h culture, and (2) IL-10 is a potent anti-inflammatory

cytokine that plays a crucial, and often essential, role in preventing inflammatory pathology and it is produced as a synthesis inhibitory factor for a negative feedback mechanism to limit over pro-inflammatory cytokine response toward Mtb infection (50). Once pro-inflammatory cytokines have been suppressed, IL-10 might not need to be plentifully produced. Nevertheless, we have shown that glibenclamide enhances IL-10 levels *in vitro*. In Thailand, East Asian (w/Beijing) strains predominated in both TB meningitis and pulmonary TB disease (56). However, our study used only Mtb H37Rv, the most studied strain of TB in research laboratories (57), and BCG, with which most Thai people have been vaccinated (58). It is possible that the magnitude of cytokines produced from human monocytes may be different in response to East Asian Mtb strains.

Obesity and T2DM are now recognized as chronic proinflammatory diseases (59). Previous studies found that short-chain fatty acids inhibit Mtb-induced pro-inflammatory cytokine production from human PBMCs (60), and poor glycemic control is a risk factor for TB infection (61). Moreover, an imbalance in the ratio of M1 and M2 macrophages, with increased cytokine production from M1 macrophages and/or reduced anti-inflammatory signals from M2 macrophages leads to adipose tissue dysfunction and impairs glucose tolerance. However, the characteristics of our samples showed that Thai DM individuals had similar BMI results as healthy controls at the time of enrollment. Also, previous studies proposed that M2 macrophages strongly promote pancreatic beta-cell proliferation (62), with enhancing beta-cell mass could be an ideal cure for DM. Linking these observations to our data, indicating that glibenclamide promotes M2 markers, suggests that another positive effect of glibenclamide on diabetes is carried out by macrophages exhibiting an M2 phenotype. The K_{ATP} channel is also known to influence the phenotype of prepolarized macrophages and inhibition of K_{ATP} channel promotes M2, while opening of K_{ATP} channel augments M1 marker expression in a human monocyte cell line (22). Therefore, as glipizide is a partial inhibitor of K_{ATP} channel, we could not expect to observe an effect on cytokine production and killing activity of primary human monocytes against Mtb infection. Another major anti-diabetic drug, metformin, a candidate for host-directed therapy for TB (63), was reported to reduce pro-inflammatory cytokine production in response to *E. coli* LPS (64) and approach to target Mtb by pharmacologically stimulating intracellular mycobacteria clearance through autophagy (65). Moreover, metformin was observed to inhibit macrophage differentiation via AMPK-mediated inhibition of STAT3 activation and to inhibit TNF- α and MCP-1 production (66). These are consistent with our data, which show a reduction in TNF- α and IL-6 against LPS and IL-6, IL-8, MCP-1, and RANTES in response to Mtb infection in T2DM individuals who were being treated with metformin. However, the killing function of monocytes from T2DM who were being treated with metformin is not impaired.

The possible mechanism to explain how glibenclamide is associated with M1 and M2 marker alteration could be

(1) pre-differentiated/pre-polarized macrophages presented an expression pattern of potassium subunits that facilitated more efficient glibenclamide binding (22) and might directly modulate macrophage polarization, and (2) the reduction of IL-1 β level through inflammasome which triggered the inhibition of potassium channel by glibenclamide (8) might result in cytokine imbalance, especially TNF- α , IL-8, and IL-6 in this study and lead to M1 and M2 marker alteration. This switch between M1 and M2 state may indicate how the innate immune balance is maintained by macrophage subsets during bacterial infection.

Taken together, this is the first report to describe that glibenclamide impairs mycobactericidal ability of primary human monocytes of T2DM individuals in response to Mtb by reducing M1 and promoting M2 polarization. Our data suggests that treatment with glibenclamide may result in increased susceptibility of T2DM individuals to TB and other bacterial infectious diseases.

AUTHOR CONTRIBUTIONS

GB, HF, and GL conceived the research, oversaw the study, and the data analysis. CK and SP performed the experiments and the data analysis. CK, SP, GB, HF, and GL interpreted the data and wrote the manuscript. All authors read, commented on, and agreed on the content of the manuscript.

FUNDING

This work was supported by Newton Fund—Thailand Office of Higher Education Committee Institutional Links, Mekong Health Science Research Institute, The Centre for Research and Development of Medical Diagnostic Laboratories and Research Incubator Programme, Faculty of Associated Medical Sciences, Khon Kaen University, Thailand. Travel grant was supported by researcher links, Newton Fund. Satria Arief Prabowo (SP) received a Ph.D. scholarship from the Indonesian Endowment Fund for Education (LPDP).

ACKNOWLEDGMENTS

The authors wish to acknowledge the help of Wipawee Seanwongsa and members of The Office of Disease Prevention and Control 10 and Dara Kodarsa and members of Yang Lum Health Promoting Hospital for sample collection and research site of preliminary study in Ubon Ratchathani. We thank Carolynne Stanley for sample collection and all supports at London School of Hygiene and Tropical Medicine (LSHTM). We also thank Natasha Spink, Felipe Cia, and Sam Willcocks for the supervision of work performed bio-containment level 3 at LSHTM.

SUPPLEMENTARY MATERIAL

The Supplementary Material for this article can be found online at: <https://www.frontiersin.org/articles/10.3389/fimmu.2018.02109/full#supplementary-material>

REFERENCES

- World Health Organisation. Global Tuberculosis Report 2017. WHO (2017).
- Houben RM, Dodd PJ. The global burden of latent tuberculosis infection: a re-estimation using mathematical modelling. *PLoS Med.* (2016) 13:e1002152. doi: 10.1371/journal.pmed.1002152
- Jeon CY, Murray MB. Diabetes mellitus increases the risk of active tuberculosis: a systematic review of 13 observational studies. *PLoS Med.* (2008) 5:e152. doi: 10.1371/journal.pmed.005015208-PLME-RA-0743
- Zheng C, Hu M, Gao F. Diabetes and pulmonary tuberculosis: a global overview with special focus on the situation in Asian countries with high TB-DM burden. *Glob Health Action* (2017) 10:1–11. doi: 10.1080/16549716.2016.1264702
- Faurholt-Jepsen D, Range N, PrayGod G, Jeremiah K, Faurholt-Jepsen M, Aabye MG, et al. The role of anthropometric and other predictors for diabetes among urban Tanzanians with tuberculosis. *Int J Tuberc Lung Dis.* (2012) 16:1680–5. doi: 10.5588/ijtld.12.0360
- Kibirige D, Ssekitooleko R, Mutebi E, Worodria W. Overt diabetes mellitus among newly diagnosed Ugandan tuberculosis patients: a cross sectional study. *BMC Infect Dis.* (2013) 13:122. doi: 10.1186/1471-2334-13-122
- World Health Organisation. Global Status Report on Noncommunicable Disease 2010. WHO (2010).
- Lamkanfi M, Mueller JL, Vitari AC, Misaghi S, Fedorova A, Deshayes K, et al. Glyburide inhibits the Cryopyrin/Nalp3 inflammasome. *J Cell Biol.* (2009) 187:61–70. doi: 10.1083/jcb.200903124
- Hermann LS, Schersten B, Bitzen PO, Kjellstrom T, Lindgarde F, Melander A. Therapeutic comparison of metformin and sulfonylurea, alone and in various combinations. A double-blind controlled study. *Diabetes Care* (1994) 17:1100–9.
- Hamon Y, Luciani MF, Becq F, Verrier B, Rubartelli A, Chimini G. Interleukin-1beta secretion is impaired by inhibitors of the Atp binding cassette transporter, ABC1. *Blood* (1997) 90:2911–5.
- Kewcharoenwong C, Rinchai D, Utitpan K, Suwannasae D, Bancroft GJ, Ato M, et al. Glibenclamide reduces pro-inflammatory cytokine production by neutrophils of diabetes patients in response to bacterial infection. *Sci Rep.* (2013) 3:3363. doi: 10.1038/srep03363
- Kewcharoenwong C, Rinchai D, Nithichanon A, Bancroft GJ, Ato M, Lertmengkolchai G. Glibenclamide impairs responses of neutrophils against Burkholderia pseudomallei by reduction of intracellular glutathione. *Sci Rep.* (2016) 6:34794. doi: 10.1038/srep34794
- Scriba TJ, Coussens AK, Fletcher HA. Human immunology of tuberculosis. *Microbiol Spectr.* (2017) 5:1–24. doi: 10.1128/microbiolspec.TB2-0016-2016
- Rogers PM. A study of the blood monocytes in children with tuberculosis. *New Eng J Med.* (1928) 198:740–9. doi: 10.1056/nejm192805241981410
- Dooley KE, Chaisson RE. Tuberculosis and diabetes mellitus: convergence of two epidemics. *Lancet Infect Dis.* (2009) 9:737–46. doi: 10.1016/S1473-3099(09)70282-8
- Murray PJ. Macrophage polarization. *Annu Rev Physiol.* (2017) 79:541–66. doi: 10.1146/annurev-physiol-022516-034339
- Lee J, Tam H, Adler L, Ilstad-Minnihan A, Macaubas C, Mellins ED. The MHC class II antigen presentation pathway in human monocytes differs by subset and is regulated by cytokines. *PLoS ONE* (2017) 12:e0183594. doi: 10.1371/journal.pone.0183594PONE-D-17-22627
- Ambarus CA, Santegoets KC, van Bon L, Wenink MH, Tak PP, Radstake TR, et al. Soluble immune complexes shift the TLR-induced cytokine production of distinct polarized human macrophage subsets towards IL-10. *PLoS ONE* (2012) 7:e35994. doi: 10.1371/journal.pone.0035994PONE-D-11-25255
- Jaguin M, Houlbert N, Fardel O, Lecreur V. Polarization profiles of human M-CSF-generated macrophages and comparison of M1-markers in classically activated macrophages from GM-CSF and M-CSF origin. *Cell Immunol.* (2013) 281:51–61. doi: 10.1016/j.cellimm.2013.01.010S0008-8749(13)00023-3
- Tarique AA, Logan J, Thomas E, Holt PG, Sly PD, Fantino E. Phenotypic, functional, and plasticity features of classical and alternatively activated human macrophages. *Am J Respir Cell Mol Biol.* (2015) 53:676–88. doi: 10.1165/rcmb.2015-0012OC
- Lugo-Villarino G, Verollet C, Maridonnetu-Parini I, Neyrolles O. Macrophage polarization: convergence point targeted by *Mycobacterium tuberculosis* and HIV. *Front Immunol.* (2011) 2:43. doi: 10.3389/fimmu.2011.00043
- Li C, Levin M, Kaplan DL. Bioelectric modulation of macrophage polarization. *Sci Rep* (2016) 6:21044. doi: 10.1038/srep21044
- Niopas I, Dafsis AC. A validated high-performance liquid chromatographic method for the determination of glibenclamide in human plasma and its application to pharmacokinetic studies. *J Pharm Biomed Anal.* (2002) 28:653–7. doi: 10.1016/S0731-7085(02)00013-4
- Fletcher HA, Tanner R, Wallis RS, Meyer J, Manjaly ZR, Harris S, et al. Inhibition of mycobacterial growth *in vitro* following primary but not secondary vaccination with *Mycobacterium bovis* BCG. *Clin Vaccine Immunol.* (2013) 20:1683–9. doi: 10.1128/CVI.00427-13
- Moliva JI, Turner J, Torrelles JB. Immune responses to bacillus calmette-guerin vaccination: why do they fail to protect against *Mycobacterium tuberculosis*? *Front Immunol.* (2017) 8:407. doi: 10.3389/fimmu.2017.00407
- Jonsson A, Hallengren B, Rydberg T, Melander A. Effects and serum levels of glibenclamide and its active metabolites in patients with type 2 diabetes. *Diabetes Obes Metab.* (2001) 3:403–9. doi: 10.1046/j.1463-1326.2001.00152.x
- DeFronzo RA. Pharmacologic therapy for type 2 diabetes mellitus. *Ann Intern Med.* (2000) 133:73–4. doi: 10.7326/0003-4819-133-1-200007040-00016
- Yang J, Zhang L, Yu C, Yang XF, Wang H. Monocyte and macrophage differentiation: circulation inflammatory monocyte as biomarker for inflammatory diseases. *Biomark Res.* (2014) 2:1. doi: 10.1186/2050-7771-2-1
- Association AD. Standards of medical care in diabetes-2017. *Diabetes Care* (2017) 40(Suppl. 1):S64–74.
- Joshi N, Caputo GM, Weitekamp MR, Karchmer AW. Infections in patients with diabetes mellitus. *N Engl J Med.* (1999) 341:1906–12. doi: 10.1056/NEJM199912163412507
- Shah BR, Hux JE. Quantifying the risk of infectious diseases for people with diabetes. *Diabetes Care* (2003) 26:510–3. doi: 10.2337/diacare.26.2.510
- Chanchamroen S, Kewcharoenwong C, Sussaengrat W, Ato M, Lertmengkolchai G. Human polymorphonuclear neutrophil responses to Burkholderia pseudomallei in healthy and diabetic subjects. *Infect Immun.* (2009) 77:456–63. doi: 10.1128/IAI.00503-08
- Koh GC, Peacock SJ, van der Poll T, Wiersinga WJ. The impact of diabetes on the pathogenesis of sepsis. *Eur J Clin Microbiol Infect Dis.* (2012) 31:379–88. doi: 10.1007/s10096-011-1337-4
- Nitzan O, Elias M, Chazan B, Saliba W. Urinary tract infections in patients with type 2 diabetes mellitus: review of prevalence, diagnosis, and management. *Diabetes Metab Syndr Obes.* (2015) 8:129–36. doi: 10.2147/DMSO.S51792dms0-8-129
- Chiao HY, Wang CY, Wang CH. Salmonella abscess of the anterior chest wall in a patient with type 2 diabetes and poor glycemic control: a case report. *Ostomy Wound Manage* (2016) 62:46–9.
- Cheng AC, Currie BJ. Melioidosis: epidemiology, pathophysiology, and management. *Clin Microbiol Rev.* (2005) 18:383–416. doi: 10.1128/CMR.18.2.383-416.2005
- Sasindran SJ, Torrelles JB. *Mycobacterium tuberculosis* infection and inflammation: what is beneficial for the host and for the bacterium? *Front Microbiol.* (2011) 2:2. doi: 10.3389/fmicb.2011.00002
- Koh GC, Schreiber MF, Bautista R, Maude RR, Dunachie S, Limmathurotsakul D, et al. Host responses to melioidosis and tuberculosis are both dominated by interferon-mediated signaling. *PLoS ONE* (2013) 8:e54961. doi: 10.1371/journal.pone.0054961
- Balboa L, Romero MM, Basile JI, Sabio y Garcia CA, Schierloh P, Yokobori N, et al. Paradoxical role of CD16+CCR2+CCR5+ monocytes in tuberculosis: efficient APC in pleural effusion but also mark disease severity in blood. *J Leukoc Biol.* (2011) 90:69–75. doi: 10.1189/jlb.1010577
- Lastrucci C, Benard A, Balboa L, Pingris K, Souriant S, Poincloux R, et al. Tuberculosis is associated with expansion of a motile, permissive and immunomodulatory CD16(+) monocyte population via the IL-10/STAT3 axis. *Cell Res.* (2015) 25:1333–51. doi: 10.1038/cr.2015.123
- Gutierrez MG, Master SS, Singh SB, Taylor GA, Colombo MI, Deretic V. Autophagy is a defense mechanism inhibiting BCG and *Mycobacterium tuberculosis* survival in infected macrophages. *Cell* (2004) 119:753–66. doi: 10.1016/j.cell.2004.11.038
- Fletcher HA, Filali-Mouhim A, Nemes E, Hawkrigde A, Keyser A, Njikan S, et al. Human newborn Bacille Calmette-Guerin vaccination and risk

- of tuberculosis disease: a case-control study. *BMC Med.* (2016) 14:76. doi: 10.1186/s12916-016-0617-3
43. Dorhoi A, Kaufmann SH. Versatile myeloid cell subsets contribute to tuberculosis-associated inflammation. *Eur J Immunol.* (2015) 45:2191–202. doi: 10.1002/eji.201545493
 44. Kahnert A, Seiler P, Stein M, Bandermann S, Hahnke K, Mollenkopf H, et al. Alternative activation deprives macrophages of a coordinated defense program to *Mycobacterium tuberculosis*. *Eur J Immunol.* (2006) 36:631–47. doi: 10.1002/eji.200535496
 45. Boillat-Blanco N, Tumbo AN, Perreau M, Amelio P, Ramaiya KL, Mganga M, et al. Hyperglycaemia is inversely correlated with live *M. bovis* BCG-specific CD4(+) T cell responses in Tanzanian adults with latent or active tuberculosis. *Immun Inflamm Dis.* (2018) 6:345–53. doi: 10.1002/iid3.222
 46. Liu Y, Bao P, Wang D, Li Z, Li Y, Tang L, et al. Evaluation of the in vivo efficacy of novel monosubstituted sulfonylureas against H37Rv and extensively drug-resistant tuberculosis. *Jpn J Infect Dis.* (2014) 67:485–7. doi: 10.7883/yoken.67.485
 47. 8. Pharmacologic Approaches to Glycemic Treatment: Standards of Medical Care in Diabetes—2018. *Diabetes Care* (2018) 41(Suppl. 1):S73–85. doi: 10.2337/dc18-S008
 48. Kratochvill F, Neale G, Haverkamp JM, Van de Velde LA, Smith AM, Kawachi D, et al. TNF Counterbalances the emergence of M2 tumor macrophages. *Cell Rep.* (2015) 12:1902–14. doi: 10.1016/j.celrep.2015.08.033
 49. Schleicher U, Paduch K, Debus A, Obermeyer S, König T, Kling JC, et al. TNF-mediated restriction of arginase 1 expression in myeloid cells triggers type 2 NO synthase activity at the site of infection. *Cell Rep.* (2016) 15:1062–75. doi: 10.1016/j.celrep.2016.04.001
 50. Flynn JL, Goldstein MM, Chan J, Triebold KJ, Pfeffer K, Lowenstein CJ, et al. Tumor necrosis factor- α is required in the protective immune response against *Mycobacterium tuberculosis* in mice. *Immunity* (1995) 2:561–72.
 51. Mantovani A, Sica A, Sozzani S, Allavena P, Vecchi A, Locati M. The chemokine system in diverse forms of macrophage activation and polarization. *Trends Immunol.* (2004) 25:677–86. doi: 10.1016/j.it.2004.09.015
 52. Ouchi N, Parker JL, Lugus JJ, Walsh K. Adipokines in inflammation and metabolic disease. *Nat Rev Immunol.* (2011) 11:85–97. doi: 10.1038/nri2921
 53. Mauer J, Chaurasia B, Goldau J, Vogt MC, Ruud J, Nguyen KD, et al. Signaling by IL-6 promotes alternative activation of macrophages to limit endotoxemia and obesity-associated resistance to insulin. *Nat Immunol.* (2014) 15:423–30. doi: 10.1038/ni.2865
 54. Fu XL, Duan W, Su CY, Mao FY, Lv YP, Teng YS, et al. Interleukin 6 induces M2 macrophage differentiation by STAT3 activation that correlates with gastric cancer progression. *Cancer Immunol Immunother.* (2017) 66:1597–608. doi: 10.1007/s00262-017-2052-5
 55. Nagabhushanam V, Solache A, Ting LM, Escaron CJ, Zhang JY, Ernst JD. Innate inhibition of adaptive immunity: *Mycobacterium tuberculosis*-induced IL-6 inhibits macrophage responses to IFN- γ . *J Immunol.* (2003) 171:4750–7. doi: 10.4049/jimmunol.171.9.4750
 56. Faksri K, Xia E, Ong RT, Tan JH, Nonghanphithak D, Makhao N, et al. Comparative whole-genome sequence analysis of *Mycobacterium tuberculosis* isolated from tuberculous meningitis and pulmonary tuberculosis patients. *Sci Rep.* (2018) 8:4910. doi: 10.1038/s41598-018-23337-y
 57. Camus JC, Pryor MJ, Medigue C, Cole ST. Re-annotation of the genome sequence of *Mycobacterium tuberculosis* H37Rv. *Microbiology* (2002) 148(Pt 10):2967–73. doi: 10.1099/00221287-148-10-2967
 58. Zwerling A, Behr MA, Verma A, Brewer TF, Menzies D, Pai M. The BCG world atlas: a database of global BCG vaccination policies and practices. *PLoS Med.* (2011) 8:e1001012. doi: 10.1371/journal.pmed.1001012
 59. Kraakman MJ, Murphy AJ, Jandeleit-Dahm K, Kammoun HL. Macrophage polarization in obesity and type 2 diabetes: weighing down our understanding of macrophage function? *Front Immunol.* (2014) 5:470. doi: 10.3389/fimmu.2014.00470
 60. Lachmandas E, van den Heuvel CN, Damen MS, Cleophas MC, Netea MG, van Crevel R. Diabetes mellitus and increased tuberculosis susceptibility: the role of short-chain fatty acids. *J Diabetes Res.* (2016) 2016:6014631. doi: 10.1155/2016/6014631
 61. Pal R, Ansari MA, Hameed S, Fatima Z. Diabetes mellitus as hub for tuberculosis infection: a snapshot. *Int J Chronic Dis.* (2016) 2016:5981574. doi: 10.1155/2016/5981574
 62. Xiao X, Gaffar I, Guo P, Wiersch J, Fischbach S, Peirish L, et al. M2 macrophages promote beta-cell proliferation by up-regulation of SMAD7. *Proc Natl Acad Sci USA.* (2014) 111:E1211–20. doi: 10.1073/pnas.1321347111
 63. Restrepo BI. Metformin: candidate host-directed therapy for tuberculosis in diabetes and non-diabetes patients. *Tuberculosis* (2016) 101S:S69–72. doi: 10.1016/j.tube.2016.09.008
 64. Arai M, Uchiba M, Komura H, Mizuochi Y, Harada N, Okajima K. Metformin, an antidiabetic agent, suppresses the production of tumor necrosis factor and tissue factor by inhibiting early growth response factor-1 expression in human monocytes *in vitro*. *J Pharmacol Exp Ther.* (2010) 334:206–13. doi: 10.1124/jpet.109.164970
 65. Schiebler M, Brown K, Hegyi K, Newton SM, Renna M, Hepburn L, et al. Functional drug screening reveals anticonvulsants as enhancers of mTOR-independent autophagic killing of *Mycobacterium tuberculosis* through inositol depletion. *EMBO Mol Med.* (2015) 7:127–39. doi: 10.15252/emmm.201404137
 66. Vasamsetti SB, Karnewar S, Kanugula AK, Thatipalli AR, Kumar JM, Kotamraju S. Metformin inhibits monocyte-to-macrophage differentiation via AMPK-mediated inhibition of STAT3 activation: potential role in atherosclerosis. *Diabetes* (2015) 64:2028–41. doi: 10.2337/db14-1225

Conflict of Interest Statement: The authors declare that the research was conducted in the absence of any commercial or financial relationships that could be construed as a potential conflict of interest.

The reviewer AT and handling Editor declared their shared affiliation.

Copyright © 2018 Kewcharoenwong, Prabowo, Bancroft, Fletcher and Lertmemongkolchai. This is an open-access article distributed under the terms of the Creative Commons Attribution License (CC BY). The use, distribution or reproduction in other forums is permitted, provided the original author(s) and the copyright owner(s) are credited and that the original publication in this journal is cited, in accordance with accepted academic practice. No use, distribution or reproduction is permitted which does not comply with these terms.



RESEARCH ARTICLE

REVISED High monocyte to lymphocyte ratio is associated with impaired protection after subcutaneous administration of BCG in a mouse model of tuberculosis [version 2; referees: 2 approved]

Andrea Zelmer ¹, Lisa Stockdale¹, Satria A. Prabowo ¹, Felipe Cia¹, Natasha Spink¹, Matthew Gibb ^{1,2}, Ayad Eddaoudi³, Helen A. Fletcher ¹

¹London School of Hygiene and Tropical Medicine, Department of Immunology and Infection, Keppel Street, London, WC1E 7HT, UK
²Baylor Institute for Immunology Research, 3434 Live Oak Street, Dallas, Texas, 75204, USA
³UCL Great Ormond Street Institute of Child Health, 30 Guilford Street, London, WC1N 1EH, UK

v2 First published: 08 Mar 2018, 7:296 (doi: [10.12688/f1000research.14239.1](https://doi.org/10.12688/f1000research.14239.1))
 Latest published: 27 Jun 2018, 7:296 (doi: [10.12688/f1000research.14239.2](https://doi.org/10.12688/f1000research.14239.2))

Abstract

Background: The only available tuberculosis (TB) vaccine, Bacillus Calmette-Guérin (BCG), has variable efficacy. New vaccines are therefore urgently needed. Why BCG fails is incompletely understood, and the tools used for early assessment of new vaccine candidates do not account for BCG variability. Taking correlates of risk of TB disease observed in human studies and back-translating them into mice to create models of BCG variability should allow novel vaccine candidates to be tested early in animal models that are more representative of the human populations most at risk. Furthermore, this could help to elucidate the immunological mechanisms leading to BCG failure. We have chosen the monocyte to lymphocyte (ML) ratio as a correlate of risk of TB disease and have back-translated this into a mouse model.

Methods: Four commercially available, inbred mouse strains were chosen. We investigated their baseline ML ratio by flow cytometry; extent of BCG-mediated protection from *Mycobacterium tuberculosis* infection by experimental challenge; vaccine-induced interferon gamma (IFN γ) response by ELISPOT assay; and tissue distribution of BCG by plating tissue homogenates.

Results: The ML ratio varied significantly between A/J, DBA/2, C57Bl/6 and 129S2 mice. A/J mice showed the highest BCG-mediated protection and lowest ML ratio, while 129S2 mice showed the lowest protection and higher ML ratio. We also found that A/J mice had a lower antigen specific IFN γ response than 129S2 mice. BCG tissue distribution appeared higher in A/J mice, although this was not statistically significant.

Conclusions: These results suggest that the ML ratio has an impact on BCG-mediated protection in mice, in alignment with observations from clinical studies. A/J and 129S2 mice may therefore be useful models of BCG vaccine variability for early TB vaccine testing. We speculate that failure of BCG to protect from TB disease is linked to poor tissue distribution in a ML high immune environment.

Keywords

Tuberculosis, animal models, BCG, vaccine, ML ratio, mice

Open Peer Review

Referee Status:

	Invited Referees	
	1	2
REVISED		
version 2 published 27 Jun 2018	report	
version 1 published 08 Mar 2018	report	report

1 **Nacho Aguilo**, University of Zaragoza, Spain

2 **Maximiliano G Gutierrez**, Francis Crick Institute, USA

Discuss this article

Comments (0)



This article is included in the [World TB Day](#) collection.

Corresponding author: Andrea Zelmer (andrea.zelmer@lshtm.ac.uk)

Author roles: **Zelmer A:** Formal Analysis, Funding Acquisition, Investigation, Methodology, Supervision, Visualization, Writing – Original Draft Preparation, Writing – Review & Editing; **Stockdale L:** Investigation, Writing – Review & Editing; **Prabowo SA:** Investigation, Writing – Review & Editing; **Cia F:** Investigation, Writing – Review & Editing; **Spink N:** Investigation, Writing – Review & Editing; **Gibb M:** Investigation, Writing – Review & Editing; **Eddaoudi A:** Investigation, Methodology, Writing – Review & Editing; **Fletcher HA:** Conceptualization, Funding Acquisition, Methodology, Supervision, Writing – Review & Editing

Competing interests: No competing interests were disclosed.

How to cite this article: Zelmer A, Stockdale L, Prabowo SA *et al.* **High monocyte to lymphocyte ratio is associated with impaired protection after subcutaneous administration of BCG in a mouse model of tuberculosis [version 2; referees: 2 approved]** *F1000Research* 2018, 7:296 (doi: [10.12688/f1000research.14239.2](https://doi.org/10.12688/f1000research.14239.2))

Copyright: © 2018 Zelmer A *et al.* This is an open access article distributed under the terms of the [Creative Commons Attribution Licence](#), which permits unrestricted use, distribution, and reproduction in any medium, provided the original work is properly cited. Data associated with the article are available under the terms of the [Creative Commons Zero "No rights reserved" data waiver](#) (CC0 1.0 Public domain dedication).

Grant information: The work in this article was funded by a grant to HF from the European Commission HORIZON2020 program (TBVAC2020 grant no. 643381) and an Athena SWAN Career Re-entry award funded by the London School of Hygiene and Tropical Medicine to AZ. *The funders had no role in study design, data collection and analysis, decision to publish, or preparation of the manuscript.*

First published: 08 Mar 2018, 7:296 (doi: [10.12688/f1000research.14239.1](https://doi.org/10.12688/f1000research.14239.1))

REVISED Amendments from Version 1

This version has been revised to address the reviewers' comments. We have now included an analysis of the CD11b intermediate, CD11c+ cell population in the lung which should be enriched in alveolar macrophages (Figure 1E). We have also included a discussion about the main genetic differences between the mouse strains, and provided some clarification of experimental and technical details.

See referee reports

Introduction

Tuberculosis (TB), caused by *Mycobacterium tuberculosis* (*Mtb*) is the leading cause of death from a single infectious agent. Multidrug-resistant TB remains a public health crisis, and only one vaccine (the *M. bovis*-derived Bacillus Calmette-Guérin, BCG) is currently licensed for clinical use. To meet the sustainable development goal of ending the TB epidemic by 2030, new treatments and vaccines are both urgently needed.

BCG efficacy is highly variable^{1,2}. The reasons why BCG protects when it does and why it fails when it doesn't are incompletely understood, but are crucial to the successful design and testing of new vaccines³. Furthermore, to be able to accurately assess vaccine candidates in models where BCG both protects and does not protect very early on in the vaccine development pipeline would be highly advantageous and de-risk failure in later stage clinical trials. There is however a lack of a broad range of tools that can collectively predict with some confidence whether a vaccine will be protective.

One of the tools for very early testing of TB vaccine candidates is a mouse model. However, in order to obtain meaningful information, new vaccine candidates should be tested in models that are clinically relevant and reflect the breadth and heterogeneity of immune environments and varying BCG efficacy found in human populations. We propose that this could be achieved by back-translating observations from clinical studies, such as correlates of risk of TB disease, into animal models.

A number of correlates of risk of TB disease have recently been identified, including transcriptomic mRNA signatures in blood, T cell activation, and monocyte to lymphocyte (ML) ratio⁴⁻⁸, while others are being investigated (reviewed in 9). We have chosen the ML ratio to provide proof of principle that correlates of risk can be back-translated into the mouse to develop a model for vaccine testing that better reflects the populations most at risk of BCG failure.

In this study, we show that inbred, commercially available mouse strains have differing ML ratios, and that a high ML ratio is associated with lower BCG-mediated protection from experimental *Mtb* challenge. We further suggest that lack of BCG dissemination and/or persistence in ML high mice impairs protection.

Methods

Ethics statement

All animal work was carried out in accordance with the Animals (Scientific Procedures) Act 1986 under a license granted by the UK Home Office (PPL 70/8043), and approved locally by the London School of Hygiene and Tropical Medicine Animal Welfare and Ethics Review Body.

Animals and experiment design

The following mouse strains were used for the experiments reported here (abbreviated names used throughout the manuscript are given in brackets): A/JOlA^{Hsd} (A/J); DBA/2Ola^{Hsd} (DBA/2); C57BL/6J^{Ola}^{Hsd} (C57Bl/6); 129S2/Sv^{Hsd} (129S2). Female mice were acquired from Envigo UK at 5–7 weeks of age. Animals were housed in specific pathogen-free individually vented cages with environmental enrichment (play tunnel and tapvei block), with 12 hours light / 12 hours dark cycles, at temperatures between 19° – 23°C and relative humidity of 45 – 65%. Mice were fed sterilized diet RM1 and filtered water ad libitum, and were allowed to acclimatize for at least 5 days before the start of any experimental procedure. Mice were allocated to cages as groups of 5 by technical staff not involved in experimental procedures or data analysis, and mice of the same strain were housed together. Each cage was allocated to a treatment in no particular order, but without formal randomisation. Animal welfare was assessed twice every day before and during the study.

Two independent experiments with separate primary outcomes were carried out to obtain the data described in this report. In Experiment 1, 5 naïve mice of each strain (20 mice total) were culled by anaesthetic overdose, and cardiac blood, lungs and spleens were collected for determination of the ML ratio by flow cytometric analysis (see below for details). The primary outcome for this experiment was the ML ratio (Figure 1). In Experiment 2, parallel groups of mice (n=5 per group) were BCG-immunised or left untreated. These were allocated at the start of the study to either an immunogenicity group (IFN γ response and BCG dissemination; 10 mice per strain; 40 mice total; Figure 3 and Figure 4), or an *Mtb* challenge group (bacterial burden in lung; 10 mice per strain; 40 mice total; Figure 2). Six weeks after immunisation, mice were infected with *Mtb* or culled for isolation of cells from lung and spleen. In all, a total of 100 mice (25 per strain) was used to obtain all data presented here.

The study was not blinded.

Vaccination

The BCG Pasteur strain was obtained from Aeras (Rockville, MD, USA) as frozen aliquots. These were stored at -80°C until needed. BCG was then thawed at room temperature and diluted to a final concentration of 2 \times 10⁶ CFU/ml in physiological saline solution for irrigation (Baxter Healthcare, Newbury, UK). Each animal received a subcutaneous injection of 100 μ l BCG containing 2 \times 10⁵ CFU BCG (vaccinated groups). BCG dose was confirmed by plating of an aliquot of the prepared vaccine

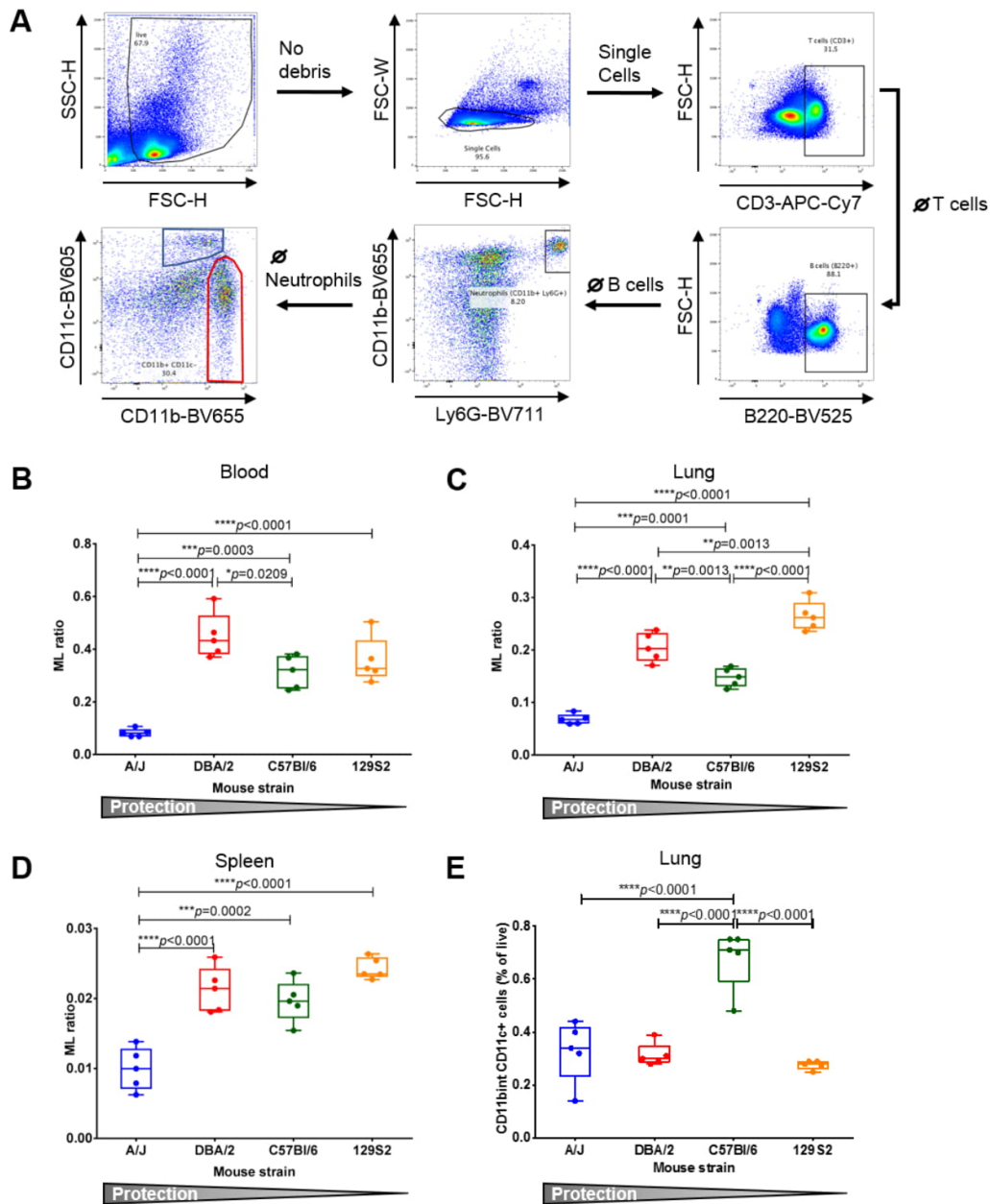


Figure 1. The ML ratio differs significantly in four different inbred mouse strains. **A** Gating strategy for flow cytometric analysis. Cells from naïve animals were fixed, stained and data acquired as described in Materials and Methods. Cell debris was gated out by use of a FSC-SSC gate, followed by gating on single cells (FSC-H and FSC-W). A sequential gating strategy was then applied to determine the frequency of T cells (CD3⁺), B cells (B220⁺), neutrophils (CD11b⁺ Ly6G⁺), monocytes/macrophages (CD11b⁺ CD11c^{low-int}, red gate) and CD11b^{int} CD11c⁺ cells (blue gate) as a percentage of single cells. Plots shown are from a sample of a C57Bl/6 spleen. **B–D** The ML ratio was calculated by dividing the percentage of monocytes/macrophages by the sum of the percentages of B and T cells. ML ratio was analysed in blood (**B**), lung (**C**) and spleen (**D**) of four different mouse strains. **E** Percentage of CD11b^{int} CD11c⁺ cells in the lung of four different mouse strains, likely to be enriched in alveolar macrophages. Each symbol represents one animal; box plots represent the median (middle line), 25th to 75th percentile (box) and minimum to maximum value (error bars). Data sets are presented in order of decreasing protection. *p* values were determined using ordinary ANOVA with Holm-Sidak test for multiple comparisons. Multiplicity adjusted *p* values are reported. A *p* value <0.05 was considered statistically significant.

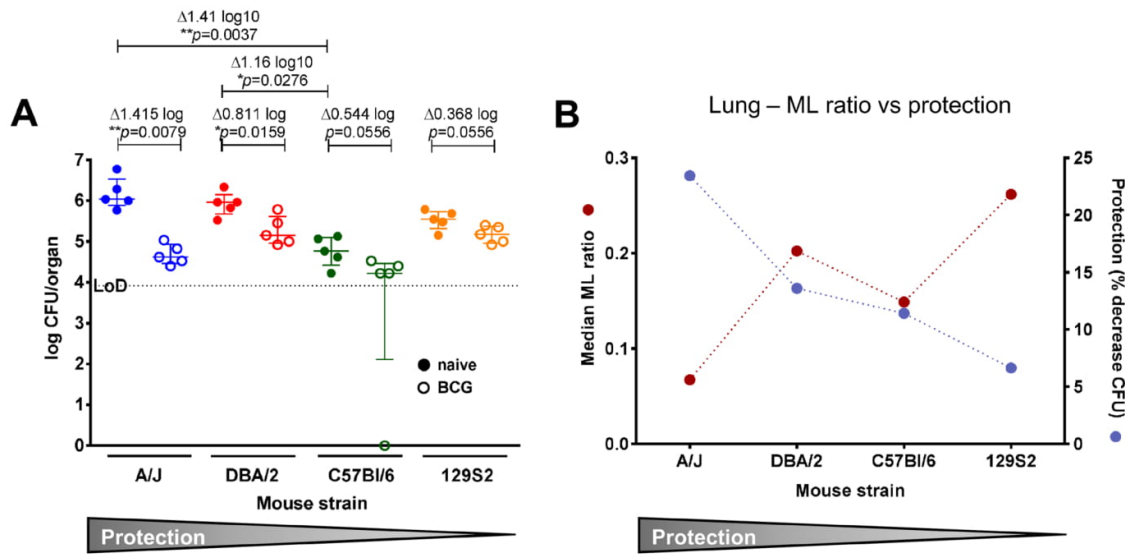


Figure 2. Protection from Mtb infection varies after BCG vaccination in ML high and low mouse strains. **A** Mice of each strain were immunised s.c. with 2×10^5 CFU BCG Pasteur (open circles) or left untreated (filled circle), and infected i.n. with 30 CFU Mtb Erdmann 6 weeks later. Bacterial burden in the lungs of all animals was enumerated 7 weeks after challenge. Each symbol represents one animal. Bacterial numbers are given as log₁₀ CFU per whole organ. No bacteria were detected in one of the C57Bl/6 samples; this value was set to zero. Δ indicates the difference in bacterial burden between naïve and BCG immunised mice. *p* values were determined by Kruskal-Wallis test with Dunn's post-test for multiple comparisons between naïve groups, and multiplicity adjusted *p* values are reported. Individual Mann-Whitney tests to compare naïve with BCG immunised groups of each mouse strain. *p* < 0.05 was considered statistically significant. Error bars represent the median and interquartile range. LoD: limit of detection. **B** ML ratio in comparison to protection in the lung of ML high and low mice. The median ML ratio in lung (red; as in Figure 1) is plotted together with protection expressed as the median % decrease in CFU (blue; as in A).

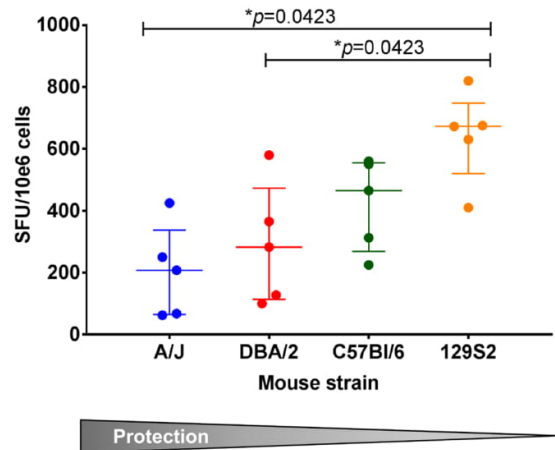


Figure 3. Antigen-specific interferon gamma response varies in splenocytes of ML high and ML low mouse strains. Splenocytes were isolated from BCG-immunised or control mice at the time of Mtb challenge (6 weeks after immunisation), and restimulated with PPD. The number of IFN γ producing cells were enumerated using an ELISPOT assay (presented as spot forming units [SFU] per 10^6 cells). Non-specific background measured in unstimulated duplicate wells was removed. Data sets are presented in order of decreasing protection. Each symbol represents one animal. *p* values were determined by using one-way ANOVA and Dunn's post test for multiple comparisons. Error bars represent the median and interquartile range. Multiplicity adjusted *p* values are reported. *p* < 0.05 was considered statistically significant.

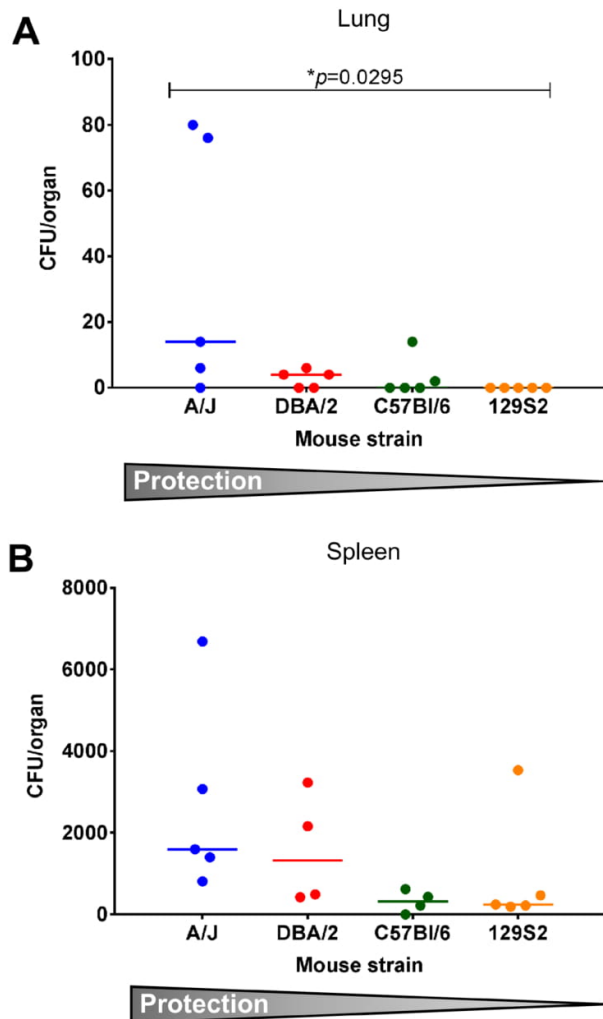


Figure 4. BCG distribution varies between lung and spleen after vaccination of ML high and ML low mice. Approximately half of each lung (A) and spleen (B) was homogenised at the time of Mtb challenge (6 weeks after immunisation) and plated on 7H11 agar plates to determine viable BCG bacteria. Total CFU per organ are reported. Data sets are presented in order of decreasing protection. Each symbol represents one animal. In some instances, bacteria could not be detected and values were set to zero. p values were determined by using Kruskal-Wallis test and Dunn's post test for multiple comparisons. Error bars represent the median and interquartile range. Multiplicity adjusted p values are reported. $p < 0.05$ was considered statistically significant.

suspension on 7H11 agar plates. Colonies were counted after 12–14 days of incubation at 37°C. Animals were then rested for 6 weeks before either infection with *Mtb*, or sacrifice for cell isolation.

BCG enumeration in tissues

Approximately half of each spleen and the right-hand side lobes of the lungs from mice in the immunogenicity group were used to determine the number of viable BCG bacteria in each organ six weeks after vaccination. Tissues were removed aseptically in a microbiological safety cabinet and placed in sterile 2 ml screwcap

vials containing 500 μ l PBS + 0.05% Tween80 and Precellys 1.4mm ceramic beads (CK14; Peqlab, Sarisbury Green, UK). A Precellys 24 homogeniser (Peqlab) was used to homogenise tissues for 15 s at 5000 rpm before plating. Each entire homogenate was plated onto two 7H11 agar plates containing 10% OADC supplement (Yorlab, York, UK) and 0.5% glycerol. Colonies were counted after 3 weeks of incubation at 37°C.

Infection with *M. tuberculosis*

Mice were infected intranasally with *M. tuberculosis* Erdman (BEI Resources, Manassas, VA, USA) 6 weeks after

BCG immunization and kept in isolators under CL-3 containment. Frozen aliquots of *Mtb* Erdman were thawed at room temperature, and diluted in saline. Mice were anaesthetized by an intraperitoneal injection of a combination of Ketamine (50 mg/kg; Ketalar Pfizer Ltd, Kent, UK) and Xylazine (10 mg/kg; Rompun; Berkshire, UK) in saline. Each animal then received 50 μ l of the inoculum, estimated to contain 30 CFU. The number of bacteria in the inoculum was confirmed by plating aliquots on 7H11 agar plates containing 10 % OADC and 0.5 % glycerol.

Seven weeks after infection, animals were killed by cervical dislocation. Lungs and spleens were removed aseptically and homogenized by mechanical disruption in sterile PBS, using the plunger of a 5 ml syringe and a 100 μ m cell strainer. A series of 10-fold dilutions of tissue homogenates in PBS with 0.05 % Tween 80 were plated onto 7H11 agar plates with 10 % OADC supplement and 0.5 % glycerol. Plates were incubated at 37 °C and colonies counted after 3 weeks.

Protection is expressed by the percent reduction of median CFU/lung in the BCG group compared to the control group for each mouse strain.

Flow cytometry

Single cell suspensions from spleens were prepared in RPMI-1640 media (Sigma-Aldrich, Dorset, UK) containing 10% heat-inactivated FBS (Labtech International Ltd, Uckfield, UK) and 2 mM L-Glutamine (Fisher Scientific, Loughborough, UK) as soon as possible after sacrifice. Spleens were mechanically disrupted by mashing through a 100 μ m cell strainer using the rubber end of the plunger from a 5ml syringe. Lungs were collected into RPMI-1640 media without FBS and cut into small pieces of approx. 2mm³ before incubation with 0.5mg/ml Liberase TL (Sigma-Aldrich) and 10 μ g/ml DNase (Sigma-Aldrich). The enzyme reaction was stopped by adding an equal amount of media containing 10% FBS and the tissue was mashed as above to obtain single cells. Cells were fixed and red blood cells lysed by adding lyse-fix solution (PhosFlow; Becton Dickinson, Oxford, UK). After fixing, cell suspensions were made up in PBS + 1% FBS.

Approximately 10⁶ cells were stained with the following antibody cocktail in BD Brilliant Stain buffer as per manufacturer's instructions (Becton Dickinson): CD3-APC/Cy7 (clone 17A2, 1:80), B220-BV510 (clone RA3-6B2, 1:40), Ly6G-BV711 (clone 1A8, 1:40), CD11b-BV650 (clone M1/70, 1:60), CD11c-BV605 (clone N418, 1:40). All antibodies were purchased from Biologend (via Fisher Scientific).

Cells from each tissue from one mouse per strain were used as fluorescence minus one (FMO) controls. These were stained with the antibody cocktail as described above, but without one of the antibodies. This was done for each antibody. FMO controls were used to guide gating.

OneComp beads (eBioscience via Fisher Scientific, Loughborough, UK) were stained with single antibodies as per manufacturer's instructions and used to calculate compensation

using the automatic function in FlowJo version 10.4. Compensation matrices were manually checked and adjusted where necessary.

Analysis was carried out using FlowJo version 10.4.

The ML ratio was calculated by dividing the percentage of monocytes/macrophages (Mono_Mac) (B220⁻ CD3⁻ Ly6G⁻ CD11b⁺ CD11c^{low-int}) relative to single cells by the percentage of B cells (B220⁺) and T cells (CD3⁺): Mono_Mac (% of single cells) / [B cells (% of single cells) + T cells (% of single cells)]

IFN- γ ELISPOT

To quantify IFN- γ secreting antigen-specific splenocytes, single cell suspensions were prepared by mechanical disruption of the remaining spleen samples from the immunogenicity group through a 100 μ m cell strainer as soon as possible after sacrifice. After lysis of red blood cells, single cell suspensions were made up in RPMI-1640 media containing 10% heat-inactivated FBS and 2 mM L-Glutamine. 96-well microtiter ELISPOT plates (MAIPS4510, Millipore, Watford, UK) were coated with 10 μ g/ml rat anti-mouse IFN- γ (clone AN18, Mabtech, Nacka Strand, Sweden). Free binding sites were blocked with RPMI-1640 supplemented with 10% heat-inactivated FBS and 2 mM L-Glutamine. 2 \times 10⁵ of total splenocytes were added and incubated in duplicate with PPD (10 μ g/ml), supplemented RPMI as a negative control, or Phorbol myristate acetate (PMA) (0.1 μ g/ml, Sigma-Aldrich) and Phytohemagglutinin (PHA) (1 μ g/ml, Sigma-Aldrich) as a positive control. After overnight incubation at 37°C in 5% CO₂, IFN- γ was detected with 1 μ g/ml biotin labelled rat anti-mouse antibody (clone R4-6A2, Mabtech) and 1 μ g/ml alkaline phosphatase-conjugated streptavidin (Mabtech). The enzyme reaction was developed with BCIP/NBT substrate (5-Bromo-4-chloro-3-indolyl phosphate/Nitro blue tetrazolium) (MP Biochemicals, UK) and stopped by washing the plates with tap water when individual spots could be visually detected (up to 5min). ELISPOT plates were analysed using an automatic plate reader. IFN- γ -specific cells are expressed as number of spot-forming units (SFU) per million spleen cells after non-specific background was subtracted using negative control wells.

Statistical analysis

Groups of animals were compared, and a *p* value of <0.05 was considered statistically significant. Statistical analysis was carried out using GraphPad Prism version 6. The specific test used for each analysis is described in the figure legends.

Results

The ML ratio differs significantly in four inbred mouse strains

Four commercially available inbred mouse strains were chosen to investigate the impact of the baseline ML ratio on BCG vaccine efficacy. A/J, DBA/2, C57Bl/6 and 129S2 mice were selected to represent varying monocyte frequencies and a range of BCG-mediated protection based on available data (Jax Phenome Database <https://phenome.jax.org>; ^{10,11}). To allow the direct comparison of the ML ratio between strains, animals were age and sex matched and all samples were processed at the same time, stained with aliquots of the same antibody cocktail, and

data acquired as a batch. All animals used in this experiment were included in the analysis.

We found significant differences between mouse strains in their baseline ML ratio in blood, spleen, and lung (Figure 1). Across all tissues, A/J mice showed the lowest ML ratio (Figure 1 B–D). In spleen and blood, the ML ratio of DBA/2, C57Bl/6 and 129S2 mice was higher than A/J, but only minor differences were found between those three strains (Figure 1 B and D). In the lung, differences between all strains were more apparent (Figure 1C). 129S2 mice had the highest ML ratio, with DBA/2 and C57Bl/6 showing intermediate levels. These differences in ML ratio were mostly driven by differing frequencies in monocytes/macrophages, with minor differences in B and T cell frequencies between mouse strains (Figure. S1–S3).

Dataset 1. Flow cytometry raw data

<http://dx.doi.org/10.5256/f1000research.14239.d207942>

This file contains the data underlying the analysis of the ML ratio and cell subsets in blood, spleen, and lung shown in Figure 1, Figure 2B, Figure S1, Figure S2, and Figure S3.

To assess the impact of these differences in ML ratio on BCG efficacy in our model, we infected mice of all strains with virulent *Mtb* Erdmann.

Mouse strains with varying ML ratios are differentially protected from *Mtb* infection by BCG

Mice of each strain were vaccinated s.c. with BCG, or left untreated, and infected with *Mtb* Erdmann six weeks later. The extent of protection by BCG was measured by determining the bacterial burden in lung and spleen of vaccinated and control mice (Figure 2). All mice were immunised with the same inoculum of BCG and infected using the same inoculum of *Mtb*, so that results of the different strains are directly comparable. All animals were included in the analysis and no unexpected adverse events were observed. No more than 10% weight loss was recorded over the duration of the experiment. We found varying degrees of protection (Figure 2A). A/J mice were the most protected with a difference in median CFU (Δ) between vaccinated and control groups of $1.41 \log_{10}$, followed by DBA/2 ($\Delta 0.81 \log_{10}$) and C57Bl/6 ($\Delta 0.54 \log_{10}$), and 129S2 mice were the least protected ($\Delta 0.37 \log_{10}$). Interestingly, the mouse strain with the highest ML ratio in the lung showed the lowest protection (129S2), and the strain with the lowest ML ratio showed the highest protection (A/J; Figure 2B). Some differences were also observed in the innate susceptibility between strains, most notably C57Bl/6 mice were significantly less susceptible than DBA/2 ($\Delta 1.16 \log_{10}$ CFU) or A/J mice ($\Delta 1.41 \log_{10}$ CFU). Alveolar macrophages play an important role in the defence against respiratory pathogens, however they are not included in the gate used here to quantify monocytes/macrophages (Figure 2A). While we did not include specific markers for this cell population, they carry a CD11b intermediate (CD11bint), CD11c+ phenotype. We found that the frequency of CD11bint CD11c+ cells was significantly higher in C57Bl/6 mice compared to the other mouse strains (Figure 2E).

Next, to investigate whether differential BCG-mediated protection from *Mtb* infection was associated with a differential immune response, we carried out an IFN γ ELISPOT assay.

Dataset 2. *Mtb* challenge CFU raw data

<http://dx.doi.org/10.5256/f1000research.14239.d197118>

This files contains the raw data as colony forming units (CFU) of the graphs in Figure 2.

A differential antigen-specific IFN γ response is associated with differential protection

To assess the immune response to mycobacterial antigens in the differentially protected mouse strains, splenocytes from mice vaccinated with BCG were stimulated with PPD, and the number of IFN γ -producing cells was measured by ELISPOT (Figure 3). IFN γ is a cytokine associated with control of infection in mice¹² and reduced risk of TB disease in humans⁶. We found that there were significantly more antigen-specific IFN γ producing splenocytes in 129S2 mice than in A/J or DBA/2 mice, both of which were better protected by BCG from *Mtb* challenge than 129S2 mice.

Since BCG is a live mycobacterium, and monocytes and macrophages are the natural host cells for these organisms, it was plausible that a high ML ratio and high IFN γ production in 129S2 mice impair BCG survival and dissemination to and/or persistence in tissues, and thus prevent the formation of a protective immune response in the lung.

Dataset 3. ELISPOT raw data

<http://dx.doi.org/10.5256/f1000research.14239.d197136>

This file contains the raw data for the graph shown in Figure 3

BCG dissemination to lung and spleen is impaired in ML high mice

To determine the extent to which BCG is found in lungs and spleens after s.c. administration, we plated organ homogenates onto 7H11 agar plates and enumerated viable BCG after 3 weeks of culture (Figure 4). We generally found low numbers of bacteria per organ, especially in the lung, where the bacterial count did not exceed 80 CFU/lung in any sample. Moderate differences were detected between mouse strains. Most notably, the most protected ML low A/J mice had the highest number of BCG in the lung, while no BCG was detectable in the lung of the least protected ML high 129S2 mice.

These data led us to speculate that certain host immune-environments, such as a high ML ratio, can influence BCG dissemination and/or persistence, which in turn could impact BCG efficacy.

The data presented here are from one experiment as detailed in the Methods section. To ensure reproducibility, we have endeavoured to include as much experimental detail as possible to allow others to repeat the study and confirm the results. Groups of animals of all strains received the same treatments at the same time to

minimise technical variation. We are therefore confident that the major differences between strains are true biological differences.

Dataset 4. BCG distribution raw data

<http://dx.doi.org/10.5256/f1000research.14239.d197137>

This file contains the raw data as colony forming units (CFU) for the graph shown in Figure 4.

Discussion

The varying efficacy of BCG has long been a concern for the control of the TB epidemic. Numerous factors have been discussed as contributors to this, such as population differences, different BCG strains, vaccination schedules, exposure to environmental mycobacteria, co-infections with viruses and/or parasites, and geographical location^{1,3,13–16}. While BCG works in some populations and protects children from pulmonary and extra-pulmonary disease, new vaccines are urgently needed for the populations where BCG fails to protect, such as adolescents and adults in endemic areas^{1,2}. The incomplete understanding of the mechanisms behind BCG failure, together with limited tools for early assessment of vaccine efficacy, are hampering the development of new vaccines. In order to allow early vaccine testing in a model that better represents the populations most at risk of TB disease, we have taken a correlate of risk observed in human studies and back-translated it into a mouse model. The monocyte to lymphocyte (ML) ratio is a non-specific marker of inflammation and has been shown to be associated with risk of TB disease in several populations, including pregnant HIV infected women, people starting anti-retroviral therapy, BCG vaccinated infants and latently *Mtb* infected adolescents^{7,8,17–19}. Scriba *et al.* show a cascade of inflammatory events as adolescents progress towards disease, which appears to start with increased Type I/II IFN signalling, followed by an increase in monocytes and a decrease in lymphocytes¹⁹. An increased risk of TB disease in BCG vaccinated individuals with a high ML ratio indicates that BCG is failing in those populations.

In order to provide proof of principle that the ML ratio, and observations from human studies more generally, can be back-translated to develop more clinically relevant mouse models, we chose to use commercially available, genetically tractable inbred mouse strains. We could show that these have highly varying ML ratios in blood, spleen, and lung, and that these differences, particularly in the lung, were associated with varying BCG-mediated protection from *Mtb* infection. Using mouse strains with genetically different backgrounds means that there are likely other confounding factors that could impact vaccine efficacy. This is exemplified by the DBA/2 mice, which are well protected despite having a relatively high ML ratio across all tissues. This could be due to the fact that they have a higher neutrophil frequency than some of the other strains (data not shown). Although confounding factors may be at play here, this would also be the case in a clinical setting since an altered ML ratio can have different underlying causes. An increased ML ratio is an indicator for inflammation, likely driven by monocytosis during inflammation. Some factors that are thought to influence BCG

efficacy also drive inflammation, such as co-infection with viruses or parasites, malnutrition, or exposure to environmental mycobacteria. However, as manipulation of ML ratio *in vitro* impacts on ability to control mycobacterial growth, it is likely that ML ratio itself is contributing to TB risk, independent of the factor driving inflammation²⁰. It is also possible that host genetic factors determine baseline inflammation and ML ratio²¹. If this is the case in TB endemic populations, inbred mouse strains with naturally varying ML ratios may be a useful model for BCG vaccine variability.

There are genetic differences between the inbred mouse strains used in this study, some of which have been well described, while others are likely to be unknown. Among the most well described genetic factors is the mutation of the interleukin-3 (IL-3) receptor alpha subunit gene in *A/J* mice, which leads to impaired IL-3 signalling and reduced proliferation of haematopoietic stem cells and their differentiation into myeloid precursors. This is likely to play a role in the low ML ratio observed in these mice^{22,23}. *A/J* mice additionally carry a defect in the gene for Naip5, an intracellular pattern recognition receptor involved in control of proliferation of intracellular pathogens^{24,25}. It may thus have an effect on BCG persistence and dissemination. C57Bl/6 mice carry a polymorphism in the *slc11a1* (formerly *nramp1*) gene, which has been shown to determine susceptibility or resistance to intravenous infection with BCG as defined by BCG load in the spleen²⁶. It does not seem to determine susceptibility to primary *Mtb* infection in mice, and the effect on BCG efficacy is not well studied²⁷. In addition, different inbred mouse strains carry different MHC haplotypes. For the strains used in this study, they are as follows: 129S2, H2^b; C57Bl/6, H2^b; *A/J*, H2^d; DBA/2, H2^d. Each one confers the ability to recognise a slightly different range of epitopes, although there is overlap. This may also impact BCG-mediated immunity.

It is currently unclear what the relative contributions are of genetic and environmental factors to a change in ML ratio²¹. Does a naturally high ML ratio in an individual make them more prone to TB disease, or do other factors including *Mtb* itself drive up the ML ratio, causing BCG to fail? Does a naturally high ML ratio in an individual exacerbate an inflammatory response initiated by environmental factors? There is striking heterogeneity in the immune response to BCG in infants vaccinated at birth, including in the ML ratio and cytokine responses¹⁷. This points towards an involvement of host factors, as the influence of environmental factors would be limited so early in life. On the other hand, Scriba *et al.* observe increases in inflammation and ML ratio over time in adolescents as an individual progresses towards active TB disease and diagnosis¹⁹. This may point towards the pathogen itself as the cause of an altered immune environment.

Interestingly, we found a higher number of antigen-specific IFN γ -producing splenocytes in unprotected 129S2 mice compared to protected *A/J* mice at the time of *Mtb* challenge. This seemed counterintuitive at first, but is in line with recent findings showing that a sub-population of BCG-vaccinated infants with an increased ML ratio showed increased

T cell-mediated cytokine production, and this was associated with increased risk of TB disease¹⁷. High monocyte count and pro-inflammatory cytokines are indicators for inflammation. It is possible that BCG efficacy is impaired in inflammatory immune environments, which may be caused by a variety of factors, such as chronic viral infection, age, malnutrition, or prolonged contact with environmental mycobacteria, all factors thought to impact BCG efficacy. Ultimately, BCG is administered into host immune environments with a heterogeneity that is not fully characterised or understood, yet may have implications for its efficacy.

The exact mechanisms behind an altered BCG vaccine efficacy in a ML high immune environment are currently unknown. Our data indicate that impaired dissemination and/or persistence of BCG may play a role in initiating an effective local immune response. A study by Kaveh and colleagues has shown that BCG persists for up to 16 months in lymph nodes and spleen of Balb/c mice and that persistence of live bacilli contributes to optimal protection from *M. bovis* challenge²⁸. Direct investigation of this phenomenon in humans is not possible; there are however reports that indicate that BCG can disseminate and persist for years in a variety of organs in humans^{29,30}. It is therefore plausible that an immune environment that impairs survival of BCG also impairs vaccine efficacy, although we did not determine in this study whether the absence of live bacilli in lungs of 129S2 mice is due to lack of dissemination or lack of persistence.

The absolute numbers of BCG might be under-estimated in this study as we only enumerated bacilli that were readily growing on standard 7H11 agar plates. Use of PCR methods or culture with resuscitation promoting factors may increase yield and allow for detection of dormant bacilli and their contribution to protection^{31,32}.

If impaired dissemination and/or persistence in certain immune environments is indeed reducing BCG vaccine efficacy, it is reasonable to assume that other live mycobacterial vaccines would have similar limitations. Variability in the ML ratio and more general heterogeneity in the host immune environment should thus be taken into account when designing new live TB vaccines or vaccines based on boosting BCG.

To circumvent potentially impaired dissemination of parenterally administered live vaccines, mucosal administration of live vaccines could be considered. Recent evidence shows that mucosal administration of BCG confers increased protection in animal models, for example by inducing homing of T cells into protected mucosal niches³³⁻³⁵. This agrees with the notion that BCG needs to be present in the lungs to initiate a protective immune response in this organ. Furthermore, subunit vaccines should not show decreased efficacy in ML high immune environments if our hypothesis is correct. Both these possibilities will need careful investigation to shed light on the mechanisms behind BCG failure.

We did not investigate the phenotype of monocytes/macrophages or T cells in this study, although it is likely that this plays

a role. In particular, inflammatory monocytes might lead to killing of BCG. It will be interesting in future to investigate this, as well as comparing the ML ratio and immune cell phenotypes before and after BCG vaccination in the different mouse strains and locations.

We found a significantly higher proportion of CD11b^{int} CD11c⁺ cells in the lungs of C57Bl/6 mice, which are likely to be enriched in alveolar macrophages. Interestingly, C57Bl/6 mice are also the strain least susceptible to *Mtb* infection without BCG vaccination. While the frequency of this population does not seem to be associated with BCG-mediated protection after subcutaneous administration of the vaccine, it could play a role after intranasal vaccination. Alveolar macrophages are located on the luminal side of the epithelium, therefore encountering antigens and pathogens taken up from environmental air. The monocyte/macrophage population included in our ML ratio on the other hand is likely to be of interstitial nature, residing on the basal side of the epithelium and encountering antigens from the blood stream.

While our data on the susceptibility of naïve mouse strains to *Mtb* infection agrees with other studies³⁶, we found some discrepancies between the data presented here and previously published data on BCG-mediated protection. A study using DBA/2 mice has shown that these mice are not protected by s.c. administration of BCG, but control infection with *Mtb* better when vaccinated i.n.¹¹ This is in contrast to our finding that DBA/2 mice are protected from *Mtb* challenge after s.c. vaccination. However, there are some differences between these two studies that may explain the different findings: a different source of mice was used; protection was assessed at 8 weeks vs 6 weeks after vaccination; the BCG strain and *Mtb* strain differed; and the *Mtb* dose used for challenge was three times higher in the study by Aguilo and colleagues compared to ours. Another report detailing the susceptibility of different mouse strains to *Mtb* challenge shows that A/J mice are notably less protected than C57Bl/6 mice¹⁰, while in our hands the opposite is the case. There are important differences between the two studies, including the age and sex of mice used, the time point after vaccination at which protection was measured, and the use of different BCG and *Mtb* strains. In combination, these factors may lead to a differing extent of protection. With particular relevance to this study, the immune cell frequency between male and female animals differs in A/J mice. For example, dataset Donahue5 on the Jackson Laboratory Mouse Phenome Database indicates a higher percentage of monocytes in blood for males compared to females, while T cells are less frequent in males, leading to a higher ML ratio in males³⁷.

In conclusion, the back-translation of a correlate of risk of TB disease, the ML ratio, into an animal model is a step forward for better tools to study the immune mechanisms behind BCG vaccine failure and to test vaccines in a model more relevant to populations most at risk. Hopefully other risk factors can also be back-translated in the future to obtain a more complete picture of vaccine efficacy at very early stages of testing. We would encourage the use of more diverse mouse models in TB vaccine testing and development to reflect the heterogeneity of immune environments found in human populations.

Data availability

Dataset 1: Flow cytometry raw data – This file contains the data underlying the analysis of the ML ratio and cell subsets in blood, spleen, and lung shown in [Figure 1](#), [Figure 2B](#), [Figure S1](#), [Figure S2](#), and [Figure S3](#). [10.5256/f1000research.14239.d207942](https://doi.org/10.5256/f1000research.14239.d207942)³⁸

Dataset 2: Mtb challenge CFU raw data – This files contains the raw data as colony forming units (CFU) of the graphs in [Figure 2](#). [10.5256/f1000research.14239.d197118](https://doi.org/10.5256/f1000research.14239.d197118)³⁹

Dataset 3: ELISPOT raw data – This file contains the raw data for the graph shown in [Figure 3](#). [10.5256/f1000research.14239.d197136](https://doi.org/10.5256/f1000research.14239.d197136)⁴⁰

Dataset 4: BCG distribution raw data – This file contains the raw data as colony forming units (CFU) for the graph shown in [Figure 4](#). [10.5256/f1000research.14239.d197137](https://doi.org/10.5256/f1000research.14239.d197137)⁴¹

Competing interests

No competing interests were disclosed.

Grant information

The work in this article was funded by a grant to HF from the European Commission HORIZON2020 program (TBVAC2020 grant no. 643381) and an Athena SWAN Career Re-entry award funded by the London School of Hygiene and Tropical Medicine to AZ.

The funders had no role in study design, data collection and analysis, decision to publish, or preparation of the manuscript.

Acknowledgements

We would like to thank Christopher Sasseti for helpful discussions and selecting the mouse strains, and Stephanie Canning for expert technical assistance with flow cytometry studies.

Supplementary material

Figure S1: The frequency of T cells varies in tissues of ML high and ML low mouse strains. T cell (CD3⁺) frequencies were determined in blood (A), lung (B) and spleen (C) of four different mouse strains using the gating strategy described in [Figure 2A](#). The ML ratio was calculated using these data. Each symbol represents one animal; box plots represent the median (middle line), 25th to 75th percentile (box) and minimum to maximum value (error bars). Data sets are presented in order of decreasing protection. *p* values were determined using ordinary ANOVA with Holm-Sidak test for multiple comparisons. Multiplicity adjusted *p* values are reported. A *p* value <0.05 was considered statistically significant.

[Click here to access the data.](#)

Figure S2: The frequency of B cells varies in tissues of ML high and ML low mouse strains. B cell frequencies (B220⁺) were determined in blood (A), lung (B) and spleen (C) of four different mouse strains using the gating strategy described in [Figure 2A](#). The ML ratio was calculated using these data. Each symbol represents one animal; box plots represent the median (middle line), 25th to 75th percentile (box) and minimum to maximum value (error bars). Data sets are presented in order of decreasing protection. *p* values were determined using ordinary ANOVA with Holm-Sidak test for multiple comparisons. Multiplicity adjusted *p* values are reported. A *p* value <0.05 was considered statistically significant.

[Click here to access the data.](#)

Figure S3: The frequency of monocytes/macrophages varies in tissues of ML high and ML low mouse strains. Monocyte/macrophage (CD11b⁺ CD11c^{low-int}) frequencies were determined in blood (A), lung (B) and spleen (C) of four different mouse strains using the gating strategy described in [Figure 2A](#). The ML ratio was calculated using these data. Each symbol represents one animal; box plots represent the median (middle line), 25th to 75th percentile (box) and minimum to maximum value (error bars). Data sets are presented in order of decreasing protection. *p* values were determined using ordinary ANOVA with Holm-Sidak test for multiple comparisons. Multiplicity adjusted *p* values are reported. A *p* value <0.05 was considered statistically significant.

[Click here to access the data.](#)

References

- Mangtani P, Abubakar I, Ariti C, *et al.*: **Protection by BCG vaccine against tuberculosis: a systematic review of randomized controlled trials.** *Clin Infect Dis.* 2014; **58**(4): 470–80. [PubMed Abstract](#) | [Publisher Full Text](#)
- Colditz GA, Brewer TF, Berkey CS, *et al.*: **Efficacy of BCG vaccine in the prevention of tuberculosis. Meta-analysis of the published literature.** *JAMA.* 1994; **271**(9): 698–702. [PubMed Abstract](#) | [Publisher Full Text](#)

3. Dockrell HM, Smith SG: **What Have We Learnt about BCG Vaccination in the Last 20 Years?** *Front Immunol.* 2017; **8**: 1134.
[PubMed Abstract](#) | [Publisher Full Text](#) | [Free Full Text](#)
4. Zak DE, Penn-Nicholson A, Scriba TJ, *et al.*: **A blood RNA signature for tuberculosis disease risk: a prospective cohort study.** *Lancet.* 2016; **387**(10035): 2312–22.
[PubMed Abstract](#) | [Publisher Full Text](#) | [Free Full Text](#)
5. Berry MP, Graham CM, McNab FW, *et al.*: **An interferon-inducible neutrophil-driven blood transcriptional signature in human tuberculosis.** *Nature.* 2010; **466**(7309): 973–7.
[PubMed Abstract](#) | [Publisher Full Text](#) | [Free Full Text](#)
6. Fletcher HA, Snowden MA, Landry B, *et al.*: **T-cell activation is an immune correlate of risk in BCG vaccinated infants.** *Nat Commun.* 2016; **7**: 11290.
[PubMed Abstract](#) | [Publisher Full Text](#) | [Free Full Text](#)
7. Naranbhai V, Hill AV, Abdoal Karim SS, *et al.*: **Ratio of monocytes to lymphocytes in peripheral blood identifies adults at risk of incident tuberculosis among HIV-infected adults initiating antiretroviral therapy.** *J Infect Dis.* 2014; **209**(4): 500–9.
[PubMed Abstract](#) | [Publisher Full Text](#) | [Free Full Text](#)
8. Naranbhai V, Moodley D, Chipato T, *et al.*: **The association between the ratio of monocytes:lymphocytes and risk of tuberculosis among HIV-infected postpartum women.** *J Acquir Immune Defic Syndr.* 2014; **67**(5): 573–5.
[PubMed Abstract](#) | [Publisher Full Text](#) | [Free Full Text](#)
9. Petruccioli E, Scriba TJ, Petrone L, *et al.*: **Correlates of tuberculosis risk: predictive biomarkers for progression to active tuberculosis.** *Eur Respir J.* 2016; **48**(6): 1751–63.
[PubMed Abstract](#) | [Publisher Full Text](#) | [Free Full Text](#)
10. Smith CM, Proulx MK, Olive AJ, *et al.*: **Tuberculosis Susceptibility and Vaccine Protection Are Independently Controlled by Host Genotype.** *mBio.* 2016; **7**(5): pii: e01516–6.
[PubMed Abstract](#) | [Publisher Full Text](#) | [Free Full Text](#)
11. Aguilo N, Alvarez-Arguedas S, Uranga S, *et al.*: **Pulmonary but Not Subcutaneous Delivery of BCG Vaccine Confers Protection to Tuberculosis-Susceptible Mice by an Interleukin 17-Dependent Mechanism.** *J Infect Dis.* 2016; **213**(5): 831–9.
[PubMed Abstract](#) | [Publisher Full Text](#)
12. Cooper AM, Dalton DK, Stewart TA, *et al.*: **Disseminated tuberculosis in interferon gamma gene-disrupted mice.** *J Exp Med.* 1993; **178**(6): 2243–7.
[PubMed Abstract](#) | [Publisher Full Text](#) | [Free Full Text](#)
13. Brosch R, Gordon SV, Garnier T, *et al.*: **Genome plasticity of BCG and impact on vaccine efficacy.** *Proc Natl Acad Sci U S A.* 2007; **104**(13): 5596–601.
[PubMed Abstract](#) | [Publisher Full Text](#) | [Free Full Text](#)
14. Muller J, Matsumiya M, Snowden MA, *et al.*: **Cytomegalovirus infection is a risk factor for TB disease in Infants.** *bioRxiv.* 2017; 222846.
[Publisher Full Text](#)
15. Lalor MK, Ben-Smith A, Gorak-Stolinska P, *et al.*: **Population differences in immune responses to Bacille Calmette-Guérin vaccination in infancy.** *J Infect Dis.* 2009; **199**(6): 795–800.
[PubMed Abstract](#) | [Publisher Full Text](#) | [Free Full Text](#)
16. Chatterjee S, Natman TB: **Helminth-induced immune regulation: implications for immune responses to tuberculosis.** *PLoS Pathog.* 2015; **11**(11): e1004582.
[PubMed Abstract](#) | [Publisher Full Text](#) | [Free Full Text](#)
17. Fletcher HA, Filali-Mouhim A, Nemes E, *et al.*: **Human newborn bacille Calmette-Guérin vaccination and risk of tuberculosis disease: a case-control study.** *BMC Med.* 2016; **14**(1): 76.
[PubMed Abstract](#) | [Publisher Full Text](#) | [Free Full Text](#)
18. Naranbhai V, Kim S, Fletcher H, *et al.*: **The association between the ratio of monocytes:lymphocytes at age 3 months and risk of tuberculosis (TB) in the first two years of life.** *BMC Med.* 2014; **12**(1): 120.
[PubMed Abstract](#) | [Publisher Full Text](#) | [Free Full Text](#)
19. Scriba TJ, Penn-Nicholson A, Shankar S, *et al.*: **Sequential inflammatory processes define human progression from *M. tuberculosis* infection to tuberculosis disease.** *PLoS Pathog.* 2017; **13**(11): e1006687.
[PubMed Abstract](#) | [Publisher Full Text](#) | [Free Full Text](#)
20. Naranbhai V, Fletcher HA, Tanner R, *et al.*: **Distinct Transcriptional and Anti-Mycobacterial Profiles of Peripheral Blood Monocytes Dependent on the Ratio of Monocytes: Lymphocytes.** *EBioMedicine.* 2015; **2**(11): 1619–26.
[PubMed Abstract](#) | [Publisher Full Text](#)
21. Lin BD, Willemssen G, Fedko IO, *et al.*: **Heritability and GWAS Studies for Monocyte-Lymphocyte Ratio.** *Twin Res Hum Genet.* 2017; **20**(2): 97–107.
[PubMed Abstract](#) | [Publisher Full Text](#)
22. Ichihara M, Hara T, Takagi M, *et al.*: **Impaired interleukin-3 (IL-3) response of the A/J mouse is caused by a branch point deletion in the IL-3 receptor alpha subunit gene.** *EMBO J.* 1995; **14**(5): 939–950.
[PubMed Abstract](#) | [Free Full Text](#)
23. Morris CF, Salisbury J, Kobayashi M, *et al.*: **Interleukin 3 alone does not support the proliferation of bone marrow cells from A/J mice: a novel system for studying the synergistic activities of IL-3.** *Br J Haematol.* 1990; **74**(2): 131–137.
[PubMed Abstract](#) | [Publisher Full Text](#)
24. Kang TJ, Lee GS, Kim SK, *et al.*: **Comparison of two mice strains, A/J and C57BL/6, in caspase-1 activity and IL-1beta secretion of macrophage to *Mycobacterium leprae* infection.** *Mediators Inflamm.* 2010; **2010**: 1–5, 708713.
[PubMed Abstract](#) | [Publisher Full Text](#) | [Free Full Text](#)
25. Lamkanfi M, Amer A, Kanneganti TD, *et al.*: **The Nod-like receptor family member Naip5/Birc1e restricts *Legionella pneumophila* growth independently of caspase-1 activation.** *J Immunol.* 2007; **178**(12): 8022–8027.
[PubMed Abstract](#) | [Publisher Full Text](#)
26. Sellers RS, Clifford CB, Treuting PM, *et al.*: **Immunological variation between inbred laboratory mouse strains: points to consider in phenotyping genetically immunomodified mice.** *Vet Pathol.* 2012; **49**(1): 32–43.
[PubMed Abstract](#) | [Publisher Full Text](#)
27. North RJ, LaCourse R, Ryan L, *et al.*: **Consequence of *Nramp1* deletion to *Mycobacterium tuberculosis* infection in mice.** *Infect Immun.* 1999; **67**(11): 5811–5814.
[PubMed Abstract](#) | [Free Full Text](#)
28. Kaveh DA, Garcia-Pelayo MC, Hogarth PJ: **Persistent BCG bacilli perpetuate CD4 T effector memory and optimal protection against tuberculosis.** *Vaccine.* 2014; **32**(51): 6911–8.
[PubMed Abstract](#) | [Publisher Full Text](#)
29. Tajima Y, Takagi R, Nakajima T, *et al.*: **An infant with asymptomatic hepatic granuloma probably caused by bacillus Calmette-Guérin (BCG) vaccination found incidentally at autopsy: a case report.** *Cases J.* 2008; **1**(1): 337.
[PubMed Abstract](#) | [Publisher Full Text](#) | [Free Full Text](#)
30. Gormsen H: **On The Occurrence Of Epithelioid Cell Granulomas In The Organs Of Bcg-Vaccinated Human Beings.** *Acta Pathol Microbiol Scand Suppl.* 1956; **38**(Suppl 111): 117–20.
[PubMed Abstract](#) | [Publisher Full Text](#)
31. Loraine J, Pu F, Turapov O, *et al.*: **Development of an *In Vitro* Assay for Detection of Drug-Induced Resuscitation-Promoting-Factor-Dependent Mycobacteria.** *Antimicrob Agents Chemother.* 2016; **60**(10): 6227–33.
[PubMed Abstract](#) | [Publisher Full Text](#) | [Free Full Text](#)
32. Jin TH, Qu T, Raina A, *et al.*: **Identification of Growth Promoting Effect of rBCG/BCG Culture Supernatant and Its Potential Applications.** *WJV.* 2013; **2013**(02): 32–8.
[Publisher Full Text](#)
33. Lai R, Afkhami S, Haddadi S, *et al.*: **Mucosal immunity and novel tuberculosis vaccine strategies: route of immunisation-determined T-cell homing to restricted lung mucosal compartments.** *Eur Respir Rev.* 2015; **24**(136): 356–60.
[PubMed Abstract](#) | [Publisher Full Text](#)
34. Perdomo C, Zedler U, Kühl AA, *et al.*: **Mucosal BCG Vaccination Induces Protective Lung-Resident Memory T Cell Populations against Tuberculosis.** *mBio.* 2016; **7**(6): pii: e01686–16.
[PubMed Abstract](#) | [Publisher Full Text](#) | [Free Full Text](#)
35. Jeyanathan M, Afkhami S, Khera A, *et al.*: **CXCR3 Signaling Is Required for Restricted Homing of Parenteral Tuberculosis Vaccine-Induced T Cells to Both the Lung Parenchyma and Airway.** *J Immunol.* 2017; **199**(7): 2555–69.
[PubMed Abstract](#) | [Publisher Full Text](#)
36. Chackerian AA, Behar SM: **Susceptibility to *Mycobacterium tuberculosis*: lessons from inbred strains of mice.** *Tuberculosis (Edinb).* 2003; **83**(5): 279–85.
[PubMed Abstract](#) | [Publisher Full Text](#)
37. Donahue L, Morgan J: **Donahue 5.** Mouse Phenome Database. (Accessed: 9 February 2018).
[Reference Source](#)
38. Zelmer A, Stockdale L, Prabowo SA, *et al.*: **Dataset 1 in: High monocyte to lymphocyte ratio is associated with impaired protection after subcutaneous administration of BCG in a mouse model of tuberculosis.** *F1000Research.* 2018.
[Data Source](#)
39. Zelmer A, Stockdale L, Prabowo SA, *et al.*: **Dataset 2 in: High monocyte to lymphocyte ratio is associated with impaired protection after subcutaneous administration of BCG in a mouse model of tuberculosis.** *F1000Research.* 2018.
[Data Source](#)
40. Zelmer A, Stockdale L, Prabowo SA, *et al.*: **Dataset 3 in: High monocyte to lymphocyte ratio is associated with impaired protection after subcutaneous administration of BCG in a mouse model of tuberculosis.** *F1000Research.* 2018.
[Data Source](#)
41. Zelmer A, Stockdale L, Prabowo SA, *et al.*: **Dataset 4 in: High monocyte to lymphocyte ratio is associated with impaired protection after subcutaneous administration of BCG in a mouse model of tuberculosis.** *F1000Research.* 2018.
[Data Source](#)



The TB vaccine H56 + IC31 dose-response curve is peaked not saturating: Data generation for new mathematical modelling methods to inform vaccine dose decisions



Sophie J. Rhodes^{a,*}, Andrea Zelmer^{b,1}, Gwenan M. Knight^{a,c}, Satria Arief Prabowo^b, Lisa Stockdale^b, Thomas G. Evans^d, Thomas Lindenstrøm^e, Richard G. White^{a,2}, Helen Fletcher^{b,2}

^a TB Modelling Group, CMMID, TB Centre, London School of Hygiene and Tropical Medicine, UK

^b Immunology and Infection Department, London School of Hygiene and Tropical Medicine, UK

^c National Institute for Health Research Health Protection Research Unit in Healthcare Associated Infection and Antimicrobial Resistance, Imperial College London, UK

^d TomegaVax, Portland, OR, United States

^e Statens Serum Institut, Copenhagen, Denmark

ARTICLE INFO

Article history:

Received 12 July 2016

Received in revised form 4 October 2016

Accepted 22 October 2016

Available online 2 November 2016

ABSTRACT

Introduction: In vaccine development, dose-response curves are commonly assumed to be saturating. Evidence from tuberculosis (TB) vaccine, H56 + IC31 shows this may be incorrect. Mathematical modelling techniques may be useful in efficiently identifying the most immunogenic dose, but model calibration requires longitudinal data across multiple doses and time points.

Aims: We aimed to (i) generate longitudinal response data in mice for a wide range of H56 + IC31 doses for use in future mathematical modelling and (ii) test whether a 'saturating' or 'peaked' dose-response curve, better fit the empirical data.

Methods: We measured IFN- γ secretion using an ELISPOT assay in the splenocytes of mice who had received doses of 0, 0.1, 0.5, 1, 5 or 15 μ g H56 + IC31. Mice were vaccinated twice (at day 0 and 15) and responses measured for each dose at 8 time points over a 56-day period following first vaccination. Summary measures Area Under the Curve (AUC), peak and day 56 responses were compared between dose groups. Corrected Akaike Information Criteria was used to test which dose-response curve best fitted empirical data, at different time ranges.

Results: (i) All summary measures for dose groups 0.1 and 0.5 μ g were higher than the control group ($p < 0.05$). The AUC was higher for 0.1 than 15 μ g dose. (ii) There was strong evidence that the dose-response curve was peaked for all time ranges, and the best dose is likely to be lower than previous empirical experiments have evaluated.

Conclusion: These results suggest that the highest, safe dose may not always optimal in terms of immunogenicity, as the dose-response curve may not saturate. Detailed longitudinal dose range data for TB vaccine H56 + IC31 reveals response dynamics in mice that should now be used to identify optimal doses for humans using clinical data, using new data collection and mathematical modelling.

© 2016 The Authors. Published by Elsevier Ltd. This is an open access article under the CC BY-NC-ND license (<http://creativecommons.org/licenses/by-nc-nd/4.0/>).

1. Introduction

Vaccines are one of the most important and cost-effective interventions in public health [1]. However, development from vaccine discovery to licensure is costly; in the region of US\$0.8 billion [2]. Mistakes in vaccine development may cause not only a waste of resources (both financial and experimental) but also ultimately,

delay licensure of an effective vaccine. A key decision in development is vaccine dose amount (hereafter dose), which, if chosen optimally would achieve maximum vaccine efficacy, with minimal side effects.

It is common practise in pre-clinical and clinical trials that vaccine dose is increased incrementally until a maximum safe dose that promotes an effective response (usually an antibody response) is achieved; it is assumed that this response will then saturate [3]. This saturating relationship between dose and host response has been the standard assumption in vaccine development and many vaccines have proceeded through to the late stages of development with this method as a basis for dose choice [4,5].

* Corresponding author.

E-mail address: sophie.rhodes@lshtm.ac.uk (S.J. Rhodes).

¹ Joint first authors.

² Joint senior authors.

However, in tuberculosis (TB) vaccine development, early pre-clinical studies in mice with the IC31 adjuvanted fusion protein TB10.4 /Ag85B (H4) revealed that low antigen doses were both more immunogenic and provided increased protection relative to high doses [6]. In accordance, a clinical study showed that responses after vaccination with the same H4 + IC31 vaccine were not different between the 5 and 15 µg doses, decreased at 50 µg and were minimal for the 150 µg dose [7]. In a latently infected target population, vaccination with an analogous vaccine H56 (an ESAT-6/Ag85B/Rv2620 fusion protein vaccine) also adjuvanted with IC31 (H56 + IC31) showed that out of two doses tested in Quantiferon-positive (QTF+) individuals, the lowest dose (15 µg H56 + IC31) was more effective at inducing polyfunctional CD4+ T cell responses than the higher dose (50 µg H56 + IC31) [8]. Of note, the higher dose (50 µg) of the related first-generation Hybrid vaccine H1 + IC31 was taken forward to a First-in-man study, which may have led to suboptimal vaccine evaluation [9]. Although immunogenicity not only depends on antigen dose, but indeed also on the type and nature of the adjuvant employed, the incorrect assumption that a higher dose is preferred per se for protein vaccines (or other platforms) has further been brought into question by vaccines using other types of adjuvants [10].

Translational quantitative analysis methods to inform dose decision-making already exist in the drug development world. Pharmacokinetic/Pharmacodynamic (PK/PD) modelling uses mechanistic mathematical methods to describe how dose influences drug dynamics over time [11,12]. Translational modelling to predict human PK/PD parameters based on animal data is a key stage in model-based drug dose decision-making [12–14], and is often required by regulators during development. Although pharmacokinetic data is often not available for vaccines, pharmacokinetics is dependent on dose and regimen, and thus analogies to dose finding for vaccines are relevant. No translational quantitative methods are applied in vaccine development, as the chosen vaccine dose to be tested in a clinical environment is usually based on qualitative assessment of the pre-clinical data [15], which has the potential to ignore or underutilise dose-response information.

To address this gap, we are proposing the new field of *Immunosimulation/Immunodynamic (IS/ID) modelling*, analogous to that of PK/PD modelling, to make more informed human vaccine dosing decisions based on animal response data. In this field, models will be created to describe the underlying mechanisms that determine the immune response dynamics (immunodynamics) following vaccination, e.g. the influence of the innate and regulatory systems for T cell expansion and contraction (immunostimulation). These models will then be calibrated to dose ranging data from animals and model parameters “mapped” to known human response data. Subsequently, dose-response curve in humans can be predicted, providing information on the most effective range of doses to be first evaluated in clinical trials. In this larger body of work, we will apply these methods on the aforementioned TB vaccine, H56 + IC31 by measuring IFN-γ after vaccination over time.

As in model-based drug development, extensive longitudinal data are required. Published data on a wide dynamic range of doses and time points do not exist for H56 + IC31, where dose-ranging studies have only ever been conducted on minimal pre-specified time points [6]. As such, we conducted and report here an experiment in which we vaccinated mice with a wide range of doses of H56 + IC31 and measured responses extensively over time. These data outlined in this paper will be used in future IS/ID modelling to further our knowledge in mice, non-human primates and humans. In this paper, we aim to (i) generate longitudinal response data in mice for a wide range of H56 + IC31 doses for use in future mathematical modelling and (ii) test whether a ‘saturating’ or ‘peaked’ dose-response curve, better fit the empirical data.

2. Materials and methods

2.1. Ethics statement

All animal work was carried out in accordance with the Animals (Scientific Procedures) Act 1986 under a license granted by the UK Home Office (PPL 70/8043), and approved by the LSHTM Animal Welfare and Ethics Review Body.

2.2. Animals

Female CB6F1 mice were acquired from Charles River UK at 6–8 weeks of age. Animals were housed in specific pathogen-free individually vented cages, were fed ad libitum, and were allowed to acclimatize for at least 5 days before the start of any experimental procedure.

2.3. Vaccination

The experimental vaccine H56 (comprising *Mycobacterium tuberculosis* antigens Ag85B-ESAT-6-Rv2660c [16], provided by Statens Serum Institute (SSI), Copenhagen, Denmark) was formulated in IC31® adjuvant (provided by SSI on behalf of Valneva Technologies) and 10 mM Tris-HCl buffer (pH 7.4) as described in [17] to obtain a final volume of 200 µl/mouse. The adjuvant IC31® consists of a mixture of the cationic peptide KLK (NH₂-KLKL5KLK-COOH) and the oligodeoxynucleotide ODN1a (oligo-(dIdC)13). Adjuvant doses were 100 nmol peptide and 4 nmol oligonucleotide for every vaccine (H56) dose. Antigen doses of 0.1, 0.5, 1, 5 or 15 µg of H56 + 100/4 nmol IC31 (hereafter, H56 + IC31) were administered per animal at day 0 and 15, the same dose was used at both vaccination times within a group. Control animals received no vaccination. The vaccine was administered subcutaneously into the left or right leg flap.

2.4. IFN-γ ELISPOT

IFN-γ secreting CD4+ T cells were measured using the ELISPOT assay. Single cell suspensions of mouse splenocytes were prepared by mechanical disruption of spleens through a 100 µm cell strainer on the day of sacrifice. After lysis of red blood cells, single cell suspensions were made up in antibiotic-free media [RPMI-1640 (Sigma-Aldrich, Dorset, UK) + 10% heat-inactivated FBS (Labtech International Ltd, Uckfield, UK) + 2 mM L-Glutamine (Fisher Scientific, Loughborough, UK)]. 96-well microtiter ELISPOT plates (MAIP54510, Millipore, Watford, UK) were coated with 10 µg/ml rat anti-mouse IFN-γ (clone AN18, Mabtech, Nacka Strand, Sweden). Free binding sites were blocked with RPMI 1640 supplemented as described above. 2.5×10^5 of total splenocytes were added and incubated in duplicate with H56 (10 µg/ml), supplemented RPMI as a negative control, or Phorbol myristate acetate (PMA) (50 µg/ml, Sigma-Aldrich) and Phytohemagglutinin (PHA) (10 µg/ml, Sigma-Aldrich) as a positive control. After 24 or 48 h of incubation at 37 °C in 5% CO₂, IFN-γ was detected with 1 µg/ml biotin labelled rat anti-mouse antibody (clone R4-6A2, Mabtech) and 1 µg/ml alkaline phosphatase-conjugated streptavidin (Mabtech). The enzyme reaction was developed with BCIP/NBT substrate (5-Bromo-4-chloro-3-indolyl phosphate/Nitro blue tetrazolium) (MP Biochemicals, UK) and stopped by washing the plates with tap water when individual spots could be visually detected (up to 5 min). ELISPOT plates were analysed using an automatic plate reader. IFN-γ-specific cells are expressed as number of spot-forming units (SFU) per million spleen cells after non-specific background was subtracted using negative control wells.

2.5. Experimental schedule

ELISPOTs were carried out at 2, 7, 9, 14, 16, 21, 28, and 56 days after the first vaccination for all doses. Five mice were used per time point per dose group (equating to 40 mice in a dose group from initiation to conclusion of the experiment). This schedule was designed to reflect the H56 + IC31 phase I clinical trial schedule [8] and previous experimental schedules in mice using the H-series vaccines by SSI in CB6F1 mice [6,16,18,19].

2.6. Statistical methods

2.6.1. Summary of IFN- γ response data after two vaccinations with TB vaccine H56+IC31 for future mathematical modelling

The Wilcoxon test was used to test for differences in IFN- γ responses generated as a result of the two ELISPOT incubation times (on data pooled across dose groups and time points). The following summary measures were used to quantify responses over time: Area Under the Curve (AUC), day 56 response, peak response between first and second vaccination and peak response post-second vaccination (peaks may occur at different times as they were defined as the highest median response measured in the respective time period). As IFN- γ responses over time within a dose group were not dependent (each taken from an individual mouse spleen), AUC was calculated using 200 samples of the possible combinations of the five mice per dose group over time. Full details of this method are outlined in [Supplementary material and Fig. S1](#). The non-parametric Dunn test was used to compare the summary measures between the dose groups and a Bonferroni correction applied to account for comparisons across multiple groups. A p -value < 0.05 was considered significant.

2.6.2. Determine the shape of dose-response curve when examined at varying sample times and the best dose predicted by fitted curves

To assess the shape of the dose-response curve (IFN- γ SFU per million splenocytes versus dose), a saturating or peaked curve was fitted to all IFN- γ responses against the (\log_{10} transformed) doses using nonlinear regression, in the software Prism (v 7 for Mac, GraphPad Software, California USA, www.graphpad.com). Briefly, the aim of nonlinear regression is to find the parameters that minimise the sum of the squared residuals from all data points to the curve (see [Supplementary material for description](#)). We choose a sigmoidal equation as the saturating curve and the gamma probability density function (pdf) as the peaked curve (see [Supplementary for equations](#)). The choice of the gamma pdf was due to the hypothesis that the dose response, once peaked, will not increase again and will never decrease to a zero response. To establish which of the shapes best described the dose-response curves the goodness-of-fit measure, the corrected Akaike information criteria (AICc) was compared, where a lower AICc indicates a better fit. A difference in AICc value between curve fits of greater than seven was considered strong evidence of a better fit and a difference in AICc of greater than ten was considered absolute evidence of a better fit [20] ([Table S1](#)). To assess how the dose-response curve changed with time, the response data was pooled into three time ranges: between the first and second vaccination (day 2, 7, 9, 14 aggregated), post-second vaccination (day 21, 28 and 56 aggregated) and day 56 responses. The best dose was defined as the dose that produced the maximum IFN- γ response as predicted by the fitted curves.

3. Results

3.1. Summary of IFN- γ response data after two vaccinations with TB vaccine H56+IC31 for future mathematical modelling

Splenocyte-derived IFN- γ responses did not differ for the 24 versus the 48 h ELISPOT incubation times when responses were pooled over all dose groups and time points (p -value = 0.67, [Fig. S2](#)). Therefore, an incubation time of 24 h was used in the following analyses.

The IFN- γ responses over time for each dose group are shown in [Fig. 1](#) (significance of the changes in dynamics over time are in [Table S2](#)). Out of the samples taken to calculate the AUC, the common significance trend showed that dose groups 0.1, 0.5 and 1 μ g had significantly higher AUC than the control group, and the dose group 0.1 μ g had significantly higher AUC than dose group 15 μ g ([Fig. 2, Table S3](#)). Peak responses between first and second vaccination were significantly higher in the dose groups 0.1, 1, 5 μ g than in the control group and for post-second vaccination, dose groups 0.1, 0.5 and 5 μ g were significantly higher than the control group ([Figs. 1 and 2, Table 1](#)). Similarly, day 56 responses were significantly higher for the dose groups 0.1, 0.5 and 1 μ g than the control group and the dose group 0.5 μ g was higher than 15 μ g. However, this did not reach statistical significance ([Figs. 1 and 2, Table 1](#)). For all summary measures, no other comparisons between dose groups were statistically significantly different ([Fig. 2, Table 1](#)).

3.2. Determine the shape of dose-response curve when examined at varying sample times and the best dose predicted by fitted curves

To establish the shape of the dose-response curve (IFN- γ SFU per million splenocytes versus dose), we fitted either a saturating or peaked function for three time ranges. There was strong evidence that the peaked curve was a better fit to the response data between first and second vaccination ([Fig. 3A, Table S4](#)) with a AICc difference of 7.5 favouring the peaked (gamma) curve. The AICc difference was 18.8 and 10.9 for the post-second vaccination ([Fig. 3B, Table S5](#)) and day 56 ([Fig. 3C, Table S6](#)) response data, suggesting absolute support for the peaked curve for both these time ranges. The best dose predicted by the peaked fitted curve for the time ranges; between first and second vaccination, post-second vaccination and day 56 were 0.026, 0.11 and 0.25 μ g, respectively (transformed from \log_{10} scale, [Fig. 3](#)). Due to the right-skewed nature of the responses the best saturation curve had an almost immediate increase followed by immediate plateau for all time ranges ([Fig. 3](#)). As such it was not possible to obtain a best predicted dose using the saturation model as, in this case, all doses generated the same response.

4. Discussion

Our future aim is to apply the new field of Immunostimulation/immunodynamic (IS/ID) modelling to translate vaccine dose-response information between animals and humans and thus quantitatively inform vaccine dose decision-making. To begin initial examination of such methods, we conducted a longitudinal dose-ranging experiment of the novel TB vaccine H56 + IC31 in mice, and a mathematical analysis of the dose-response curve over time.

We successfully generated an intensive time course of IFN- γ response data to vaccination where AUC and peak analysis showed a trend toward higher responses over time in the lower doses than in the higher doses. By using mathematical curve fitting, we showed that the IFN- γ dose-response follows a peaked shape instead of the commonly assumed saturation shape for all time

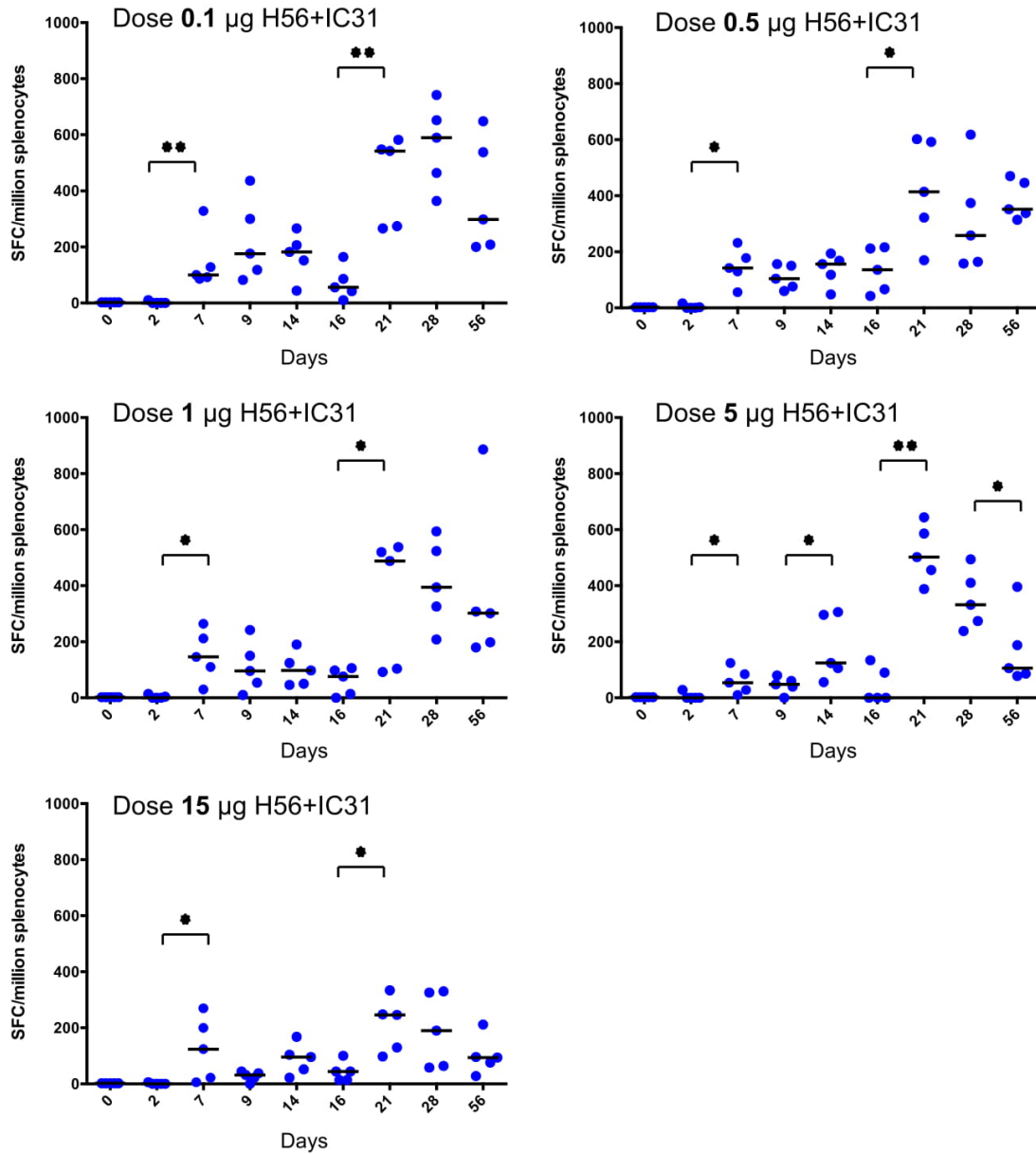


Fig. 1. Median IFN- γ responses (horizontal black bars) and responses of individual mice per time point (blue points) for each dose. As the control group did not receive H56 + IC31, the median of all responses from the control group (which did not significantly change throughout the experiment) was used to represent all mice at baseline. The Wilcoxon test was used to compare consecutive time points, where * equals to p-value < 0.05 and ** p-value < 0.01 (Table S2). (For interpretation of the references to colour in this figure legend, the reader is referred to the web version of this article.)

ranges. This was most apparent post-second vaccination, and trended toward that curve shape after the first dose. Using the peaked fitted curve, we were able to determine which dose may provide the maximal predicted IFN- γ response in mice. Our results indicate this was at a low range; between 0.02 and 0.25 μg H56 + IC31. It must be noted that, there is uncertainty associated with our predictions for best dose which is apparent in Tables S4–S6, where the standard error was high for some gamma distribution function parameters, particularly for the time ranges between first and second vaccination and post-second vaccination. This is poten-

tially due to a lack of response information between dose 0 and 0.1 μg , which would provide information on the increase of the peaked curve. Despite this, as we show a definitive decline in the dose-response at the higher dose range (approximately after dose 1 μg H56 + IC31), our predicted best dose range show compelling evidence that lower doses than previously explored in mice using very similar vaccines [6,16,18,21,22], would be preferential. Importantly, as previous evidence suggest the human dose-response may be of a similar shape for the H-series of vaccines from SSI [7,8] (although higher in magnitude), this implies that previously tested

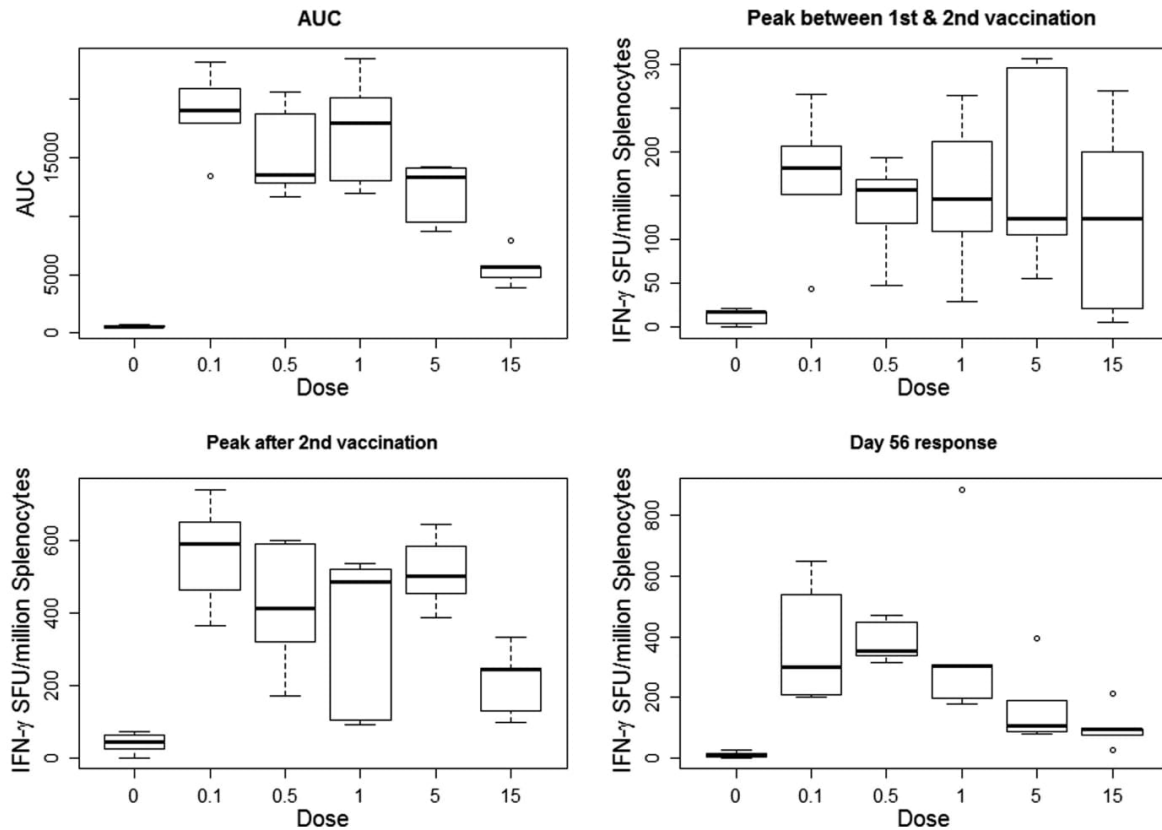


Fig. 2. AUC calculated from number of IFN- γ secreting CD4+ T cells after two vaccinations with H56 + IC31 from individual mice spleens, number of IFN- γ secreting CD4+ T cells between first and second vaccination, after second vaccination and day 56 by dose (μg H56 + 100 nmol IC31). Dose 0 equates to the control group. The plot for AUC is representative of the 200 samples taken to establish statistical differences in AUC by dose (see methods). X axis not to scale.

Table 1

Median (IQR) values for the summary measures day 56 response, peak between first and second vaccination and post-second vaccination IFN- γ responses by dose. Significance in the summary measures was tested between dose groups using the non-parametric Dunn test with a Bonferroni correction. Those comparisons between dose groups with a p-value < 0.05 or 0.05 < p-value < 0.1 (starred) are displayed. Abbreviations: IQR = interquartile range, vacc = vaccination.

Dose group (μg H56 + IC31)	Median day 56 response (IQR)	Significantly different from dose	Median Peak between 1st and 2nd vacc (IQR)	Significantly different from dose	Median Peak post 2nd vacc (IQR)	Significantly different from dose
Control	10 (2–14)	0.1, 0.5, 1	18 (4–18)	0.1, 1, 5	44 (26–64)	0.1, 0.5, 5
0.1	298 (208–538)	Control	182 (152–206)	Control	590 (464–652)	Control
0.5	352 (338–446)	Control, 15*	156 (118–168)	–	414 (322–592)	Control
1	302 (198–308)	Control	146 (110–212)	Control	488 (104–520)	–
5	106 (86–188)	–	124 (106–296)	Control	502 (456–586)	Control
15	94 (76–96)	0.5*	124 (22–200)	–	246 (130–248)	–

clinical dose ranges may also have been too high to capture the optimal response in terms of immunogenicity.

We use the frequency of IFN- γ secreting CD4+ T cells measured using the ELISPOT assay as our chosen immune response readout to reflect the current convention in TB vaccine development for dose selection. IFN- γ is a cytokine shown to be associated with control of infection or decreased risk of TB disease [23], however these findings have been a topic of controversy in TB vaccine development [24]. In previous work by Aagaard et al. in the vaccine H4 + IC31, results showed that mice vaccinated with a lower dose (0.5 μg H4) experienced significantly higher IFN- γ responses than higher doses (5 and 15 μg H4) and, significantly stronger protection against *Mtb.* infection (measured by *Mtb.* colony forming units) than the higher doses, in two independent challenge exper-

iments [6]. These results support our choice of IFN- γ as a readout. We also compliment Aagaard et al.'s study by measuring the IFN- γ response at multiple time points, thus assessing trends in the dose-response curve over time.

It is possible that varying dose may alter the function or type of CD4 T cell secreting IFN- γ , which the ELISPOT assay will not detect. Further lab assays such as flow cytometry should be used in the future work to determine the function or type of cell produced as a result of varying dose, which may then be used in clinical trials for human dose selection.

Dose concentration feasibility and animal cost and overall numbers limited the size of our study. By testing in larger groups of mice at potentially fewer time points, we may have gained greater certainty in response differences and fitted dose-response curves.

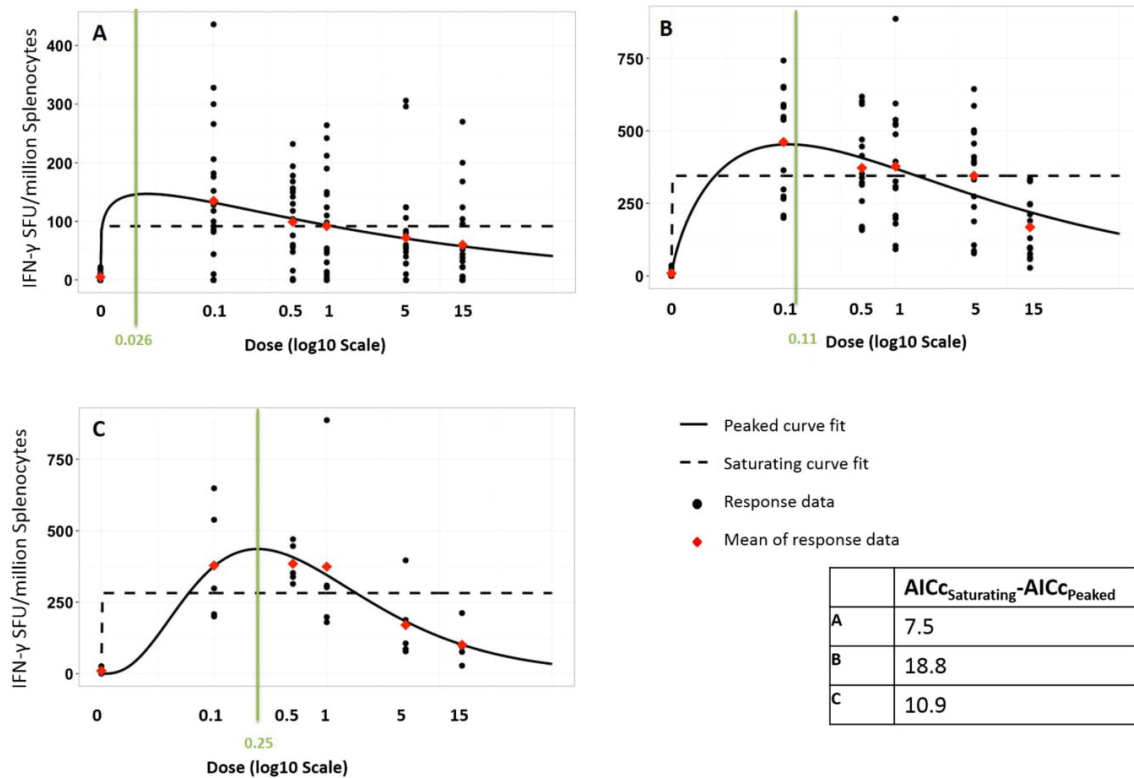


Fig. 3. Results of the dose-response curve fitting analysis for the time ranges (A) between first and second vaccination (aggregated responses from days 2, 7, 9 and 14), (B) post-second vaccination (days 21, 28 and 56) and C. Day 56 (last time point). Black points correspond to the number of IFN- γ secreting CD4+ T cells from one mouse spleen in response to vaccination for the relevant time range, red diamonds show the mean of the responses, the black solid lines are the peaked (gamma) fit, the black dashed line show the saturating (sigmoidal) curve fit and the vertical green line indicated the best dose as predicted by the peaked curve fit. The table shows the differences in AICc for A,B and C between the saturating and peaked curve fits. The x-axis is $\log_{10}(\text{dose: } \mu\text{g H56 + IC31}) + 2$ to transform the dose to a log scale and to ensure positivity, but x-axis labels show the non-logged value for clarity (to avoid infinite values, control (dose 0) is not logged).

However, we chose the extensive time course to determine detailed dynamics of the vaccine response and dose-response curves over time, since this has been performed infrequently in the past. We believe a higher maximum dose may have better defined the decline in the dose-response curve. As the size of the study was limited, we concentrated efforts on the lower doses, where previous exploration is lacking; however, we found that the probable best dose is still lower than the minimum dose used here.

We have identified the following areas for further research. The mathematical curve fitting we conducted has provided the basis for further optimised studies in animals, i.e. we now know that the dose range that captures the probable best dose should be 0–0.3 $\mu\text{g H56 + IC31}$ (based on our predicted best dose values) not the initial 0–15 $\mu\text{g H56 + IC31}$ (a reduction of 98% in the range). Expanding the dose range in the lower end between 0 and 0.1 μg will further increase our best dose predictions, as the peaked curve parameters will be estimated with greater certainty. This warrants further animal studies to investigate in greater detail the host response to low dose vaccination.

Additionally, we used AUC to quantify the magnitude of the immune response for the duration of the experiment and compared AUC between dose groups. However, we do not interpret this measure as the cumulative immune response over time, as would be appropriate in drug AUC measures, but an indication of overall higher immune response magnitude. In vaccine development, dose

decisions are made based on the dose response curve at one time point (usually a long-term time point) and as such it would be advantageous to know how dose effects the dynamics of the immune response that may lead to higher average response in the long-term. As such, our future aim is to apply the new field of Immunostimulation/immunodynamic (IS/ID) modelling, where by a mechanistic mathematical model incorporating the fundamental T cell subsets involved in a Th1 immune response will be calibrated to the ELISPOT or another given measure over time. The IS/ID model will allow us to quantify how the dynamics of the immune response differ between dose groups (and across the entire mouse population) by assessing the change in model parameters by dose. To achieve this, we will use the robust statistical framework, Nonlinear Mixed Effects Modelling to calibrate the model to the data and characterise the parameters and associated parameter variation. IS/ID modelling will also be used to translate vaccine dose-response information between animals and humans. To achieve this we will utilise known allometric scaling factors for H56 + IC31 between mouse and human we aim to “map” IS/ID model parameters from one dose of the outlined experiment to existing human H56 + IC31 dose data (one dose 50 $\mu\text{g H56 + 500 nmol IC31}$). The effect of heterogeneity in target human populations (due to HIV status, existing latent infection, etc.) on IS/ID modelling parameters will be taken into account. Following this mapping, we can then use the remaining doses to predict the dose response curve in humans. This predicted human dose response

curve will be used as a guide to select further doses to test in clinical trials.

Additionally, as the antigen dose-response may also vary with the adjuvant dose and type of adjuvant, in order to fully characterise and optimise complete vaccine (H56 + IC31) dose it would be necessary to perform a checkerboard interaction pattern, the design of which could be informed by IS/ID modelling through optimal design analysis [25].

5. Conclusion

Our results suggest that the highest, safe dose is not always optimal in terms of host response as the dose-response curve is not saturating, which may also be true for vaccines against diseases other than TB. Mathematical modelling can be used on the detailed longitudinal dose range data for TB vaccine H56 + IC31 to simulate responses to optimise further experiments in mice and help to identify optimal doses for humans.

Funding

Funding for the experiment was provided by the Bill and Melinda Gates Foundation. SR is supported by a LSHTM studentship funded by Aeras. The views expressed are those of the author(s) and not necessarily those of the SSI, the NHS, the NIHR, the Department of Health or Public Health England. RGW is funded by the UK Medical Research Council (MRC) and the UK Department for International Development (DFID) under the MRC/DFID Concordat agreement that is also part of the EDCTP2 programme supported by the European Union (MR/J005088/1), the Bill and Melinda Gates Foundation (TB Modelling and Analysis Consortium: OPP1084276) and UNITAID (4214-LSHTM-Sept15; PO #8477-0-600).

Conflicts of interest

There are no conflicts of interest.

Acknowledgements

We would like to thank our collaborators at Staten Serum Institute Peter Andersen and Else Marie Agger (now at Novo Nordisk) for advising the mouse experiment schedule and Steven Kern at the Bill and Melinda Gates Foundation for facilitating experiment funding.

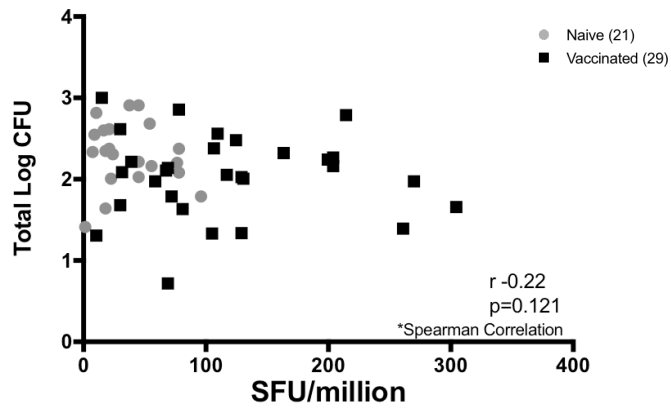
Appendix A. Supplementary material

Supplementary data associated with this article can be found, in the online version, at <http://dx.doi.org/10.1016/j.vaccine.2016.10.060>.

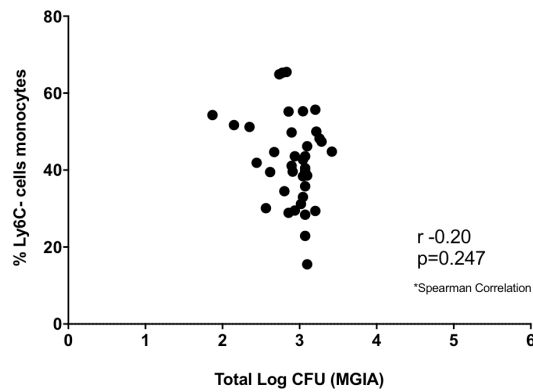
References

- [1] Han S. Clinical vaccine development. *Clin Exp Vaccine Res* 2015;4:46–53.
- [2] Dickson M, Gagnon JP. The cost of new drug discovery and development. *Discovery Med* 2004;4:172–9.
- [3] Quinn CP, Sabourin CL, Niemuth NA, Li H, Semenova VA, Rudge TL, et al. A three-dose intramuscular injection schedule of anthrax vaccine adsorbed generates sustained humoral and cellular immune responses to protective antigen and provides long-term protection against inhalation anthrax in rhesus macaques. *Clin Vaccine Immunol*: CVI 2012;19:1730–45.
- [4] Little SF, Webster WM, Norris SL, Andrews GP. Evaluation of an anti-rPA IgG ELISA for measuring the antibody response in mice. *Biol: J Int Assoc Biol Standardization* 2004;32:62–9.
- [5] Semenova VA, Schiffer J, Steward-Clark E, Soroka S, Schmidt DS, Brawner MM, et al. Validation and long term performance characteristics of a quantitative enzyme linked immunosorbent assay (ELISA) for human anti-PA IgG. *J Immunol Methods* 2012;376:97–107.
- [6] Aagaard C, Hoang TT, Izzo A, Billeskov R, Troudt J, Arnett K, et al. Protection and polyfunctional T cells induced by Ag85B-TB10.4/IC31 against *Mycobacterium tuberculosis* is highly dependent on the antigen dose. *PLoS ONE* 2009;4:e5930.
- [7] Geldenhuys H, Mearns H, Miles DJ, Tameris M, Hokey D, Shi Z, et al. The tuberculosis vaccine H4:IC31 is safe and induces a persistent polyfunctional CD4 T cell response in South African adults: a randomized controlled trial. *Vaccine* 2015;33:3592–9.
- [8] Luabeya AK, Kagina BM, Tameris MD, Geldenhuys H, Hoff ST, Shi Z, et al. First-in-human trial of the post-exposure tuberculosis vaccine H56:IC31 in *Mycobacterium tuberculosis* infected and non-infected healthy adults. *Vaccine* 2015;33:4130–40.
- [9] van Dissel JT, Arend SM, Prins C, Bang P, Tingskov PN, Lingnau K, et al. Ag85B-ESAT-6 adjuvanted with IC31 promotes strong and long-lived *Mycobacterium tuberculosis* specific T cell responses in naive human volunteers. *Vaccine* 2010;28:3571–81.
- [10] Evans TG, McElrath MJ, Matthews T, Montefiori D, Weinhold K, Wolff M, et al. QS-21 promotes an adjuvant effect allowing for reduced antigen dose during HIV-1 envelope subunit immunization in humans. *Vaccine* 2001;19:2080–91.
- [11] Wright DF, Winter HR, Duffull SB. Understanding the time course of pharmacological effect: a PKPD approach. *Br J Clin Pharmacol* 2011;71:815–23.
- [12] Mould DR, Upton RN. Basic concepts in population modeling, simulation, and model-based drug development. *CPT: Pharmacometrics Syst Pharmacol* 2012;1:e6.
- [13] Knibbe CA, Zuideveld KP, Aarts LP, Kuks PF, Danhof M. Allometric relationships between the pharmacokinetics of propofol in rats, children and adults. *Br J Clin Pharmacol* 2005;59:705–11.
- [14] Dubois VF, de Witte WE, Visser SA, Danhof M, Della Pasqua O, Cardiovascular Safety Project T, et al. Assessment of interspecies differences in drug-induced QTc interval prolongation in cynomolgus monkeys, dogs and humans. *Pharm Res* 2016;33:40–51.
- [15] Plotkin SA, Orenstein WA, Offit PA. *Vaccines*. 6th ed. Saunders; 2013.
- [16] Aagaard C, Hoang T, Dietrich J, Cardona PJ, Izzo A, Dolganov G, et al. A multistage tuberculosis vaccine that confers efficient protection before and after exposure. *Nat Med* 2011;17:189–94.
- [17] Lalvani A, Pathan AA, McShane H, Wilkinson RJ, Latif M, Conlon CP, et al. Rapid detection of *Mycobacterium tuberculosis* infection by enumeration of antigen-specific T cells. *Am J Respir Crit Care Med* 2001;163:824–8.
- [18] Hoang T, Aagaard C, Dietrich J, Cassidy JP, Dolganov G, Schoolnik GK, et al. ESAT-6 (EsxA) and TB10.4 (EsxH) based vaccines for pre- and post-exposure tuberculosis vaccination. *PLoS ONE* 2013;8:e80579.
- [19] Christensen D, Lindenstrom T, van de Wijdeven G, Andersen P, Agger EM. Syringe free vaccination with CAF01 Adjuvanted Ag85B-ESAT-6 in bioneedles provides strong and prolonged protection against tuberculosis. *PLoS ONE* 2010;5:e15043.
- [20] Burnham KP, Anderson DR. Multimodel inference: understanding AIC and BIC in model selection. *Sociol. Methods Res.* 2004;33:261–304.
- [21] Ciabattini A, Prota G, Christensen D, Andersen P, Pozzi G, Medagliani D. Characterization of the antigen-specific CD4(+) T Cell response induced by prime-boost strategies with CAF01 and CpG adjuvants administered by the intranasal and subcutaneous routes. *Front Immunol* 2015;6:430.
- [22] Elvang T, Christensen JP, Billeskov R, Thi Kim Thanh Hoang T, Holst P, Thomsen AR, et al. CD4 and CD8 T cell responses to the M. tuberculosis Ag85B-TB10.4 promoted by adjuvanted subunit, adenovector or heterologous prime boost vaccination. *PLoS ONE* 2009;4:e5139.
- [23] Fletcher HA, Snowden MA, Landry B, Rida W, Satti I, Harris SA, et al. T-cell activation is an immune correlate of risk in BCG vaccinated infants. *Nature Commun* 2016;7:11290.
- [24] Kagina BM, Abel B, Scriba TJ, Hughes EJ, Keyser A, Soares A, et al. Specific T cell frequency and cytokine expression profile do not correlate with protection against tuberculosis after bacillus Calmette-Guérin vaccination of newborns. *Am J Respir Crit Care Med* 2010;182:1073–9.
- [25] Chien JY, Friedrich S, Heathman MA, de Alwis DP, Sinha V. Pharmacokinetics/pharmacodynamics and the stages of drug development: role of modeling and simulation. *AAPS J* 2005;7:E544–59.

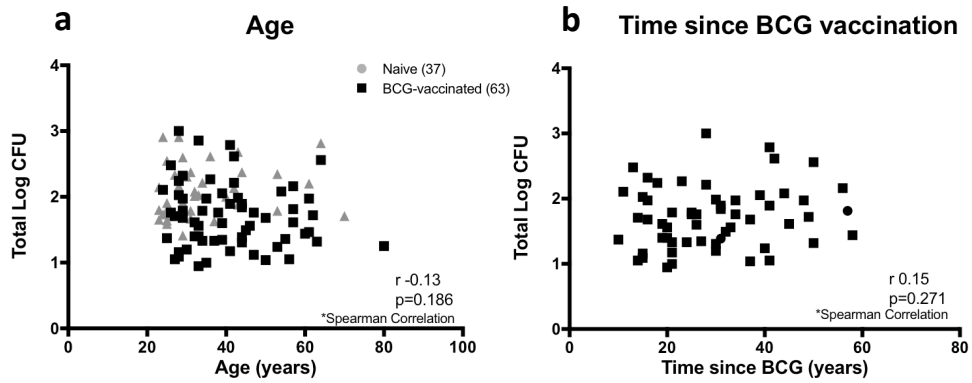
APPENDIX 8. Additional data



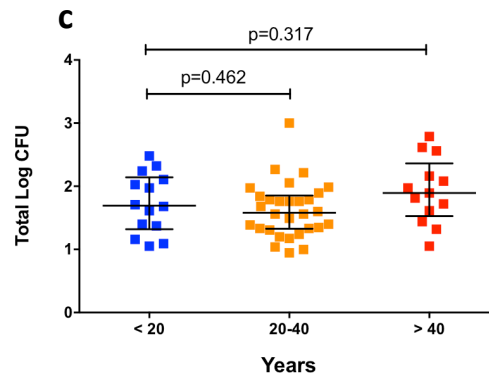
Appendix 8A (Figure). Correlation between IFN- γ ELISpot response and mycobacterial growth. Statistical significance was tested using Spearman's correlation. A p value < 0.05 was considered significant. n= 21 naïve and 29 BCG-vaccinated.



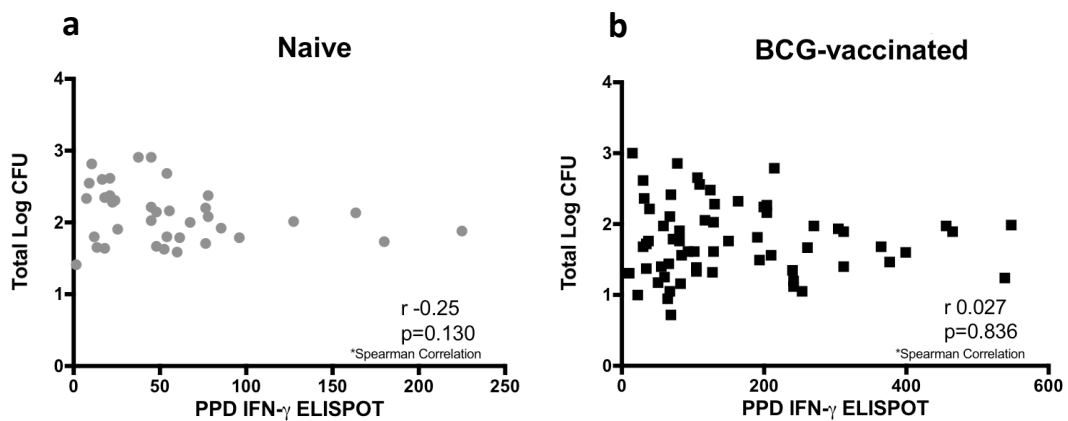
Appendix 8B (Figure). Correlation between the frequency of Ly6C⁺ monocytes/macrophages and mycobacterial growth control following RUTI vaccination across time points. Statistical significance was tested using Spearman's correlation. A p value < 0.05 was considered significant. n= 42 mice.



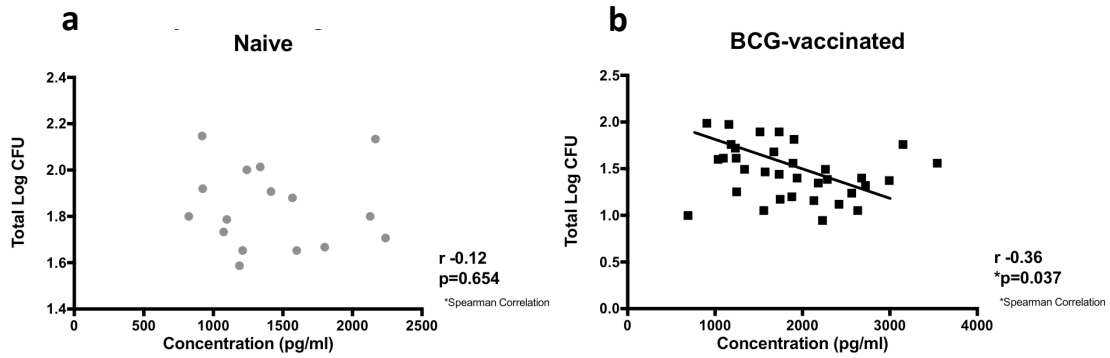
Time since BCG vaccination - Stratified



Appendix 8C (Figure). Correlation between the age of participants (a) and time since vaccination (b) with *ex vivo* mycobacterial growth. Statistical significance was tested using Spearman’s correlation. An analysis was also performed by stratifying the time since BCG vaccination (c), unpaired t-test. A p value < 0.05 was considered significant. n= 37 naïve and 63 BCG-vaccinated.



Appendix 8D (Figure). Correlation between IFN- γ ELISpot response and mycobacterial growth in the naïve (a) and BCG-vaccinated (b) groups. Statistical significance was tested using Spearman’s correlation. A p value < 0.05 was considered significant. n= 37 naïve and 63 BCG-vaccinated.



Appendix 8E (Figure). Correlation between the production of perforin and mycobacterial growth inhibition in the naïve (a) and BCG-vaccinated (b) groups. Statistical significance was tested using Spearman’s correlation. A p value < 0.05 was considered significant. n= 16 naïve and 34 BCG-vaccinated.

BCG-specific cytokine ⁺ T-cells	Correlation with CMV-specific cytokine ⁺ T-cells					
	All participants		Naïve		BCG-vaccinated	
	r	p-value	r	p-value	r	p-value
IFN- γ ⁺ CD4 T-cells	0.19	0.2515	0.51	0.0758	0.068	0.7369
IL-2 ⁺ CD4 T-cells	0.13	0.4253	0.0	0.99	0.11	0.5999
TNF- α ⁺ CD4 T-cells	-0.046	0.7761	-0.19	0.5513	0.021	0.9180
IFN- γ ⁺ CD8 T-cells	0.042	0.7990	-0.26	0.4103	0.065	0.7473
IL-2 ⁺ CD8 T-cells	-0.18	0.2775	-0.078	0.8205	-0.2	0.3158
TNF- α ⁺ CD8 T-cells	0.18	0.2675	-0.27	0.5385	0.21	0.2887

Appendix 8F (Table). Correlation between BCG-specific T-cell response and CMV-specific T-cell response. Associations were assessed from total 50 participants, as well as from each naïve (n=16) and BCG-vaccinated (n=34) groups respectively (Spearman’s correlation). Correlations were investigated from 3 different subsets of BCG-specific cytokine⁺ CD4 and CD8 T-cells expressing IFN- γ ⁺, IL-2⁺ or TNF- α ⁺ with each respective CMV-specific T-cell. A p value <0.05 was considered statistically significant.

CMV-specific cytokine ⁺ T-cells	Correlation with NK cells			
	Cytokine NK cell		Cytotoxic NK cell	
	r	p-value	r	p-value
IFN- γ ⁺ CD4 T-cells	0.25	0.1176	0.27	0.0898
IL-2 ⁺ CD4 T-cells	0.23	0.1596	0.25	0.1225
TNF- α ⁺ CD4 T-cells	0.26	0.0995	0.28	0.0795
IFN- γ ⁺ CD8 T-cells	0.047	0.7713	0.16	0.3232
IL-2 ⁺ CD8 T-cells	0.071	0.6634	0.081	0.6212
TNF- α ⁺ CD8 T-cells	0.028	0.8633	0.23	0.1621

Appendix 8G (Table). Correlation between CMV-specific T-cell response and NK-cells frequency. Associations were investigated with cytokine-producing and cytotoxic NK cell populations, respectively. A p value <0.05 was considered statistically significant (Spearman’s correlation). n= 50 participants (16 naïve, 34 BCG-vaccinated).